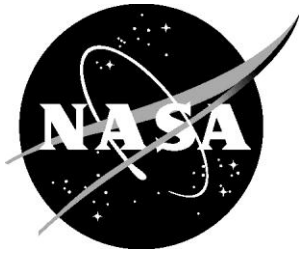


NASA/CR–2013-217797



System-Level Experimental Validations for Supersonic Commercial Transport Aircraft Entering Service in the 2018-2020 Time Period

Phase I Final Report

*Todd E. Magee, Peter A. Wilcox, Spencer R. Fugal, and Kurt E. Acheson
Boeing Research and Technology, Huntington Beach, California*

*Eric E. Adamson, Alicia L. Bidwell, and Stephen G. Shaw
Boeing Commercial Airplanes, Seattle, Washington*

NASA STI Program . . . in Profile

Since its founding, NASA has been dedicated to the advancement of aeronautics and space science. The NASA scientific and technical information (STI) program plays a key part in helping NASA maintain this important role.

The NASA STI program operates under the auspices of the Agency Chief Information Officer. It collects, organizes, provides for archiving, and disseminates NASA's STI. The NASA STI program provides access to the NASA Aeronautics and Space Database and its public interface, the NASA Technical Report Server, thus providing one of the largest collections of aeronautical and space science STI in the world. Results are published in both non-NASA channels and by NASA in the NASA STI Report Series, which includes the following report types:

- **TECHNICAL PUBLICATION.** Reports of completed research or a major significant phase of research that present the results of NASA Programs and include extensive data or theoretical analysis. Includes compilations of significant scientific and technical data and information deemed to be of continuing reference value. NASA counterpart of peer-reviewed formal professional papers, but having less stringent limitations on manuscript length and extent of graphic presentations.
- **TECHNICAL MEMORANDUM.** Scientific and technical findings that are preliminary or of specialized interest, e.g., quick release reports, working papers, and bibliographies that contain minimal annotation. Does not contain extensive analysis.
- **CONTRACTOR REPORT.** Scientific and technical findings by NASA-sponsored contractors and grantees.

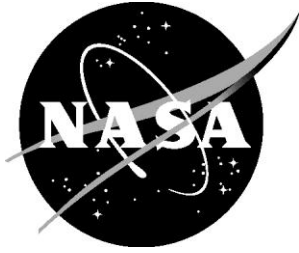
- **CONFERENCE PUBLICATION.** Collected papers from scientific and technical conferences, symposia, seminars, or other meetings sponsored or co-sponsored by NASA.
- **SPECIAL PUBLICATION.** Scientific, technical, or historical information from NASA programs, projects, and missions, often concerned with subjects having substantial public interest.
- **TECHNICAL TRANSLATION.** English-language translations of foreign scientific and technical material pertinent to NASA's mission.

Specialized services also include organizing and publishing research results, distributing specialized research announcements and feeds, providing information desk and personal search support, and enabling data exchange services.

For more information about the NASA STI program, see the following:

- Access the NASA STI program home page at <http://www.sti.nasa.gov>
- E-mail your question to help@sti.nasa.gov
- Fax your question to the NASA STI Information Desk at 443-757-5803
- Phone the NASA STI Information Desk at 443-757-5802
- Write to:
STI Information Desk
NASA Center for AeroSpace Information
7115 Standard Drive
Hanover, MD 21076-1320

NASA/CR–2013-217797



System-Level Experimental Validations for Supersonic Commercial Transport Aircraft Entering Service in the 2018-2020 Time Period

Phase I Final Report

*Todd E. Magee, Peter A. Wilcox, Spencer R. Fugal, and Kurt E. Acheson
Boeing Research and Technology, Huntington Beach, California*

*Eric E. Adamson, Alicia L. Bidwell, and Stephen G. Shaw
Boeing Commercial Airplanes, Seattle, Washington*

National Aeronautics and
Space Administration

Langley Research Center
Hampton, Virginia 23681-2199

Prepared for Langley Research Center
under Contract NNL08AA16B/NNL10AA00T

February 2013

Available from:

NASA Center for AeroSpace Information
7115 Standard Drive
Hanover, MD 21076-1320
443-757-5802

TABLE OF CONTENTS

ABSTRACT..... 9

1.0 EXECUTIVE SUMMARY 10

2.0 SCOPE OF ACTIVITY..... 11

2.1 Project Objectives and Goals 11

2.2 Project Scope 12

2.3 Project Plan and Schedule..... 13

2.4 Project Organization 16

2.5 Project Deliverables 16

3.0 LOW-BOOM CONCEPT DEVELOPMENT 18

3.1 Preliminary Concept Definition..... 18

3.2 Preliminary Engine Sizing 26

3.3 Preliminary Design Definition..... 31

3.4 Final Design Definition..... 35

3.5 Low-Boom Concept Analysis, Gate 1 Review 36

3.6 Second OML Design, Alternate Part Definition 45

3.7 Additional Boom Optimization Studies After Gate Review 48

4.0 LOW-BOOM CONCEPT WIND TUNNEL MODEL PREPARATION 53

4.1 QEVC Boom Model 1 53

4.2 QEVC Boom Model 2 55

4.3 QEVC Performance Model 1 57

4.4 Bodies of Revolution 61

5.0 EVALUATION OF EXISTING NASA PRESSURE RAILS..... 63

5.1 Overview..... 63

5.2 Probe 64

5.3 Wall Rail 65

5.4 Mast Rail..... 67

5.5 Results of Evaluation 68

6.0 NEW PRESSURE MEASUREMENT RAIL INSTRUMENTATION 70

6.1 Overview..... 70

6.2 Blade Rail..... 72

7.0 VALIDATION WIND TUNNEL TEST 74

7.1 Overview..... 74

7.2 Test Objectives and Test Plan..... 75

7.3 Facility Hardware and Instrumentation..... 77

7.4 Test Performance and Productivity 81

7.5 Data Quality and Test Results..... 94

7.6 Wind Tunnel Test Summary and Conclusions	125
8.0 CFD AND VALIDATION ANALYSIS.....	126
8.1 Overview.....	126
8.2 Summary of CFD Cases.....	128
8.3 Body of Revolution CFD vs. Test Pressure Signature Comparisons.....	135
8.4 Boom Model CFD vs. Test Pressure Signature and F&M Comparisons.....	142
8.5 Performance Model CFD vs. Test Pressure Signature and F&M Comparisons	159
8.6 Additional Tare and Interference Assessments.....	169
8.7 CFD Validation Summary and Conclusions	179
9.0 RECOMMENDATIONS AND FUTURE WORK.....	180
10.0 SUMMARY AND CONCLUSION.....	181
11.0 NOMENCLATURE.....	183
12.0 REFERENCES.....	186

LIST OF FIGURES

Figure 2.3-1. Phase I Master Schedule	15
Figure 2.4-1. Supersonic Experimental Validation Project Organization.....	16
Figure 2.5-1. Boeing N+2 Supersonic Experimental Validation Project Deliverables.....	17
Figure 3.1-1. 765-076E General Arrangement	19
Figure 3.1-2. 765-076F General Arrangement.....	20
Figure 3.1-3. 765-076G General Arrangement.....	21
Figure 3.1-4. 765-100A General Arrangement.....	22
Figure 3.1-5. Initial Design Target.....	23
Figure 3.1-6. Changes to -076I to Create QEVC2.....	24
Figure 3.1-7. 765-076I Compared to QEVC2 Concept	24
Figure 3.1-8. QEVC2 General Arrangement	25
Figure 3.1-9. QEVC2 Drag and Boom Levels Relative to Project Targets	25
Figure 3.2-1. Concept Flow Path for Mixed-Flow Turbofan Provided by Rolls-Royce (Unscaled).....	26
Figure 3.2-2. Cross-Section of Concept Propulsion System Installation.....	27
Figure 3.2-3. Notional Inlet Concept	27
Figure 3.2-4. Impact of Inlet Turning on Propulsion System Installation and Performance	28
Figure 3.2-5. Effect of Freestream Mach on Propulsion System Installation and Performance.....	28
Figure 3.2-6. Over-wing Inlet Design Mach.....	29
Figure 3.2-7. Notional Concept Propulsion System Compared With Flow-Through Placeholder Nacelle.....	30
Figure 3.2-8. Front View of Propulsion System Installation	30
Figure 3.2-9. Notional Nacelle with 2D Inlet and Nozzle Design Concepts	31
Figure 3.3-1. Initial Optimization Results ($M = 1.8$, $CL = 0.104$).....	32
Figure 3.3-2. 8038 Drag and Boom Levels Relative to Project Targets	33
Figure 3.3-3. 7038 Drag and Boom Levels Relative to Project Targets	33
Figure 3.3-4. 6007 Drag and Boom Levels Relative to Project Targets.....	34
Figure 3.3-5. 6007 Final Surface and Centerline Pressure ($M = 1.8$, $CL = 0.1039$).....	35
Figure 3.4-1. QEVC3 General Arrangement	36
Figure 3.5-1. Sonic Boom and Performance Metric Tracking for the Low-Boom Design.....	37
Figure 3.5-2. The Low-Boom Concept Has Robust Sonic Boom Characteristics at Multiple Mach Numbers.....	39
Figure 3.5-3. Low-Boom Concept Signature Characteristics at Off-Design CLs	40
Figure 3.5-4. The Low-Boom Concept Has Robust Signature Characteristics at Off-Track Locations.....	41
Figure 3.5-5. Low-Boom Concept Longitudinal Cruise Aerodynamics.....	42
Figure 3.5-6. Fuel Layout for the Low-Boom Concept	43
Figure 3.5-7. Low-Boom Concept Performance Analysis by Comparison With the 765-076E.....	44
Figure 3.5-8. The Low-Boom Concept CG Envelope	45
Figure 3.6-1. 8668 Compared to 6007 ($Mach = 1.6$).....	46

Figure 3.6-2. 8668 Compared to 6007 (Mach = 1.8).....	47
Figure 3.6-3. 8679 Compared to 8668 (Mach = 1.6).....	47
Figure 3.6-4. Surface Pressure and Flow Field for 8679 Geometry (M = 1.6, CL = 0.14).....	48
Figure 3.7-1. Optimum Under-Track Signature Comparing Nacelle On (Green) With Nacelle Off (Blue) (M = 1.6, CL = 0.14).....	49
Figure 3.7-2. Optimum Off-Track Signature Comparing Nacelle On (Green) With Nacelle Off (Blue) (M = 1.6, CL = 0.14).....	49
Figure 3.7-3. Surface Pressure and Centerline Pressure for Geometry Optimized with no Nacelle (M = 1.6, CL = 0.14).....	50
Figure 3.7-4. Under-Track Signatures for Optimum Results with Different Off-Track Weightings (M = 1.6, CL = 0.14).....	51
Figure 3.7-5. 45-deg Off-Track Signatures for Optimum Results with Different Off-Track Weightings (M = 1.6, CL = 0.14).....	51
Figure 3.7-6. Surface Pressure Distribution for Different Off-Track Weighting (M = 1.6, CL = 0.14).....	52
Figure 4.1-1. Preliminary Boom Model 1 Layout Shown at Gate 1 Review.....	53
Figure 4.1-2. Boom Model 1 Assembly Shown at PDR.....	54
Figure 4.1-3. Boom Model 1 Modular Parts.....	55
Figure 4.2-1. Boom Model 1 and Boom Model 2 and Associated Modular Hardware.....	56
Figure 4.3-1. Force Model Layout Shown at Gate 1 Review.....	57
Figure 4.3-2. Performance Model 1 Assembly.....	58
Figure 4.3-3. Performance Model Modular Parts.....	58
Figure 4.3-4. Performance Wind Tunnel Model and Associated Modular Part.....	60
Figure 4.4-1. Geometric Comparison Between AS1, AS2, and AS3.....	61
Figure 4.4-2. AS1 Model Installed in NASA Ames 9' x 7' Wind tunnel.....	62
Figure 4.4-3. AS2 Model Installed in NASA Ames 9' x 7' Wind tunnel.....	62
Figure 4.4-4. AS3 Model Installed in NASA Ames 9' x 7' Wind tunnel.....	62
Figure 5.1-1. Examples of Past Sonic Boom Pressure Measurement Techniques and Factors That Determine Their Selection.....	64
Figure 5.2-1. NASA Single Probes Used in the 2008 Sonic Boom Test.....	65
Figure 5.2-2. Single Probe Uncertainty Based on Repeat Run Data From 2008 Test.....	65
Figure 5.3-1. NASA Wall Rail Used in the 2008 Sonic Boom Test.....	66
Figure 5.3-2. Wall Rail Uncertainty Based on Short-Term Repeatability From 2008 Test Data.....	66
Figure 5.4-1. NASA Mast Rail Used in the 2008 Sonic Boom Test.....	67
Figure 5.4-2. Mast Rail Uncertainty Based on Short-Term Repeatability From the 2008 Test Data.....	67
Figure 5.4-3. Qualitative Comparison of Uncertainty between the Single Probe, Wall Rail, and Mast Rail.....	68
Figure 5.5-1. Final Evaluation.....	69
Figure 6.1-1. Example of Observed Variation in Near-field Signature with Spatial Location in the Wind Tunnel.....	71
Figure 6.2-1. Installation of the 14" Blade Rail on the NASA Ames 9' x 7' Window Blanks.....	72

Figure 6.2-2. The 14" Pressure Instrumented Blade Rail	73
Figure 6.2-3. The 14" Blade Rail Installed in the NASA Ames 9' x 7' Wind Tunnel	73
Figure 7.1-1. NASA Ames 9' x 7' Supersonic Wind Tunnel Facility Layout.....	74
Figure 7.3-1. 2-in Sonic Boom Pressure Rail for AS-0229	77
Figure 7.3-2. Installation of 2-in Sonic Boom Pressure Rail on North Wall Aft Window Blank.....	78
Figure 7.3-3. Photograph of the 2-in Sonic Boom Pressure Rail Installed in the NASA Ames 9' x 7' Test Section	78
Figure 7.3-4. Sting and Sting Spacer Hardware.....	79
Figure 7.3-5. Installed Sting and Sting Spacer Hardware	79
Figure 7.4-1. BM1 Model with VS2 Strut Installed in the NASA Ames 9' x 7' Wind Tunnel.....	82
Figure 7.4-2. Sting Supported PM1 Model Installed in the NASA Ames 9' x 7' Wind Tunnel	82
Figure 7.4-3. Ames AS0229 Test Productivity	85
Figure 7.5-1. Typical BOR Pressure Data Repeatability, M = 1.60	95
Figure 7.5-2. Typical BOR Pressure Data Repeatability, M = 1.80	96
Figure 7.5-3. Typical Boom Model Pressure Data Repeatability, M = 1.60	97
Figure 7.5-4. Typical Boom Model Pressure Data Repeatability, M = 1.80	98
Figure 7.5-5. Typical Performance Model Pressure Data Repeatability, M = 1.60.....	99
Figure 7.5-6. Typical Performance Model Pressure Data Repeatability, M = 1.80.....	100
Figure 7.5-7. Typical BOR Reference Run Pressure Data Repeatability, M = 1.60, H = ~86".....	102
Figure 7.5-8. Typical BOR Reference Run Pressure Data Repeatability, M = 1.80, H = ~86".....	103
Figure 7.5-9. Typical Boom Model Reference Run Pressure Data Repeatability, M = 1.60, H = ~86"	104
Figure 7.5-10. Typical Boom Model Reference Run Pressure Data Repeatability, M = 1.80, H = ~86"	105
Figure 7.5-11. Typical BOR Pressure Data Variation with Angle of Attack, M = 1.60.....	107
Figure 7.5-12. Typical BOR Pressure Data Variation with Angle of Attack, M = 1.80.....	108
Figure 7.5-13. Typical Boom Model Pressure Data Variation with Angle of Attack, M = 1.60.....	109
Figure 7.5-14. Typical BM Pressure Data Variation with Angle of Attack, M = 1.80	110
Figure 7.5-15. Typical Performance Model Pressure Data Variation with Angle of Attack, M = 1.60	111
Figure 7.5-16. Typical Performance Model Pressure Data Variation with Angle of Attack, M = 1.80	112
Figure 7.5-17. Typical BOR F&M Data Quality, M = 1.60	114
Figure 7.5-18. Typical BOR F&M Data Quality, M = 1.80	115
Figure 7.5-19. Typical BM F&M Data Repeatability, M = 1.60	116
Figure 7.5-20. Typical BM F&M Data Repeatability, M = 1.80	117
Figure 7.5-21. Typical PM F&M Data Repeatability, M = 1.60	118
Figure 7.5-22. Typical PM F&M Data Repeatability, M = 1.80	119
Figure 7.5-23. Typical Boom Model F&M Height Variation, M = 1.60.....	121
Figure 7.5-24. Typical Boom Model F&M Height Variation, M = 1.80.....	122
Figure 7.5-25. Typical Performance Model F&M Height Variation, M = 1.60	123

Figure 7.5-26. Typical Performance Model F&M Height Variation, M = 1.80	124
Figure 8.1-1. Available NASA Ames 9' x 7' Supersonic Wind Tunnel AS-0229 Test Configurations.....	127
Figure 8.3-1. AS1 Pressure Signature Comparison of OVERFLOW vs. Test, M = 1.60.....	136
Figure 8.3-2. AS1 Pressure Signature Comparison of OVERFLOW vs. Test, M = 1.80.....	137
Figure 8.3-3. AS2 Pressure Signature Comparison of OVERFLOW vs. Test, M = 1.60.....	138
Figure 8.3-4. AS2 Pressure Signature Comparison of OVERFLOW vs. Test, M = 1.80.....	139
Figure 8.3-5. AS3 Pressure Signature Comparison of OVERFLOW vs. Test, M = 1.60.....	140
Figure 8.3-6. AS3 Pressure Signature Comparison of OVERFLOW vs. Test, M = 1.80.....	141
Figure 8.4-1. BM1, Configuration 4, Pressure Signature Comparison of OVERFLOW vs. Test, M = 1.60.....	143
Figure 8.4-2. BM1, Configuration 4, Pressure Signature Comparison of OVERFLOW vs. Test, M = 1.80.....	144
Figure 8.4-3. BM2, Configuration 9, Pressure Signature Comparison of OVERFLOW vs. Test, M = 1.60.....	145
Figure 8.4-4. BM2, Configuration 9, Pressure Signature Comparison of OVERFLOW vs. Test, M = 1.80.....	146
Figure 8.4-5. BM1, Configuration 4, F&M Comparison of OVERFLOW vs. Test, M = 1.60	147
Figure 8.4-6. BM1, Configuration 4, F&M Comparison of OVERFLOW vs. Test, M = 1.80	148
Figure 8.4-7. BM2, Configuration 9, F&M Comparison of OVERFLOW vs. Test, M = 1.60	148
Figure 8.4-8. BM2, Configuration 9, F&M Comparison of OVERFLOW vs. Test, M = 1.80	149
Figure 8.4-9. BM1, Configuration 4 to BM2, Configuration 9, Pressure and F&M Increments—Comparison of OVERFLOW vs. Test	150
Figure 8.4-10. BM1, Configuration 4 to BM2, Configuration 9, Pressure and F&M Increments, M = 1.60, Comparison of OVERFLOW vs. Test.....	151
Figure 8.4-11. BM1, Configuration 4 to BM2, Configuration 9, Pressure and F&M Increments, M = 1.80, Comparison of OVERFLOW vs. Test.....	152
Figure 8.4-12. BM1 Configuration Effects—Comparison of OVERFLOW vs. Test.....	154
Figure 8.4-13. BM1, Configuration 4, Alpha Variation—Comparison of OVERFLOW vs. Test.....	156
Figure 8.4-14. BM1, Configuration 5, Alpha Variation—Comparison of OVERFLOW vs. Test.....	157
Figure 8.4-15. BM1, Configuration 7, Alpha Variation—Comparison of OVERFLOW vs. Test.....	158
Figure 8.5-1. PM1, Configuration 1, Pressure Signature Comparison of OVERFLOW vs. Test, H = 60.....	160
Figure 8.5-2. PM1, Configuration 3, Pressure Signature Comparison of OVERFLOW vs. Test, H = 60.....	161
Figure 8.5-3. PM1, Configuration 3, Pressure Signature Comparison of OVERFLOW vs. Test, H = 60.....	162
Figure 8.5-4. PM1, Configuration 1, F&M Comparison of OVERFLOW vs. Test, M = 1.60.....	163
Figure 8.5-5. PM1, Configuration 1, F&M Comparison of OVERFLOW vs. Test, M = 1.80.....	164
Figure 8.5-6. PM1, Configuration 3, F&M Comparison of OVERFLOW vs. Test, M = 1.60.....	164

Figure 8.5-7. PM1, Configuration 3, F&M Comparison of OVERFLOW vs. Test, M = 1.80.....	165
Figure 8.5-8. PM1, Configuration 1 to PM1, Configuration 3, Pressure and F&M Increments—Comparison of OVERFLOW vs. Test	166
Figure 8.5-9. PM1, Configuration 1 to PM1, Configuration 3, Pressure and F&M Increments, M = 1.60 Comparison of OVERFLOW vs. Test	167
Figure 8.5-10. PM1, Configuration 1 to PM1, Configuration 3, Pressure and F&M Increments, M = 1.80 Comparison of OVERFLOW vs. Test.....	168
Figure 8.6-1. CFD-Based Reynolds Number Correction for BM1, Configuration 4, M = 1.60.....	170
Figure 8.6-2. CFD-Based Reynolds Number Correction for BM1, Configuration 4, M = 1.80.....	171
Figure 8.6-3. CFD-Based Reynolds Number Correction for BM1, Configuration 4, M = 1.60 and 1.80.....	172
Figure 8.6-4. CFD-Based Reynolds Number Correction for PM1, Configuration 3, M = 1.60	173
Figure 8.6-5. CFD-Based Reynolds Number Correction for PM1, Configuration 3, M = 1.80	174
Figure 8.6-6. CFD-Based Reynolds Number Correction for PM1, Configuration 3, M = 1.60 and 1.80.....	175
Figure 8.6-7. CFD-Based Upper Swept Strut Correction for BM1, Configuration 4, M = 1.60 and 1.80.....	176
Figure 8.6-8. CFD-Based Upper Swept Strut Correction for BM1, Configuration 4, M = 1.60 and 1.80.....	177
Figure 8.6-9. Experimental Results with CFD-Based Corrections Applied for BM1, Configuration 4, M = 1.60 and 1.80.....	178

LIST OF TABLES

Table 2.1-1. Technical Goals for the N+2 Experimental Validation Project.....	12
Table 3.3-1. Optimization Parameters	31
Table 3.3-2. Initial Optimization Force Results at $M = 1.8$	32
Table 3.3-3. Final Optimization Force Results at $M = 1.8$	34
Table 3.6-1. Optimization Parameters	46
Table 3.7-1. Nacelle Off-Design Comparison	50
Table 3.7-2. Optimization Results for Different Off-Track Weighting ($M = 1.6$).....	52
Table 4.1-1. Boom Model 1 Modular Parts	54
Table 4.2-1. Boom Model 2 Modular Parts	55
Table 4.3-1. Performance Model 1 Modular Parts.....	59
Table 7.2-1. As-Run Test Plan.....	76
Table 7.4-1. As-Run Summary	86
Table 8.2-1. CFD Cases for BOR Models	129
Table 8.2-2. CFD Cases for BM Models	130
Table 8.2-3. CFD Cases for PM Models.....	133

ABSTRACT

This report describes the work conducted by The Boeing Company under American Recovery and Reinvestment Act (ARRA) and NASA funding to experimentally validate the conceptual design of a supersonic airliner feasible for entry into service in the 2018 to 2020 timeframe (NASA N+2 generation). The report discusses the design, analysis and development of a low-boom concept that meets aggressive sonic boom and performance goals for a cruise Mach number of 1.8. The design is achieved through integrated multidisciplinary optimization tools. The report also describes the detailed design and fabrication of both sonic boom and performance wind tunnel models of the low-boom concept. Additionally, a description of the detailed validation wind tunnel testing that was performed with the wind tunnel models is provided along with validation comparisons with pretest Computational Fluid Dynamics (CFD). Finally, the report describes the evaluation of existing NASA sonic boom pressure rail measurement instrumentation and a detailed description of new sonic boom measurement instrumentation that was constructed for the validation wind tunnel testing.

1.0 EXECUTIVE SUMMARY

This report describes the work conducted under ARRA and NASA funding on the Boeing N+2 Supersonic Experimental Validation project to experimentally validate the conceptual design of a supersonic airliner feasible for entry into service in the 2018 to 2020 timeframe (NASA N+2 generation). The goal of the project is to develop a low-boom configuration optimized for minimum sonic boom levels and maximum performance efficiency, with special emphasis on shaping the aft sonic boom signature. The NASA Supersonics Project sonic boom goal for N+2 concepts is 65 to 70 PLdB. This is a very aggressive goal that can be achieved only through integrated multidisciplinary optimization tools validated in relevant ground and, later, flight environments. The Boeing N+2 Supersonic Experimental Validation project comprises the detailed aerodynamic design of an N+2 low-boom supersonic airliner configuration (ARRA-funded) and wind tunnel tests (NASA-funded) to validate the design.

The report is broken down into seven sections. The first technical section (Section 2) describes the complete Boeing N+2 Experimental Validation efforts, including both ARRA- and NASA-funded activities. The second section of the report details the low-boom design and analysis effort that resulted in a low-boom concept. The third section focuses on the design and fabrication of two low-boom wind tunnel models and one cruise performance wind tunnel model. Also included in the section is information on the fabrication of a new pressure measurement rail, and model-support hardware required to appropriately position the model relative to the rail in the tunnel. The fourth section focuses on the Boeing evaluation of existing NASA sonic boom pressure measurement rails for measuring sonic booms in wind tunnels. The fifth section provides a description of the validation wind tunnel test that took place at the NASA Ames 9' x 7' supersonic wind tunnel. The sixth section provides the CFD validation with wind tunnel data. Finally, in the seventh section (Section 8) some recommendations and future work are discussed.

For this project, a set of priorities and goals was developed to eventually enable a viable N+2 supersonic airliner that meets the 65- to 70-PLdB requirement. The primary goal was to develop a low-boom concept with a shaped front and aft signature that achieves an under-track perceived loudness of 85 PLdB. The low-boom concept should have robust sonic boom characteristics that persist at off-design and off-track locations. The secondary goal was to design a low-boom concept that meets the cruise aerodynamic performance levels of the 765-076E configuration developed under the Boeing N+2 Supersonic System study. This concept was analyzed in other areas such as fuel loading, stability, trim, and center-of-gravity. The aircraft design was not required to close in all areas; however, shortfalls were identified and noted for future work.

The ARRA- and NASA- funded work was successful in meeting all contract objectives. A low-boom concept was developed that passed the required gate review. Additional optimization work was conducted to determine the sensitivity of certain design variables on sonic boom levels and performance goals. An alternate low-boom concept was developed to enhance the validation work, and three wind tunnel models were designed and fabricated, including two sonic boom models and one cruise performance wind tunnel model. The existing NASA pressure rails were evaluated, and a recommendation for a new sonic boom pressure rail was made. Two new sonic boom pressure rails were fabricated and tested. A validation wind tunnel test using the concept wind tunnel models was conducted at the NASA Ames 9' x 7' supersonic wind tunnel. Finally, the data that was gathered during the wind tunnel test was compared with pre-test CFD results and validated the low-boom design. Several issues surfaced during the Phase I project concerning flow quality in the NASA Ames 9' x 7' supersonic wind tunnel. These issues are discussed in the report and recommendations for solution are provided.

2.0 SCOPE OF ACTIVITY

Overview

Since 1968, the FAA has banned civil supersonic flight over the continental United States (FAA Part 91.817) without a specific waiver. For all supersonic aircraft operating at the time, and in fact since then, the sonic boom produced as a result of flight at supersonic speeds has been deemed to be too annoying to the public at large to be declared acceptable. Limiting supersonic-capable commercial aircraft to subsonic speed over land has been a major obstacle to the development of second-generation commercial supersonic aircraft after the Concorde.

At the beginning of the 21st century, a renewed interest in sonic boom research had occurred, focused on solving the problems that hinder the furtherance of a new generation of civil supersonic aviation. Since then, significant research has been conducted that shows that it is possible to design a supersonic airplane with a very low sonic boom level by shaping the outer mold-line (OML). In August 2003, the first flight demonstration of this technology was successful in showing that the sonic boom signature can be shaped by shaping the OML and that this signature-shaping persists to the ground. This flight experiment, called the Shaped Sonic Boom Demonstrator (SSBD), was a vital first step in validating the approach (ref. 1). Although the SSBD successfully demonstrated signature shaping on the front of an aircraft, it was readily apparent that to reduce the sonic boom noise, the entire aircraft and resultant sonic boom signature needed shaping. With advances in multidisciplinary optimization (MDO), complete aircraft shaping is now possible. Successfully implementing MDO, Boeing and others have developed the necessary techniques to design low-boom aircraft. The goal of this project was not only to conduct further low-boom concept designs using the latest techniques, but also to validate these methods in a wind tunnel environment.

This project is funded by ARRA and NASA. In this section, a brief outline of the project follows which describes Boeing tasks using both ARRA and NASA funds.

2.1 Project Objectives and Goals

There are two main objectives for this project. The first objective is to validate the sonic boom and performance characteristics of an N+2-class supersonic vehicle specifically designed for low-boom operation. The second main objective is to assess the effect of nacelle and nozzle shaping on sonic boom levels and cruise performance for an N+2-class supersonic vehicle. The project is broken down into two distinct 18-month phases to address each of these objectives. The first phase of the project was designed to address the sonic boom and performance validation. The specific objectives for Phase I are listed below.

Phase I objective: Validate the low-boom configuration and its cruise efficiency.

- Starting with an N+2 supersonic vehicle, optimize the configuration to meet specified sonic boom and supersonic aerodynamic performance goals.
- Ensure that the low-boom concept sonic boom signature has front and aft signature shaping.
- Ensure that the low-boom concept has robust signature characteristics in under-track, off-track, and off-design flight conditions (i.e., Mach and CL).
- Validate the concept through sonic boom and supersonic performance wind tunnel testing.

Phase II objective: Assess the effect of nacelle and nozzle shaping on sonic boom and cruise performance.

- Starting with the Phase I supersonic vehicle, further optimize the configuration to meet sonic boom and cruise efficiency goals based on the lessons learned in Phase I testing.
- Focus special attention on the effects of the inlet and plume on the sonic boom signature and supersonic cruise efficiency.
- Consider the interaction of the plume on aft signature shaping.
- Validate the new design through wind tunnel testing.

Note: Only Phase I objectives were addressed with ARRA funding.

Table 2.1-1 illustrates the goals for the project, the most important of which is the 85-PLdB under-track sonic boom noise level with front and aft signature shaping. The second most important goal is the lift/drag (L/D) ratio remaining as good as the 765-076E configuration (i.e., $L/D \geq 7.0$ at Mach = 1.6). In this study, Boeing chose to design the concept to the low end of the scale, with 35 passengers. The remaining goals are essentially fallouts of the previous three goals. Although aircraft design is not required to close in all disciplines, all disciplines (e.g., aerodynamics, stability and control, and mass properties) are to be assessed, and those that do not close are to be noted for future research.

Table 2.1-1. Technical Goals for the N+2 Experimental Validation Project

Goal	Phase I	Phase II
Objective	Validation of low-boom configuration and efficiency	Effect of nacelle and nozzle shaping on sonic boom and efficiency
Sonic Boom (PLdB)	85 PLdB with front and aft shaping	85 PLdB with front and aft shaping
Lift/Drag Ratio	As good as 765-076E	As good as 765-076E
Cruise Speed	Mach 1.6–1.8	Mach 1.6 to 1.8
Range	4000 nmi	4000 nmi
Payload (Passengers)	35 to 70	35 to 70
Fuel Efficiency (passenger miles per lb of fuel)	Fallout	Fallout
Tools Used/Validated	Gen 3.0	Gen 3.5
Sonic Boom Design Tools	Nonlinear CFD-based shape optimization	Nonlinear CFD-based shape optimization with propulsion effects
Optimization Tools	MDOPT and TRANAIR	MDOPT and TRANAIR
Analysis Tools	MDA	MDA
CFD Tools	OVERFLOW, Cart3d, and TRANAIR	OVERFLOW, Cart3d, with adjoint, and TRANAIR
Sonic Boom Tools	MDBOOM and Zephyrus	MDBOOM and Zephyrus

2.2 Project Scope

This project employs a phased and gated approach to experimentally validate a supersonic N+2 low-boom concept. As discussed previously, the project is broken down into two 18-month phases. In Phase I, which is covered in this final report, a low-boom concept would be developed that met the goals and objectives discussed in section 2.1. Once the concept was designed, its sonic boom and performance would be assessed using high-fidelity CFD. The results of this assessment would then be presented at a gate review with NASA. If the concept sufficiently met project goals, it would pass the gate review and enter fabrication and testing. Two wind tunnel models were then to be fabricated, a sonic boom and a performance wind tunnel model, which would be tested at a NASA wind tunnel facility. Both sonic boom

and aerodynamic performance testing would be conducted. After testing, validation analysis would be conducted through the evaluation of the test data and pretest CFD predictions, and the results documented and presented to NASA. A second gate review would then be held to determine whether or not the project should advance to Phase II.

The scope of Phase II essentially mirrors the Phase I effort, except that the focus is now on the effect of the inlet and nozzle plume on the sonic boom and the aircraft aerodynamic performance. The low-boom concept in Phase II is updated based on lessons learned in Phase I. Additional design work is conducted that leverages nacelle and nozzle shaping with aircraft integration to achieve low sonic boom noise and high installed propulsion efficiency. The design must pass a gate review similar to the one conducted in Phase I. Upon passing this gate review, two wind tunnel models are fabricated, one sonic boom model and one cruise performance model. Upon completion of the wind tunnel models, sonic boom and cruise performance wind tunnel testing are conducted. Following this testing, validation is conducted using the wind tunnel test data and pretest CFD, and the results are documented and presented to NASA.

Only the concept design, analysis, and wind tunnel model fabrication in Phase I are funded by ARRA. The remainder of the project is funded by NASA.

2.3 Project Plan and Schedule

The project plan is broken down by WBS, with each phase having similar items. The Phase I project plan is listed below.

Phase I

- 3.1 Development of Generation 3.0 Geometry (ARRA-funded task).
 - 3.1.1—Develop low-boom concept.
 - 3.1.2—Assess low-boom concept and preliminary model mount system.
 - 3.1.3—Gate Review 1.
- 3.2 Fabrication of Experimental Validation Hardware (ARRA-funded task).
- 3.3 Evaluation of Existing NASA Sonic Boom Pressure Rails (ARRA-funded task).
- 3.4 Validation Analysis.
- 3.5 Test Planning, Pretest Support, and Post-test Support.
- 3.6 Wind Tunnel Test Support.
- 3.7 Technical Management, Planning, and Deliverables.
 - 3.7.1—ARRA-funded tasks.
 - 3.7.2—NASA-funded tasks (Gate Review 2 is included in this WBS item).

In Phase I, ARRA-funded activities include WBS items 3.1, 3.2, 3.3, and 3.7.1. The remaining WBS items are NASA-funded activities.

The Phase II project plan is listed below.

Phase II

- 3.8 Development of Updated Propulsion Effects Geometry.
 - Gate Review 3.
- 3.9 Fabrication of Experimental Validation Hardware.
- 3.10 Validation Analysis.
- 3.11 Test Planning, Pretest Support, and Post-test Support.
- 3.12 Wind Tunnel Test Support.
- 3.13 Technical Management, Planning, and Documentation.

All WBS elements in Phase II are NASA-funded activities.

From the project plan, an integrated master schedule was developed. During the 14 months of the ARRA-funded part of the project, the master schedule changed somewhat to capture developments in the project. Specific changes included the early start of the NASA pressure rail evaluation and the continued design and analysis activities following Gate Review 1. The continued design activities focused on gathering additional sensitivity and optimization data to improve the resultant validation. It was also decided with NASA to consolidate the two wind tunnel tests into one larger sonic-boom and performance test in WBS 3.5 and 3.6.

Three additional tasks were added during Phase I to cover hardware development that was not in the original plan. This new hardware included two pressure measurement rail concepts and additional model support hardware. The specific new WBS elements are listed below.

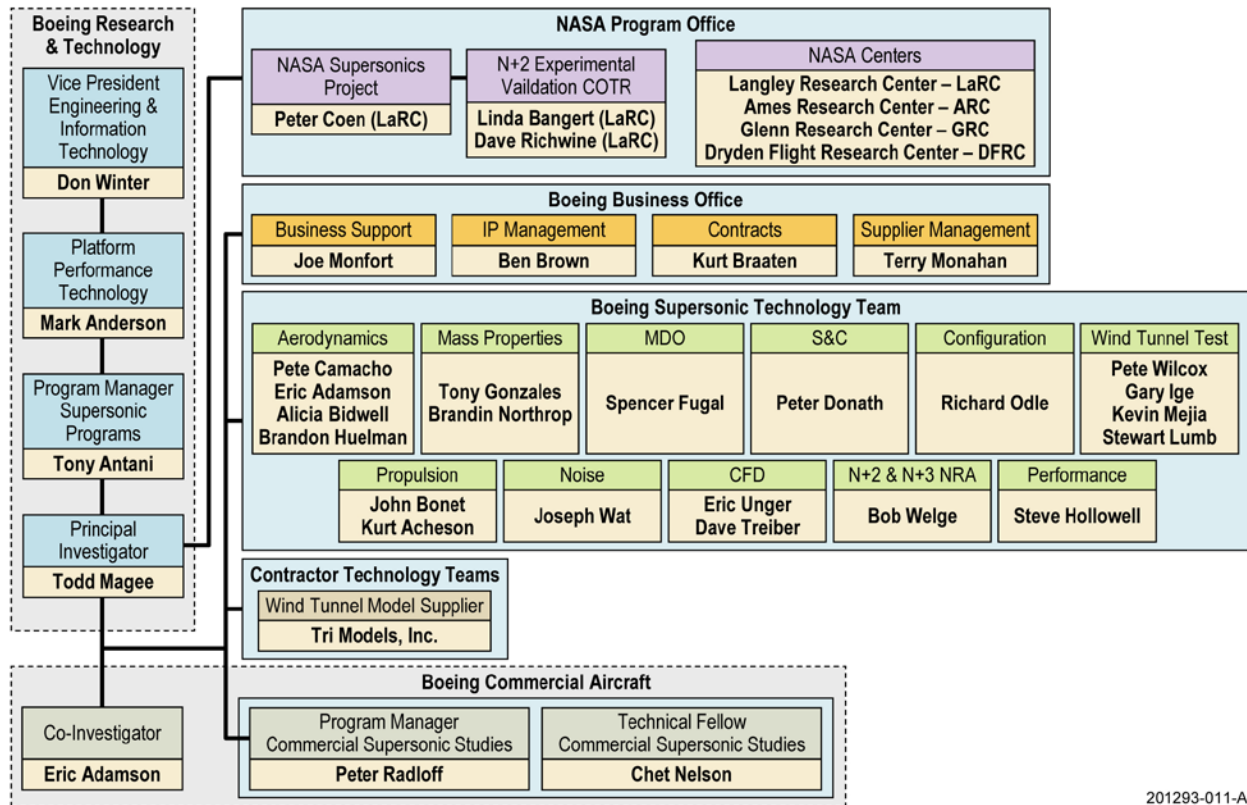
- 3.14 Sonic boom measurement rail design and fabrication (Blade Rail)
- 3.15 Alternate sonic boom measurement rail design, analysis, and fabrication
- 3.16 New sting and spacer

The first pressure measurement rail (WBS 3.14) was based on the NASA Blade Rail design and the second pressure measurement rail (WBS 3.15) was based on the Boeing short rail design. Figure 2.3-1 shows the resulting Phase I master schedule.

The Phase I ARRA-funded period completed at the end of February 2011. Phase I under NASA funding continued until the end of June 2011.

2.4 Project Organization

Figure 2.4-1 shows the project organization. NASA leadership for the project consists of Peter Coen (NASA Supersonics Project manager) and Linda Bangert (N+2 Experimental Validation contracting officer's technical representative [COTR]). The project principal investigator is Todd Magee, and the project co-investigator is Eric Adamson. Personnel from both Boeing Research & Technology and Boeing Commercial Airplanes were involved in the project. A single supplier, Tri Models, Inc., was selected for wind tunnel model fabrication. Boeing functional leadership and technical contributors also are identified in Figure 2.4-1.



201293-011-A

Figure 2.4-1. Supersonic Experimental Validation Project Organization

2.5 Project Deliverables

The project has 60 deliverables, as listed in Figure 2.5-1. At the time of this writing, several Phase II delivery dates are in flux, so only the Phase I deliverables are shown.

The remainder of the report focuses specifically on the Phase I project. The Phase II information in this section was provided for continuity. A second report will be provided at the end of Phase II.

Figure 2.5-1. Boeing N+2 Supersonic Experimental Validation Project Deliverables

#	Phase	Deliverable	Due Date (Months After Contract Award)	Comments
1	Phase 1	ARRA - CAD definition for N+2 OML designed with generation 3.0 tools	Aug-10	Complete
2	Phase 1	ARRA - Preliminary boom model mount design	Aug-10	Complete
3	Phase 1	ARRA - Sonic boom wind tunnel model (Model #1a)	Feb-11	Complete
4	Phase 1	ARRA - Required support hardware for Model #1a	Feb-11	Complete
5	Phase 1	ARRA - Model #1a documentation (drawings, stress report, quality report)	Feb-11	Complete
6	Phase 1	ARRA - Model #1a support hardware documentation	Feb-11	Complete
7	Phase 1	ARRA - Supersonic cruise performance wind tunnel model (Model #2a)	Feb-11	Complete
8	Phase 1	ARRA - Required support hardware for Model #2a	Feb-11	Complete
9	Phase 1	ARRA - Model #2a documentation (drawings, stress report, quality report)	Feb-11	Complete
10	Phase 1	ARRA - Model #2a support hardware documentation	Feb-11	Complete
11	Phase 1	ARRA - NASA Pressure rail evaluation PowerPoint file	Jun-10	Complete
12	Phase 1	Phase 1 validation report	Jun-11	Complete
13	Phase 1	Sonic boom wind tunnel test plan - Test #1 (1 performance & 1 boom)	Apr-11	Complete
14	Phase 1	Sonic boom wind tunnel test report - Test #1 (1 performance & 1 boom)	Jun-11	Complete
15	Phase 1	Deleted per Mod. 11 (included in #13 above)		
16	Phase 1	Deleted per Mod. 11 (included in #14 above)		
17	Phase 1	ARRA – technical report for tasks 3.1 – 3.3	Feb-11	Complete
18	Phase 1	ARRA - monthly progress reports	Jan-11 - Feb-11	Complete
19	Phase 1	ARRA - 2010 FAP Annual Meeting PowerPoint Presentation	Feb-11	Complete
20	Phase 1	ARRA - Technical Interchange Meeting #1 briefing	May-10	Complete
21	Phase 1	ARRA - Technical Interchange Meeting #2 briefing	Jan-11	Complete
22	Phase 1	ARRA - Gate Review #1 briefing	Aug-10	Complete
23	Phase 1	ARRA FAR Clause 52.204-11 reporting	Compliance with all clause reporting requirements	Complete
24	Phase 1	Phase 1 final report for tasks 3.1 – 3.7 (NASA CR)	Sep-11	Complete
25	Phase 1	Monthly progress reports	Mar-11 - Sep-11	Complete
26	Phase 1	Gate Review #2 briefing	Jul-11	Complete
27	Phase 1	Phase 1 review briefing	Aug-11	Complete
28	Phase 1	Boeing Sonic Boom Measurement Rail Documentation	Nov-10	Complete
29	Phase 1	Boeing Pressure Rail Performance Documentation	Feb-11	Complete
				Additional Phase I deliverables added after the start of the contract
50	Phase 1	Gate Review #R1 briefing	Oct-10	Complete
51	Phase 1	Sonic boom measurement rail	Nov-10	Complete
52	Phase 1	Interim Annual Report	Dec-10	10 days prior to contract award anniversary, Complete
53	Phase 1	Alternate sonic boom pressure rail PDR briefing	Jan-11	Complete
54	Phase 1	Alternate sonic boom pressure rail	Mar-11	Delivered to NASA Ames 9' x 7' supersonic wind tunnel March 7, 2011
55	Phase 1	Alternate sonic boom pressure rail documentation	Mar-11	Complete
56	Phase 1	Alternate rail evaluation report	Jun-11	Complete
57	Phase 1	New 28" sting	Mar-11	Delivered to NASA Ames 9' x 7' supersonic wind tunnel March 15, 2011
58	Phase 1	New 28" sting Documentation	Mar-11	Complete
59	Phase 1	New 40" spacer	Mar-11	Delivered to NASA Ames 9' x 7' supersonic wind tunnel March 15, 2011
60	Phase 1	New 40" spacer Documentation	Mar-11	Complete
61		Contract award on Dec 17, 2009		

3.0 LOW-BOOM CONCEPT DEVELOPMENT

Overview

Low-boom concept development encompassed three phases that spanned an overall period of 8 months.

The first phase was associated with the conceptual design definition, which lasted just longer than 3 months. During this period, a seed configuration was devised and screening analysis and optimizations on configuration details such as planform, body length, and tail design were then performed. The intent of the conceptual design definition phase was to perform sufficient analysis to ensure that the down-selected preliminary concept configuration had sufficient degrees of freedom and the basic characteristics necessary to meet project requirements once detailed design commenced. For configuration-tracking purposes, the preliminary concept was called the Quiet Experimental Validation Concept 2 (QEVC2). Following preliminary concept definition, a preliminary engine sizing effort was conducted to ensure that any configuration changes made since the original 765-076 were compatible with the propulsion concept.

The second phase, low-boom concept development, was the primary design phase. Throughout this period and starting with the QEVC2 as a baseline, detailed low-boom optimization studies were performed and progress toward meeting N+2 project requirements was monitored. Four figures of merit were tracked: (1) the near-field under-track signature shape at three body lengths away, (2) the ground signature shape, (3) the total ground signature PLdB and the PLdB of just the front and rear signatures and (4) the cruise point inviscid pressure drag at $M = 1.8$ and $CL = 0.10$. The product of the primary design phase was a configuration that could meet the N+2 project requirements and would be suitable for integration with the proposed wind tunnel validation model support hardware.

The last phase of the low-boom concept development was the final design phase. In this phase, the configuration was to be assessed in greater detail for on- and off- design characteristics. It had to be checked for model support hardware tare and interference effects. It also had to pass the Gate 1 review to receive authorization for fabrication. Lastly, it had to incorporate the typical modifications required for wind-tunnel-scale geometry without unduly compromising the design and jeopardizing overall program objectives. This period lasted 2 months, with the final configuration concept termed the QEVC3.

3.1 Preliminary Concept Definition

The first stage in the development of the N+2 experimental validation models was to “freeze” the conceptual design. The contract specified that the -076E configuration was the starting point but also that the goal ground signature would be less than 85 PLdB. Figure 3.1-1 shows the -076E concept (refs. 2 and 3). It was estimated that after detailed design and optimization was complete, the vehicle sonic boom would be >91 PLdB. Consequently, three other concepts were considered: (1) 765-076F, shown in Figure 3.1-2; (2) 765-076G, shown in Figure 3.1-3; and (3) 765-100A, shown in Figure 3.1-4. Two of these concepts underwent an initial cycle of TRANAIR optimization to down-select the best candidate moving forward.

Mach = 1.8, Weight = 162 klbs, Altitude = 49,000 ft

Model	765-076E	
Item	Wing	V-tail
Reference Area (ft ²)	2516.5	377.5
Aspect Ratio	2.94	3.15
Taper Ratio	0.17	0.20
Span (ft)	86.1	34.5
LE Sweep Angle (deg)	72 / 52	48
Root Chord (in)	598.7	219.4
Tip Chord (in)	102.9	43.4
M.A.C. IN	409.2	151.0
X ¼ mac (in)	1243.9	1641.1
Ymac (in)	197.4	262.9
Total Vehicle Length (ft)	154	-
T/C	0.024	0.030
Tail Volume Coefficient	-	0.146
Tail Arm (in)	-	397.2

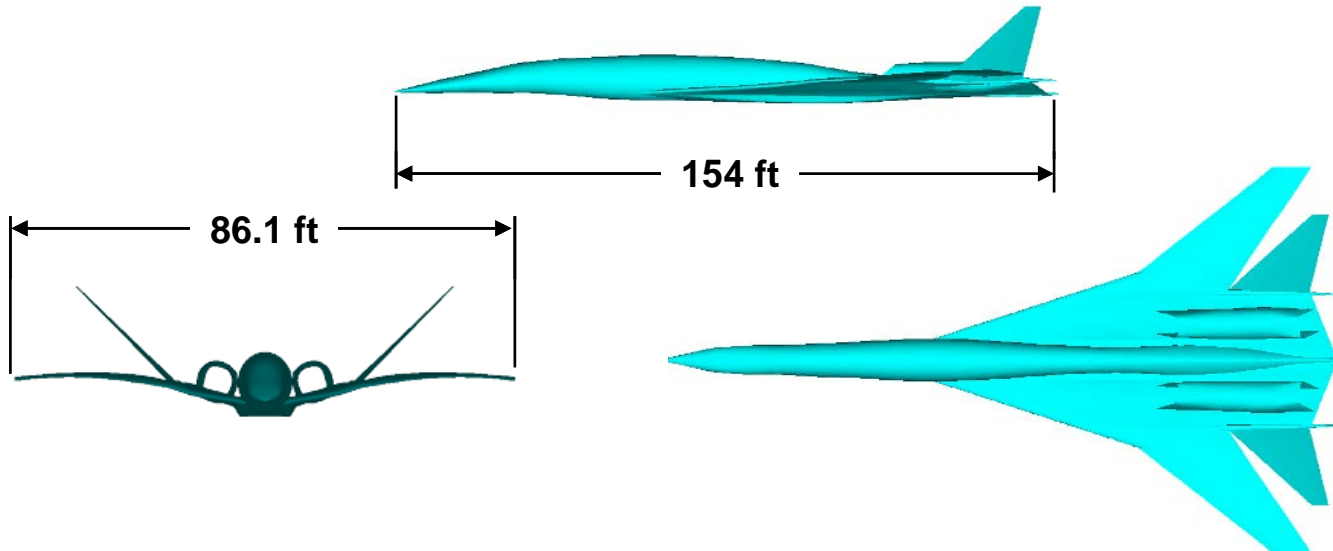
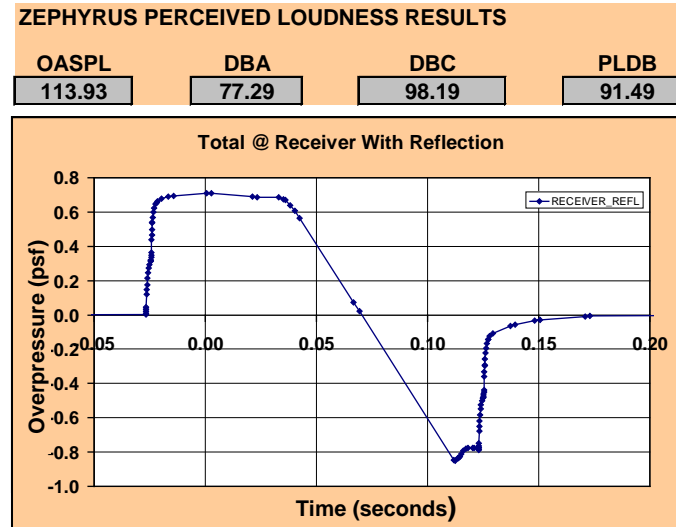


Figure 3.1-1. 765-076E General Arrangement

Mach = 1.8, Weight = 162 klbs, Altitude = 49,000 ft

Model	765-076F	
Item	Wing	V-tail
Reference Area (ft ²)	2516.5	377.5
Aspect Ratio	2.94	3.15
Taper Ratio	0.17	0.20
Span (ft)	86.1	34.5
LE Sweep Angle (deg)	72 / 52	48
Root Chord (in)	598.7	219.4
Tip Chord (in)	102.9	43.4
M.A.C. IN	409.2	151.0
X ¼ mac (in)	1483.9	1881.1
Ymac (in)	197.4	262.9
Total Vehicle Length (ft)	174	-
T/C	0.024	0.030
Tail Volume Coefficient	-	0.146
Tail Arm (in)	-	397.2

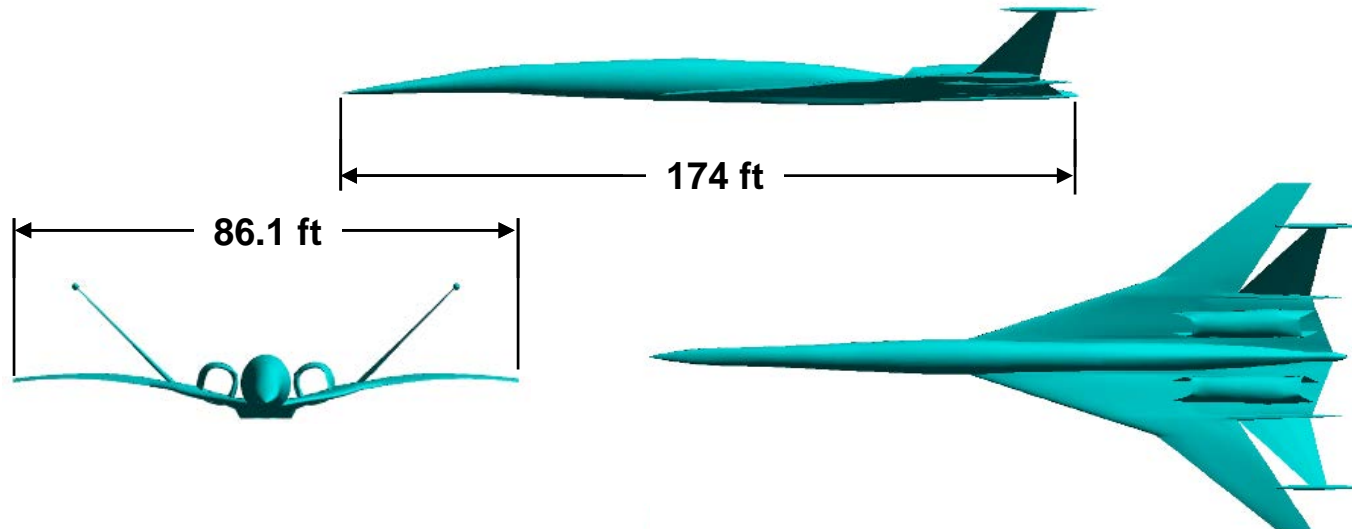
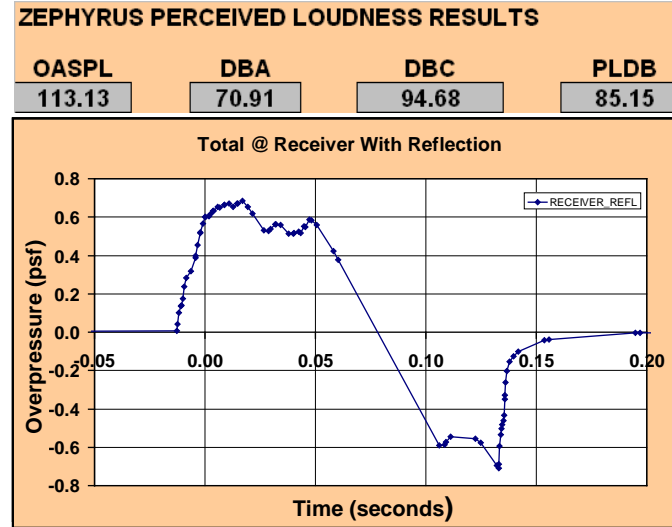


Figure 3.1-2. 765-076F General Arrangement

Mach = 1.8, Weight = 162 klbs, Altitude = 49,000 ft

Model	765-076G	
Item	Wing	V-tail
Reference Area (ft ²)	2516.5	377.5
Aspect Ratio	2.94	3.15
Taper Ratio	0.17	0.20
Span (ft)	86.1	34.5
LE Sweep Angle (deg)	72 / 52	48
Root Chord (in)	598.7	219.4
Tip Chord (in)	102.9	43.4
M.A.C. IN	409.2	151.0
X ¼ mac (in)	1783.9	2181.1
Ymac (in)	197.4	262.9
Total Vehicle Length (ft)	196	-
T/C	0.024	0.030
Tail Volume Coefficient	-	0.146
Tail Arm (in)	-	397.2

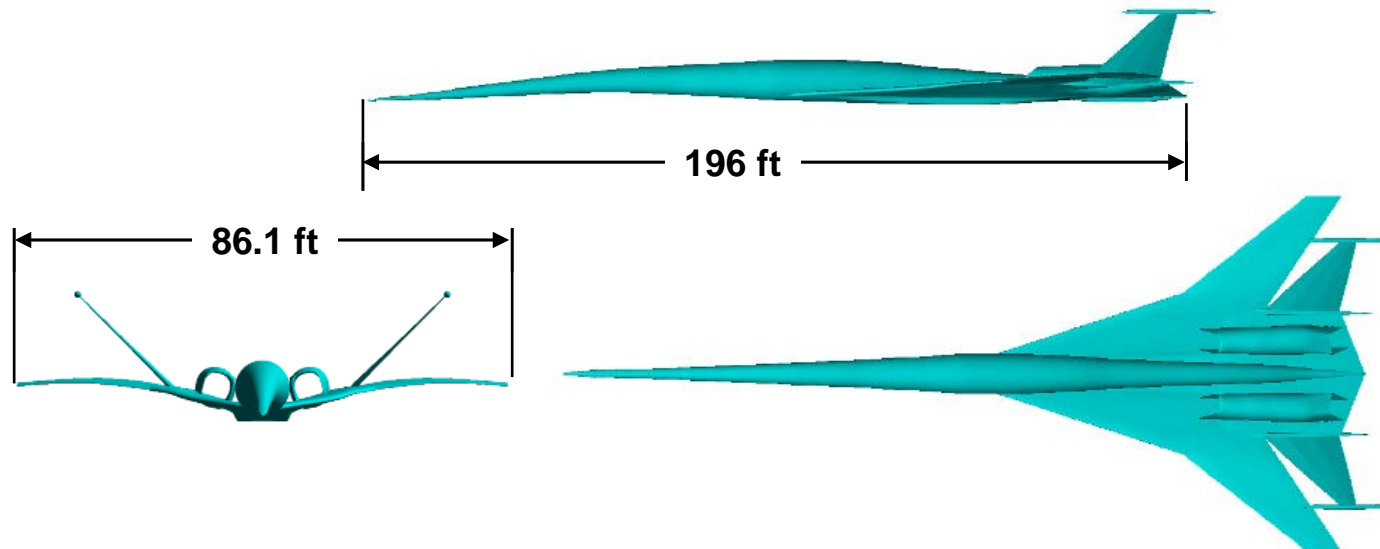
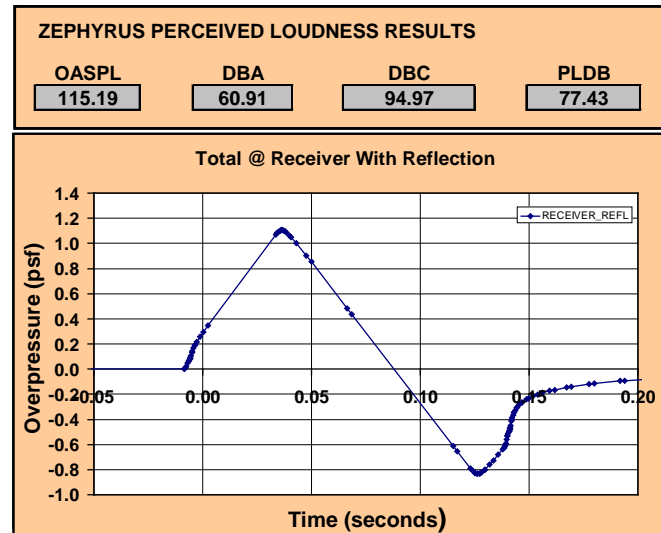


Figure 3.1-3. 765-076G General Arrangement

Mach = 1.8, Weight = 162 klbs, Altitude = 49,000 ft

Model	765-100A	
Item	Wing	V-tail
Reference Area (ft ²)	2586.3	387.9
Aspect Ratio	2.87	3.15
Taper Ratio	0.17	0.20
Span (ft)	86.1	34.5
LE Sweep Angle (deg)	71 / 52	48
Root Chord (in)	647.2	222.4
Tip Chord (in)	73.8	44.0
M.A.C. IN	436.5	153.1
X ¼ mac (in)	1667.8	2113.8
Ymac (in)	189.8	263.5
Total Vehicle Length (ft)	202	-
T/C	0.024	0.030
Tail Volume Coefficient	-	0.153
Tail Arm (in)	-	446.0

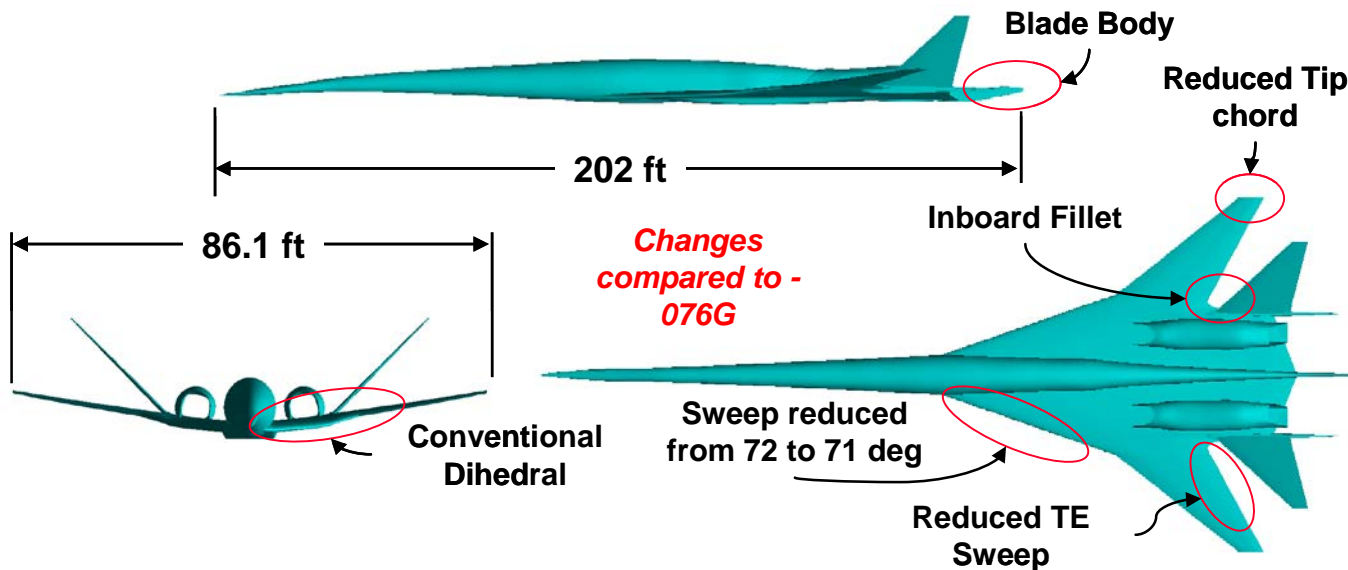
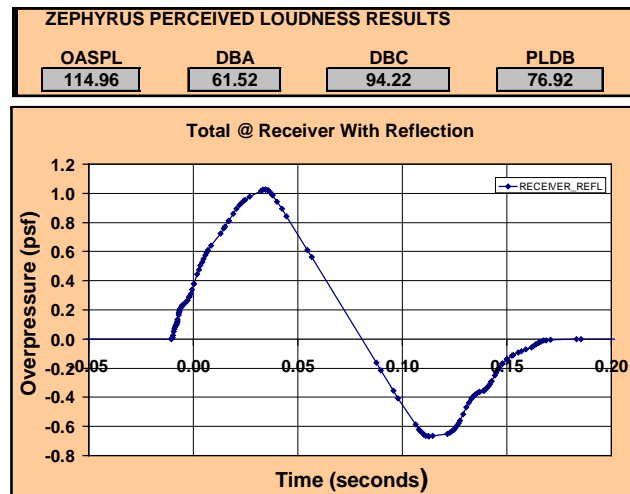


Figure 3.1-4. 765-100A General Arrangement

In all, during a 1-month period, 12 TRANAIR designs were completed to define the initial concept. The TRANAIR designs included W/B/N/V optimizations for L/D, and W/B and W/B/N/V for sonic boom run on the 765-076F configuration. The W/B optimizations for sonic boom were run on the -100A configuration at M = 1.6 and 1.8. With the configuration variables used in the initial TRANAIR designs, there was a distinct tradeoff between lowering drag and lowering boom. At the completion of the TRANAIR designs, it was decided that the starting configuration should have the -076F planform and the -100A body. This composite concept was designated the 765-076I. The initial target for ground signature was set at 76.92 PLdB (Figure 3.1-5).

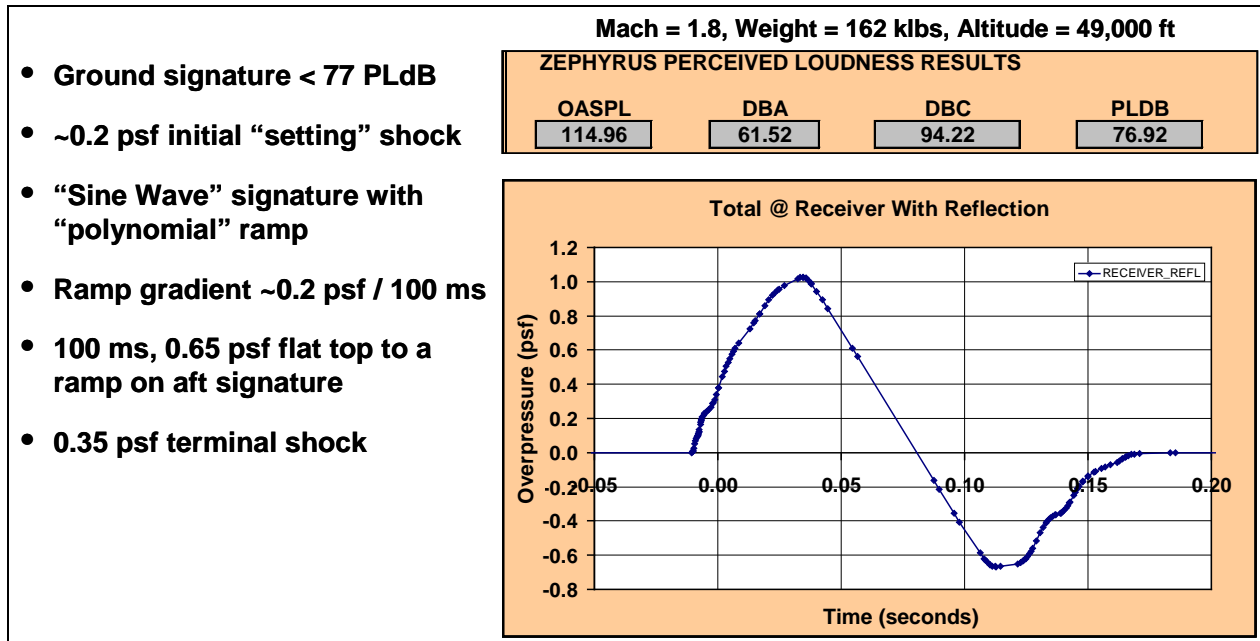


Figure 3.1-5. Initial Design Target

Lofts of the 765-076I vehicle concept were created and a computational mesh was developed for analysis and optimization in OVERFLOW. Before detailed optimization, the -076I drag was approximately 30 counts higher than the N+2 goal, and the boom signature was 13 PLdB higher (99 PLdB versus the goal of <85 PLdB).

Next, a series of independent studies were conducted to refine individual configuration features. The initial QEVC2 was the culmination of these studies. Figure 3.1-6 shows the list of detailed design features refined in the design period between definition of the 765-076I and the QEVC2. Figure 3.1-7 shows the comparison of the two concepts and their relative performance. Figure 3.1-8 shows the QEVC2 general arrangement. Figure 3.1-9 identifies the QEVC2 drag and boom levels relative to project goals.

Changes Relative to -076I

- 1) New raked V-tail (20% smaller, T/C=3.%)
- 2) Ogive/raked wing tip
- 3) 6 ft tail raked winglet
- 4) Wing/Body blending
- 5) Inboard leading edge droop
- 6) Large strake with smoothing
- 7) New forebody with body rotated down 0.5 deg
- 8) Recessed gear fairing
- 9) Re-optimized camber and twist

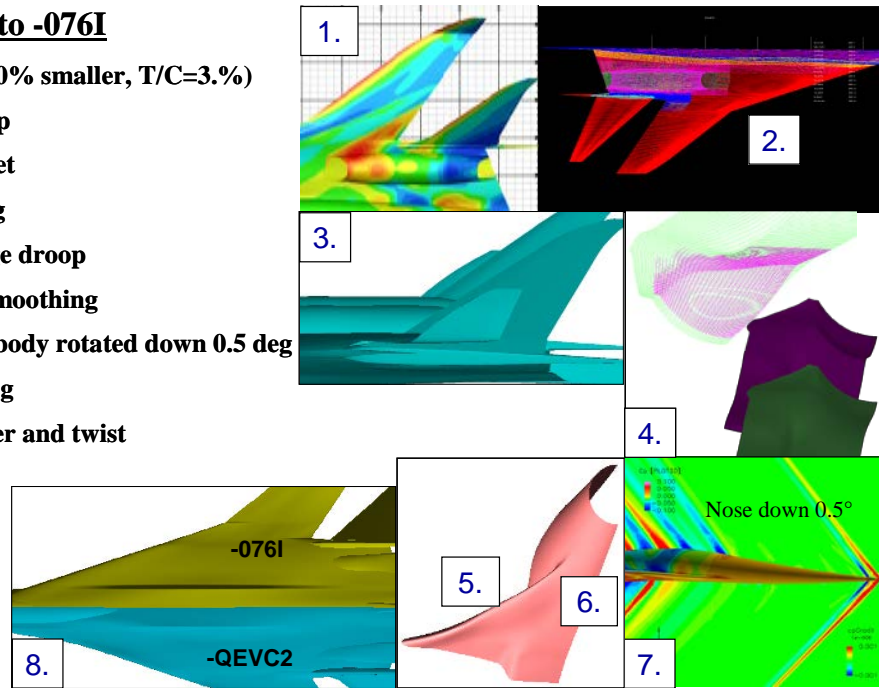
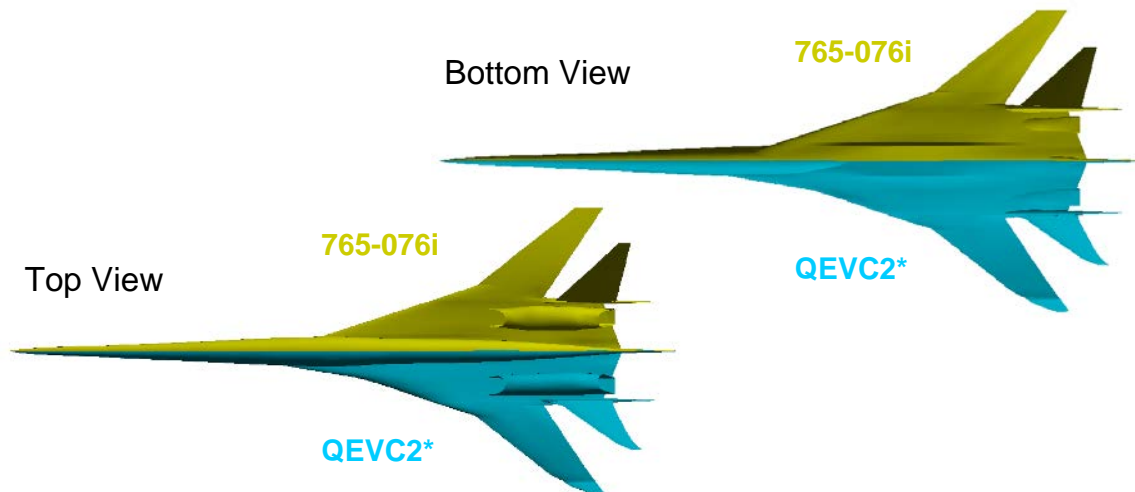


Figure 3.1-6. Changes to -076I to Create QEVC2



	α	C_{Li}	C_{Di}	C_{Mi}	
765-076i	3.053	.10391	.01084	-.02946	$S_{ref} = 181188.0 \text{ in}^2$ $c_{ref} = 409.2 \text{ in}$ $x_{cg} = 1663.9 \text{ in}$ $z_{cg} = 0.0 \text{ in}$
QEVC2*	2.940	.10392	.00904	-.03958	
*smoothed					

Figure 3.1-7. 765-076I Compared to QEVC2 Concept

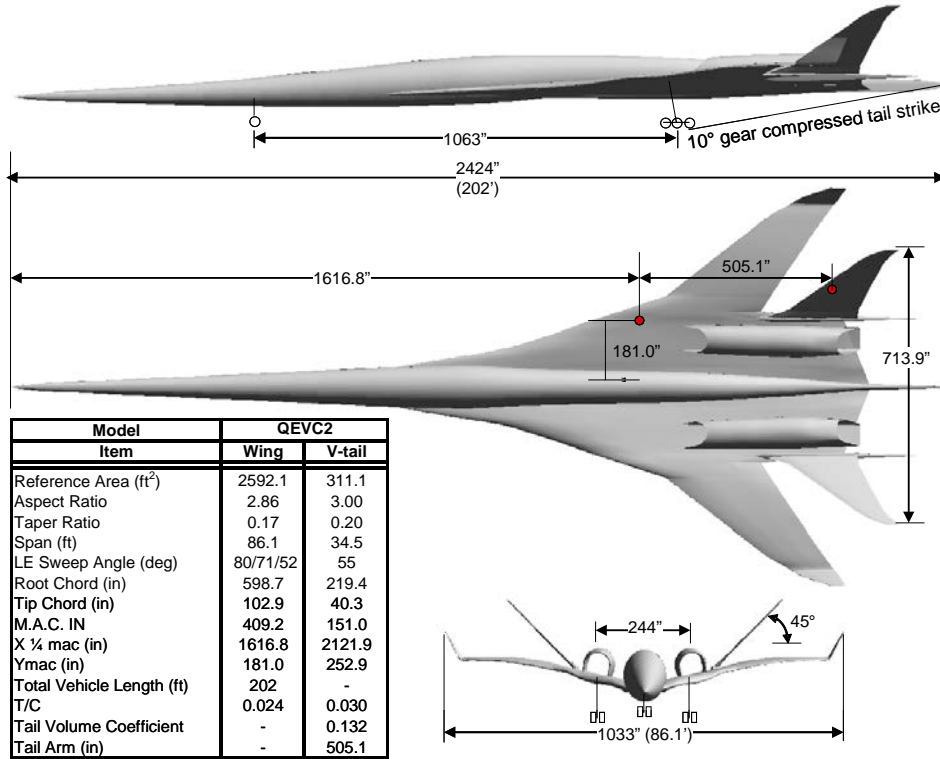


Figure 3.1-8. QEVC2 General Arrangement

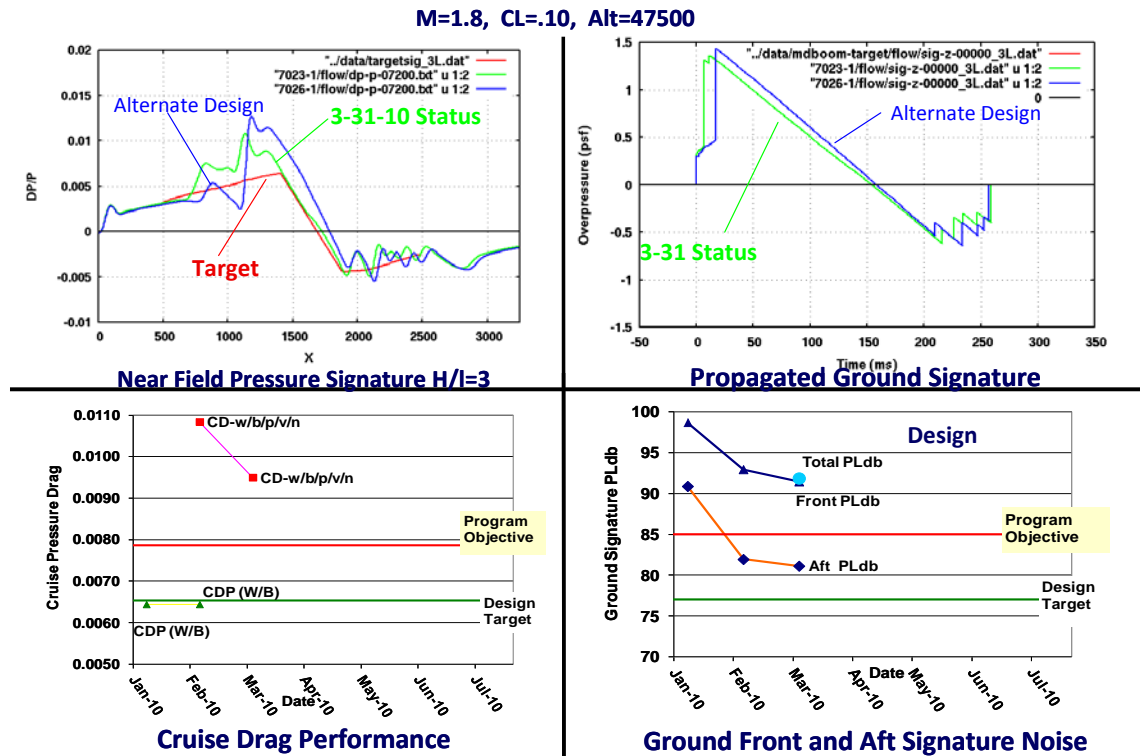


Figure 3.1-9. QEVC2 Drag and Boom Levels Relative to Project Targets

3.2 Preliminary Engine Sizing

A top-level assessment of the propulsion system installation was conducted to ensure that the nacelle used during the validation phase was representatively sized. The baseline engine configuration and installation concept were established through trade studies conducted under the N+2 Supersonic Concept Development and Systems Integration project, NASA NRA 4.71, completed in July 2009. Of particular interest were the inlet and diffuser designs, which will be central to the Phase II portion of this validation project.

The aircraft of interest for this study will have a design cruise Mach number between 1.6 and 1.8. For this initial sizing exercise, a Mach 1.6 cruise level was assumed. A design for Mach 1.8 cruise will be developed during Phase II.

The engine model used for this analysis was configured from the dual-spool, mixed-flow turbofan model developed by the Georgia Institute of Technology. The general flow path of this engine is depicted in a Rolls-Royce cross-section concept shown in Figure 3.2-1. Georgia Tech's Numerical Propulsion System Simulation (NPSS) engine model was cycled to be sized consistently for the QEVC 2 vehicle with a 41,000-lb sea-level static thrust level. The result is an engine with a 69-in fan diameter and a length of 149 in. With a bypass ratio of 3.72 in cruise, this engine represents a compromise to provide relatively low jet velocities at takeoff (<1,200 ft/s) and low specific fuel consumption (SFC) in cruise, while limiting the growth of fan diameter to retain reasonably low cruise drag and installed weight levels.

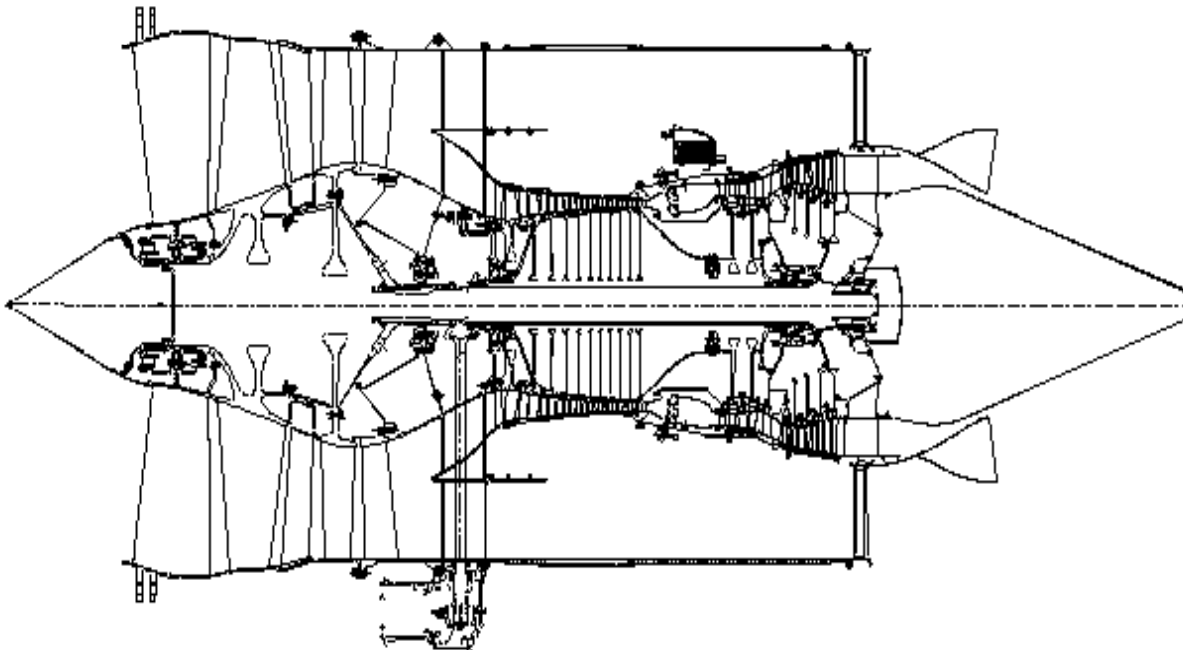


Figure 3.2-1. Concept Flow Path for Mixed-Flow Turbofan Provided by Rolls-Royce (Unscaled)

Figure 3.2-2 shows the concept installation. The target installation features a fixed-aperture, bleed-less and diverter-less inlet design to minimize weight, complexity, and cost. Given the selection of a Mach 1.6 cruise speed; there is a reasonable prospect of achieving target performance and distortion levels. At a Mach 1.8 cruise level, it is more likely that ramp bleed or a diverter will be required to maintain tolerable engine fan face distortion levels throughout the flight envelope.

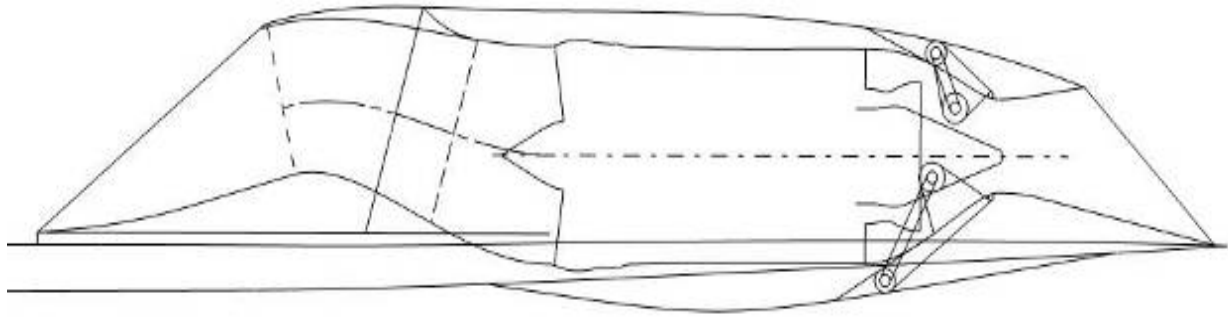


Figure 3.2-2. Cross-Section of Concept Propulsion System Installation

The inlet concept is shown in more detail in Figure 3.2-3. To maximize inlet total pressure recovery in cruise, the inlet must incorporate several features. First, most of the compression must be completed isentropically to minimize shock losses. In addition, the diffuser must be short to minimize diffuser skin friction losses. Furthermore, in an effort to minimize drag, the inlet will be run to near-critical to minimize spillage drag and nacelle scrubbing losses.

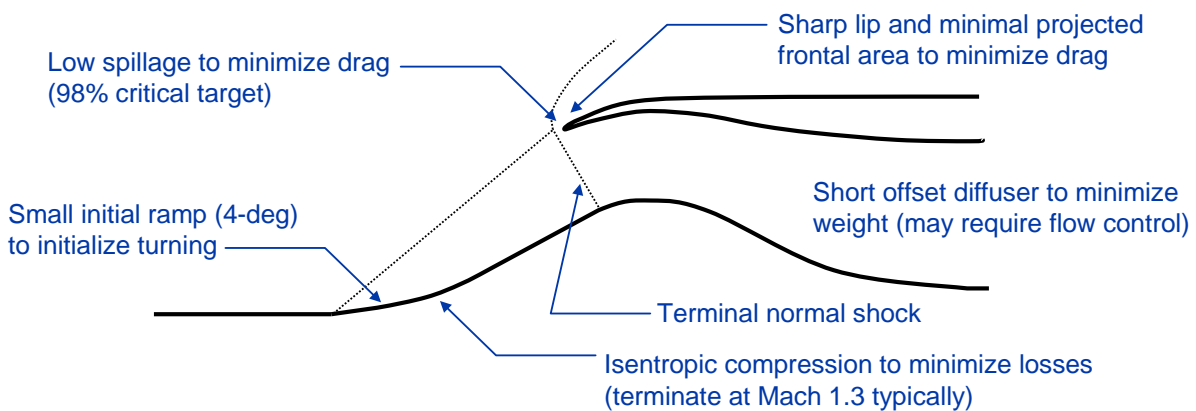
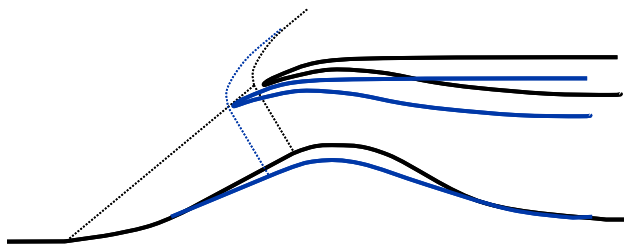


Figure 3.2-3. Notional Inlet Concept

Note that an isentropic compression system requires additional frontal area and running length relative to an inlet using shocks to compress the flow. As illustrated in Figure 3.2-4, if less turning is accomplished, the inlet can be made more compact. The shock losses incurred through the compression of the compact inlet, however, will lead to a significant increase in SFC. At a Mach 1.6 cruise speed, the volume required to implement isentropic compression is relatively modest and remains competitive in trade studies with shock compression inlet systems.



- Black: baseline concept with terminal normal shock at Mach 1.3
- Blue: more compact inlet with terminal normal shock at Mach 1.4
 - reduced frontal area
 - shorter diffuser with less reflex

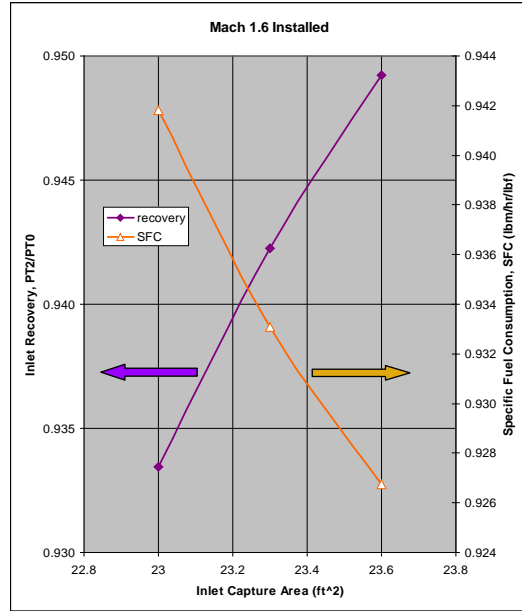


Figure 3.2-4. Impact of Inlet Turning on Propulsion System Installation and Performance

As cruise Mach increases, the frontal area required for the isentropic ramp alone will produce a considerable increase in capture area, which will lead directly to significant increases in structural weight and drag. When these penalties are included in the propulsion system performance assessment, the increase is dramatic (fig. 3.2-5). Thus, as expected, the amount of external isentropic compression that is practical diminishes as cruise Mach number increases.

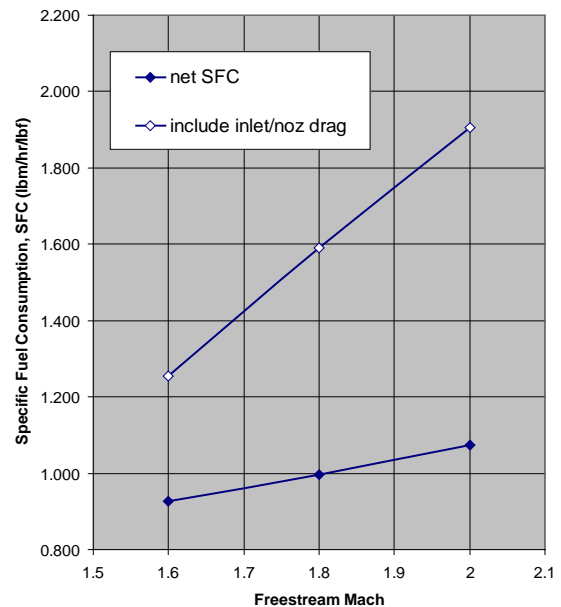
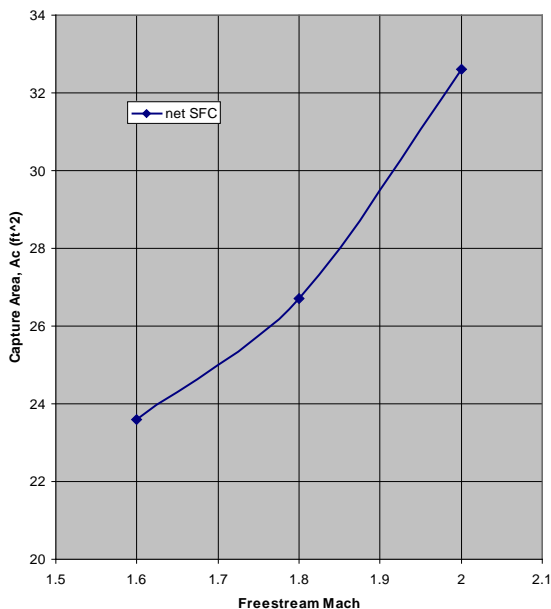


Figure 3.2-5. Effect of Freestream Mach on Propulsion System Installation and Performance

The propulsion system under consideration here is over-the-wing mounted. This arrangement adds an additional design challenge for the propulsion system. When mounted under the wing, the propulsion

system can leverage wing pressurization to help compress the flow. The opposite is true when mounted over the wing, as the flow field has been accelerated to generate a suction force. This means that the propulsion system must be designed for a higher effective Mach number. The amount of flow acceleration is a direct function of the angle of attack (AOA). The effect has been reported previously (fig. 3.2-6) and is corroborated by Boeing CFD analysis of this configuration. Given a nominal cruise Mach of 1.6 and an AOA of 2 deg, the inlet will see an oncoming Mach of 1.67 and must be designed accordingly.

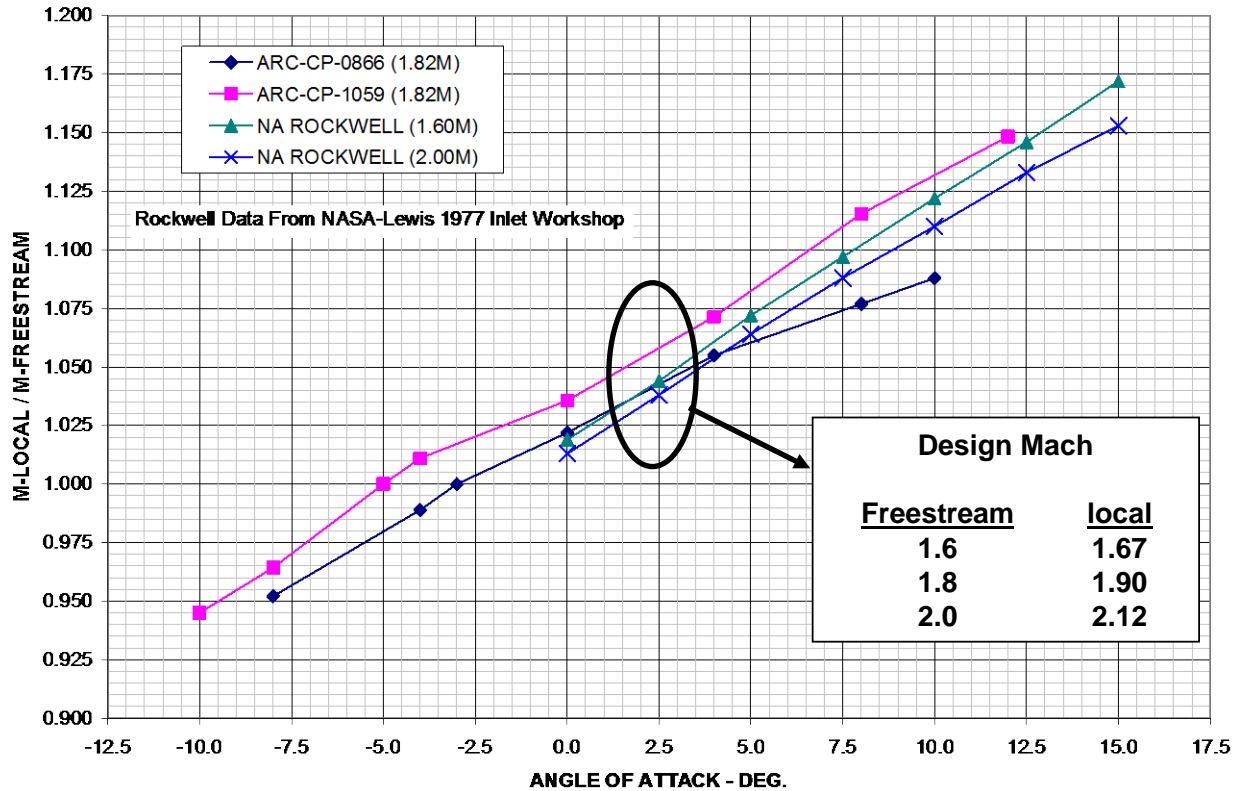


Figure 3.2-6. Over-wing Inlet Design Mach

Given this background, an initial layout of a 2D external compression inlet was incorporated on QEVC2e. As shown in Figures 3.2-7 and 3.2-8, the installation is similar in size and scale to the placeholder nacelle. A cutaway of the propulsion system installation (fig. 3.2-9) reveals that this inlet and nozzle each were drawn very short, which represents a risk that target inlet performance and operability levels may not be achievable because of diffuser flow separation, or that sufficient volume is provided for mechanical integration of the nozzle and thrust reverser. Even with these caveats, this approach represents a reasonable starting point in the effort to maximize airplane performance.

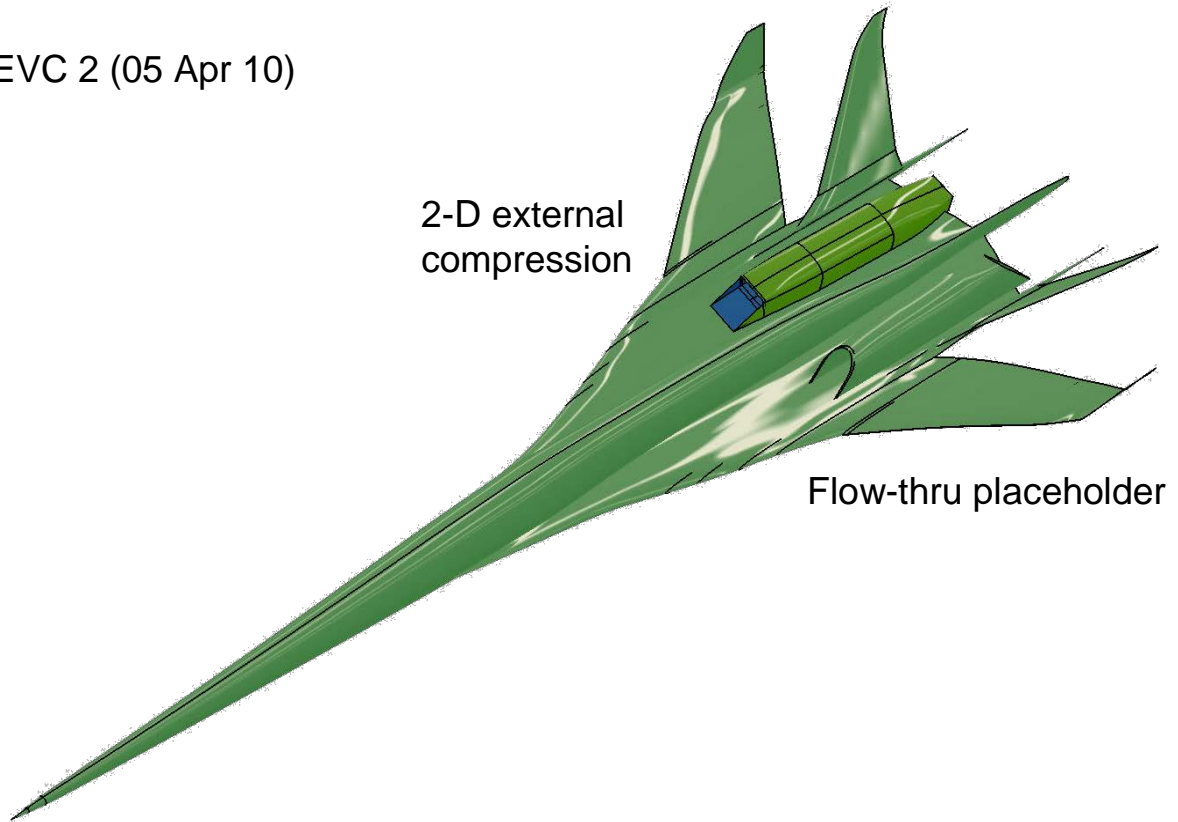


Figure 3.2-7. Notional Concept Propulsion System Compared With Flow-Through Placeholder Nacelle

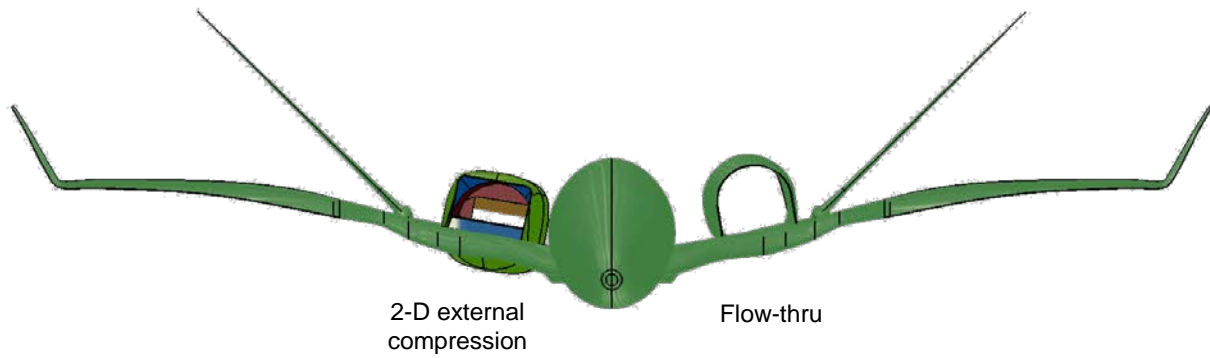


Figure 3.2-8. Front View of Propulsion System Installation

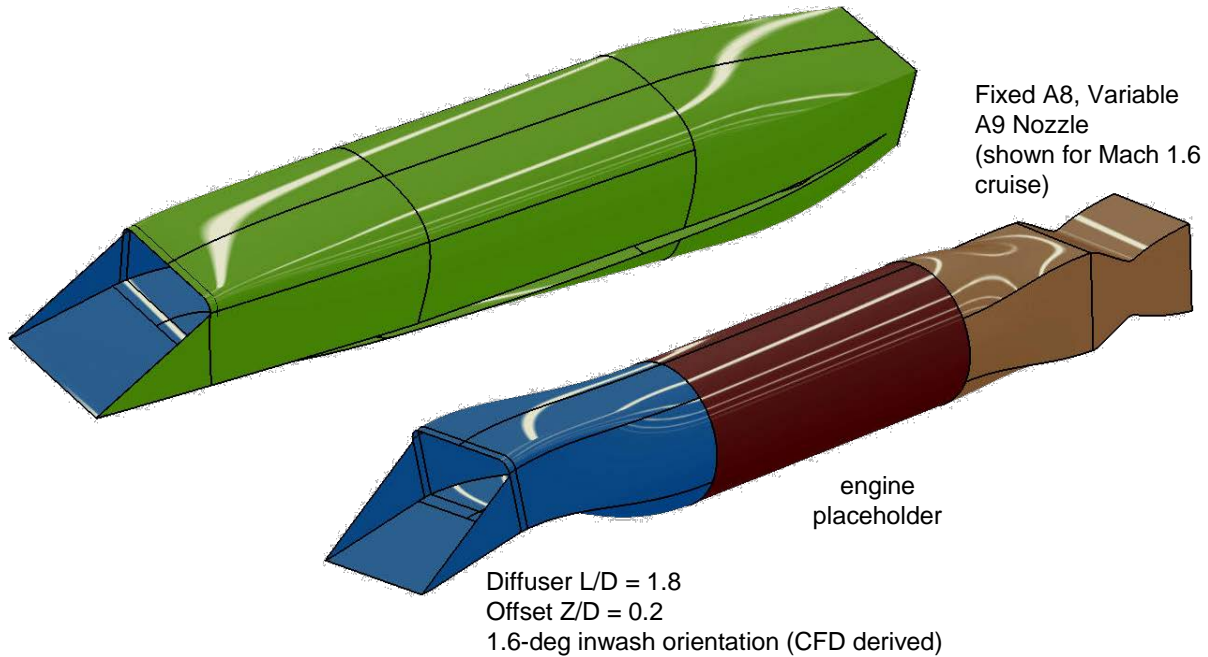


Figure 3.2-9. Notional Nacelle with 2D Inlet and Nozzle Design Concepts

3.3 Preliminary Design Definition

Following the definition of the QEVC2 concept, several months were devoted to detailed configuration optimizations to develop a preliminary design that would meet project objectives for both boom and L/D. The initial optimizations were set up to attain the best possible under-track signature without concern for drag, pitching moment or off-track signature. The starting geometry was the QEVC seed geometry, and the optimization was run at $M = 1.8$, with lift constrained to 0.1039. The pitching moment observed with the original geometry was -0.04. The initial objective was to match a target under-track pressure distribution at three body lengths below the aircraft. The target under-track pressure distribution was one that provided a shaped ~ 77 PLdB ground signature (Figure 3.1-5). Table 3.3-1 shows the optimization parameters.

Table 3.3-1. Optimization Parameters

	Optimization for Preliminary Design
Starting geometry	QEVC seed
Mach	1.8
Lift coefficient	0.1039
Pitching moment	No constraint

After several optimization and refinement iterations with this objective, a new model was created to predict the difference from the target signature. Several more iterations of the optimization process produced the blue signature shown in Figure 3.3-1. The QEVC seed signature is shown in green, and the target is shown in red. Both the forward and aft signatures are significantly better than the starting signature, but the forward signature produces an N-wave at the ground. The lift, drag and pitching

moment for this optimized configuration are listed in Table 3.3-2, which shows a one-count reduction in drag and a more negative pitching moment.

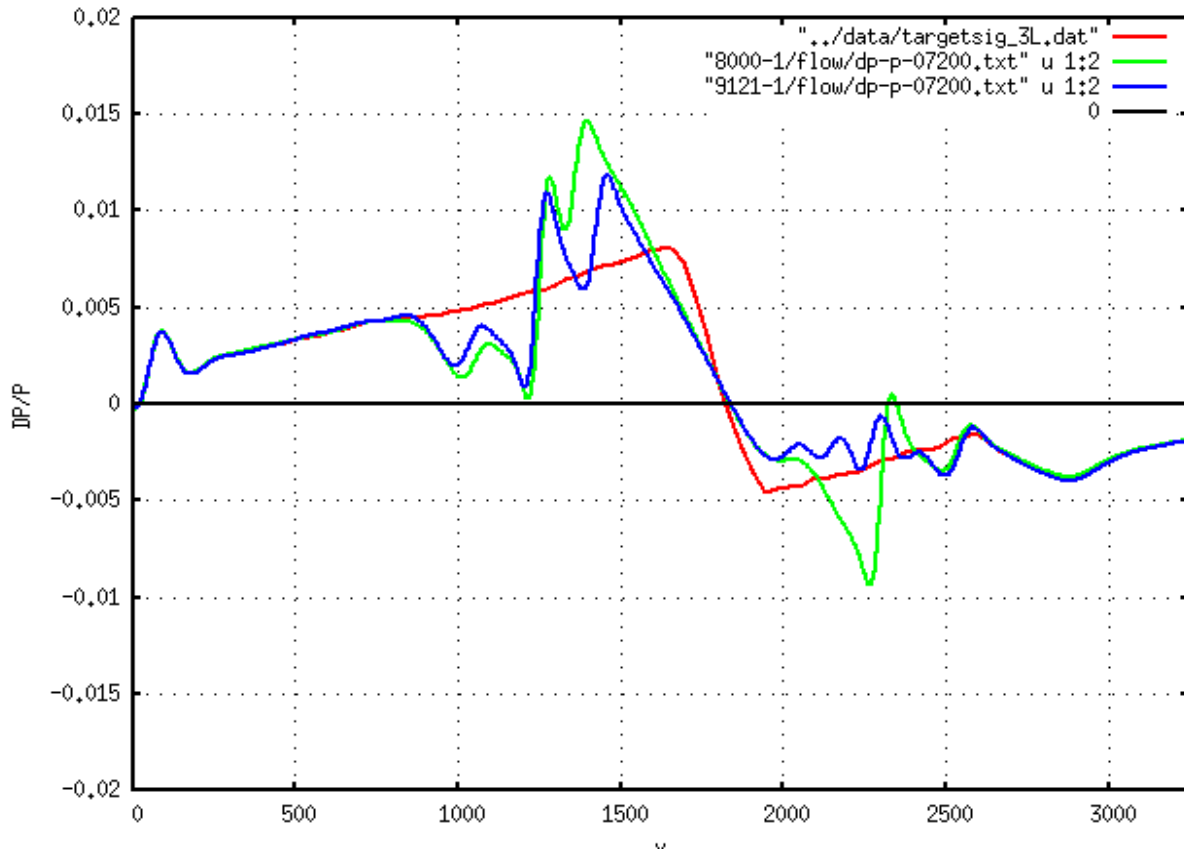


Figure 3.3-1. Initial Optimization Results (M = 1.8, CL = 0.104)

Green is seed signature; blue is optimized signature.

Table 3.3-2. Initial Optimization Force Results at M = 1.8

Subcase	Description	Alpha	CL	CD	CM
8000	QEVc seed	2.957	0.1039	0.00893	-0.0396
9121	Optimization I DOE result	3.008	0.1039	0.00883	-0.0418

The geometry that results from the optimization process typically has some obvious features in the off-body pressure signature that must be fixed, but the limited design space in this case would not allow it. These features are fixed with additional local refinement cycles. The first design that came close to meeting project goals was the QEVc-8038. Figure 3.3-2 shows where the 8038 drag and boom levels were relative to project goals. The 8038 was further refined to become the QEVc-7038. For similar under-track ground PLdB levels, the 7038 improved the off-track signatures and had a 4.8-count drag reduction compared with the 8038. Figure 3.3-3 identifies the 7038 drag and boom levels relative to the program goals.

M=1.8, CL=.10, Alt=47500

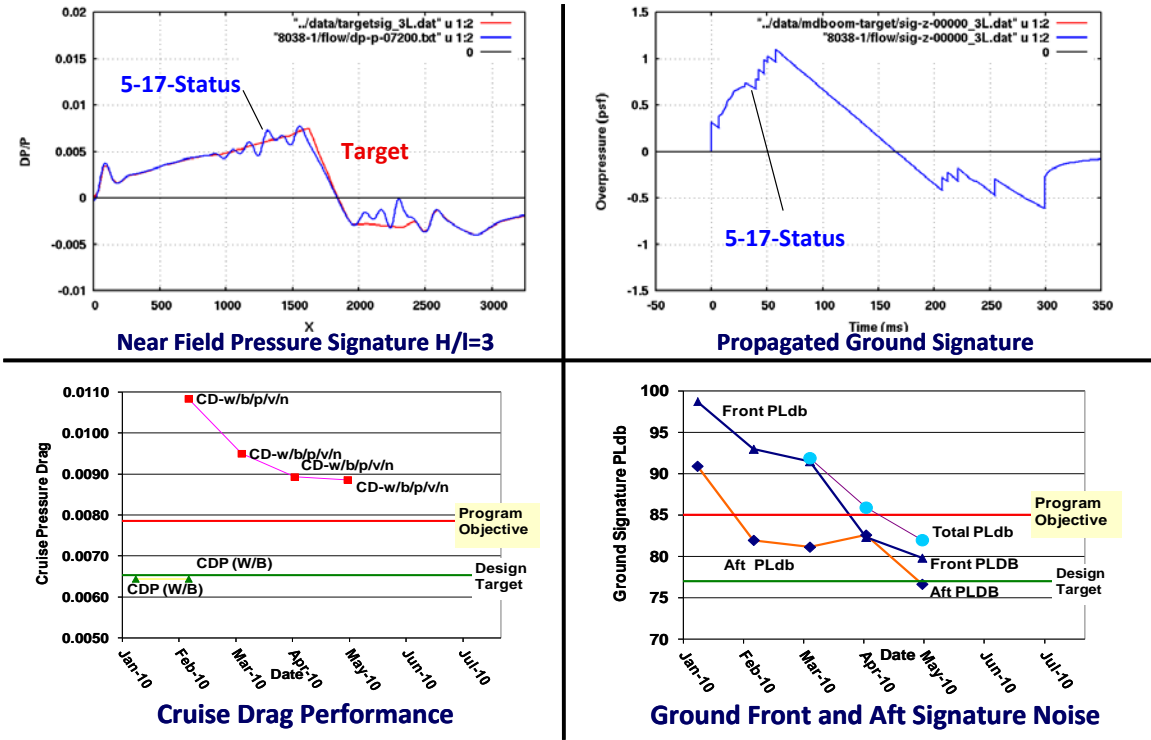


Figure 3.3-2. 8038 Drag and Boom Levels Relative to Project Targets

M=1.8, CL=.10, Alt=47500

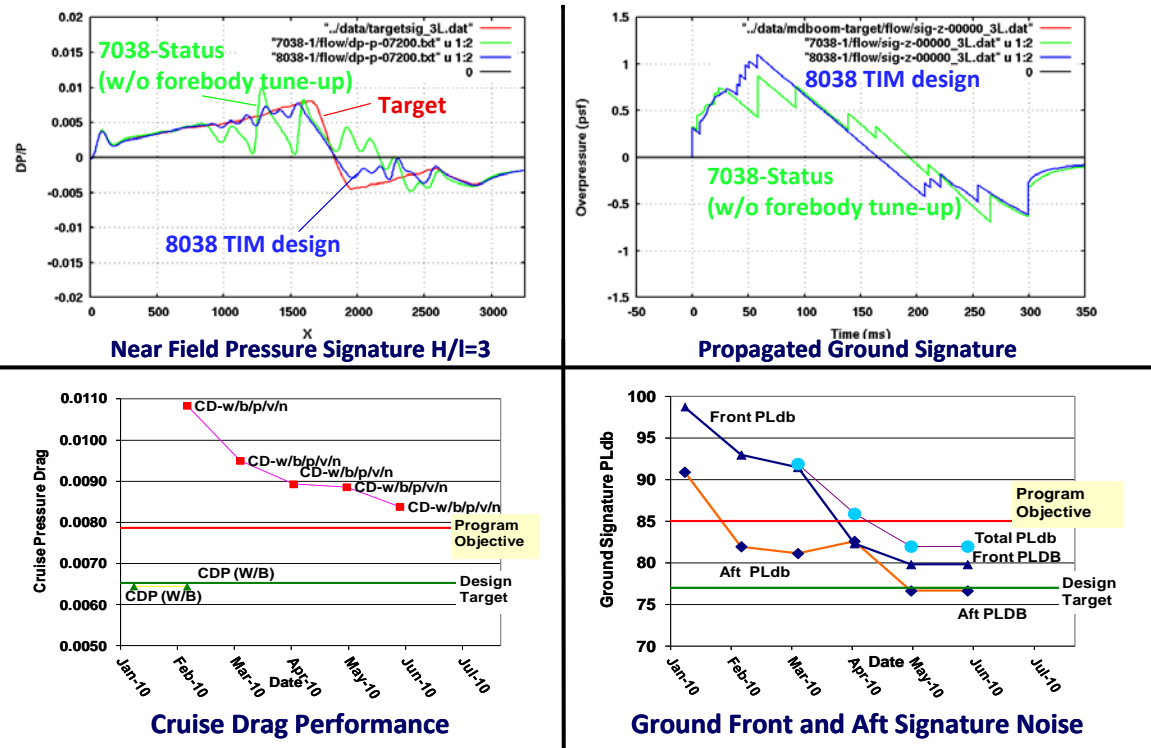


Figure 3.3-3. 7038 Drag and Boom Levels Relative to Project Targets

Table 3.3-3. Final Optimization Force Results at M = 1.8

Subcase	Description	Alpha	CL	CD	CM
8000	QEVG seed	2.957	0.1039	0.008931	-0.0396
6007	Optimization I final result (includes hand fixes)	3.282	0.1039	0.008933	-0.0341

Based on NASA feedback provided at the monthly status review at the end of June 2010, the 7038 design was discarded. Additional optimizations favoring an aft flat-top signature shape were conducted, starting with the 8038 as a seed. The resultant design, the 6007, was agreed upon to be a more suitable geometry for an experimental validation model. Table 3.3-3 shows the lift, drag, and pitching moment comparison between the 6007 and the QEVG seed configuration. Figure 3.3-4 identifies the 6007 drag and boom levels relative to project goals. Figure 3.3-5 shows 6007 final surface and centerline pressure (M = 1.8, CL = 0.1039). The QEVG -6007 was submitted for approval at the Gate 1 Review.

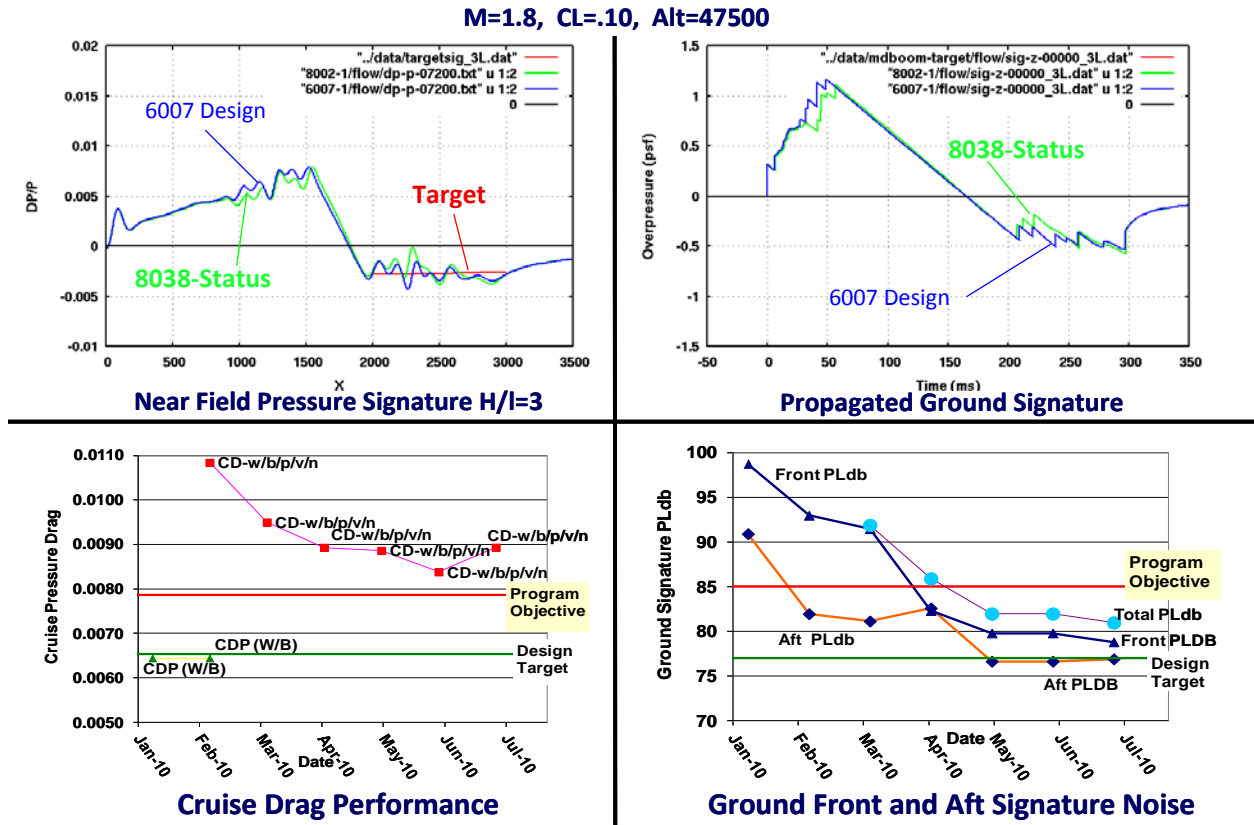


Figure 3.3-4. 6007 Drag and Boom Levels Relative to Project Targets

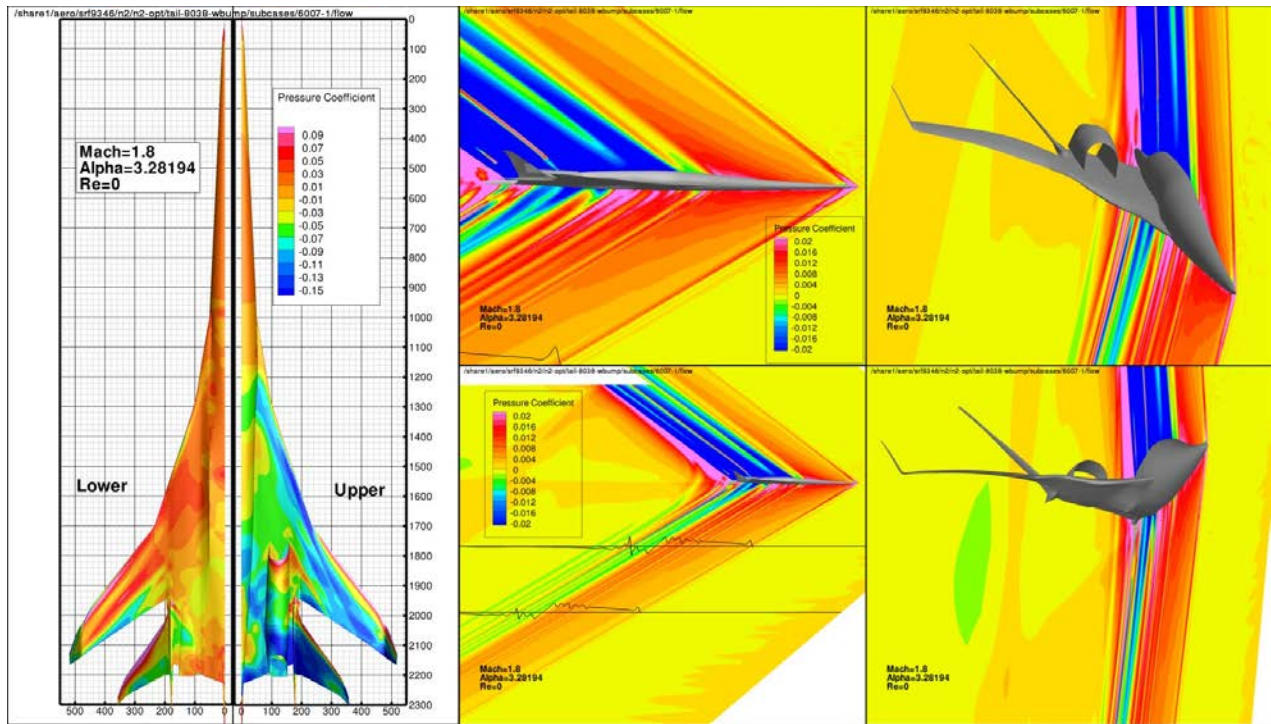


Figure 3.3-5. 6007 Final Surface and Centerline Pressure (M = 1.8, CL = 0.1039)

3.4 Final Design Definition

There were three basic criteria for passing Gate 1 Review: (1) the low-boom concept had to meet the <85 PLdB shaped ground signature and have L/D comparable to the -076E N+2 concept, (2) the off-design boom and drag characteristics needed to be evaluated to ensure that the concept was not so point-designed that an experimental validation would be exceedingly difficult, and (3) the proposed mounting systems for the models would not excessively change the results.

For the Gate 1 Review, ground signatures and near-field pressure distributions at multiple distances away from the aircraft were prepared for several different lift coefficients at Mach numbers of 1.6 and 1.8. Given the schedule constraints and the geometric and boom similarities between the 8038 and the 6007 configuration, the tare and interference effects of the large model flared aft-body (aft sting-mounted model) and the small model upper swept strut were deemed modest and within acceptable bounds. (Section 3.5 provides details on these results.)

The 6007 concept passed the Gate 1 Review and was approved to proceed to fabrication. To meet the manufacturing requirements of small-scale wind tunnel models, the 6007 geometry had to be altered in several ways before the machining of parts could begin. For the performance model, the aft-body had to be flared to have a constant cross-section from the mid-body aft to provide clearance for the internal balance and aft sting support system. The sharp wing leading and trailing edges, nacelle inlet and nozzle, and V-tail leading and trailing edges were increased to a finite thickness of 0.22 inch full-scale. For the boom model, the sharp wing leading and trailing edges, nacelle inlet and nozzle, and V-tail leading and trailing edges were increased to a finite thickness of 0.62 inch full-scale. The nacelles had to be moved inboard 5 inches, and the support pod thickness needed to be increased by 50%. In addition, the V-tail wing tips and winglet needed to be increased from an original $t/c = 3\%$ to 4.5%. Each of these features was checked with analysis in OVERFLOW before approval for fabrication was given. Figure 3.4-1 shows

the general arrangement for the configuration (6007 [i.e., QEVC3]) that passed the Gate 1 Review.

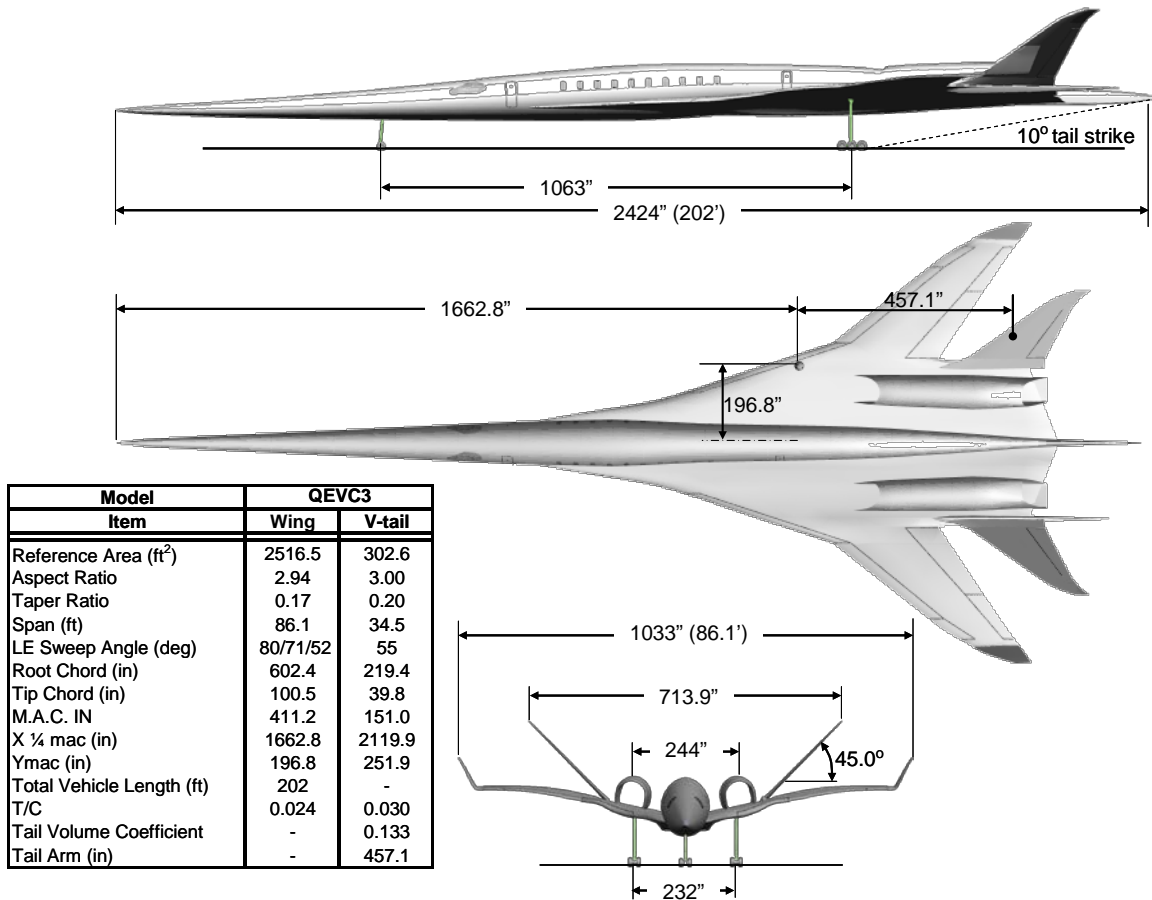


Figure 3.4-1. QEVC3 General Arrangement

3.5 Low-Boom Concept Analysis, Gate 1 Review

Once the low-boom design had achieved the sonic boom and performance goals, the configuration was analyzed in detail in several areas. These areas included sonic boom analysis, cruise aerodynamics, performance analysis and cruise trim CG. Each of these areas was presented during the low-boom Gate 1 Review on 13 August 2010. At the end of the gate review, the concept was deemed suitable to proceed with conducting validation testing.

Sonic Boom Analysis

The intent of this analysis was to demonstrate that the low-boom design met the sonic boom goals for the project; specifically, that the under-track signature was 85 PLdB or lower, the signature had fore and aft shaping, the signature was robust at off-design Mach and CL conditions and that it had robust off-track signature characteristics. The tools used for this analysis included both Euler (Cart3d [ref. 4]) and OVERFLOW ([ref. 5]) and Navier-Stokes (OVERFLOW) solvers to determine the near-field pressure distributions and two different wave propagation codes (MDBOOM/MDPLOT [ref. 6] and Zephyrus [refs. 7 and 8] / Loudboom) to determine the ground signatures. A brief description of the Zephyrus code is provided in Section 11. The results from the Zephyrus code were used to determine if the ground signature perceived loudness was below the 85 PLdB goal. During the design phase, however,

MDBOOM was used for the ground signature assessment because of its speed and efficiency. During design, the two main design goals (85 PLdB and L/D as good as the -076E) were tracked by month. Figure 3.5-1 shows the final metric summary chart. In the figure, the upper left plot tracks the near-field pressure signature, the plot in the upper right-hand corner tracks the propagated ground signature, the plot in the lower left-hand corner tracks the cruise pressure drag and the plot in the lower right-hand corner tracks the ground PLdB. The 6007 design was analyzed for the gate review.

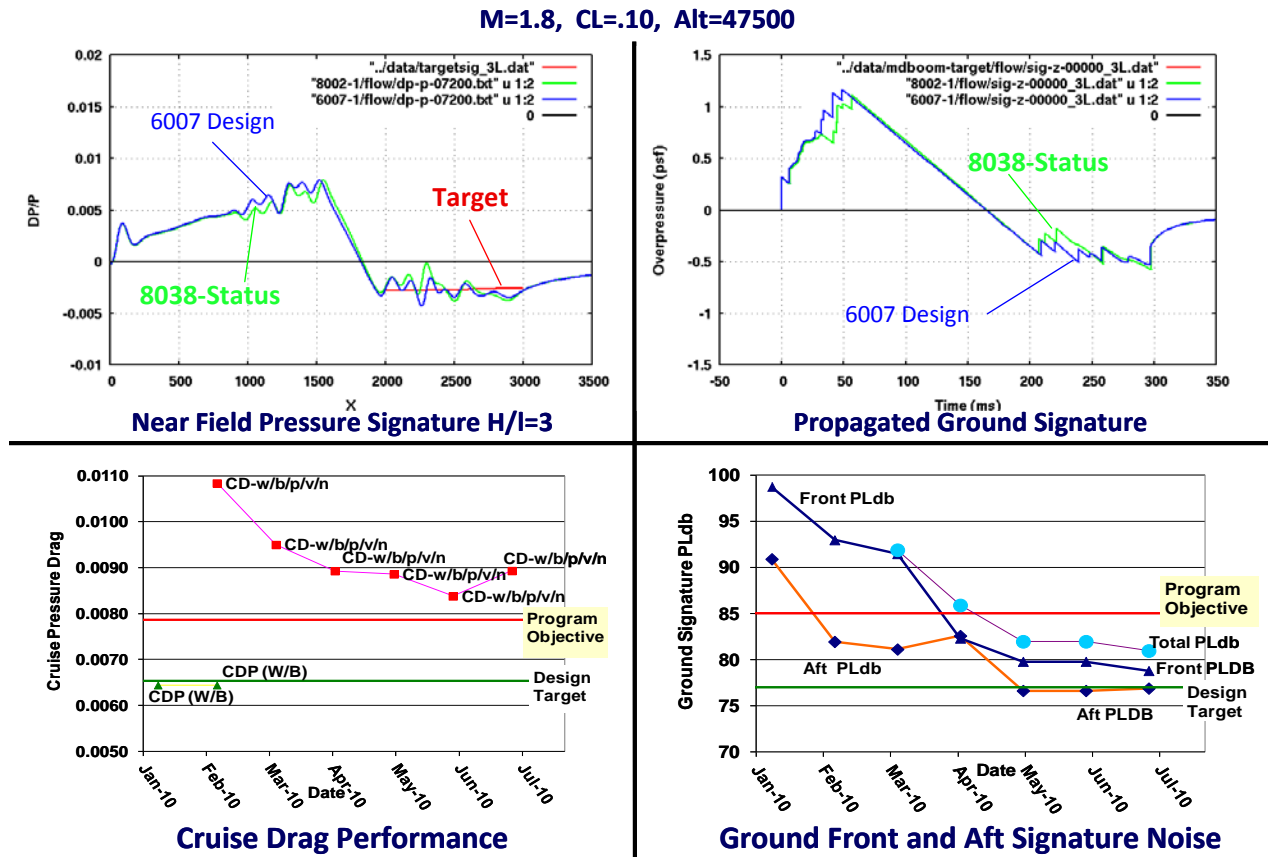


Figure 3.5-1. Sonic Boom and Performance Metric Tracking for the Low-Boom Design

In Figure 3.5-2, the detailed sonic boom analysis using OVERFLOW and Zephyrus is shown for two Mach numbers, the design Mach = 1.8 and the off-design Mach = 1.6. In the upper portion of the curve, the near-field pressure distribution is shown for several H/L locations. Essentially, stable near-field distributions are achieved for H/L locations of 2.0 or more. When an H/L is not shown in a sonic boom figure, it is assumed that H/L = 3. In the lower half of Figure 3.5-2, the ground signature is shown for both Mach = 1.8 and Mach = 1.6 and for the same H/L variations. For H/L values of 2.0 or more, shaped fore and aft ground signatures are achieved for the low-boom concept at both Mach numbers. In addition, all ground signatures are below the 85 PLdB goal, with the lowest one at ~81 PLdB.

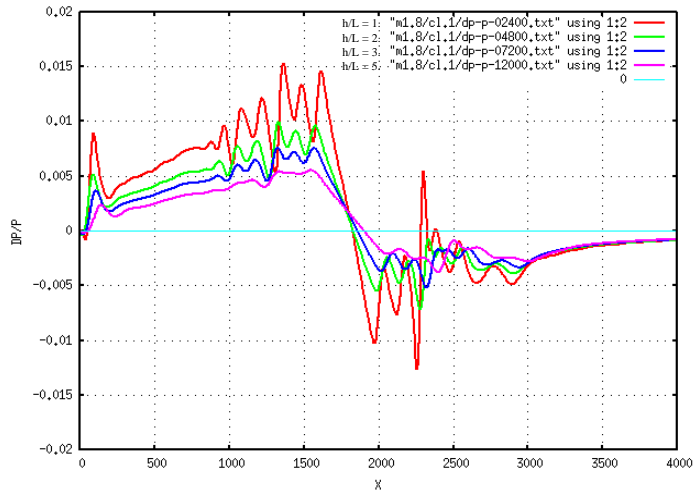
The low-boom concept also was examined at off-design CLs at each Mach number to determine whether signature-shaping persists to the ground and the perceived loudness is still below the 85 PLdB goal. Figure 3.5-3 shows this for Mach = 1.6 and 1.8, at H/L = 3 for three different CL values. Again, both the near-field and ground signatures are shown in the figure. From Figure 3.5-3, many off-design CLs continue to show fore and aft shaping. For a CL = 0.08 at Mach = 1.8, however, the aft signature is starting to approach an N-wave, and ground-perceived loudness is above the 85 PLdB goal. All Mach =

1.6 cases show shaped signatures for all CLs considered, and ground-perceived loudness essentially meets the 85 PLdB goal.

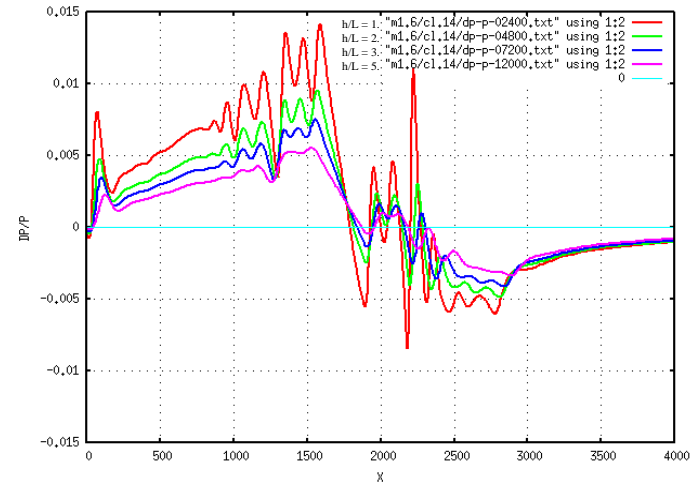
Finally, Figure 3.5-4 shows the variation of the sonic boom signature with off-track location for Mach 1.6 and 1.8 at $H/L = 3$. The near-field and ground signatures are portrayed in the same way as the previous figures. The low-boom concept retains signature-shaping and ground-perceived loudness, to some extent, when moving away from under-track. At Mach = 1.8, the shaping persists to approximately 15 deg off-track. The ground-perceived loudness also is maintained below 85 PLdB up to 10 deg off-track. At Mach = 1.6, the shaping and ground-perceived loudness remain at the goal or lower for up to 30 deg off-track. This was a favorably robust result, given that the concept was designed at the Mach = 1.8 condition.

Nearfield Signature

Mach = 1.8, CL=0.1



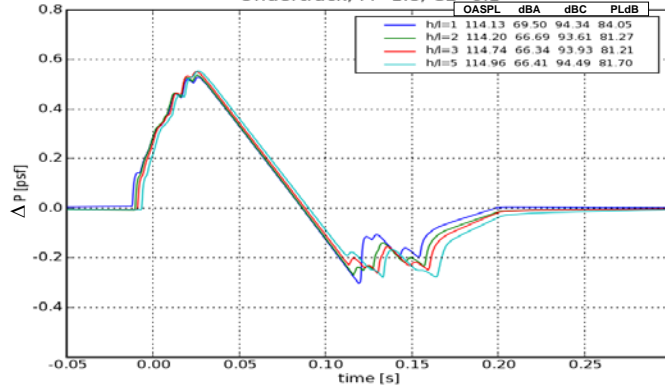
Mach = 1.6, CL=0.14



Ground Signature

Ground Pressure Signature

Undertrack, M=1.8, CL=0.1



Ground Pressure Signature

Undertrack, M=1.6, CL=0.14

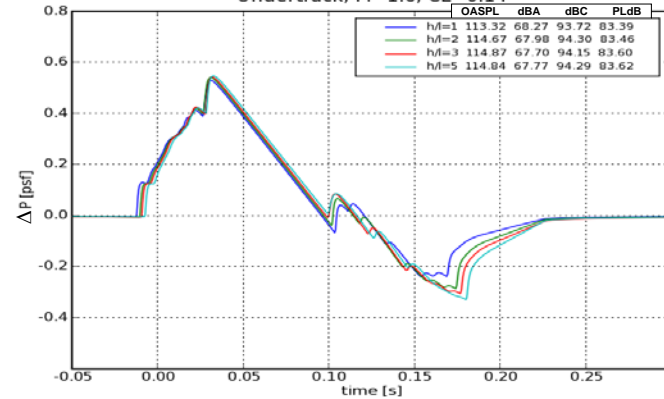
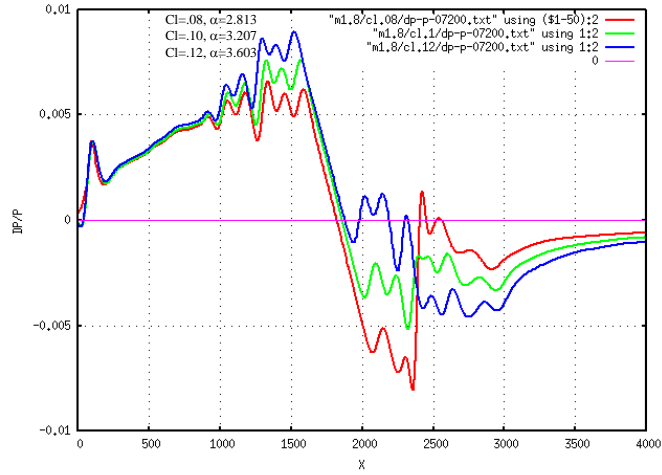


Figure 3.5-2. The Low-Boom Concept Has Robust Sonic Boom Characteristics at Multiple Mach Numbers

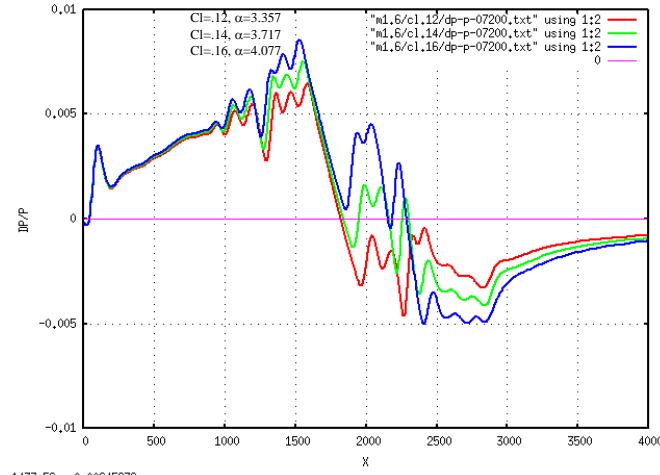
Nearfield Signature

Mach = 1.8, h/L=3



-562.874, -0.0119313

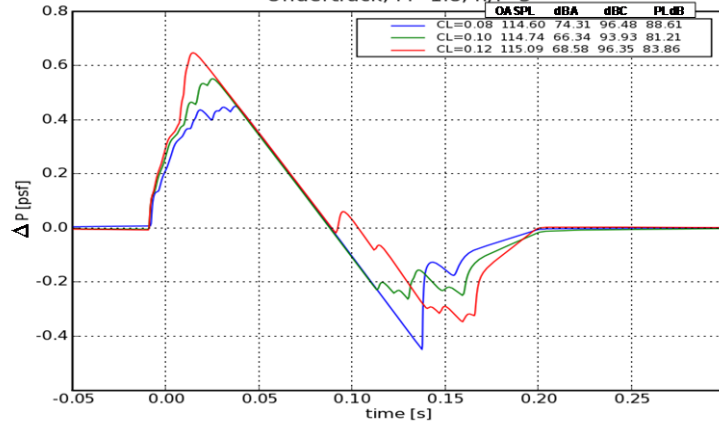
Mach = 1.6, h/L=3



1473.56, 0.00645936

Ground Signature

Ground Pressure Signature
Undertrack, M=1.8, h/l=3



Ground Pressure Signature
Undertrack, M=1.6, h/l=3

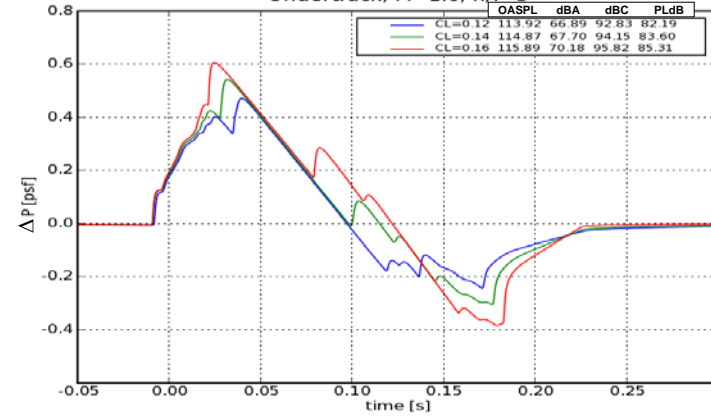
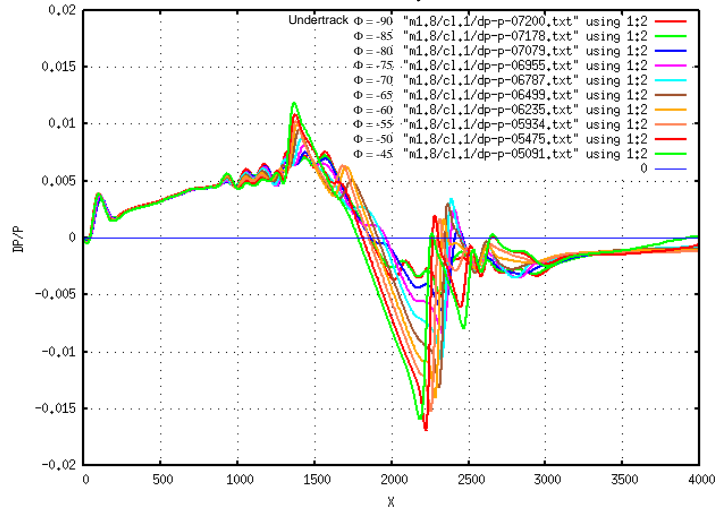


Figure 3.5-3. Low-Boom Concept Signature Characteristics at Off-Design CLs

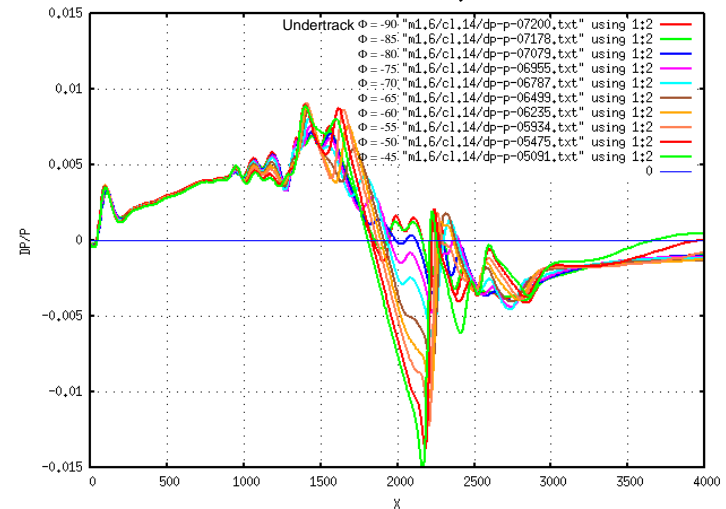
Nearfield Signature

Mach = 1.8, h/L=3



1237.93, 0.0149045

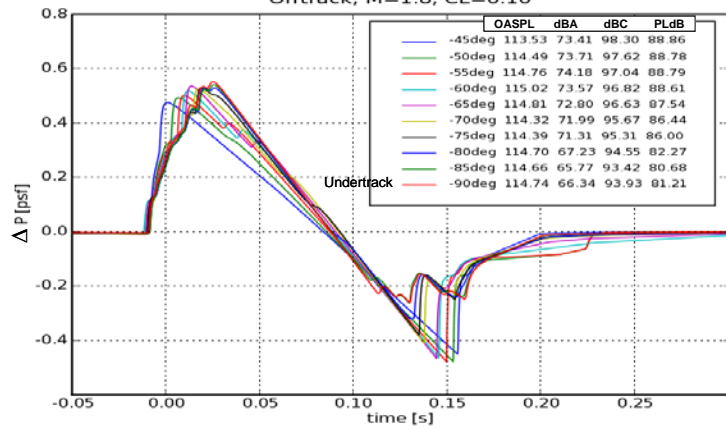
Mach = 1.6, h/L=3



2871.26, -0.00289689

Ground Signature

**Ground Pressure Signature
Offtrack, M=1.8, CL=0.10**



**Ground Pressure Signature
Offtrack, M=1.6, CL=0.14**

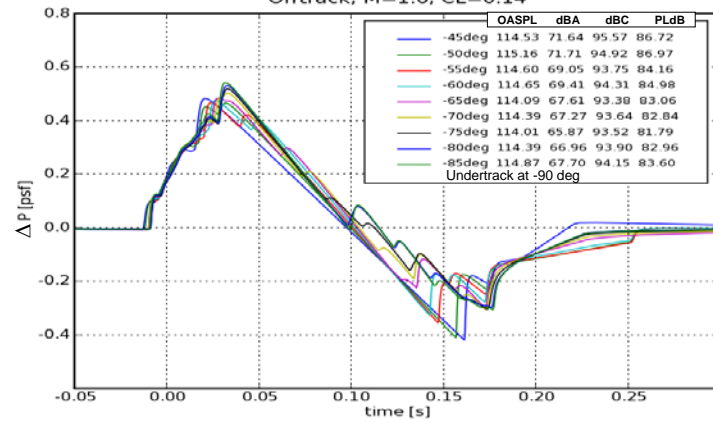


Figure 3.5-4. The Low-Boom Concept Has Robust Signature Characteristics at Off-Track Locations

Cruise Aerodynamics

A longitudinal aerodynamic analysis was conducted on the low-boom concept at the cruise condition for Mach = 1.6 and Mach = 1.8. Both Euler (Cart3d) and Navier-Stokes (OVERFLOW) analyses were conducted. Figure 3.5-5 summarizes the Navier-Stokes analysis. The upper left plot contains the lift curve versus AOA, the upper right plot contains the drag polar (CL versus CD), the lower left plot contains the L/D versus AOA and the lower right plot contains the pitching moment (CM versus CL). The pressure drag at the Mach = 1.8 design condition is ~86 counts, which is 7 counts above the -076E goal value. At the Mach = 1.8 design condition, L/D = 6.2, which is below the design goal of L/D = 7.0. With a technology projection to 2025 (and further optimization), the Mach = 1.6 performance can exceed the goals of matching the 765-076E levels. Thus, although the Mach = 1.8 aerodynamic performance does not meet the goal, the low-boom concept is sufficient for experimental validation testing. Improved drag was one reason Boeing proceeded with a second OML, which is discussed in section 3.6.

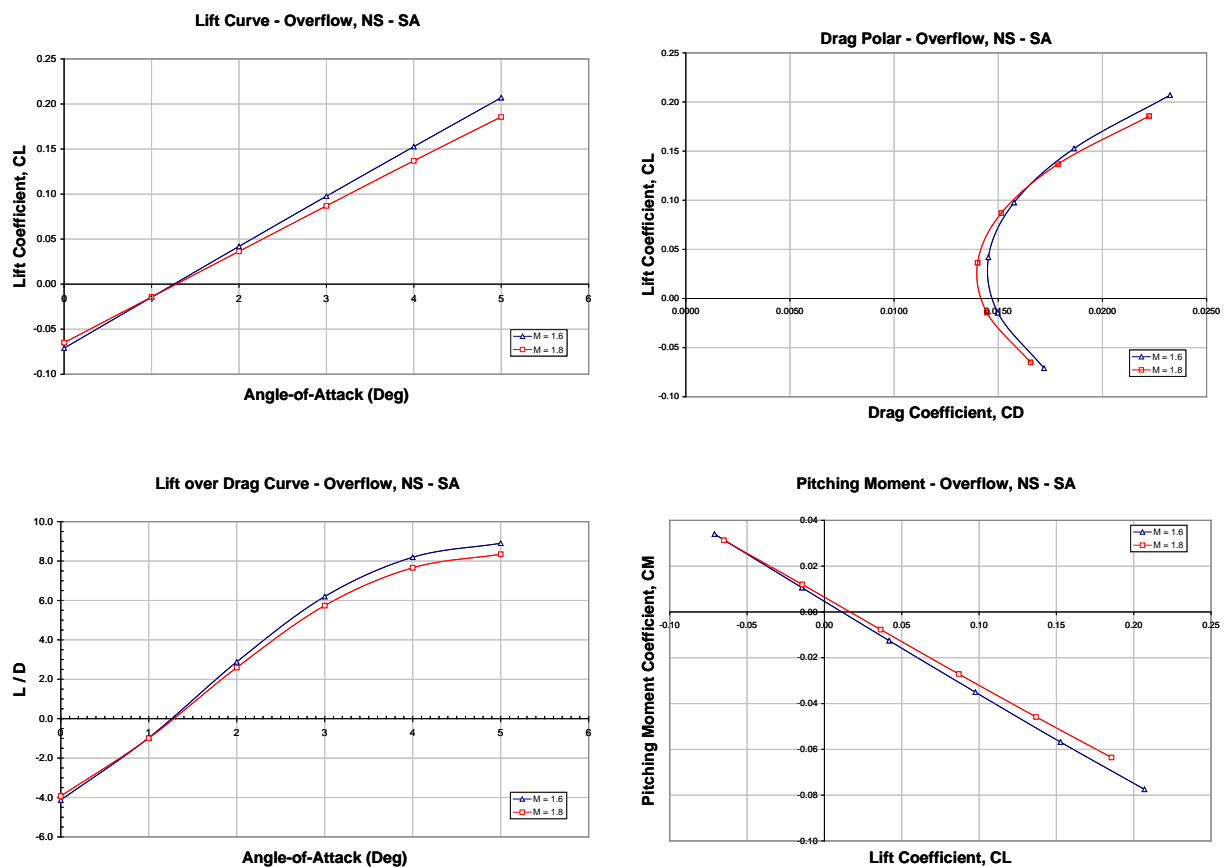


Figure 3.5-5. Low-Boom Concept Longitudinal Cruise Aerodynamics

Fuel Loading

One concern with low-boom concepts is whether enough fuel can be loaded onto the aircraft to meet the range requirement. Most low-boom concepts have very thin airfoil sections and limited space to place fuel. The low-boom concept was examined to see where fuel tanks could be placed and whether enough fuel could be loaded on the aircraft. Figure 3.5-6 summarizes the fuel tank layout and possible fuel loading. Based on this assessment, it appears that enough fuel can be loaded onto the aircraft.

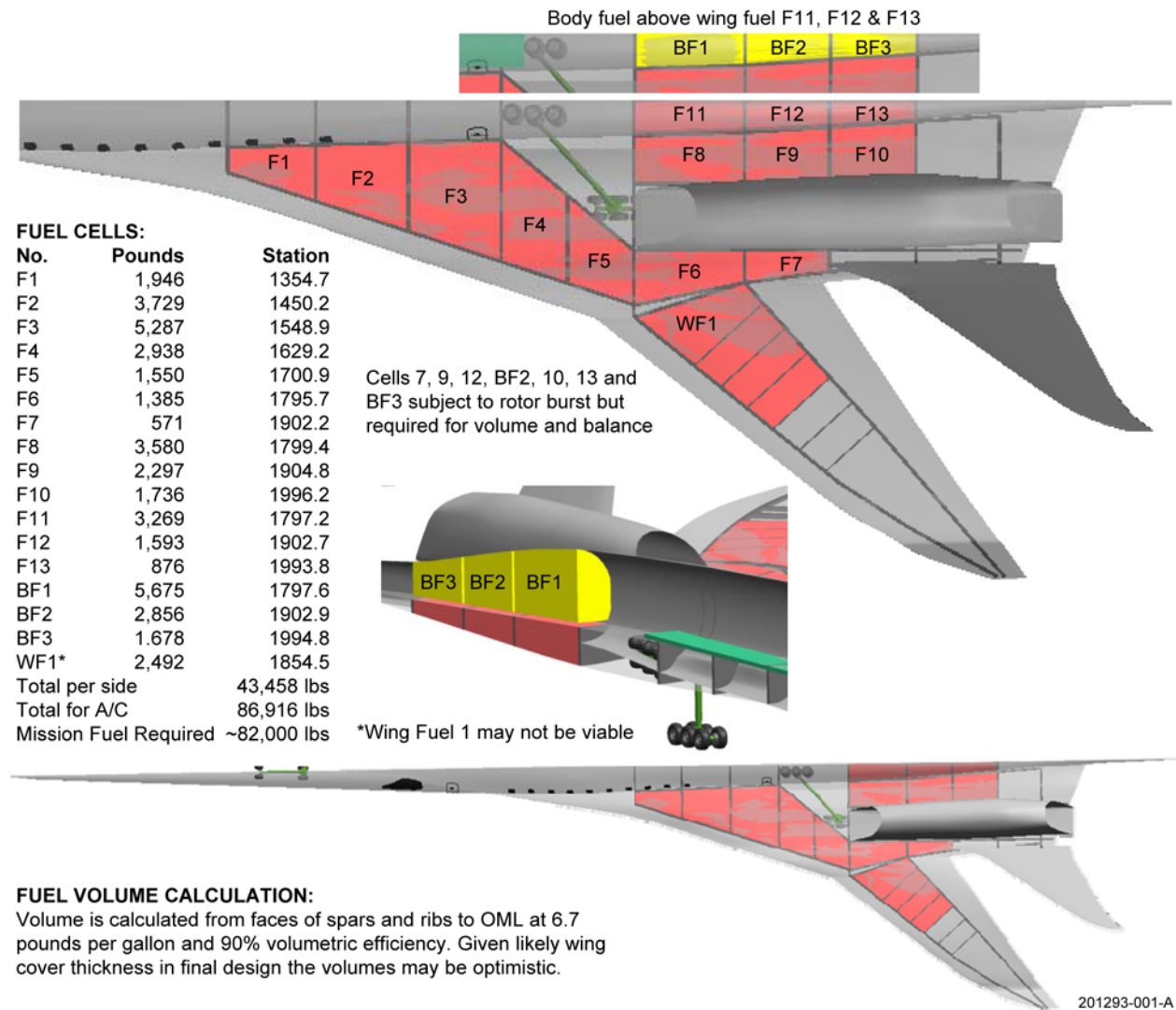


Figure 3.5-6. Fuel Layout for the Low-Boom Concept

Performance Analysis

A performance analysis for the low-boom concept was not completed, but based on a comparison with a previous analysis for the 765-076E configuration, it is possible to meet the same 2025 performance target at Mach = 1.6 with a 3% technology projection. Figure 3.5-7 shows this analysis by comparison. From the figure, at Mach = 1.6 and a mid-cruise CL = 0.16, the L/D is 8.5. The status drag (Navier Stokes-based) with a notional 3% technology projection for improvements made in design methods between 2010 and 2025 yields a L/D = 8.55, which slightly exceeds the 765-076E value. Increased L/D performance was another reason Boeing proceeded with a second OML, which is discussed in section 3.6.

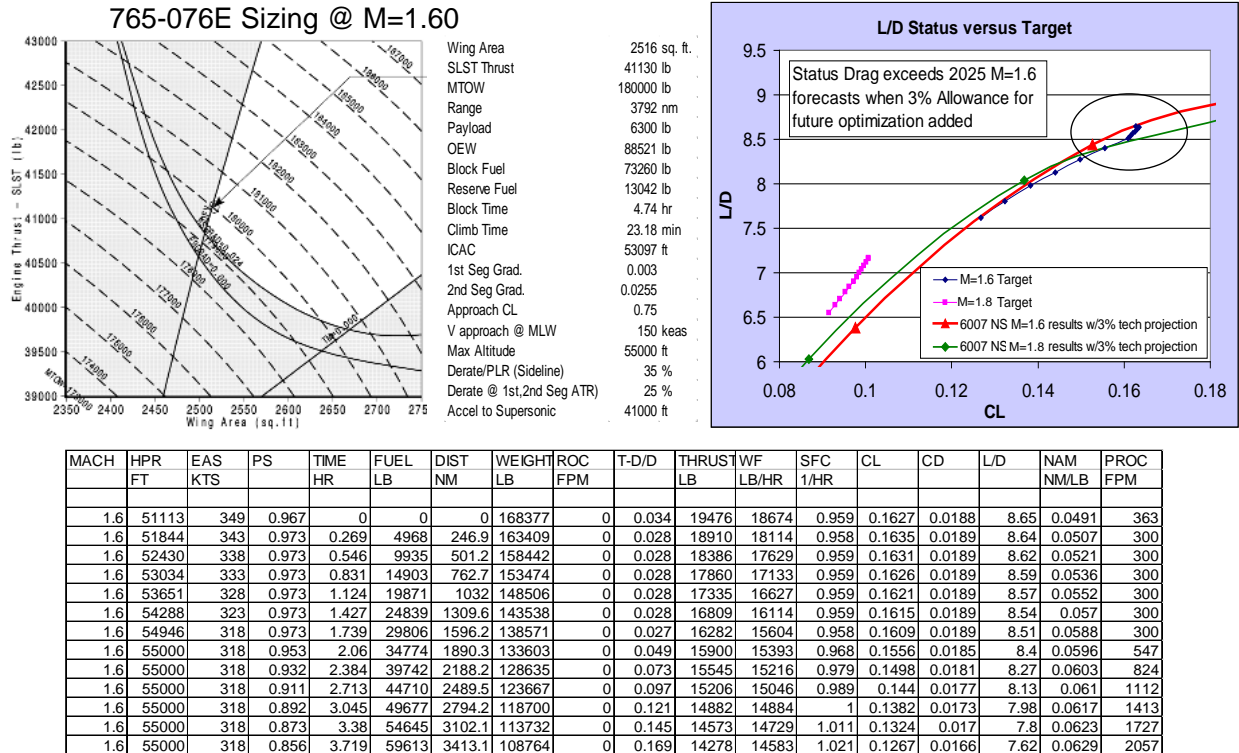


Figure 3.5-7. Low-Boom Concept Performance Analysis by Comparison With the 765-076E

Cruise Trim and CG

Challenges for low-boom concepts include cruise trim and CG. Figure 3.5-8 shows the CG envelope for the low-boom concept. Analysis showed the 6007 OML cruise CG is not within current fuel tank loadability limits. This situation arose because the seed geometry had significant tail lift (V-tail toe-in/incidence was set to 0 and not designed) and V-tail toe-in/incidence that were not originally design variables because of the complexity of the V-tail/support pod grid intersections. In addition, the majority of design activity was not executed with a CM constraint, because it was not a requirement for this phase of experimental validation. There appears, however, to be no obstacle to designing to a CG constraint in the future. Boeing plans to include variables to off-load the tail in follow-on designs discussed in section 3.6. Thus, although the status cruise CM does not meet the goal for a fully closed aircraft concept, Boeing believes that the design is sufficient for experimental validation testing.

QEVC2 Center-of-Gravity Envelope

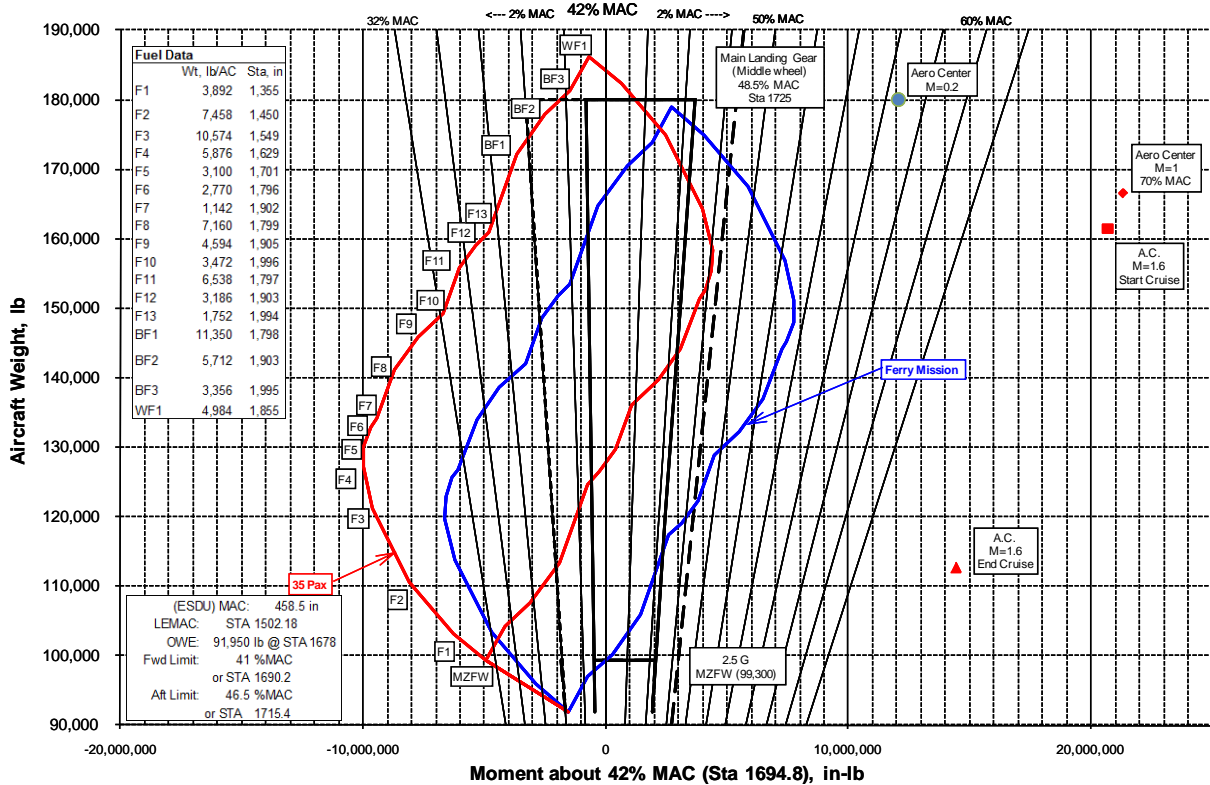


Figure 3.5-8. The Low-Boom Concept CG Envelope

3.6 Second OML Design, Alternate Part Definition

The experimental validation program was centered on two models: a large model primarily for performance validations, with some capability for boom testing; and a smaller 1/3-size model, primarily for boom measurements. In addition, the fabrication budget included resources to build several extra small parts for each model to obtain sensitivities on boom and drag to verify that the CFD validation could cover incremental effects.

For the large model, two additional outboard wings, an alternate nacelle and an alternate V-tail, were designed. One of the alternate outboard wings, along with the V-tail, was a product of using the QEVC3 concept but changing the wing and tail to minimize drag. The alternate nacelle was a 2D inlet.

For the small boom model, a different approach was taken. Instead of fabricating a series of alternate parts (e.g., a nose, gear fairing, nacelle, and tail), a complete alternate design was chosen. To ensure that the second optimization produced a geometry that would be significantly different from that produced by the first optimization, design conditions were changed from Mach = 1.8 (CL = 0.1039 to Mach = 1.6 (CL = 0.14). In addition, the weighting of objectives was adjusted so that the focus was more on drag and pitching moment than the near-field signature shape.

Table 3.6-1 compares the design criteria of Boom Models 1 and 2. The resulting 8668 design is shown

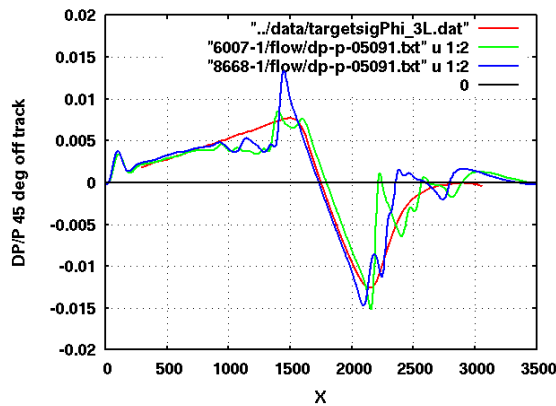
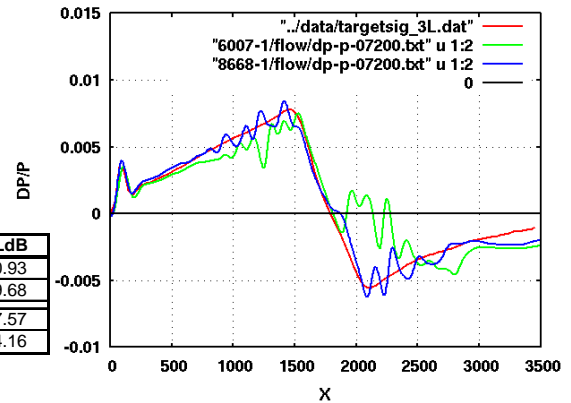
in comparison to the 6007 at $M = 1.6$ in Figure 3.6-1 and $M = 1.8$ in Figure 3.6-2. Subsequent refinements to the geometry and modifications for wind tunnel model constraints resulted in the 8679 concept. Figure 3.6-3 compares the 8679 and 8668. Boom Model 2 is the QEVC3-8679. The surface and centerline pressure for Boom Model 2 are shown in Figure 3.6-4.

Table 3.6-1. Optimization Parameters

	Boom Model 1 Optimization	Boom Model 2 Optimization
Starting geometry	QEVC seed	Optimized for low drag
Mach	1.8	1.6
Lift coefficient	0.104	0.140
Pitching moment	No constraint	Constrained to -0.02

- Final Design, 8668 signature is nearly as good as 6007
- Alternate shape chosen for “variety”
- Drag and pitching moment are much better
- ~20cts improvement at Mach=1.6

Subcase	Mach	Alpha	CL	CD	CM	Fwd PLdB	Aft PLdB	PLdB
6007	1.6	3.72	0.140	0.0106	-0.0521	79.99	71.88	80.93
8668	1.6	3.28	0.140	0.0086	-0.0238	77.20	75.49	79.68
6007	1.8	3.28	0.104	0.0089	-0.0341	76.86	70.00	77.57
8668	1.8	2.79	0.104	0.0074	-0.0073	82.07	93.46	94.16



Mach=1.6
CL=0.14

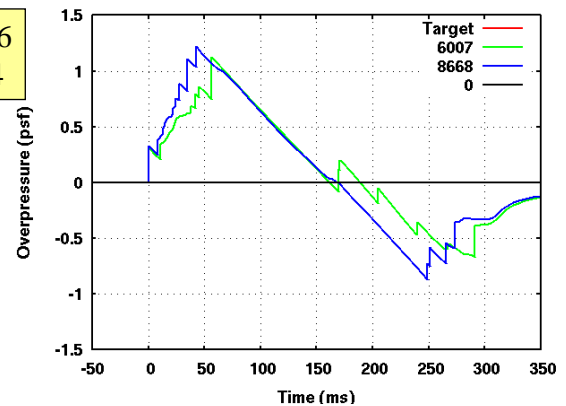
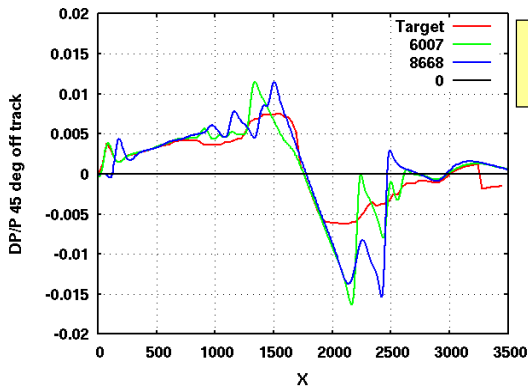
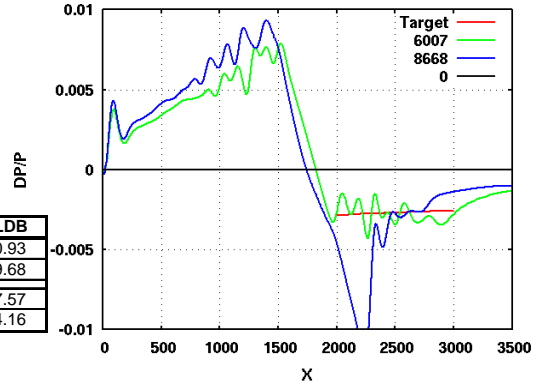


Figure 3.6-1. 8668 Compared to 6007 (Mach = 1.6)

- 8668 signature is significantly worse than 6007
 - Need to check off CL conditions since aft signature changes significantly with CL
- Drag and pitching moment are much better

Subcase	Mach	Alpha	CL	CD	CM	Fwd PLDB	Aft PLDB	PLDB
6007	1.6	3.72	0.140	0.0106	-0.0521	79.99	71.88	80.93
8668	1.6	3.28	0.140	0.0086	-0.0238	77.20	75.49	79.68
6007	1.8	3.28	0.104	0.0089	-0.0341	76.86	70.00	77.57
8668	1.8	2.79	0.104	0.0074	-0.0073	82.07	93.46	94.16



Mach=1.8
CL=0.104

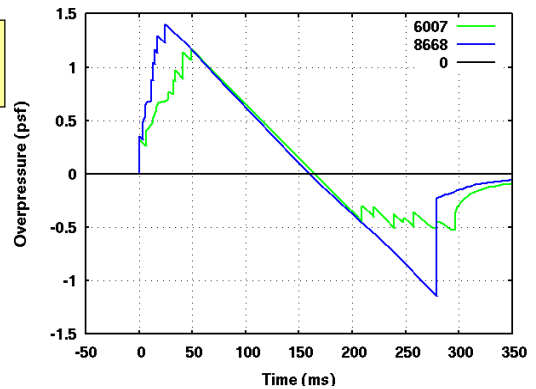
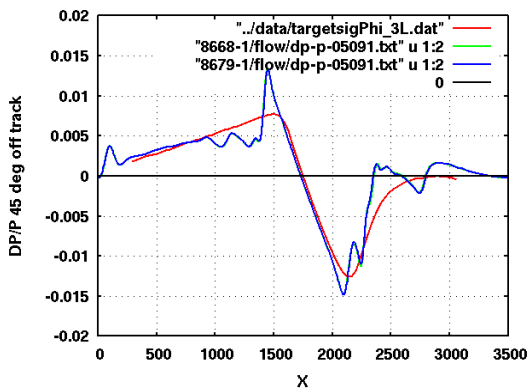
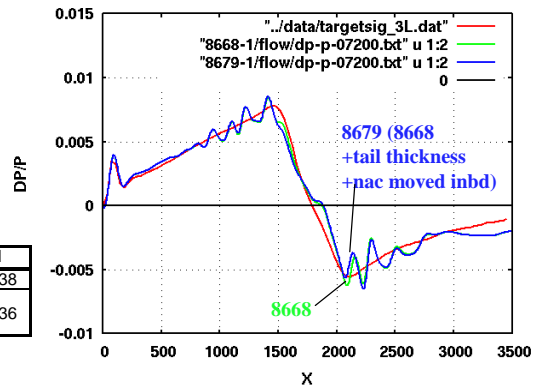


Figure 3.6-2. 8668 Compared to 6007 (Mach = 1.8)

- Manufacturing concerns resulted in several OML changes
- Move nacelle inboard 5"
- Increased tail tip thickness from 3% to 4.5%

Subcase	Description	Alpha	CL	CD	CM
8668	Hand fixed second OML	3.282	0.1400	0.0086	-0.0238
8679	Add tail thickness and move nacelle 5" inboard from 8668	3.302	0.1400	0.0088	-0.0236



Mach=1.6
CL=0.14

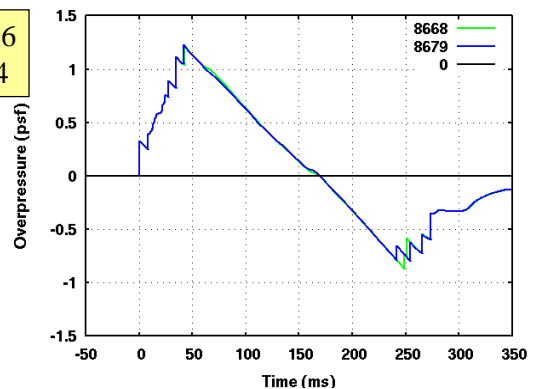


Figure 3.6-3. 8679 Compared to 8668 (Mach = 1.6)

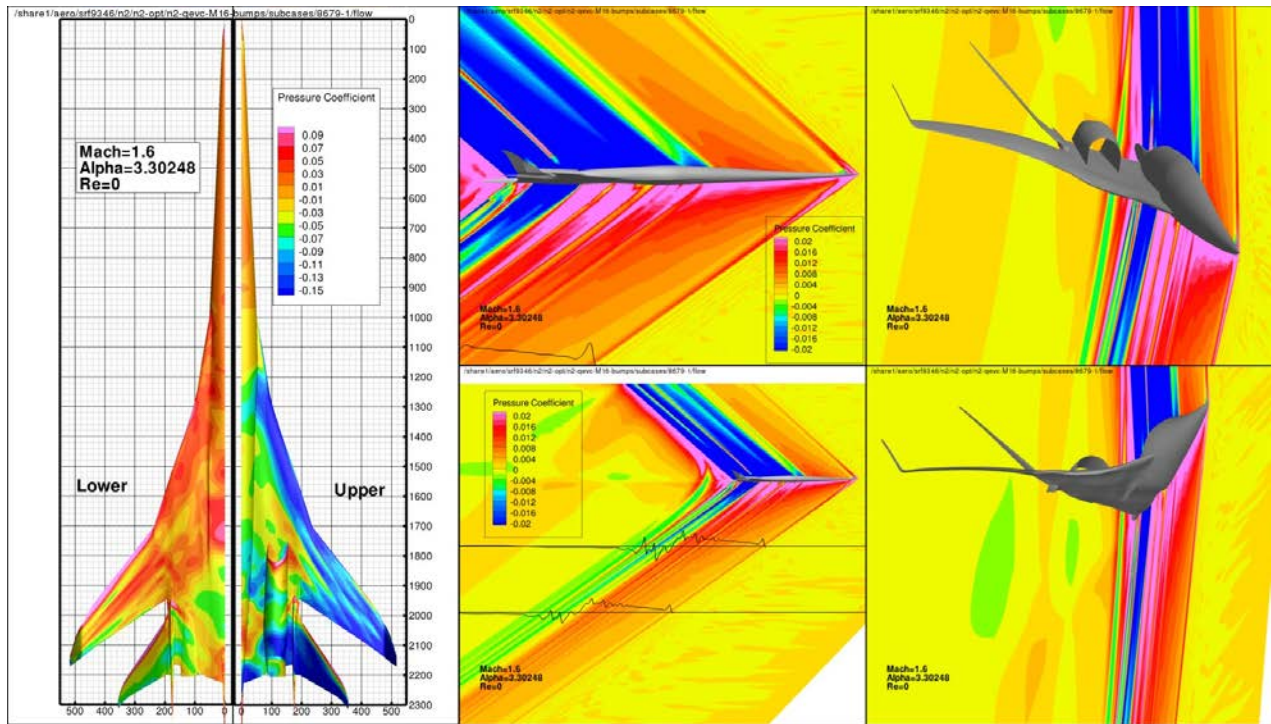


Figure 3.6-4. Surface Pressure and Flow Field for 8679 Geometry ($M = 1.6$, $CL = 0.14$)

3.7 Additional Boom Optimization Studies After Gate Review

Several additional optimization studies were conducted after the gate review to determine to what degree various aspects of the design affect the resulting low-boom configuration.

Optimization with No Nacelle

An optimization similar to Boom Model 2 was conducted with the nacelle removed from the geometry. It was found that removing the nacelle from the QEVC seed geometry results in a drag reduction of 11 counts. A drag minimization at $M = 1.6$, $CL = 0.14$, reduced the drag another 16 counts (slightly less than the 18 counts observed with the same optimization with the nacelle). The DOE optimization without the nacelle produced a signature very similar to the signature with the nacelle. Figures 3.7-1 and 3.7-2 show comparisons of the under- and off-track signatures. The under-track signature shows very little difference, whereas the peak compression in the off-track signature shows some improvement for the optimization run without the nacelle. The final forces and moments for these configurations are summarized in Table 3.7-1, and surface pressure and centerline pressure are shown in Figure 3.7-3.

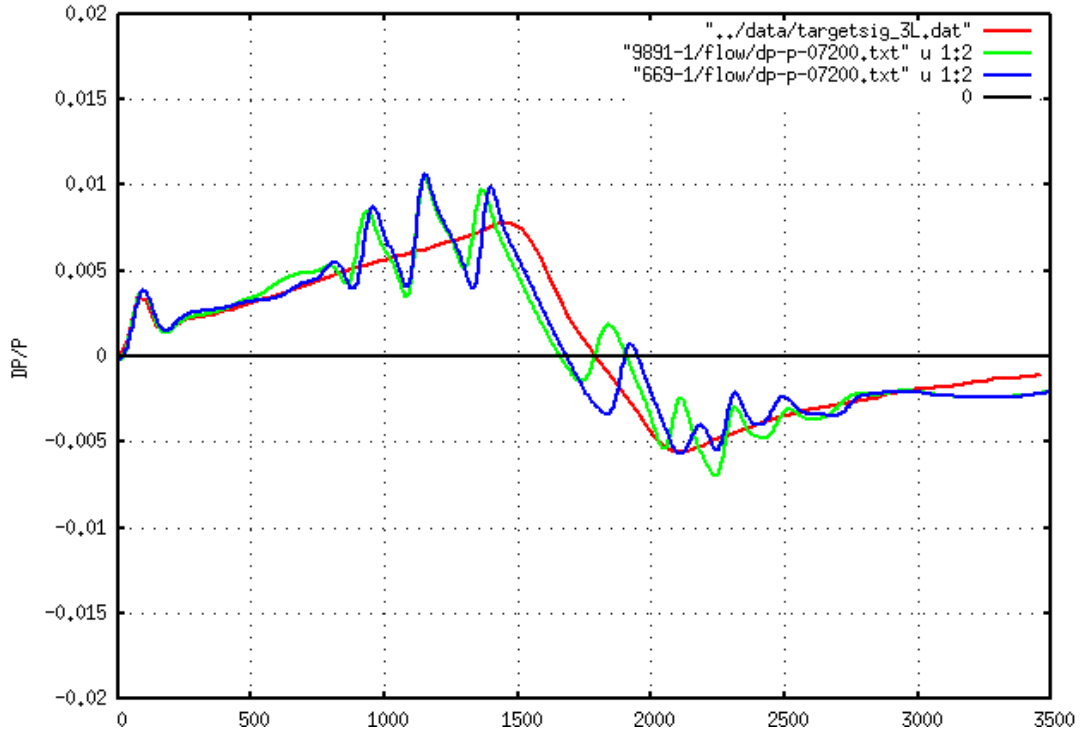


Figure 3.7-1. Optimum Under-Track Signature Comparing Nacelle On (Green) With Nacelle Off (Blue) ($M = 1.6$, $CL = 0.14$)

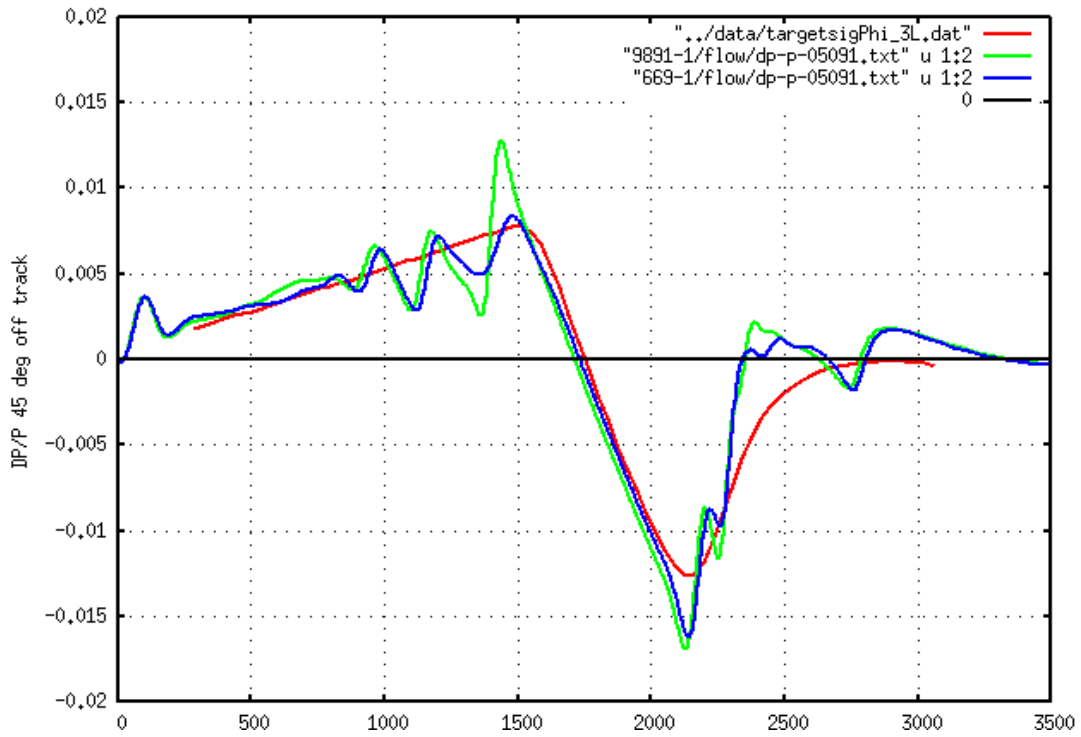


Figure 3.7-2. Optimum Off-Track Signature Comparing Nacelle On (Green) With Nacelle Off (Blue) ($M = 1.6$, $CL = 0.14$)

Table 3.7-1. Nacelle Off-Design Comparison

Subcase	Description	Alpha	CL	CD	CM
Nacelle 891	Opt point with nacelle	3.294	0.13999	0.00859	-0.0207
No nacelle 669	Opt point with no nacelle	3.459	0.14000	0.00799	-0.0201

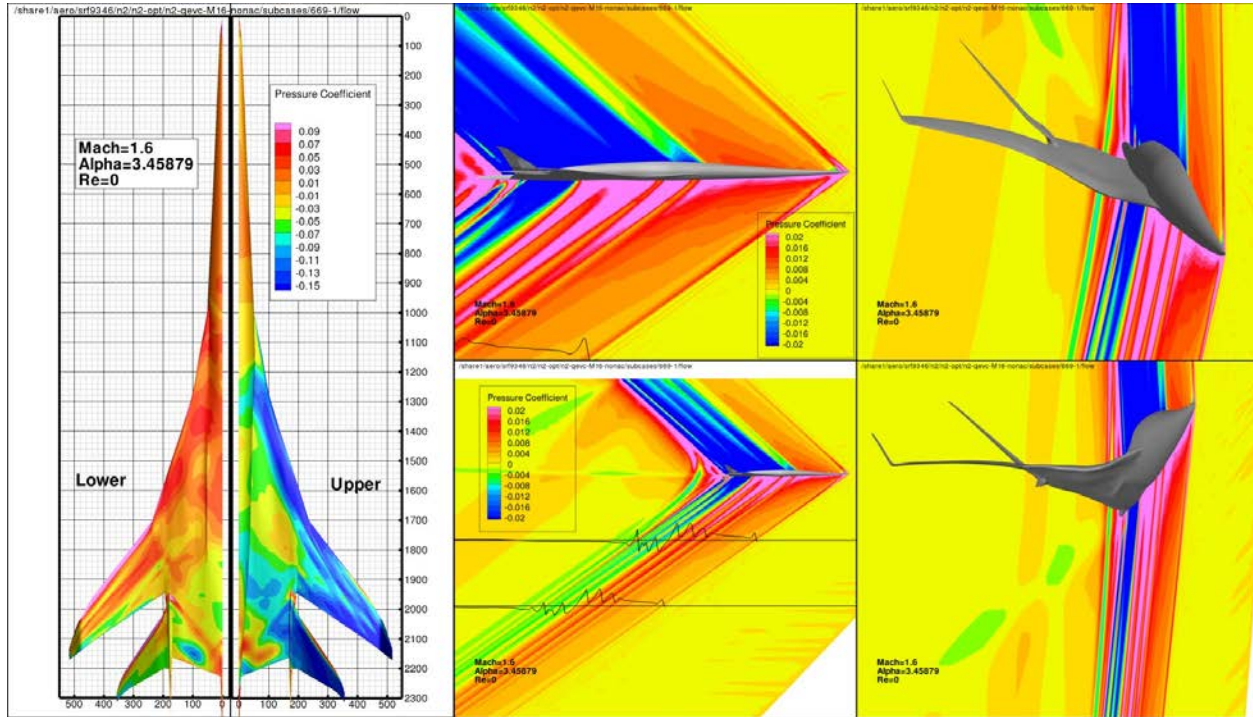


Figure 3.7-3. Surface Pressure and Centerline Pressure for Geometry Optimized with no Nacelle ($M = 1.6$, $CL = 0.14$)

Optimization with Wing Thickness Variables

Two approaches were investigated to determine how much improvement could be obtained by including wing thickness variables in an optimization. The first approach was to add thickness variables to an optimization. The second approach was to take the best site from the twist and camber optimization and modify the upper surface thickness to minimize drag. Neither of these optimizations produced results of significance.

Off-Track Signature Optimization

The Boom Model 2 optimization was run with equal weighting on under-track signature, off-track signature and drag. The final result was a geometry that has lower drag than the target and a good under-track signature. The peak compression and expansion in the off-track signature, however, is significantly higher than the under-track signature, which leads to a ground signature that gets worse when moving away from the centerline. To investigate the relationship between the under-track and off-track signatures, additional optimization was run with a higher weighting on the off-track objective. Weightings of 2x and 10x were considered, and the resulting signatures are shown in Figures 3.7-4 and 3.7-5, respectively. Table 3.7-2 summarizes the forces for these geometries. Figure 3.7-6 shows the surface pressures for these three geometries.

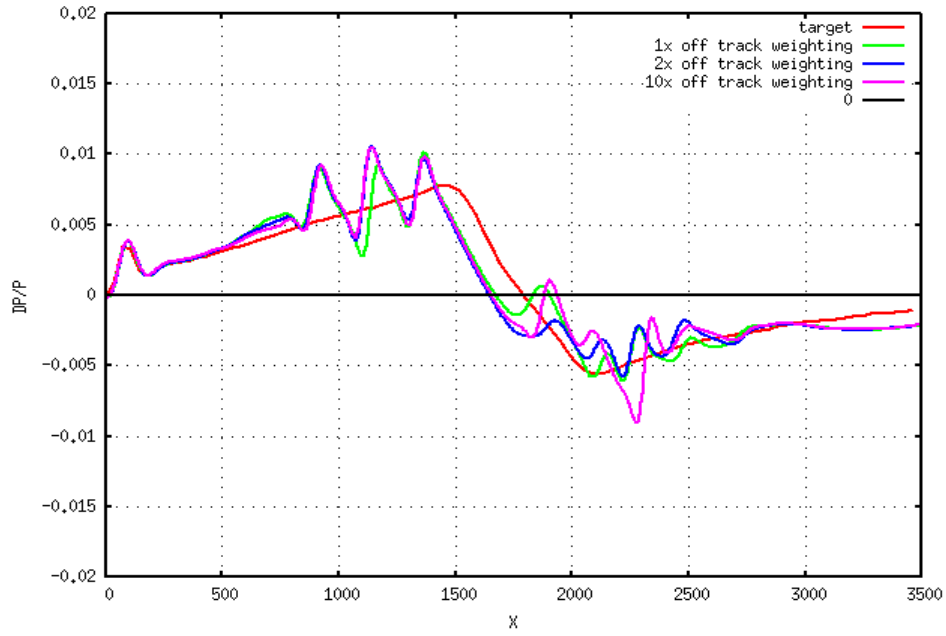


Figure 3.7-4. Under-Track Signatures for Optimum Results with Different Off-Track Weightings (M = 1.6, CL = 0.14)

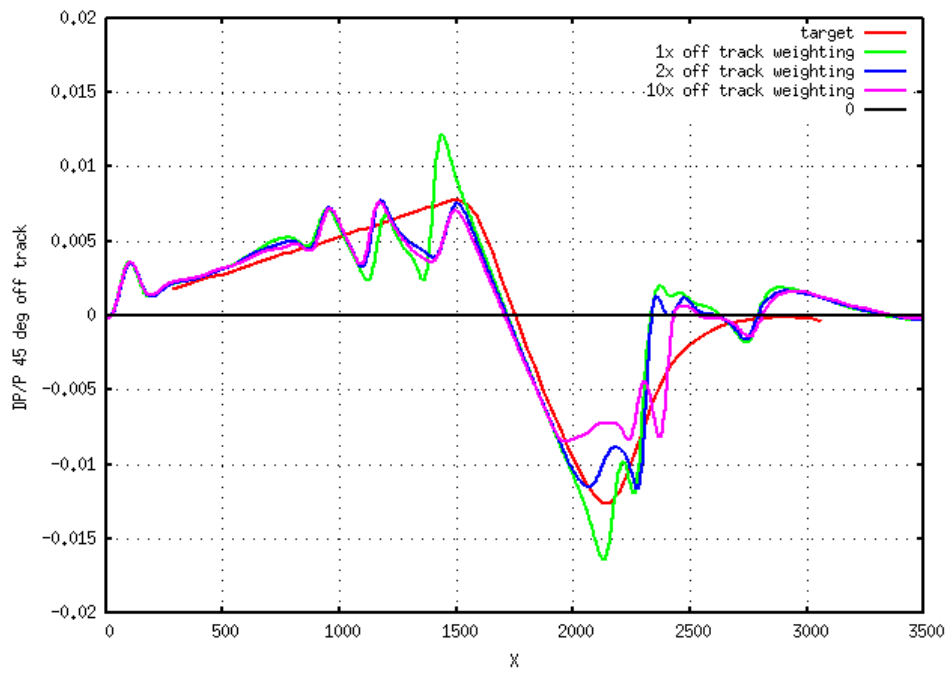


Figure 3.7-5. 45-deg Off-Track Signatures for Optimum Results with Different Off-Track Weightings (M = 1.6, CL = 0.14)

Table 3.7-2. Optimization Results for Different Off-Track Weighting (M = 1.6)

Subcase	Description	Alpha	CL	CD	CM
1064	1x off-track weight	3.382	0.139985	0.00866	-0.0203
8188	2x off-track weight	3.490	0.139983	0.00912	-0.0199
8260	10x off-track weight	3.437	0.139980	0.01006	-0.0197

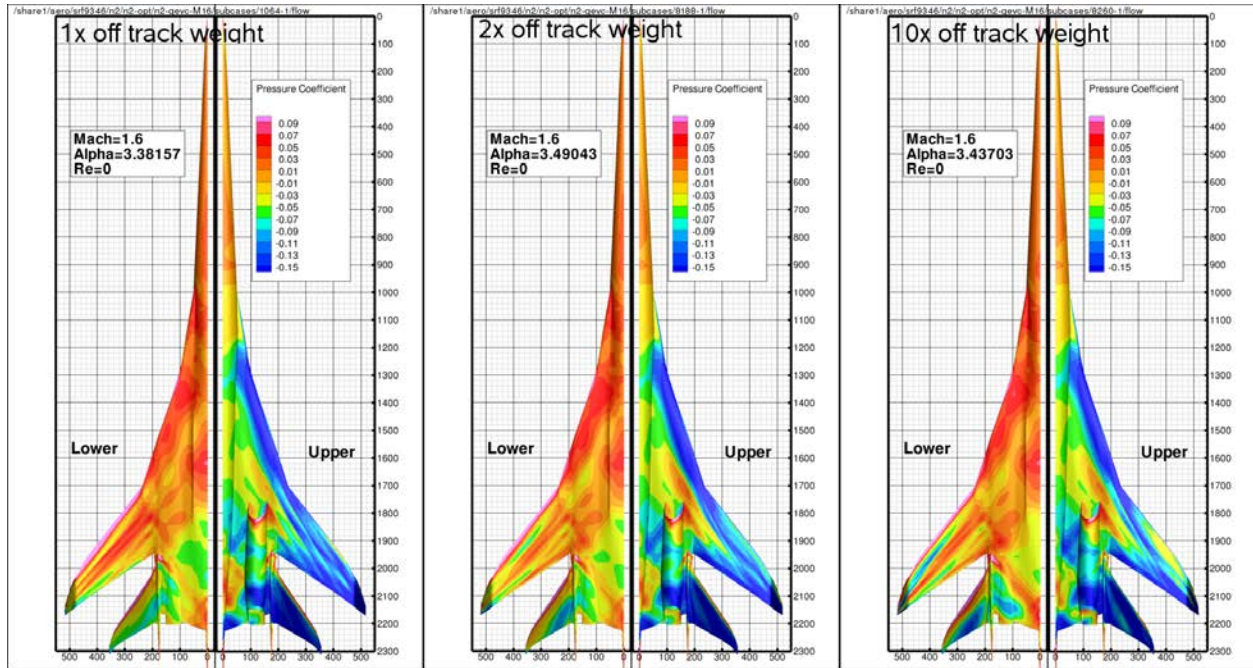


Figure 3.7-6. Surface Pressure Distribution for Different Off-Track Weighting (M = 1.6, CL = 0.14)

4.0 LOW-BOOM CONCEPT WIND TUNNEL MODEL PREPARATION

4.1 QEVC Boom Model 1

The first of the three models fabricated for experimental validation testing was a 15.75-in-long model (0.65% scale) designated Boom Model 1. The model was sized to provide the best compromise of model fidelity and ability to measure off-body sonic boom pressure signatures in a large tunnel. Figure 4.1-1 shows the layout for Boom Model 1, which was mounted with an upper swept strut that connects to an aft sting by means of a balance adapter. Figure 4.1-2 shows the overall assembly for Boom Model 1. Both a short and a long upper swept strut were manufactured, as well as strut assemblies with and without vertical stabilizer surfaces. Forces and moments are resolved with a NASA Ames-furnished 1-inch diameter six-component internal balance located within the balance adapter. The model was modular to allow for component testing and future modification as low-boom design tools and methods evolve. The model was made up of four components: (1) a removable nose, (2) a wing-body, (3) a removable wing-body-fairing lower surface (also referred to as the gear fairing) and (4) removable left-hand/right-hand (LH/RH) integrated nacelle/tail surfaces. Inlet mass flow plugs were also manufactured. Figure 4.1-3 shows the modular parts, and Table 4.1-1 lists the Boom Model 1 parts.

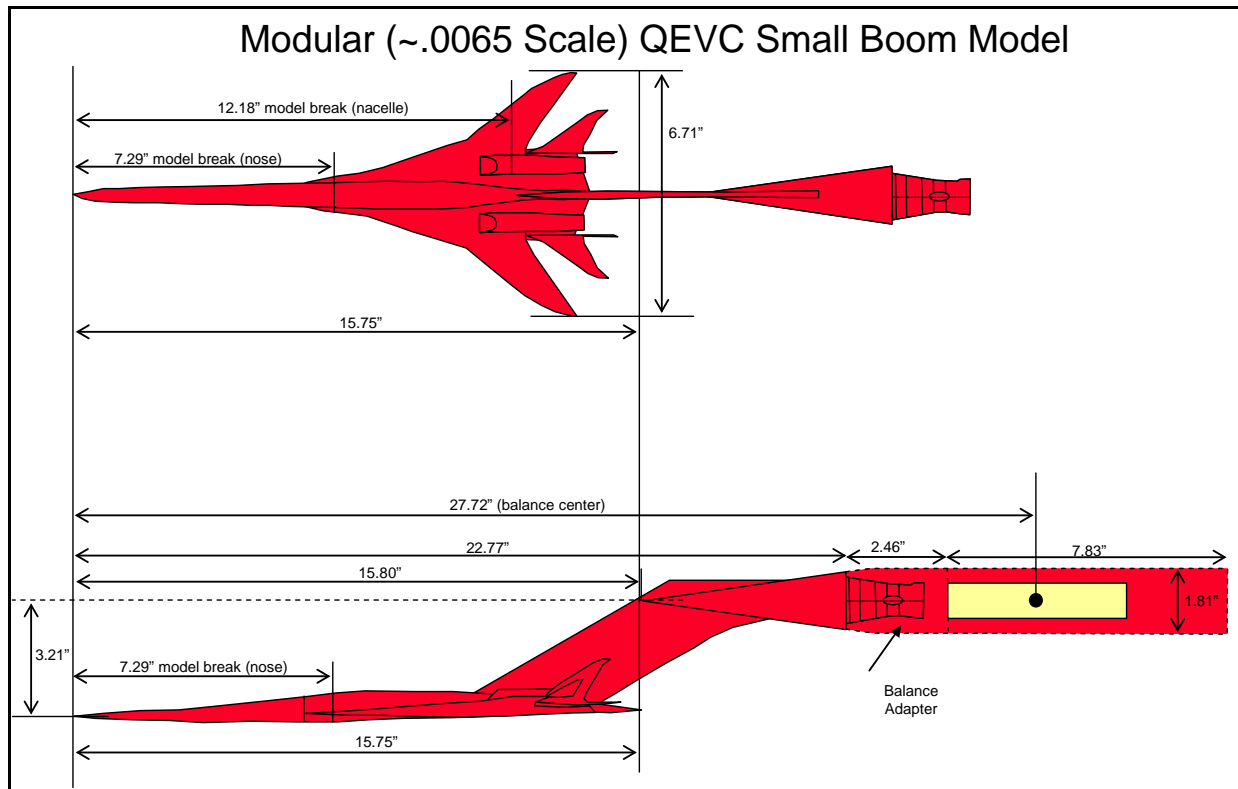


Figure 4.1-1. Preliminary Boom Model 1 Layout Shown at Gate 1 Review

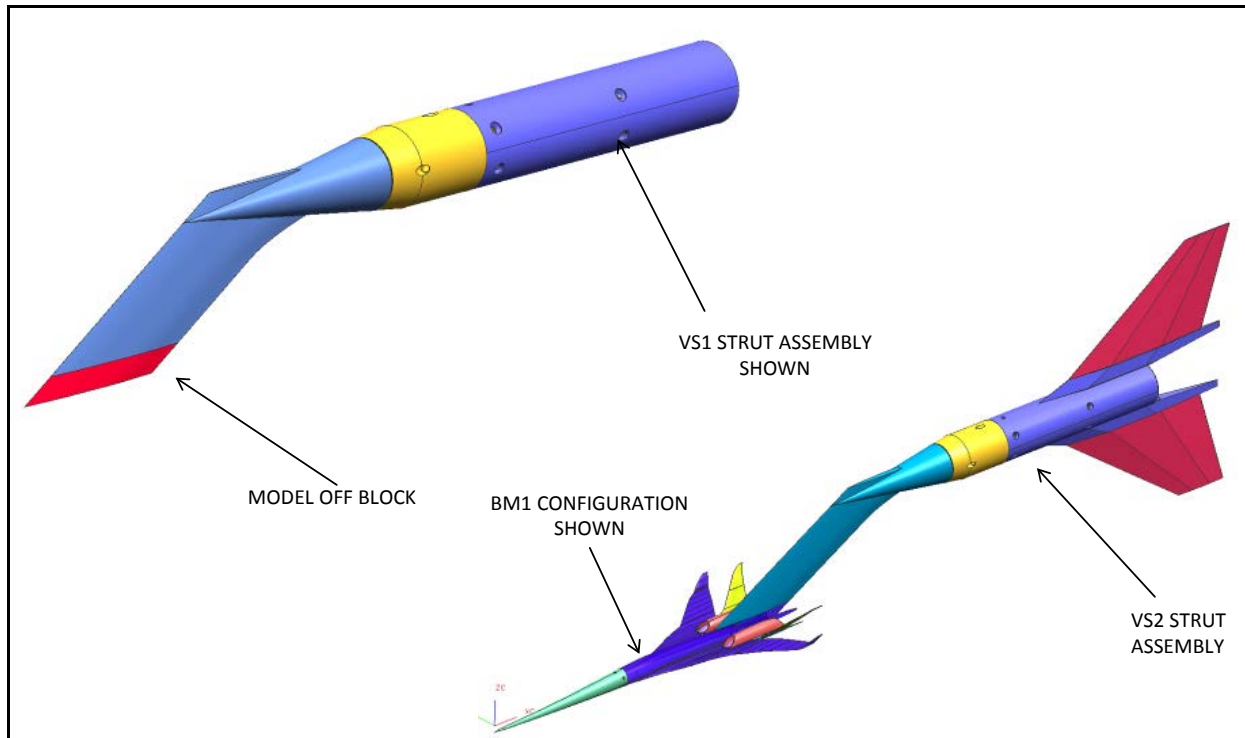


Figure 4.1-2. Boom Model 1 Assembly Shown at PDR

Table 4.1-1. Boom Model 1 Modular Parts

Small Model
<ul style="list-style-type: none"> • Boom Model 1 Geometry (W1/B1/GF1/N1/V1) <ul style="list-style-type: none"> – Wing/Body (W1) – Nose (B1) – Gear Fairing Cover plate (GF1) – LH /RH Nacelles (N1) – LH/RH Vertical Interface Pods (VP1) – LH/RH Verticals (V1)
<ul style="list-style-type: none"> • Inlet Plugs for Spillage Effects <ul style="list-style-type: none"> – LH/RH Inlet Plugs (IP1) (SLA) – LH/RH Inlet Plugs (IP2) (SLA) – LH/RH Inlet Plugs (IP3) (SLA)
<ul style="list-style-type: none"> • Cylindrical Balance Fairings (2) <ul style="list-style-type: none"> – Cylindrical Balance Fairing (BS1) – Cylindrical Balance Fairing With Fins (BS2)
<ul style="list-style-type: none"> • Conical Bal. Adapter Nose Fairing (CF1) • Detachable Upper Swept Struts (2) <ul style="list-style-type: none"> – Detachable Upper Swept Strut 1 (VS1) – Detachable Upper Swept Strut 2 (VS2)

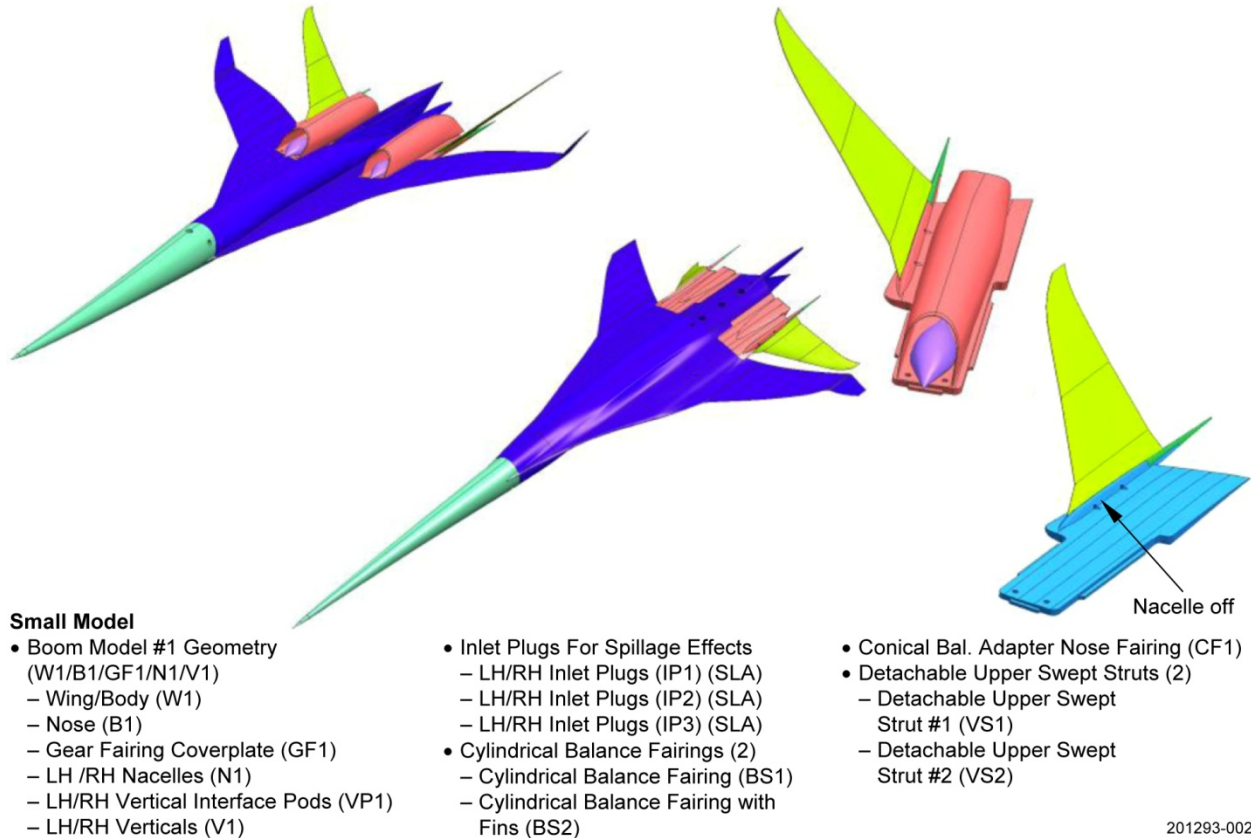


Figure 4.1-3. Boom Model 1 Modular Parts

4.2 QEVC Boom Model 2

The second model, Boom Model 2, was an alternate low-boom design with the same breakdown and general features as Boom Model 1. Table 4.2-1 lists the Boom Model 2 parts. The final fabricated parts for Boom Models 1 and 2 are shown in the photograph in Figure 4.2-1.

Table 4.2-1. Boom Model 2 Modular Parts

- | |
|--|
| <ul style="list-style-type: none"> • Boom Model 2 Geometry (W2/B2/GF2/N2/V2) <ul style="list-style-type: none"> – Wing/Body (W2) – Nose (B2) – Gear Fairing Cover plate (GF2) – LH/RH Nacelles (N2) – LH/RH Vertical Interface Pods (VP2) – LH/RH Verticals (V2) |
|--|



Figure 4.2-1. Boom Model 1 and Boom Model 2 and Associated Modular Hardware

4.3 QEVC Performance Model 1

The third model was a larger 43.31-inch-long model that was 1.79% scale. It was called Performance Model 1, but was often referred to as the force model. This model was sized to provide the best compromise of accurate force and moment assessment, with some reduced capability to measure off-body sonic boom pressure signatures in a large wind tunnel. Figure 4.3-1 shows the layout for Performance Model 1. It was mounted with an aft sting, with forces and moments resolved with the same Ames-furnished 1-inch diameter six-component internal balance as the boom models. Figure 4.3-2 shows the overall assembly for Performance Model 1. The model was also modular to allow for component testing and future modification as low-boom design tools and methods evolve. The model was made up of six components: (1) a removable nose, (2) a wing-body, (3) removable outboard wings, (4) a wing-body-fairing lower surface (also referred to as the gear fairing), (5) nacelles and (6) V-tail surfaces. The performance model was made with two additional alternate outboard wings and alternate 2D nacelles, an alternate V-tail and inlet mass flow plugs. Figure 4.3-3 shows the modular parts, and Table 4.3-1 lists the Performance Model 1 parts. A photograph of the complete performance model and associated parts are shown in Figure 4.3-4.

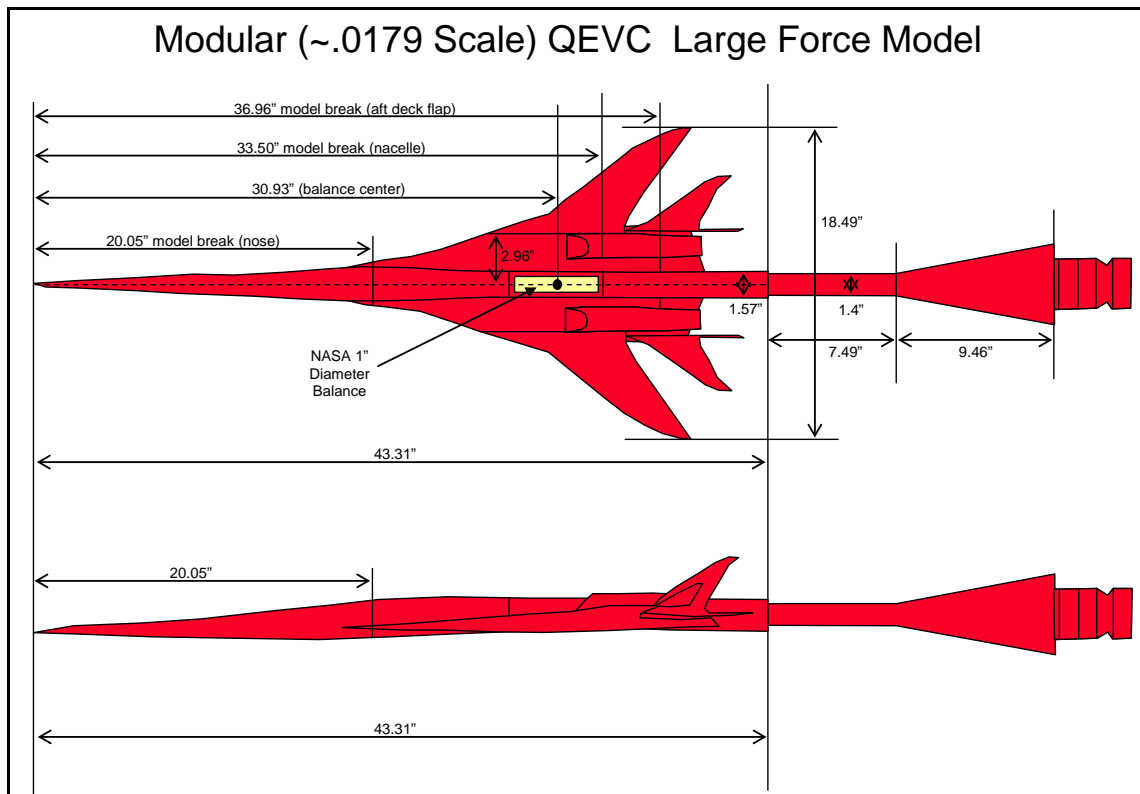


Figure 4.3-1. Force Model Layout Shown at Gate 1 Review

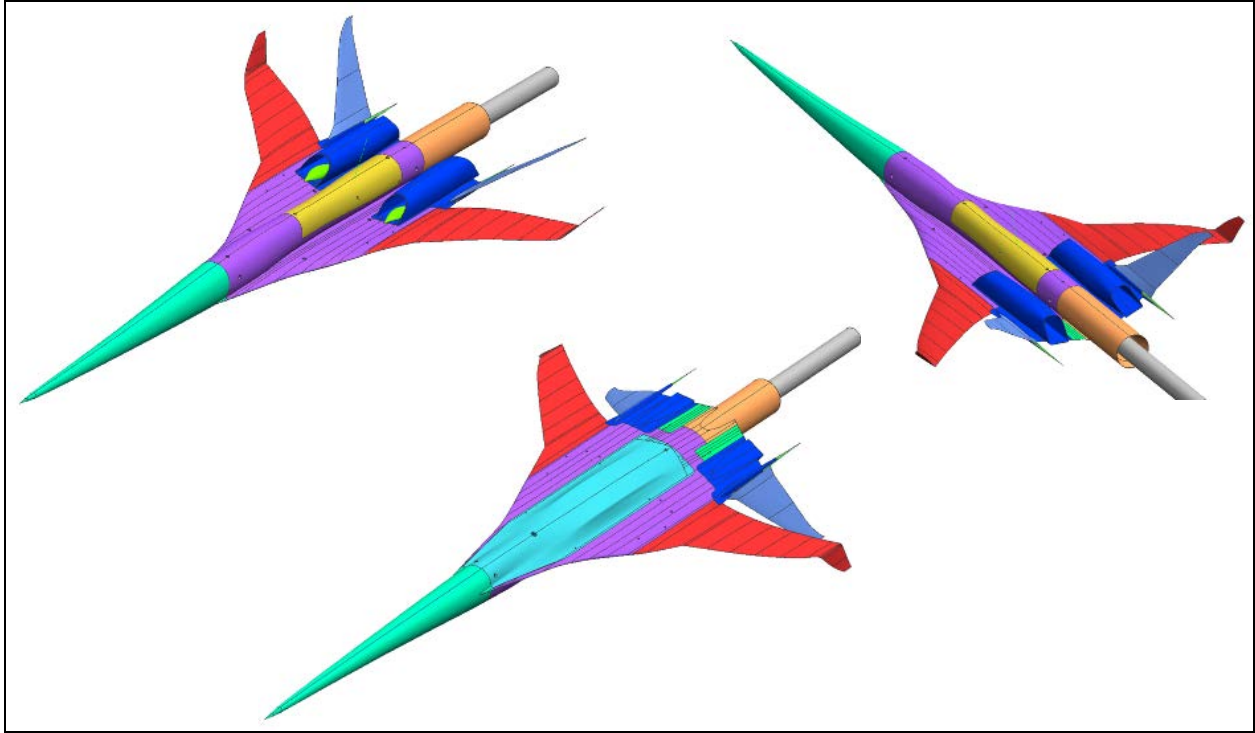


Figure 4.3-2. Performance Model 1 Assembly

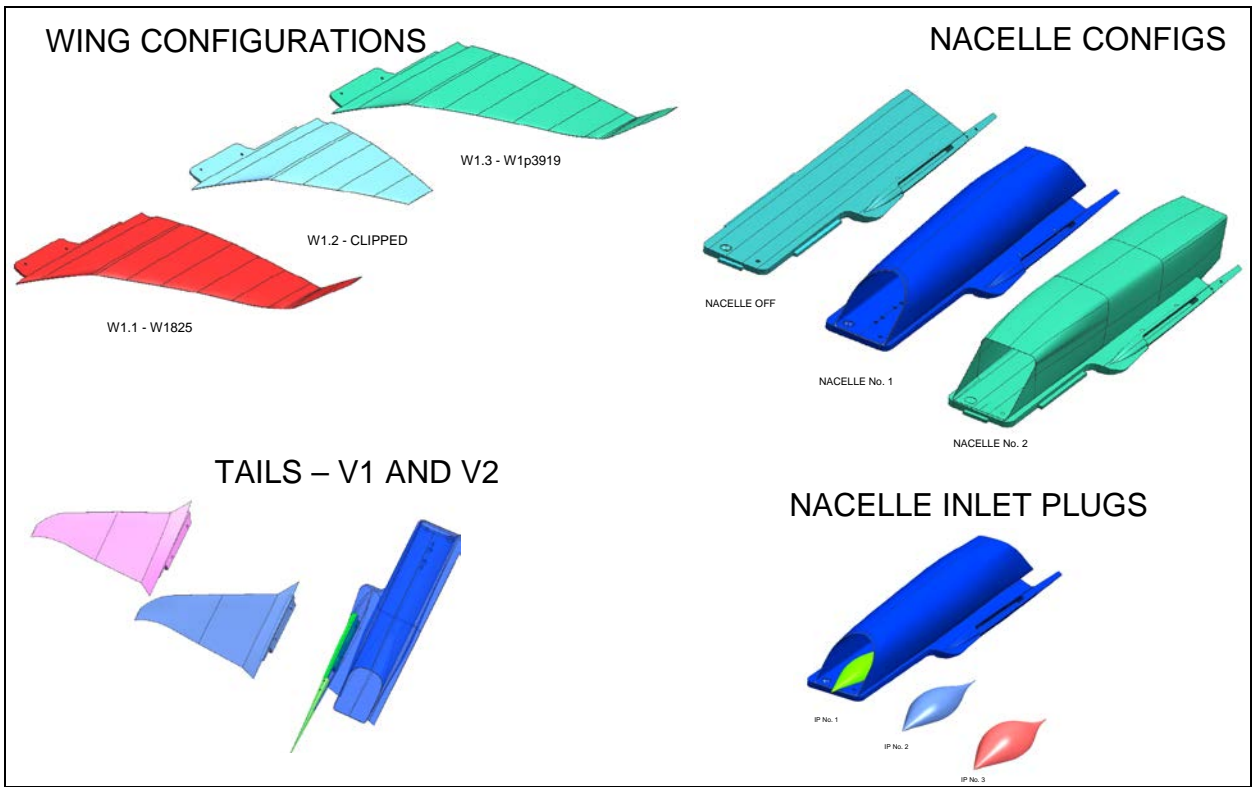


Figure 4.3-3. Performance Model Modular Parts

Table 4.3-1. Performance Model 1 Modular Parts

Large Model
• Base Model Geometry (W1B1.1GF1N1AF1VP1V1)
– Base WB With LH/RH Outboard Wing Tips (W1)
– Removable Nose (B1.1)
– Gear Fairing Cover plate (GF1)
– LH /RH Nacelles (N1)
– LH/RH Aft Deck Flaps (AF1)
– LH/RH Vertical Interface Pods (VP1)
– LH/RH Verticals (V1)
• Clipped Wing Force Model Geometry (W1.2B1.1GF1N1AF1VP1V1)
– Alt. Outboard Wing Tips (W1.2)
• Alt Nacelle Force Model Geometry (W1B1.1GF1N2AF2VP1V1)
– LH/RH Nacelles (N2)
– Alt. Aft Deck Flaps (AF2)
• Alt. Low Drag Model Geometry (W1.1B1.1GF1N1AF1VP1V2)
– Alt. Outboard Wing Tips (W1.1)
– LH/RH Verticals (V2)
• Inlet Plugs for Spillage Effects
– LH/RH Inlet Plugs (IP1) (SLA)
– LH/RH Inlet Plugs (IP2) (SLA)
– LH/RH Inlet Plugs (IP3) (SLA)



Figure 4.3-4. Performance Wind Tunnel Model and Associated Modular Part

4.4 Bodies of Revolution

Three bodies of revolution (BOR) wind tunnel models were fabricated to assess and calibrate the pressure rail instrumentation. These models each had defined near-field pressure signatures which would allow the identification of rail interference and wall reflection on the resultant measured signatures. The three BOR models were designated AS1, AS2, and AS3. The AS1 model was an existing Boeing model that has the advantages of simple geometry, a signature of the appropriate amplitude and a long constant section to monitor reflections and interferences. That model has 4 inches of shaped contour with an 80 PLdB signature. The AS2 model was a 200% scale version of AS1 to get 8 inches of signature and provide a correlation between the 30 and 60 inch offset distances proposed for the test. The AS3 model had an N+2 target signature derived from the development of BM1, was scaled by 50% to match the 8 inches of signature length and preserved the long constant cross section recovery aft of the model. Figure 4.4-1 shows a geometry comparison for the three BOR models. Photographs of the AS1, AS2, and AS3 models are shown in Figures 4.4-2, 4.4-3, and 4.4-4, respectively.

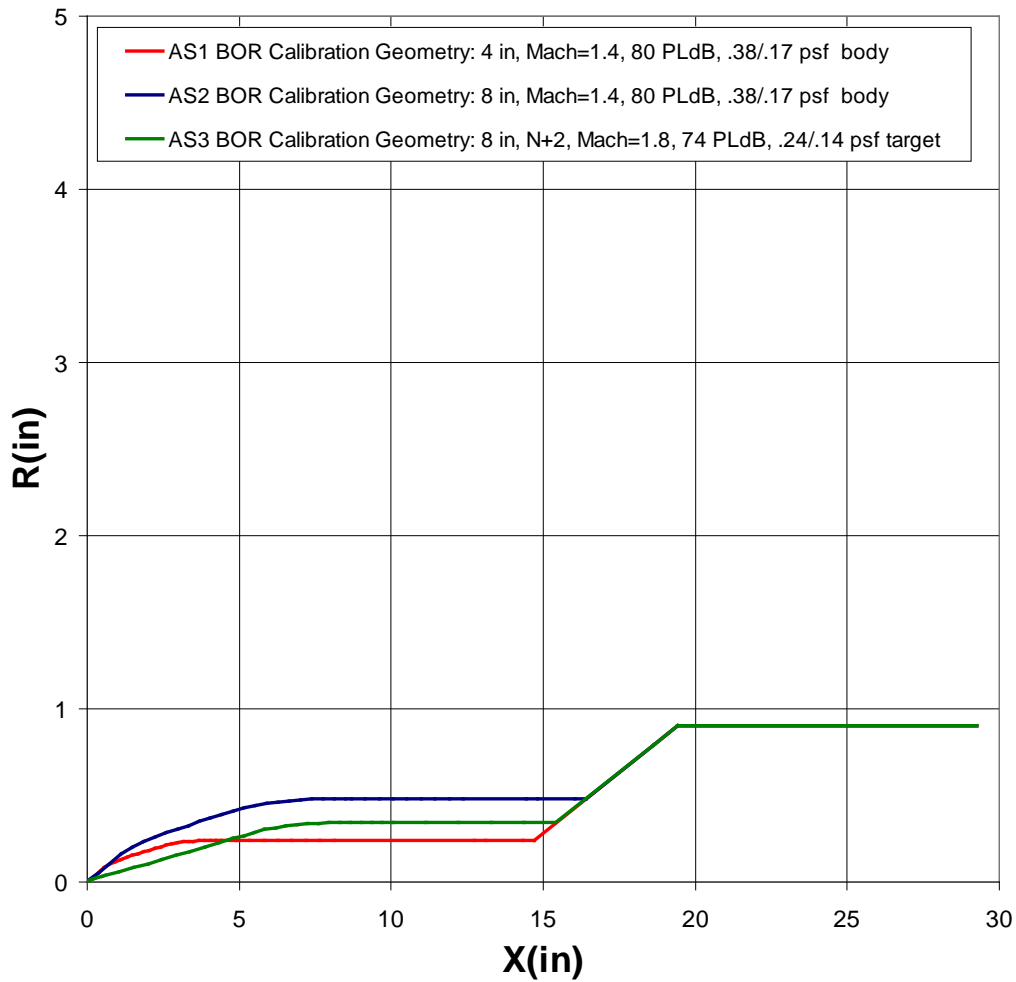


Figure 4.4-1. Geometric Comparison Between AS1, AS2, and AS3

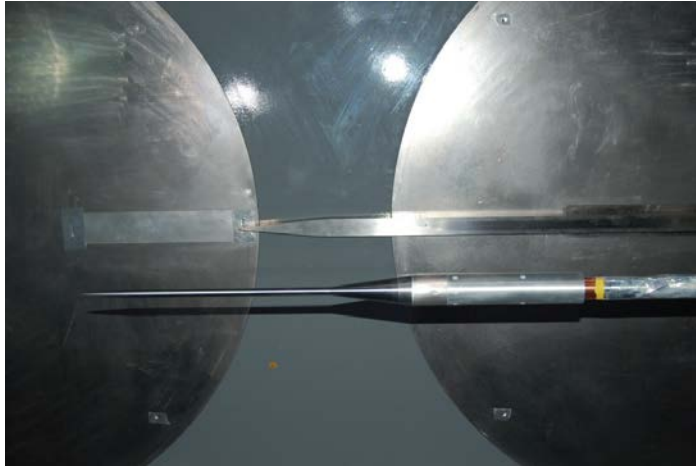


Figure 4.4-2. AS1 Model Installed in NASA Ames 9' x 7' Wind tunnel



Figure 4.4-3. AS2 Model Installed in NASA Ames 9' x 7' Wind tunnel

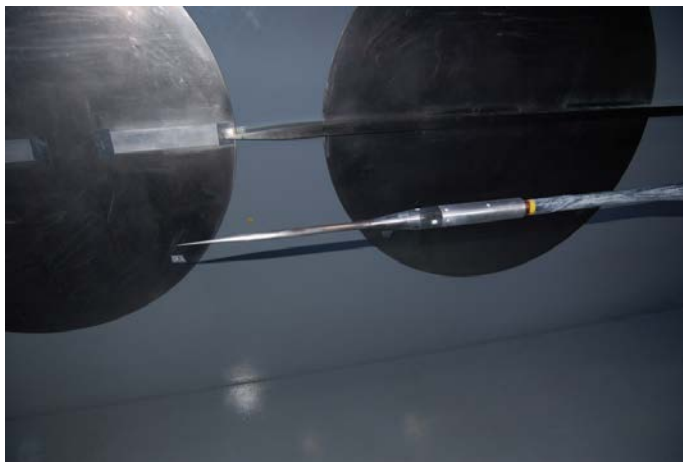


Figure 4.4-4. AS3 Model Installed in NASA Ames 9' x 7' Wind tunnel

5.0 EVALUATION OF EXISTING NASA PRESSURE RAILS

5.1 Overview

One ARRA-funded task of the contract was to evaluate the existing NASA pressure measurement rails using existing 2008 NASA Ames 9' x 7' supersonic wind tunnel data. The specific deliverable was defined as the following:

“The Contractor shall examine the data generated from recent NASA sonic boom tests (reference Section 4) that utilized the NASA sonic boom pressure rail and evaluate whether the NASA pressure rail is adequate for the proposed validation tests. The Contractor shall deliver a report containing the results and recommendations of the evaluation to NASA. The report shall address the overall data quality and criteria, test efficiency, and ease of integration with the existing tunnel(s). Government furnished information (GFI) is required for this task and shall be provided to the Contractor no later than January 31, 2010. Evaluation by the Contractor is not expected to start prior to Contractor receipt of GFI as stated above. The Contractor shall complete evaluation efforts within three months of receipt of GFI.”

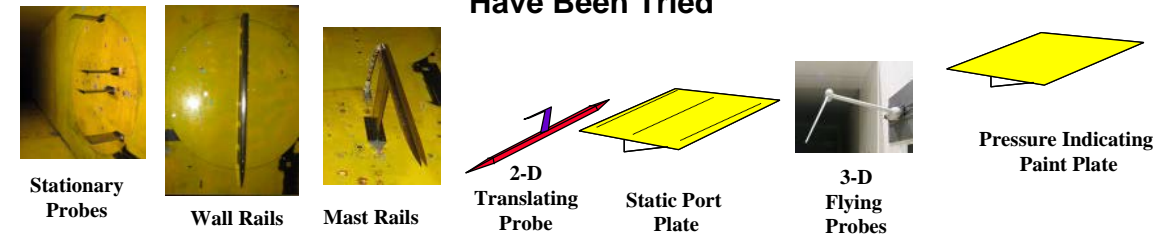
Off-body pressure measurement methods for sonic booms have been around for more than 50 years, and a variety of approaches have been used. Figure 5.1-1 shows some of the most common approaches. In addition to the three methods used in the Ames 2008 test (i.e., stationary probe, a wall rail and a mast rail), there have been methods utilizing 2D translating probes, plates with pressure belts, 3D translating and flying probes and pressure-indicating paint on plates. When selecting a methodology, a long list of considerations must be traded in accordance with the test objectives. Some methods offer less interference, others high productivity, others quicker installation time and so on. Although a comprehensive rating of each of these prior methods is possible and each method likely would have merit for some applications, this contract was directed specifically to evaluate the wall rail used in the 2008 NASA Ames 9' x 7' supersonic wind tunnel test. However, for completeness, the mast rail and the probes were also evaluated from that same 2008 wind tunnel test.

Boeing used the following criteria to evaluate the probe and the rails:

- Clean tunnel variation.
- Repeatability.
- Consistency of reflection factor.
- Complexity of installation.
- Flexibility to collect data at various heights.
- Influence of pressure gradients.
- Forebody shape.
- Productivity.

In the next three sections, each measurement device is evaluated against these criteria.

Multiple Off-Body Pressure Measurement Options Have Been Tried



Long list of considerations that must be traded

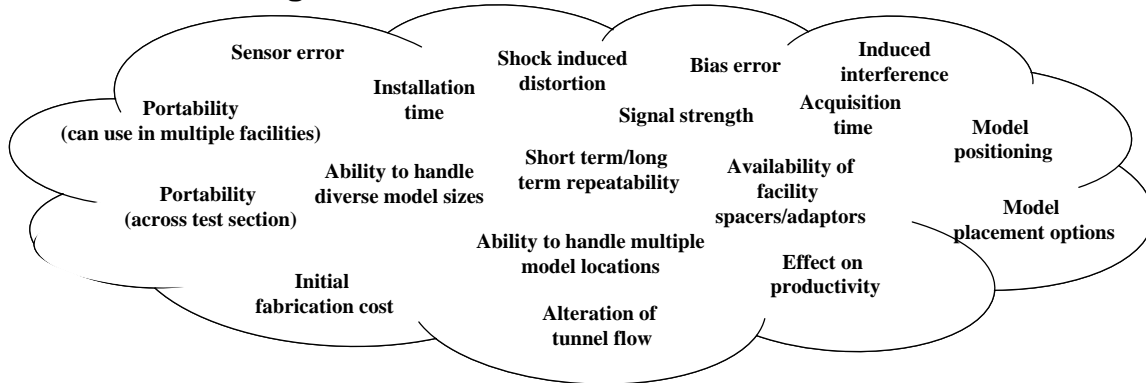


Figure 5.1-1. Examples of Past Sonic Boom Pressure Measurement Techniques and Factors That Determine Their Selection

5.2 Probe

During the 2008 NASA Ames sonic boom test at the 9' x 7' supersonic wind tunnel, single-pressure measurement probes were used for several configuration runs. These single-pressure probes were fixed to the wind tunnel wall, and the wind tunnel models were translated with a linear actuator past the probes to measure the full signature. One pressure probe was mounted on the centerline to capture the under-track near-field signature and two probes were mounted off-centerline to capture the off-track near-field signature. Figure 5.2-1 shows the probes installed in the 9' x 7' wind tunnel.

The resultant uncertainty developed from a number of repeat runs was ± 0.005 . This can be seen in the uncertainty plots shown in Figure 5.2-2.



- Single Probes**
- 3 for signatures
 - 1 centerline
 - 2 off ground track
 - 1 for reference

Ames probes with orifices located 10" from wall

201293-003

Figure 5.2-1. NASA Single Probes Used in the 2008 Sonic Boom Test

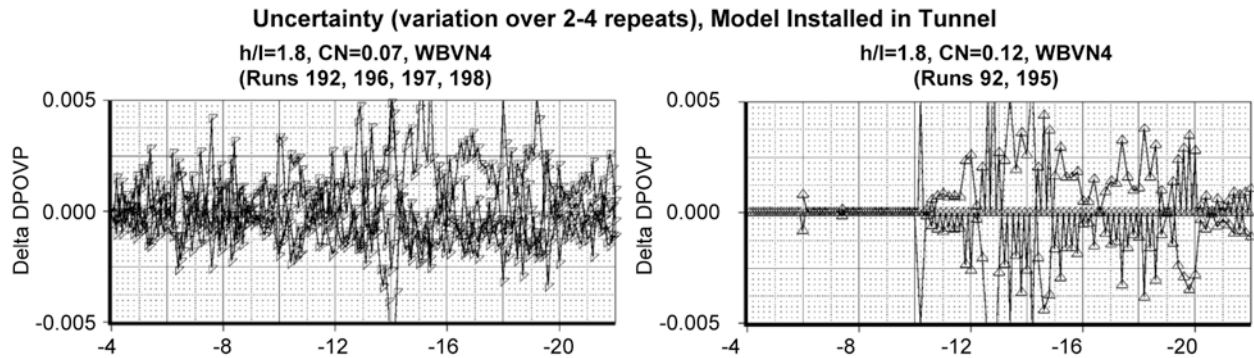


Figure 5.2-2. Single Probe Uncertainty Based on Repeat Run Data From 2008 Test

5.3 Wall Rail

During the 2008 NASA Ames sonic boom test at the 9' x 7' supersonic wind tunnel, a wall rail was used on many configurations during the test. The wall rail was fixed to the wind tunnel wall, was 5 feet long, extended 5.25 inches from the wall and included 385 pressure orifices spaced 1/8-in apart to measure the full signature at once. Figure 5.3-1 shows the wall rail installed in the 9' x 7' supersonic wind tunnel.

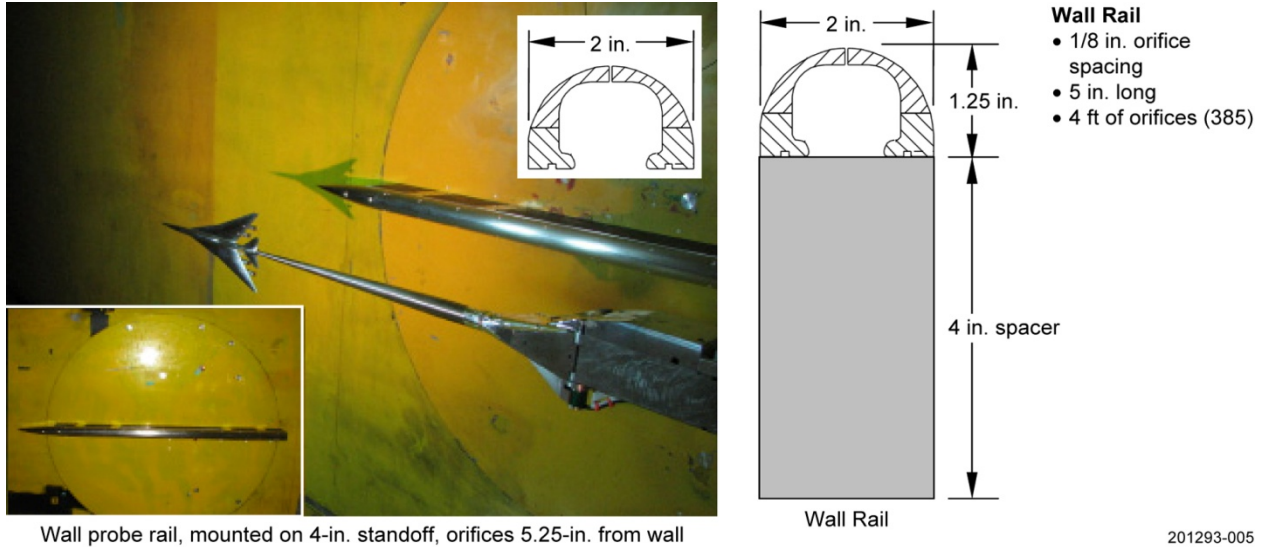


Figure 5.3-1. NASA Wall Rail Used in the 2008 Sonic Boom Test

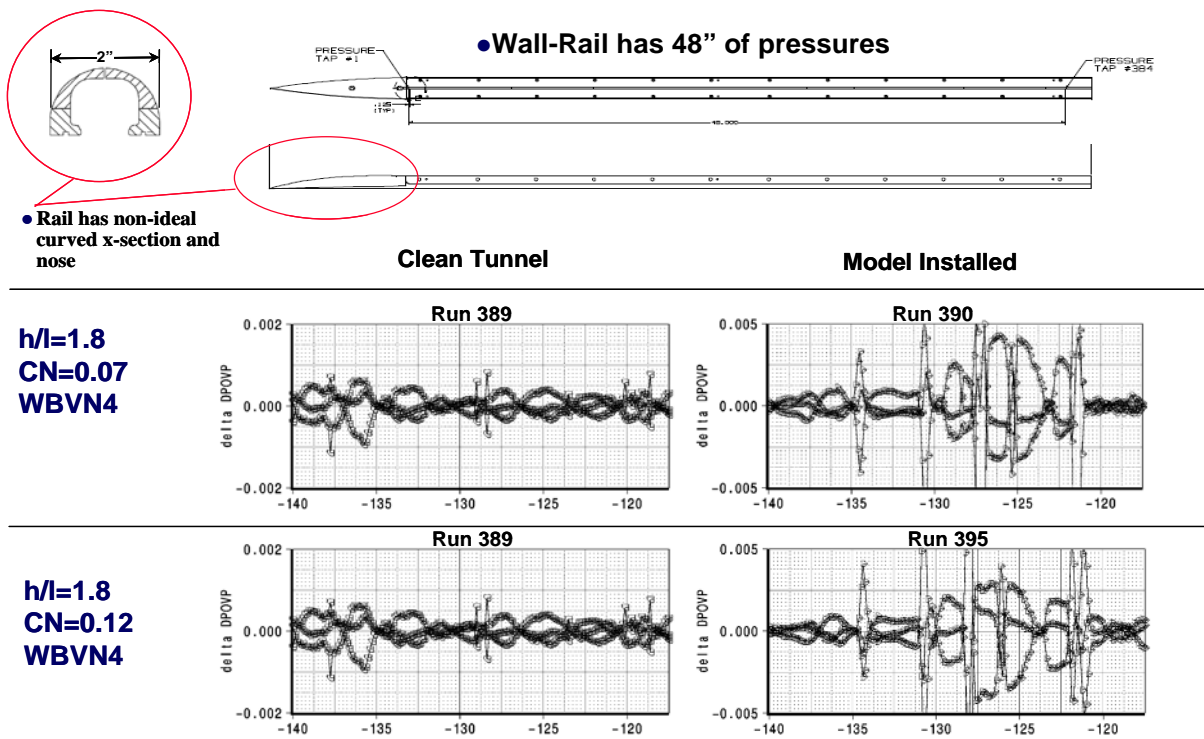


Figure 5.3-2. Wall Rail Uncertainty Based on Short-Term Repeatability From 2008 Test Data

Figure 5.3-2 shows the uncertainty for the wall rail in terms of short-term repeatability. The short-term repeatability uncertainty shown for the wall rail is in terms of a prediction interval. Typically, for each plot, the difference in dP/P for each rail static port is compared to a three-run average. The left-hand plots show the clean tunnel data, and the right-hand data show the change when a model signature is present. The resultant uncertainty of the clean tunnel data is ± 0.001 , whereas the uncertainty with the model in the tunnel is ± 0.005 .

5.4 Mast Rail

During the 2008 NASA Ames sonic boom test at the 9' x 7' supersonic wind tunnel, a mast rail also was used. The mast rail was fixed to the wind tunnel wall, was 3 feet long, extended 18 inches from the wall and included 160 pressure orifices spaced 1/8-inch apart to measure the full signature at once. Figure 5.4-1 shows the mast rail installed in the 9' x 7' wind tunnel.



Figure 5.4-1. NASA Mast Rail Used in the 2008 Sonic Boom Test

Figure 5.4-2 shows the mast rail uncertainty measured in terms of short-term repeatability. Shown here are similar short-term repeat data as were shown for the wall rail. The difference in dP/P for each rail static port is plotted compared to a three-run average. The resultant uncertainty of the data is ± 0.002 .

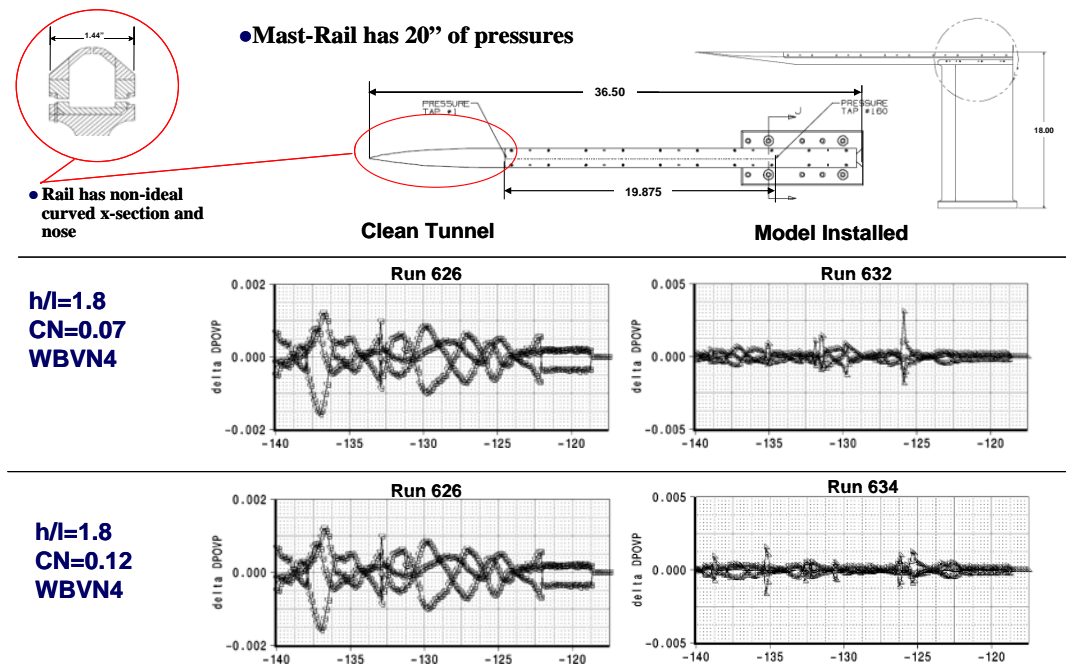


Figure 5.4-2. Mast Rail Uncertainty Based on Short-Term Repeatability From the 2008 Test Data

The prior uncertainty charts showed the respective uncertainties of the wall rail and mast rail in a quantitative way. Figure 5.4-3 illustrates similar data in a qualitative way and shows the repeatability of each rail type. These data are at the cruise lift coefficient.

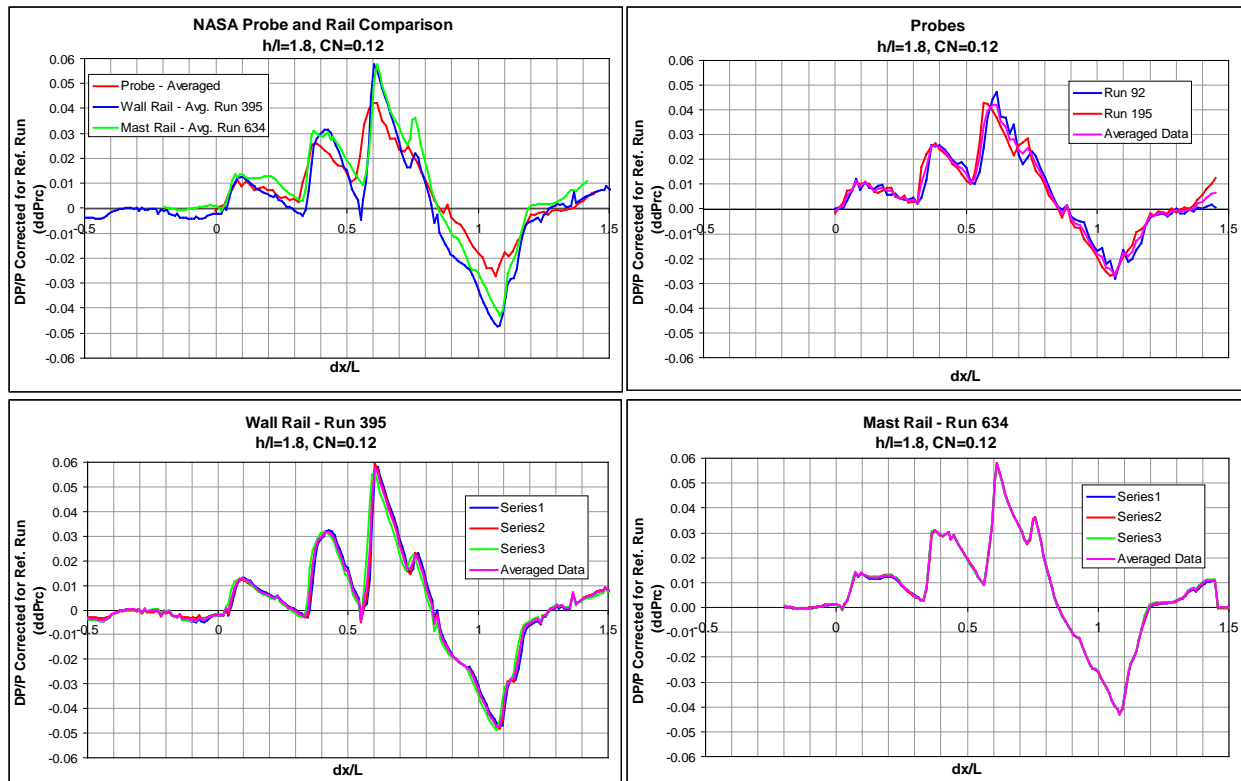


Figure 5.4-3. Qualitative Comparison of Uncertainty between the Single Probe, Wall Rail, and Mast Rail

In the upper left-hand figure is a comparison between averaged probe, averaged wall rail and averaged mast rail data. The upper right-hand figure shows two repeats of the pressure probe data compared to its average. In the lower right-hand figure, similar data (three repeats) are shown for the mast rail. The lower left-hand plot has the same data (three repeats) for the wall rail.

5.5 Results of Evaluation

The final acceptability evaluation is summarized in Figure 5.5-1. It is believed that the pressure measurement instrument used should be one that is good (green) in most areas and no worse than fair (yellow) everywhere else. There should be no fails (red). The existing wall rail fails in two areas: (1) consistency of reflection factor, and (2) forebody shape (i.e., induced interference).

Based on this evaluation, it was recommended that NASA design and fabricate a new pressure rail for future sonic boom validation testing. An improved 14" tall blade rail was subsequently fabricated and tested in later part of 2010.

Evaluation Criteria	NASA Probe	NASA Wall Rail	NASA Mast Rail
• Clean tunnel variation	●	●	●
• Repeatability	●	●	●
• Consistency of reflection factor	●	●	●
• Complexity of installation	●	●	●
• Flexibility to collect data at various heights	●	●	●
• Influence of pressure gradients	●	●	●
• Forebody shape	●	●	●
• Productivity	●	●	●

- Unacceptable
- Marginal
- Acceptable

Figure 5.5-1. Final Evaluation

6.0 NEW PRESSURE MEASUREMENT RAIL INSTRUMENTATION

6.1 Overview

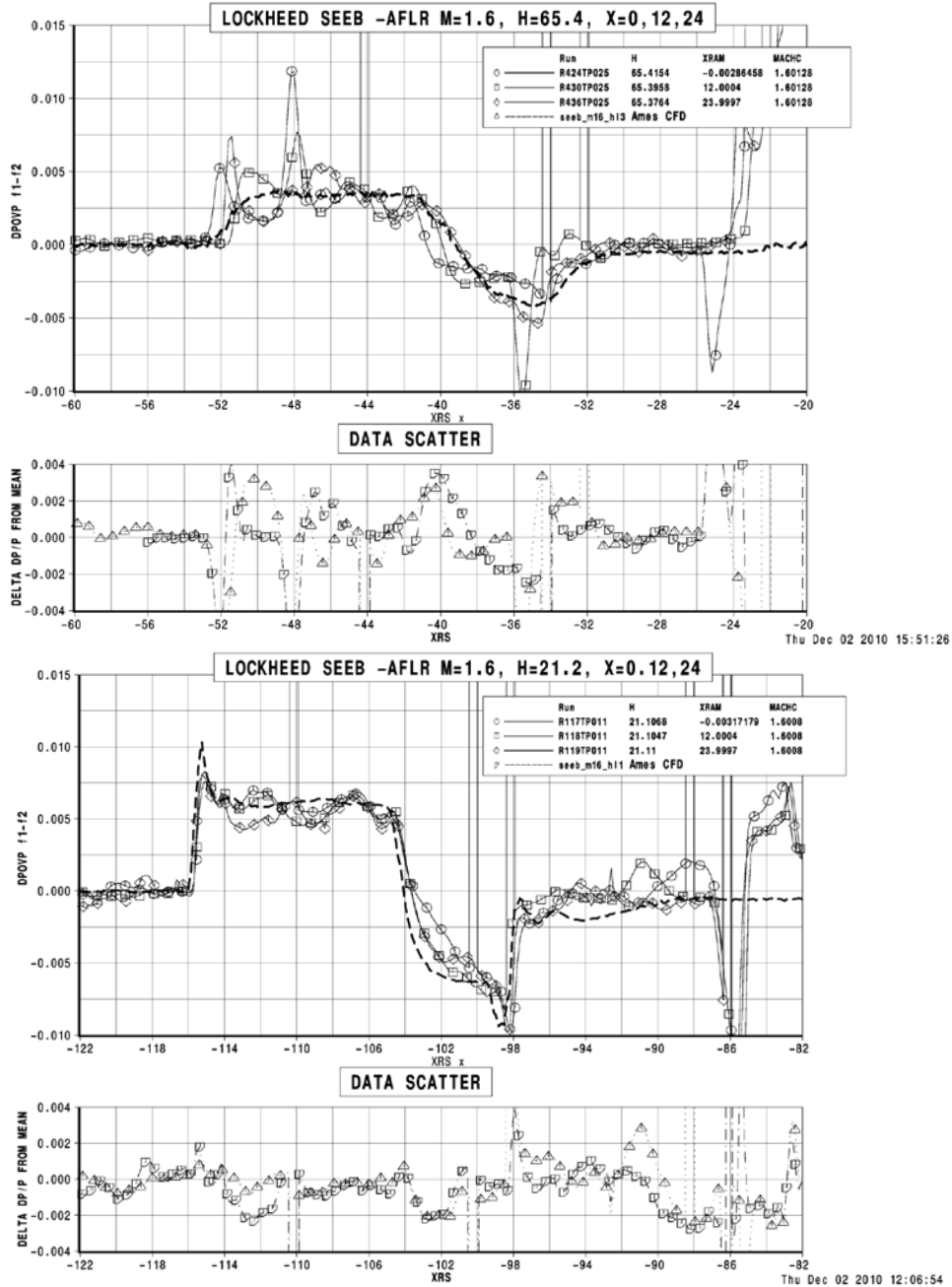
Based on the results of the evaluation of the existing NASA pressure rails, it was decided that a new pressure rail was needed. Boeing was contracted by NASA to design, fabricate and inspect a new pressure rail that would minimize the influence of rail interference on the incoming signature, provide a consistent reflection factor, was not unduly influenced by pressure gradients, had a simple installation, had flexibility to collect data at various heights and maximized test productivity. Several rail concepts were investigated during the design phase, including a 2" tall flat-topped rail (Boeing Concept) and a 14" tall blade rail (NASA Concept). The 14" tall blade rail was subsequently selected for fabrication. Tri Models Incorporated was subcontracted by Boeing to develop a detailed design of the 14" blade rail and then fabricate and inspect it. The rail was complete on Nov 1, 2010, and was shipped to the NASA Ames 9' x 7' wind tunnel for validation. The rail validation test (Ames Test AS-0220) was conducted from November 16, 2010 through December 2, 2010 as part of Lockheed Martin's statement of work. The test consisted of evaluating the rail against two body-of-revolution models and one NASA winged model (NASA Low-Boom Wing-Tail (LBWT) model). The rail validation test had several objectives.

- Evaluate suitability of the chosen rail for measuring signatures from models with different shapes and sizes.
- Demonstrate that this rail has improved accuracy over previously-tested pressure rails by showing that the shock reflection factor is consistently equal to 1.0 (within 10%) over the whole length of the rail.
- Characterize repeatability and show if it is improved over the previous rail data.
- Determine best techniques for getting good measurements with the rail; variables are:
 - Model longitudinal position (x) in tunnel (use traverse to vary by ± 12 inches).
 - Height (h/L) above the rail (in 9x7 horizontal plane).
 - Rail on forward or aft window blank.
 - Target humidity value.
 - Tolerance on holding humidity.
 - Frequency of reference runs to minimize tunnel flow variations over time, especially humidity.
- Identify/clarify issues associated with using the new rail in the cross flow/up flow environment of the 9x7 wind tunnel.
- Identify improvements of the new pressure rail over previous rails in terms of reducing the uncorrectable, adverse effects of the rail on the model shocks due to rail shape and size.

The rail validation test was very successful in gathering a significant data set to evaluate the 14" blade rail. It verified that the rail had a reflection factor of 1. Generally, the pressure data showed short-term repeatability from ± 0.0007 to ± 0.002 dP/P for the lower heights (<32") and ± 0.001 to ± 0.004 dP/P for the higher heights (>54"). This is about the same as the previous wall and mast rails. Correlation with CFD was generally good at the lower H/L's, although it did not capture all of the features in the wind tunnel data. Finally, humidity was found to have a big influence on the results. It was not only determined that humidity needs to be below 250 ppm, but that it should not vary more than ± 3 ppm within a run. In addition, the humidity for the model run should be within ± 3 ppm of the humidity for the reference run

utilized to reduce the data.

Although a lot of lessons-learned were acquired from the test, there was an observed disturbing variation in the signature with spatial location in the wind tunnel. It appeared random, but also seemed to have a sinusoidal variation with x-location in the tunnel and was more pronounced at larger H/L's. In addition, there were features in the data that were not captured with the CFD. An example of this is shown in Figure 6.1-1.



Based on these results, it appeared that the 14" rail was influencing the measured signature as a result of its size or possibly due to flow angularity (later it would be determined not to be the rail, but a number of things including flow quality, pressure lag, influence of the wind tunnel primary strut, etc). Boeing decided to use the 2" rail design for their validation test because of their experience with these types of rails in other test facilities. A new 2" rail was designed and fabricated by Tri Models Incorporated. Details about this rail are contained in section 7.3.

6.2 Blade Rail

The 14" blade rail was designed to attach to the sidewall window blanks at the NASA Ames 9' x 7' supersonic wind tunnel. The existing window blanks had a number of holes drilled in them from previous experiments, so new ones were fabricated for use with the 14" blade rail. Figure 6.2-1 shows a detailed diagram of the 14" blade rail attached to the new window blanks. The 14" blade rail was designed so that two 66" long pressure instrumented rail sections could be installed in the tunnel spanning both window blanks. However, only one instrumented rail section was fabricated due to cost constraints. The 14" blade rail is detailed in Figure 6.2-2. It is 90" long with 420 static pressure taps spaced 4 mm apart. It has an 18" leading edge section and a 6" trailing edge closeout section. It is interchangeable with either the front or aft window blank. A photograph of the 14" blade rail is shown in Figure 6.2-3.

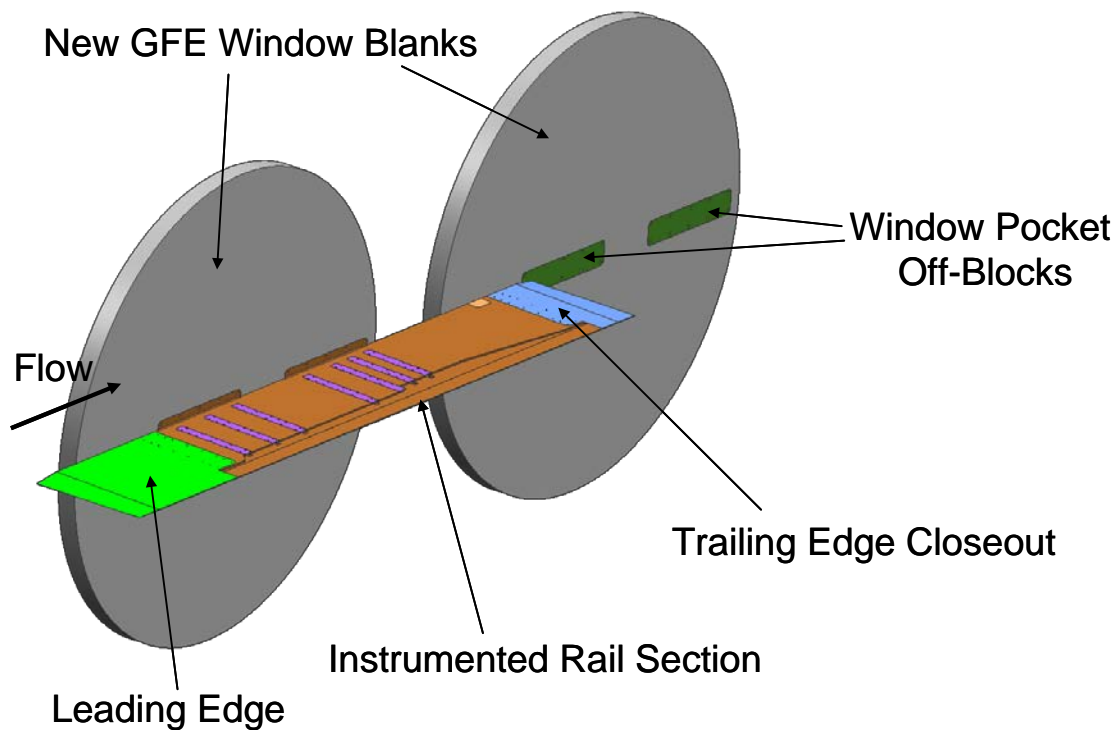


Figure 6.2-1. Installation of the 14" Blade Rail on the NASA Ames 9' x 7' Window Blanks

Key notable attributes of the 14" blade rail included a reflection factor of 1.0 (as a result of the small diameter top) and its 14" height, which minimizes the influence of the pressure signature by wall reflections for models shorter than approximately 35" at Mach numbers of 1.6. However, the 14" height does remove some H/L capability and the long pressure line lengths due to its size cause some pressure lag in the measurements.

- **Rail details:**
 - 14" from tunnel wall to tip
 - 0.050" radius tip
 - 3.5 deg included angle (1.0" base width)
 - 66" length
 - Pressure taps 4 mm (0.1575") apart
 - ~420 pressure taps
 - Leading edge and trailing edge closeout
 - Interchangeable with forward and aft window blanks

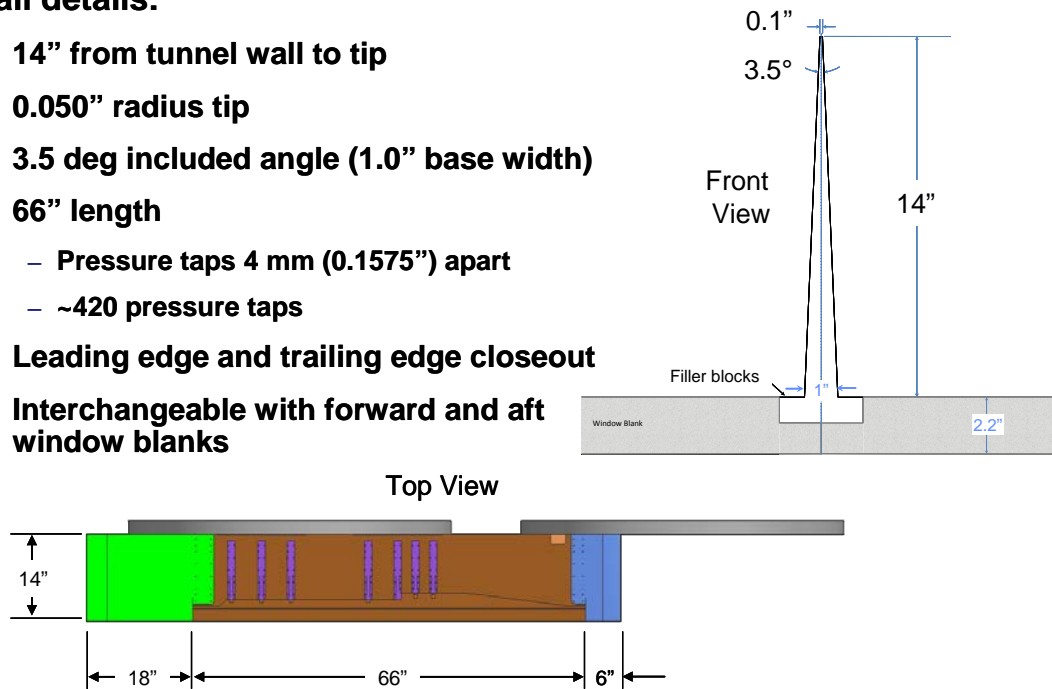


Figure 6.2-2. The 14" Pressure Instrumented Blade Rail



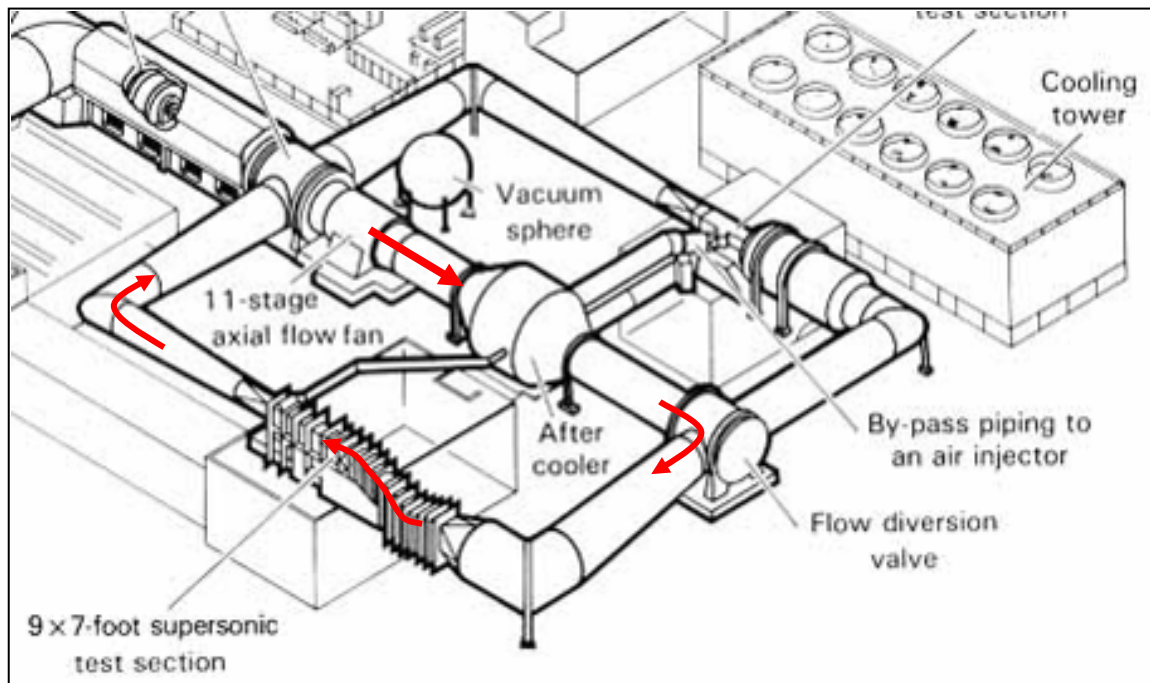
Figure 6.2-3. The 14" Blade Rail Installed in the NASA Ames 9' x 7' Wind Tunnel

7.0 VALIDATION WIND TUNNEL TEST

7.1 Overview

Compliant with Phase I, WBS 3.5 and 3.6, the planning and conduct of the experimental validation wind tunnel test of the QEVC boom and performance models were successfully completed on 22 April 2011. The validation test, referred to as Ames Test AS-0229, was conducted in the closed-return test circuit of the NASA Ames 9' x 7' supersonic wind tunnel complex at Moffett Field, California. This tunnel was chosen for its large, variable-density test section and its capability to provide extremely dry freestream flow conditions. The facility has also been used extensively in recent years for conducting other sonic boom explorations. An illustration of the facility layout is provided in Figure 7.1-1.

The test campaign, which began on 11 April and concluded on 22 April, was preceded by an extremely valuable series of monthly test-planning meetings held at the Ames test facility during the first quarter of 2011. Attended by Boeing, facility and customer representatives, the meetings were held to ensure that the intended test objectives, productivity and data quality expectations would be successfully met. Because these meetings were held concurrently with the preparation of the wind tunnel model and new ancillary hardware, issues associated with the interface of this new hardware with the wind tunnel were addressed and resolved in real time, resulting in a successful on-time integration of the test hardware.



Some Noteworthy Facility Attributes

- There are no screens or honeycomb upstream of nozzle
- The distance from the circuit elbow and nozzle is short
- The distance between the nozzle throat and test section is short
- The nozzle is asymmetric
- The test section has solid walls

Figure 7.1-1. NASA Ames 9' x 7' Supersonic Wind Tunnel Facility Layout

7.2 Test Objectives and Test Plan

The overarching purpose of the test was to experimentally validate the low sonic boom and performance characteristics of the QEVC (N+2 class) supersonic vehicle configuration that were established with CFD design and prediction tools. To accomplish this, the following test objectives were established.

- Validate and calibrate the operation of the new pressure rail using three Boeing-provided bodies-of-revolution models.
- Obtain pressure signatures from the boom and performance models.
- Obtain force data from the boom and performance models.
- Validate CFD design and prediction tools.
- Validate the productivity and data quality attributes of the NASA Ames 9' x 7' supersonic wind tunnel facility with regard to sonic boom testing.

The test was scheduled for 160 occupancy hours, over 2 weeks, on a two-shift- (first and third) per-day operation. Actual test metrics are provided in section 7.4. The “as-tested” test plan is shown in Table 7.2-1.

Table 7.2-1. As-Run Test Plan

+ 1 day →

		22:30	11:30	0:30	1:30	2:30	3:30	4:30	5:30	6:30	7:30	8:30	9:30	10:30	11:30	12:30	13:30				
		PM		AM						AM						PM					
		Third Shift: 10:30pm - 6:30am									First Shift: 6:30am - 2:30pm										
Mon. Fri		Prep Room 10 shifts																			
11	Mon	Install rail, leak & port check																			
12	Tue	AS1 Series 1 body of rev. calibration model config #1a (H=30 in, upflow, Forces undertrack, off track BOOM)									AS2 Series 2 body of rev. calibration model config #1c (H=30 in, upflow, Forces undertrack, off track BOOM)				AS3 Series 3 body of rev. calibration model config #1c (H=30 in, upflow, Forces undertrack, off track BOOM)						
13	Wed	W1/B1/N1/GF1/V1/VS1 Series 4 Full Configuration VS1 BM1 config #2 (H=30in, upflow, Forces undertrack, off track BOOM)									W1/B1/N1/GF1/V1/VS2 Series 5 Full Configuration VS2 BM1 config #4 (H=30in, upflow, Forces				W1/B1/GF1/V1/VS2 Series 6 Nac N1 Off BM1 config #5 (H=30in, upflow, Forces undertrack, off track BOOM)						
14	Thu	W1/B1/GF1/VS2 Series 7 Vert V1 & N1 Off BM1 config #7 (H=30in, upflow, Forces undertrack, off track BOOM)				W2/B2/N2/GF2/V2/VS2 Series 8 Full Configuration 2 BM2 config #9 (H=30in, upflow, Forces				W1/B1/N1/GF1/V1/VS2 Series 9 Full Configuration VS2 BM1 config #4 repeat (H=30in, upflow, Forces undertrack, off track BOOM)				CF Series 10 Cone (H=30)				AS3 Series 11 body of revolution calibration model config #1c repeat (H=30 in, upflow, Forces			
15	Fri	Add spacer: Deflection calibration of balance+stings and Models (check NF, PM)																			
18	Mon	AS2 (M=1.8) Series 13 body of rev. calibration model config #1b (H=60in/1525mm, upflow, Forces undertrack, off track BOOM)				AS3 Series 14 body of rev. calibration model config #1b (H=60in/1525mm, upflow, Forces				W1/B1/N1/GF1/V1/VS2 Series 15 Full Configuration BM1 config #4 (H=60in/1525mm, upflow, Forces				CF Series 16 Cone (H=60in/1525mm, upflow, Forces undertrack BOOM)				W1/B1/GF1/VS2 Series 17 Vert V1 & N1 Off BM1 config #7 (H=60in/1525mm, upflow, Forces			
19	Tues	W2/B2/N2/GF2/V2/VS2 Series 18 Full Configuration 2 BM2 config #9 (H=60in/1525mm, upflow, Forces undertrack, off track BOOM)				W1/B1/N1/GF1/V1/VS2 Series 19 Full Configuration VS2 BM1 config #4 repeat (H=60in/1525mm, upflow, Forces undertrack, off track BOOM)				Shift to Large Model				Shift to Large Model							
20	Wed	W1/B1.1/GF1 Series 20 Vert V1 & N1 Off PM config #1 (H=60in/1525mm, upflow, Forces undertrack, off track BOOM)				W1/B1.1/N1/GF1/V1 Series 21 Full Configuration PM config #3 (H=60in/1525mm, upflow, Forces undertrack, off track BOOM)				W1/B1.1/GF1/N1 Series 22 V-tail Off PM config #4 (H=60in/1525mm, upflow, Forces undertrack, off track BOOM)				W1/B1.1/GF1/V1 Series 23 Nac N1 Off, V-tail on PM config #2 (H=60in/1525mm, upflow, Forces undertrack, off track BOOM)				W1/B1.1/GF1/N2/V1 Series 24 Alternate Nacelle PM config #5 (H=60in/1525mm, upflow, Forces undertrack, off track BOOM)			
21	Thu	PM1_W1.3B1.1GF1N1V3 Series 25 low drag full confic PM config #9 (H=60in/1525mm, upflow, Forces undertrack, off track BOOM)				W1.3/B1.1/GF1 Series 26 low drag wing-body PM config #7 (H=60in/1525mm, upflow, Forces undertrack, off track BOOM)				W1/B1.1/GF1 Series 27 Vert V1 & N1 Off PM config #1-repeat (H=60in/1525mm, upflow, Forces undertrack, off track BOOM)				W1.1/B1.1/GF1 Series 28 Clipped Tip wing/body PM config #10 (H=60in/1525mm, upflow, Forces undertrack, off track BOOM)				W1.1/B1.1/N1/GF1/V1 Series 29 Clipped Tip full config PM config #12 (H=60in/1525mm, upflow, Forces undertrack, off track BOOM)			
22	Fri	W1/B1.1/N1/IP2/GF1/V1 Series 30 Inlet Plug spillage PM config #14 (H=60in/1525mm, upflow, Forces undertrack, off track BOOM)				AS1 Series 31 body of rev. calibration model config #1b undertrack, off track BOOM) Varying Machs, Pressures				AS1 Series 32 body of rev. calibration model config #1b undertrack, off track BOOM) Wall tape effect, multiple data point acq.				AS1 Series 33 Cone Fairing undertrack, off track BOOM) reference runs, multiple data point acq.							

7.3 Facility Hardware and Instrumentation

Pressure Rail

A new sonic boom pressure rail was fabricated for the AS-0229 test. The criteria considered in its design were minimal, clean-tunnel variation due to its presence in the tunnel test section, measurement repeatability, consistency of reflection factor, complexity of installation, future flexibility to collect data at various heights, its influence on pressure gradients, its forebody shape and productivity. Previous test results indicated that all of these criteria were either met or exceeded. The end product (the rail shown in fig. 7.3-1) was 96 inches long, 2 inches high and 1.5 inches wide, with a wedge-shaped forebody and closeout. The static pressure belt used for sonic boom signature measurement was 72 inches long, beginning at a point 18 inches aft of the rail nose, and consisted of 458 pressure orifices spaced 0.1575 inch apart, each with an internal diameter of 0.028 inch. Other dimensions of interest are shown in the figure. The modular design of the rail allows for potential future increases in rail height and pressure-surface width if desired.

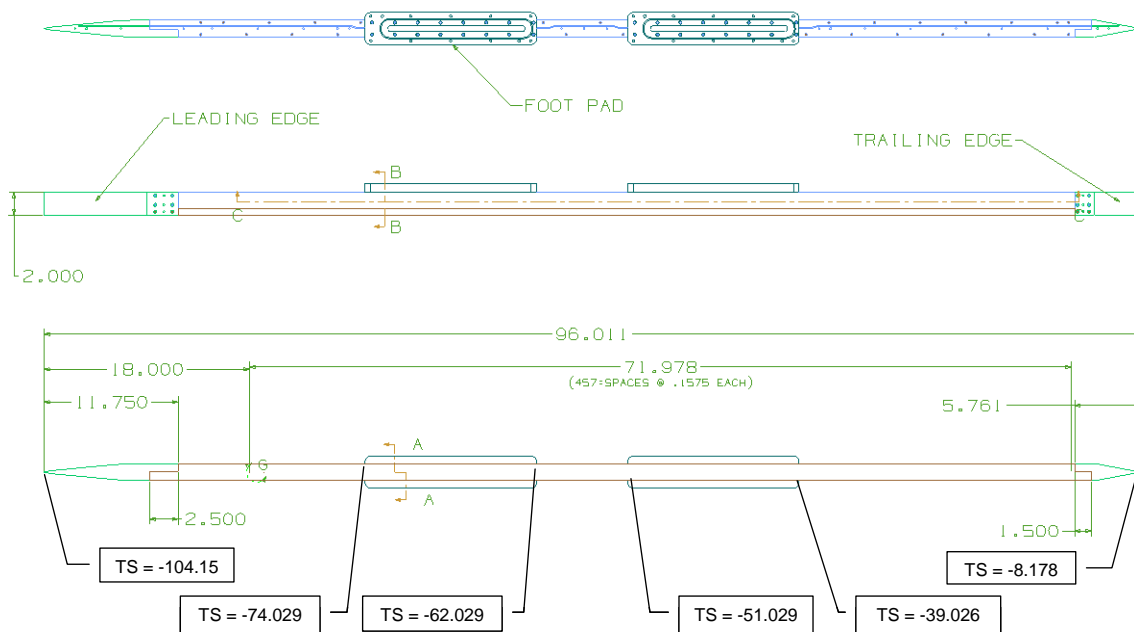


Figure 7.3-1. 2-in Sonic Boom Pressure Rail for AS-0229

The pressure rail was installed on the 9' x 7' north tunnel wall aft window blank for the entire AS-0229 test. Existing pockets in the window blank provided the interface to the two rail mounting pads. Pressure tubes from the 458 pressure orifices were routed from the rail through sealed passages in the window blank rail pockets to eight Ames-provided, 64-port PSI modules located just outside of the test section wall. An illustration and a photograph of the rail installation in the test section are shown in Figures 7.3-2 and 7.3-3, respectively.

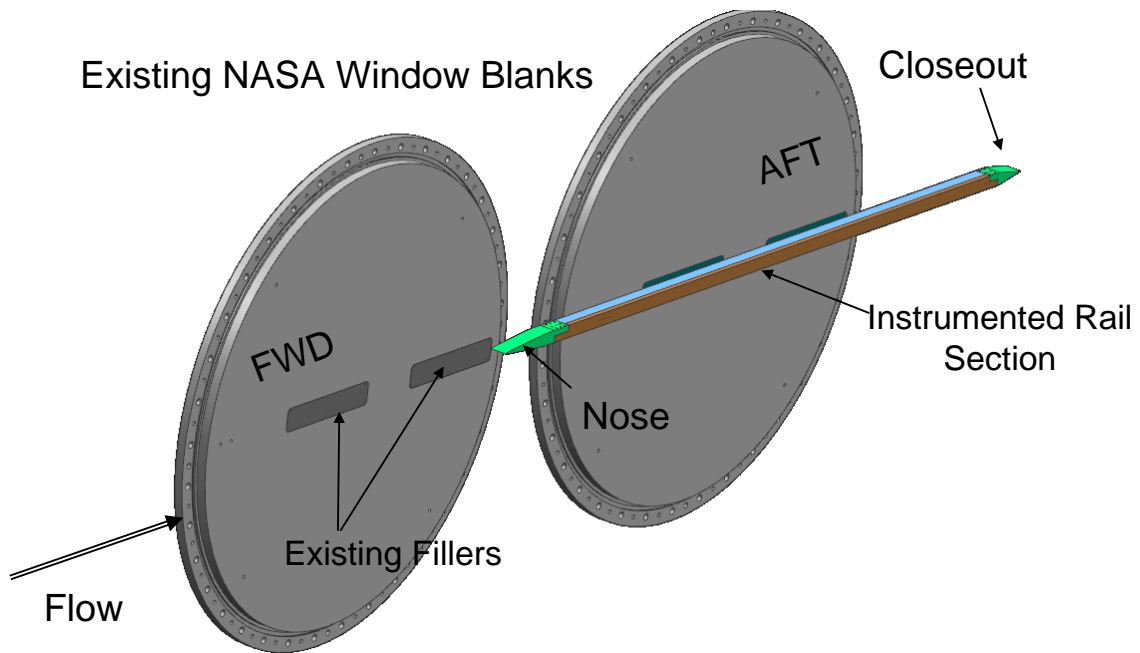


Figure 7.3-2. Installation of 2-in Sonic Boom Pressure Rail on North Wall Aft Window Blank



Figure 7.3-3. Photograph of the 2-in Sonic Boom Pressure Rail Installed in the NASA Ames 9' x 7' Test Section

Model Support Hardware

A new 28-inch-long sting and a 40-inch-long sting spacer were also provided for the AS-0229 test to accommodate the planned longitudinal and height positioning of the model in the test section relative to the pressure rail. A dimensional sketch of this hardware is shown in Figure 7.3-4. Figure 7.3-5 shows how these components integrated with the model and pressure rail in the test section. The sting was fabricated to mount to either the NASA-provided roll mechanism or to the forward end of the new spacer and to be compatible with the chosen balance. Both sting-alone and sting/spacer support sting configurations were tested.

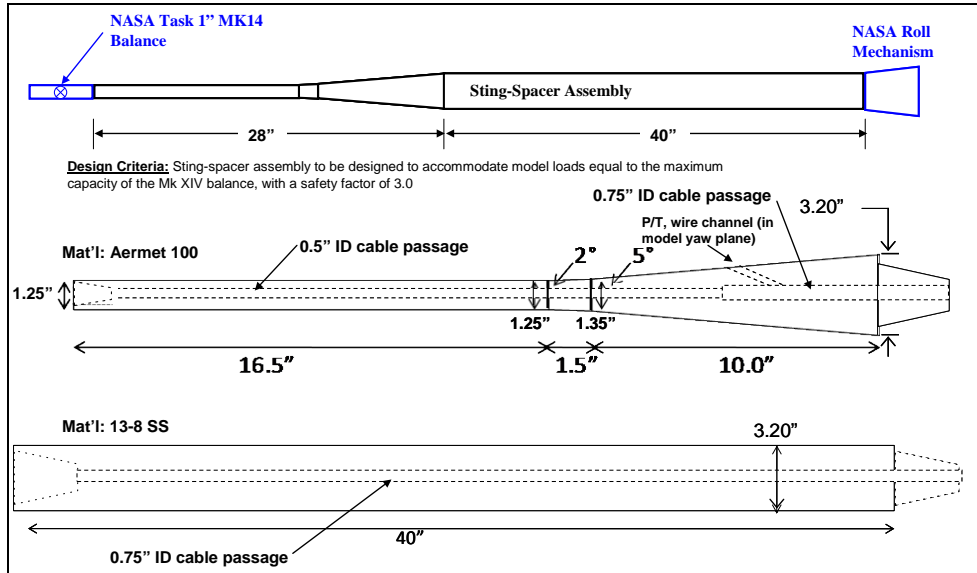


Figure 7.3-4. Sting and Sting Spacer Hardware

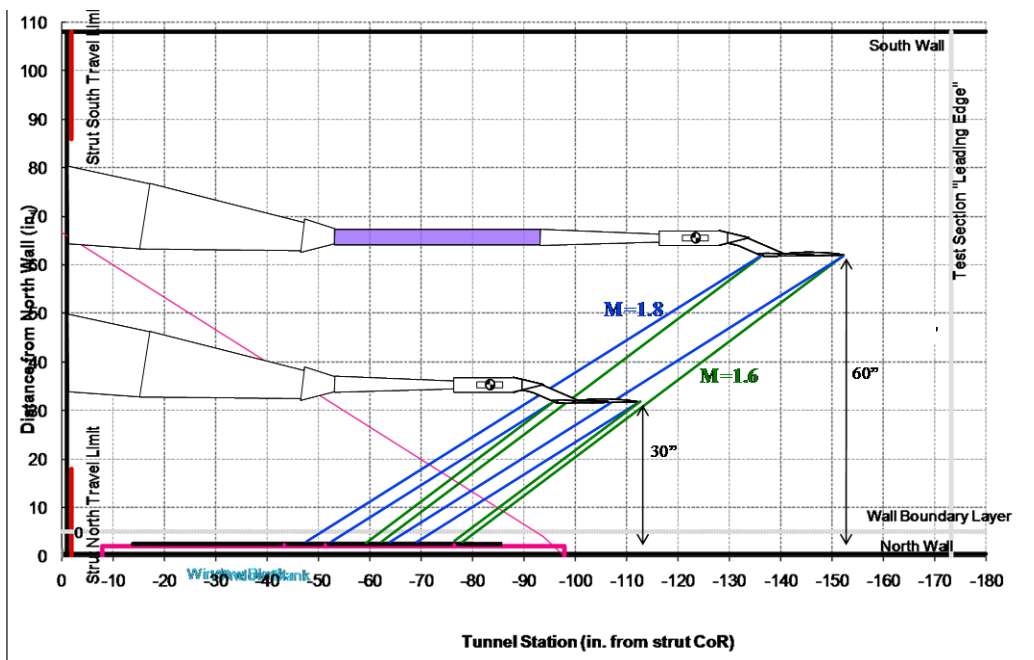


Figure 7.3-5. Installed Sting and Sting Spacer Hardware

Other model support hardware provided by NASA Ames for the AS-0229 test included their existing modified SR-57 sting adaptor, the “small model” roll mechanism with motion control system and a 1-in MK XIV C (Mk 14C) task balance (described below).

Instrumentation

The six-component, 1-inch diameter MK XIV C task balance was provided by Ames to measure model forces and moments. The force balance gage capacities were $N1/N2 = 400$ lb; $S1/S2 = 200$ lb; $RM = 250$ in-lb; and $AF = 100$ lb. The balance was calibrated by Triumph in March 2008 and its calibration verified using checkloading prior to model installation. No backup balance compatible with the QEVC models was available for the test; however, a backup was never needed.

Eight 5-psid 64-port ESP scanner modules were provided by Ames to measure the sonic boom rail pressures. The modules were de-ranged to 1.7 psid to improve the measurement resolution of the expected small sonic boom pressure signatures. A 15-psid, 64-port ESP scanner module located in the tunnel arc sector was also provided by Ames to measure the three on-board cavity pressures located at the forward end of the model sting (1 inch forward of the aft edge of the model).

A fouling circuit was installed at the forward end of the sting to detect model fouling. A thermocouple was also installed at the forward end of the strut at the balance interface to measure balance temperature at its back end. An attempt to place one at the forward end of the balance (on the model) was unsuccessful due to the wire continually becoming cut at the model-balance interface.

7.4 Test Performance and Productivity

Model Buildup

Before model installation in the test section, the balance, sting hardware and models were built up and checked out in a model preparation room (MPR) located in another building. Activities in the MPR included:

- Check-loading the balance installed on the sting with and without the 40-in spacer. Loads were applied to all six balance gages to verify the health of the balance and to determine the sting-bending characteristics used to calculate model AOA for the performance model in the tunnel.
- Characterizing the boom model deflections for both the short and long upper swept strut installations. Loads were applied to loading dimples on one of the installed boom models to determine the sting-bending characteristics used to calculate model AOA for the models in the tunnel.
- Acquiring “single-point” normal and side force check-loads for the balance/sting assembly for comparison with the same loads acquired in the test section (for troubleshooting purposes if necessary).
- Acquiring “single-point” normal force/pitching moment check-loads on the boom model for comparison in the test section (for troubleshooting purposes if necessary).
- Acquiring a “single-point” normal force check-load on the performance model for comparison in the test section (for troubleshooting purposes if necessary).
- Acquiring natural frequency characteristics for the boom model installed on the short and long struts. These data would be considered if excessive model dynamics were observed in the tunnel. However, actual model dynamics experienced during the test were manageable.
- Building up the starting configuration in preparation for installation.

Summary of Model Installations

NASA Ames tunnel personnel were responsible for the installation and checkout of all balance and support system hardware in the tunnel, while Boeing engineers were responsible for the preparation, installation and configuration changes of all models on the balance during the test. The starting configuration for the AS-0229 test was the AS1 Body of Revolution (BOR) model installed on the sting with no sting spacer to begin the nominal $H = 30$ inch (above-rail) evaluations. This was the first of three BOR models that were used to validate and calibrate the new pressure rail for sonic boom measurement. Boom Model 1 was first installed on the short (VS1) strut and then the long (VS2) strut to assess model-support system dynamics. Upon observing that the model dynamics for the long-strut installation were manageable, the decision was made to use that strut for the remainder of boom-model testing. The longer strut mitigated the contamination of the support hardware on the aft boom pressure signature. Four Boom Model 1 configurations and one Boom Model 2 configuration were installed and tested. A cone-fairing installation (for flow diagnostics) rounded out the $H = 30$ inch testing on the sting-only support system.

Models evaluated at the nominal $H = 60$ inches-above-rail height, using both the sting and spacer, were the AS1, AS2, and AS3 BOR models; the Boom Model 1 (2 configurations) and Boom Model 2 (1 configuration) models; the Performance Model 1 (10 configurations, following an initial lengthy one-shift installation); and the cone fairing. The AS1 model was reinstalled for diagnostic purposes at the end of the test. This configuration remained in the test section for follow-on NASA-Ames-funded testing that was performed after the conclusion of the AS-0229 test.

Photographs of the BM1 and PM1 wind tunnel models installed in the NASA Ames 9' x 7' wind tunnel are shown in Figures 7.4-1 and 7.4-2, respectively.



Figure 7.4-1. BM1 Model with VS2 Strut Installed in the NASA Ames 9' x 7' Wind Tunnel

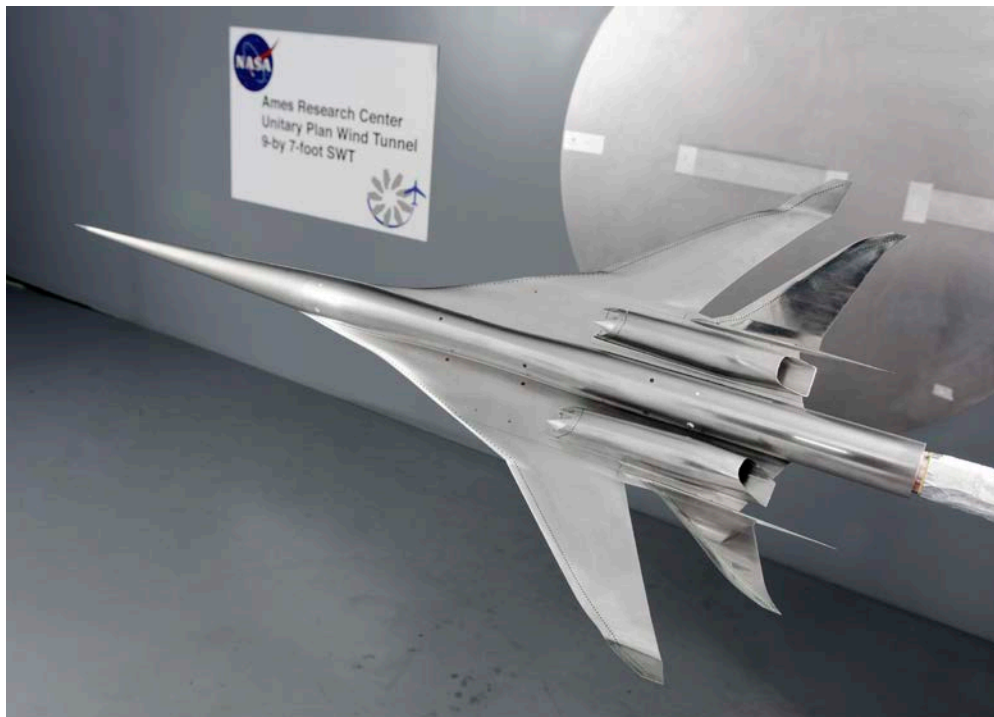


Figure 7.4-2. Sting Supported PM1 Model Installed in the NASA Ames 9' x 7' Wind Tunnel

Test Productivity

Test metrics, including facility downtime, were monitored and documented carefully and thoroughly throughout the AS-0229 test. This task was facilitated by having the Boeing test manager sit in close proximity to the tunnel operations crew, such that information and status were acquired and shared in real time. Access to the Ames test director and engineer logs also greatly aided this task. The categories associated with tunnel occupancy that were tracked included tunnel state (fan on/off and conditioning), model installation/removal and change times, and downtime (computation, instrumentation, operations, and test/data). These productivity records were documented in an Excel file called the Occ Log (ref. 25). The results from the Occ Log are summarized in tabular and graphical form in Figure 7.4-3 for convenience.

Productivity was high, especially considering the need for extensive drying time of the tunnel circuit to achieve the required low humidity levels. This can be inferred by comparison of the runs acquired per occupancy hour (6.2) vs. fan-on occupancy hour (15.4), considering lengthy model installation times but short model changes. Once on condition, the facility demonstrated an excellent run rate. Downtime was only ~8%, mostly attributable to operational and computing issues.

Test Conditions and Data Acquisition

The following nominal test conditions were established before the start of the test.

Mach	= 1.6 and 1.8.
Alpha	= -2 to +7 deg.
Beta	= -2 to +4 deg.
Phi	= 0, 15, 30, 45, 90, and 180 deg.
Pt (psf)	= 1450.
q (psf)	= 600 (Mach 1.6); 570 (Mach 1.8).
Re/ft (106)	= 2.87 (Mach 1.6); 2.71 (Mach 1.8).
Humidity	= 200 to 250 ppm; ± 3 ppm between reference and data runs.

The following data acquisition constants were established before the start of the test.

Model/pitch settling time	= 0.5 sec.
Samples per test point	= 30.
Sampling time (averaged)	= 2 sec.
Max pitch rate	= 3 deg/sec.
Average pitch rate	= 0.5 deg/sec.

The following data accuracy tolerances were established before the start of the test.

	<u>Required</u>	<u>Setting</u>
Mach number	±0.002	±0.002.
Total pressure	±1 psf	±1.5 psf (may not be attainable due to HP air addition).
Alpha	±0.05 deg	±0.05 deg (accuracy, Knuckle Sleeve Angle Source).
Beta	±0.05 deg	±0.05 deg (accuracy, Knuckle Sleeve Angle Source).
Roll	±0.1 deg	±0.1 deg.
Balance	±0.25% Full Scale (FS).	
PSI static pressures	<0.10% FS (expected); <0.05% FS (typical).	

Run Summary

A run summary that includes the nominal model setup information, wind tunnel conditions and run information (series, run number and data type) is provided in Table 7.4-1. The summary is reflective of the very comprehensive test matrix that was established for this test. The types of data runs that were acquired are categorized as shown below.

- “Inv” - Model inverted for assessment of flow angularity in the pitch plane.
- “Beta” - Model sideslip for assessment of flow angularity in the yaw plane.
- “force/press” - Model upright pitch sweep; model F&M (force and moment), flow angularity, sonic boom pressure signatures.
- “Reference” - Model up and away from pressure rail; serves as a tare for sonic boom pressure signature data.
- “Z sweep” - Height variation above pressure rail.
- “Roll sweep” - Assessment of off-track sonic boom pressure signature data.

Test Documentation

In addition to the aforementioned Occ Log, the Boeing test manager maintained a run log (ref. 26) that documented the as-run details and test conditions throughout the test and a test notes log (ref. 27) that served as a diary for the test, containing notes, observations, and progress of the test.

TEST METRICS			
	hr	%	% Total
Chargeable Fan-On	62.33	40.12	37.19
Chargeable Fan Off	44.60	28.71	26.61
Model Change	32.68	21.04	19.50
Install	15.75	10.14	9.40
Remove	0.00	0.00	0.00
Total Occupancy	155.37	100.00	92.70
Non-Occupancy			
	hr	%	% Total
Lunch	0.00	0.00	0.00
Computing	3.68	30.11	2.20
Design	0.00	0.00	0.00
Instr	0.92	7.49	0.55
Ops	6.70	54.77	4.00
Shop	0.00	0.00	0.00
Test/Data	0.93	7.63	0.56
Total	12.23	100.00	7.30
Test Total (hr)			
Total Series	29		
Total Data Runs	961		
Data Runs/Occ hr	6.19		
Data Runs/Fan-On hr	15.42		
Data Runs/Total hr	5.73		
Total Occ/Test Total	0.927		

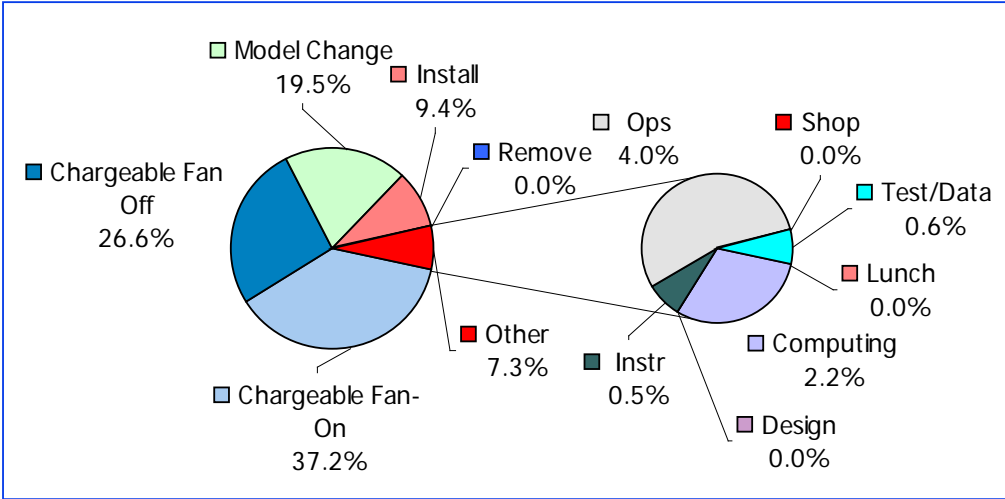


Figure 7.4-3. Ames AS0229 Test Productivity

Table 7.4-1. As-Run Summary

CFD Code	WT Code	Model Config	Series	Data	Bal	Re	Alpha	Trip	Roll Angle	Height	Mach No	
											1.60	1.80
<i>Rail Validation</i>												
AS1 Config #1a	1	AS1	1	inv	MKXIV	2.8	a1	TS0	180	30	74	94
				Beta	MKXIV	2.8	b1	TS0	0,90	30	75,76	95,96
				Reference	MKXIV	2.8	6	TS0	0	87.5	73,77,79, 81,83,86, 88,90,92	93,97,99, 101,103,106, 108,110,112
				force/press	MKXIV	2.8	a1	TS0	0	30	78,80,82, 87,89,91	98,100,102, 107,109,111
				Zsweep	MKXIV	2.8	a2	TS0	0	24-36	84,85	104,105
AS2 Config #1b	2	AS2	2	inv	MKXIV	2.8	a1	TS0	180	30	116	136
				Beta	MKXIV	2.8	b1	TS0	0,90	30	117,118	137, 138
				Reference	MKXIV	2.8	6	TS0	0	87.5	115, 119,121, 123, 125, 128, 130, 132, 134	139, 141, 143, 145, 148, 151, 153, 155
				force/press	MKXIV	2.8	a1	TS0	0	30	120, 122, 124, 129, 131, 133	140, 142, 144, 150, 152, 154
				Zsweep	MKXIV	2.8	a2	TS0	0	24-36	126, 127	147, 149
AS3 Config #1c	3	AS3	3	inv	MKXIV	2.8	a1	TS0	180	30	158	178
				Beta	MKXIV	2.8	b1	TS0	0,90	30	159, 160	179, 180
				Reference	MKXIV	2.8	6	TS0	0	87.5	157, 161, 163, 165, 167, 170, 172, 174, 176	177, 181, 183, 185, 187, 190, 192, 194, 196
				force/press	MKXIV	2.8	a1	TS0	0	30	162, 164, 166, 171, 173, 175,	182, 184, 186, 191, 193, 195
				Zsweep	MKXIV	2.8	a2	TS0	0	24-36	168, 169	188, 189

Table 7.4-1. As-Run Summary (Continued)

CFD Code	WT Code	Model Config	Series	Data	Bal	Re	Alpha	Trip	Roll Angle	Height	Mach No	
											1.60	1.80
<i>Boom Model 1 - Pressure & Force</i>												
BM1 Config#2	4	BM1_W1 B1 GF1 N1 V1 VS1	4	inv	MKXIV	2.8	a3	TS0	180	30	204,255	236
				Beta	MKXIV	2.8	b1	TS0	0	30	205,256	238
				Beta	MKXIV	2.8	b1	TS0	90	30	206,257	237
				Reference	MKXIV	2.8	6	TS0	0	83.5	202, 207, 209, 211, 213, 214, 216, 221, 224, 226, 254	229,231,233, 235,239,244, 246,249,251, 253
				force/press	MKXIV	2.8	a4	TS0	0	30	208,210,212 215,223,225	230,232,234, 245,250,252
				Roll sweep	MKXIV	2.8	a5	TS0	0-45	30	259,260, 261,262	240,241, 242,243
				Zsweep	MKXIV	2.8	a6	TS0	0	24-36	218,219	247,248
BM1 Config#4	5	BM1_W1 B1 GF1 N1 V1 VS2	5	inv	MKXIV	2.8	a3	TS0	180	30	264	283
				Reference	MKXIV	2.8	6	TS0	0	85.7	265, 268,270, 274,279	284, 287, 289, 293, 297
				force/press	MKXIV	2.8	a4	TS0	0	30	266,267,269, 280,281,282	285, 286, 288, 298, 299, 300
				Roll sweep	MKXIV	2.8	a5	TS0	0-45	30	271, 272, 273	290, 291, 292
				Zsweep	MKXIV	2.8	a6	TS0	0	24-36	276,277,278	294, 295, 296
BM1 Config#5	6	BM1_W1 B1 GF1 V1 VS2	6	Reference	MKXIV	2.8	6	TS0	0	85.7	302, 305, 309, 313, 317	321, 324, 326, 330, 334
				force/press	MKXIV	2.8	a4	TS0	0	30	303, 304, 306, 318, 319, 320	322, 323, 325, 335, 336, 337,
				Roll sweep	MKXIV	2.8	a5	TS0	0-45	30	310, 311, 312	327, 328, 329
				Zsweep	MKXIV	2.8	a6	TS0	0	24-36	314, 315, 316	331, 332, 333
BM1 Config#7	7	BM1_W1 B1 GF1 VS2	7	Reference	MKXIV	2.8	6	TS0	0	83.5	348, 351, 353, 357	361, 364, 366, 370
				force/press	MKXIV	2.8	a4	TS0	0	30	349, 350, 352	362, 363, 365
				Roll sweep	MKXIV	2.8	a5	TS0	0-45	30	354, 355, 356	367, 368, 369
				Zsweep	MKXIV	2.8	a6	TS0	0	24-36, 42,48	358, 359, 360	371, 372, 373

Table 7.4-1. As-Run Summary (Continued)

CFD Code	WT Code	Model Config	Series	Data	Bal	Re	Alpha	Trip	Roll Angle	Height	Mach No	
											1.60	1.80
<i>Boom Model 2 - Pressure & Force</i>												
BM2 Config#9	8	BM2_W2 B2 GF2 N2 V2 VS2	8	Reference	MKXIV	2.8	r1	TS0	0	85.7	382, 385, 387,391	397, 400, 402, 406
				force/press	MKXIV	2.8	a4	TS0	0	30	383, 384, 386	398, 399, 401
				Roll sweep	MKXIV	2.8	a5	TS0	0-45	30	388, 389, 390	403, 404, 405
				Zsweep	MKXIV	2.8	a6	TS0	0	24-36, 42,48	394, 395, 396	407, 408, 409
<i>Repeats</i>												
BM1 Config#4	5	BM1_W1 B1 GF1 N1 V1 VS2	9	Reference	MKXIV	2.8	r1	TS0	0	85.7	415,418,420, 424	428, 431,433, 437
				force/press	MKXIV	2.8	a4	TS0	0	30	416, 417,419	429,430, 432
				Roll sweep	MKXIV	2.8	a5	TS0	0-45	30	421, 422, 423	434, 435, 436
				Zsweep	MKXIV	2.8	a6	TS0	0	24-36, 42,48	425, 426, 427	438, 439, 440
8 deg Cone Fairing	3	CF	10	Reference	MKXIV	2.8	r1	TS0	0	87.5		
				Zsweep	MKXIV	2.8	0	TS0	0	18-36, 42,48	442,443,444	445,446,447
				Zsweep	MKXIV	2.8	3.2	TS0	0	18-36, 42,48	451,452,453	448,449,450
AS3 Config #1c	3	AS3	11	Reference	MKXIV	2.8	r1	TS0	0	87.5	459	463
				Zsweep	MKXIV	2.8	a6	TS0	0	24-36, 42,48	460, 461, 462	464,465,466
<i>Add spacer</i>												
AS1 Config #1a	1	AS1	12	Reference	MKXIV	2.8	r1	TS0	0	90	483, 485, 487, 489, 491, 493	496, 498, 500, 502, 504, 506
				Zsweep	MKXIV	2.8	a6	TS0	0	54-66	484, 486, 488, 490, 492, 494	497, 499, 501, 503, 505, 507
				Zsweep-no ref runs	MKXIV	2.8	a6	TS0	0	54-66	509, 510, 511	514, 515, 516, 517
AS1 Config #1b	2	AS2	13	inv	MKXIV	2.8	a1	TS0	-180	60	524, 525	544, 545
				inv	MKXIV	2.8	a1	TS0	-180	30	528, 529	548, 549
				Beta	MKXIV	2.8	a2	TS0	90	60	526, 527	546, 547
				Reference	MKXIV	2.8	r1	TS0	0	87	523, 530, 532, 534, 536, 538, 540, 542	543, 553,555,557, 559,561,563
				Zsweep	MKXIV	2.8	a6	TS0	0	54-66	531, 533, 535, 537, 539, 541	554,556,558, 560,562,564

Table 7.4-1. As-Run Summary (Continued)

CFD Code	WT Code	Model Config	Series	Data	Bal	Re	Alpha	Trip	Roll Angle	Height	Mach No	
											1.60	1.80
AS1 Config #1c	3	AS3	14	Reference	MKXIV	2.8	r1	TS0	0	87	571,573,575, 577,579,581,583	584,586,588, 590,592,594,596
				Zsweep	MKXIV	2.8	a6	TS0	0	54-66	572,574,576 578,580,582	585,587,589, 591,593,595
BM1 Config#4	5	BM1_W1 B1 GF1 N1 V1 VS2	15	Reference	MKXIV	2.8	r1	TS0	0	87	602,608,610,614	621, 628, 630, 634,
				inv	MKXIV	2.8	a9	TS0	-180	60	605	625
				inv	MKXIV	2.8	a9	TS0	-180	30	619	638
				Beta	MKXIV	2.8	b1	TS0	0	60	603	622
				Beta	MKXIV	2.8	b2	TS0	90	60	604	624
				force/press	MKXIV	2.8	a3	TS0	0	60	606, 607,609	626,627,629
				force/press	MKXIV	2.8	a3	TS0	0	30	620	639
				Roll sweep	MKXIV	2.8	a5	TS0	0-45	60	611,612,613	631,632,633
8 deg Cone Fairing	3	CF	16	Zsweep	MKXIV	2.8	a6	TS0	0	54-66	615,616,618	635,636,637
				Reference	MKXIV	2.8	r1	TS0	0	87.5	644,647	654
				Zsweep	MKXIV	2.8	0	TS0	0	54-66	645,648,649,650	655,656,657
BM1 Config#7	10	BM1_W1 B1 GF1 VS2	17	Zsweep	MKXIV	2.8	3.2	TS0	0	54-66	651,652,653	658,659,660
				Reference	MKXIV	2.8	r1	TS0	0	87	669, 672, 674, 678	682, 685, 687, 691
				force/press	MKXIV	2.8	a3	TS0	0	60	670, 671, 673	683, 684, 686
				Roll sweep	MKXIV	2.8	a5	TS0	0-45	60	675, 676, 677	688, 689, 690
BM2 Config#9	8	BM2_W2 B2 GF2 N2 V2 VS2	18	Zsweep	MKXIV	2.8	a6	TS0	0	54-66	679, 680, 681	692, 693, 694
				Reference	MKXIV	2.8	r1	TS0	0	87	700, 704, 708	714, 718, 722
				force/press	MKXIV	2.8	a3	TS0	0	60	701, 702, 703	715, 716, 717
				Roll sweep	MKXIV	2.8	a5	TS0	0-45	60	705, 706, 707	719, 720, 721
Repeats	5	BM1_W1 B1 GF1 N1 V1 VS2	19	Zsweep	MKXIV	2.8	a6	TS0	0	54-66	711, 712, 713	723, 724, 725
				Reference	MKXIV	2.8	r1	TS0	0	90	731, 735	737, 741
BM1 Config#4	5	BM1_W1 B1 GF1 N1 V1 VS2	19	force/press	MKXIV	2.8	a3	TS0	0	60	732, 734, 736	739, 740, 742

Table 7.4-1. As-Run Summary (Continued)

CFD Code	WT Code	Model Config	Series	Data	Bal	Re	Alpha	Trip	Roll Angle	Height	Mach No	
											1.60	1.80
<i>New Boom Model Pressure & Force</i>												
PM1 Config#1		PM1_W1B1.1GF1	20	inv	MKXIV	2.8	a1	TS1	180	60	763	791
				stream	MKXIV	2.8	a2	TS1	0	60	764	792
				Beta	MKXIV	2.8	a2	TS1	0	60	760, 761	789
				Beta	MKXIV	2.8	a2	TS1	90	60	762, 766	790
				Reference	MKXIV	2.8	r1	TS1	0	90	758, 767, 769, 771, 773, 778, 780, 783, 785, 787	788, 793, 795, 797, 799, 806, 809, 811, 813
				force/press	MKXIV	2.8	a12,a14	TS1	0	60	768, 770, 772, 779, 784, 786	794, 796, 798, 805, 810, 812
				Roll sweep Zsweep	MKXIV	2.8	a13 a15	TS1	0-45 0	60 54-66	774, 775, 776, 777 781, 782	800, 801, 802, 803 807, 808
PM1 Config#3		PM1_W1B1.1GF1N1V1	21	Reference	MKXIV	2.8	r1	TS1	0	90	819, 821, 823, 825, 830, 832, 835, 837, 839	840, 842, 844, 846, 851, 853, 856, 858, 860
				force/press	MKXIV	2.8	a12,a14	TS1	0	60	820, 822, 824, 831, 836, 838	841, 843, 845, 852, 857, 859
				Roll sweep Zsweep	MKXIV	2.8	a13 a15	TS1	0-45 0	60 54-66	826, 827, 828, 829 833, 834	847, 848, 849, 850 854, 855
				Reference	MKXIV	2.8	r1	TS1	0	90	866,868,870,872,877,879,882,884,886	887,889,891,893,898,901
PM1 Config#4		PM1_W1B1.1GF1N1	22	force/press	MKXIV	2.8	a12,a14	TS1	0	60	867,869,871,878,883,885	888,890,892
				Roll sweep Zsweep	MKXIV	2.8	a13 a15	TS1	0-45 0	60 54-66	873,874,875,876 880,881	894,895,896,897 899,900
				Reference	MKXIV	2.8	r1	TS1	0	90	906, 908, 910 912, 917, 920	921, 923,925, 927, 935
				force/press	MKXIV	2.8	a12,a14	TS1	0	60	907,909, 911	922, 924, 926
PM1 Config#2		PM1_W1B1.1GF1V1	23	Roll sweep Zsweep	MKXIV	2.8	a13 a15	TS1	0-45 0	60 54-66	913, 914, 915 918, 919	928, 929, 930, 931 933, 934

Table 7.4-1. As-Run Summary (Continued)

CFD Code	WT Code	Model Config	Series	Data	Bal	Re	Alpha	Trip	Roll Angle	Height	Mach No	
											1.60	1.80
PM1 Config#5		PM1_W1B1.1GF1N2V1	24	Reference	MKXIV	2.8	r1	TS1	0	90	942, 944, 946, 948, 953, 956	957, 959, 961, 963, 968, 971
				force/press	MKXIV	2.8	a3	TS1	0	60	943, 945, 947	958, 960, 962
				Roll sweep	MKXIV	2.8	a5	TS1	0-45	60	949, 950, 951, 952	964, 965, 966, 967
				Zsweep	MKXIV	2.8	a2,24,3,6	TS1	0	54-66	954, 955	969, 970
PM1 Config#9		PM1_W1.3B1.1GF1N1V3	25	Reference	MKXIV	2.8	r1	TS1	0	90	979, 981, 983, 985, 990, 993	994, 996, 998, 1000, 1005, 1008
				force/press	MKXIV	2.8	a3	TS1	0	60	980, 982, 984	995, 997, 999
				Roll sweep	MKXIV	2.8	a5	TS1	0-45	60	986, 987, 988, 989	1001, 1002, 1003, 1004
				Zsweep	MKXIV	2.8	a6	TS1	0	54-66	991, 992	1006, 1007
PM1 Config#7		PM1_W1.3B1.1GF1	26	Reference	MKXIV	2.8	r1	TS1	0	90	1014, 1016, 1018, 1020, 1025, 1028	1029, 1031, 1033, 1035, 1040, 1043
				force/press	MKXIV	2.8	a3	TS1	0	60	1015, 1017, 1019	1030, 1032, 1034
				Roll sweep	MKXIV	2.8	a5	TS1	0-45	60	1021, 1022, 1023, 1024	1036, 1037, 1038, 1039
				Zsweep	MKXIV	2.8	a6	TS1	0	54-66	1026, 1027	1041, 1042
PM1 Config#1		PM1_W1B1.1GF1	27	Reference	MKXIV	2.8	r1	TS1	0	90	1049, 1051, 1053, 1055, 1060, 1063	1064, 1066, 1068, 1070, 1075, 1078
				force/press	MKXIV	2.8	a3	TS1	0	60	1050, 1052, 1054	1065, 1067, 1069
				Roll sweep	MKXIV	2.8	a5	TS1	0-45	60	1056, 1057, 1058, 1059	1071, 1072, 1073, 1074
				Zsweep	MKXIV	2.8	a6	TS1	0	54-66	1061, 1062	1076, 1077
PM1 Config#10		PM1_W1.2B1.1GF1	28	Reference	MKXIV	2.8	r1	TS1	0	90	1083	1093, 1094
				force/press	MKXIV	2.8	a3	TS1	0	60	1084, 1085, 1086	1095, 1096, 1097
				Roll sweep	MKXIV	2.8	a5	TS1	0-45	60	1087, 1088, 1089, 1090	1098, 1099, 1100, 1101
				Zsweep	MKXIV	2.8	a6	TS1	0	54-66	1091, 1092	1102, 1103

Table 7.4-1. As-Run Summary (Continued)

CFD Code	WT Code	Model Config	Series	Data	Bal	Re	Alpha	Trip	Roll Angle	Height	Mach No	
											1.60	1.80
PM1 Config#12		PM1_W1.2B1.1GF1N1V1	29	Reference	MKXIV	2.8	r1	TS1	0	90	1110	1120
				force/press	MKXIV	2.8	a3	TS1	0	60	1111,1112,1113	1121,1122,1123
				Roll sweep	MKXIV	2.8	a5	TS1	0-45	60	1114,1115, 1116, 1117	1124,1125,1126,1 1227
				Zsweep	MKXIV	2.8	a6	TS1	0	54-66	1118,1119	1128,1129
PM1 Config#14		PM1_W1B1.1GF1N1P2V1	30	Reference	MKXIV	2.8	r1	TS1	0	90	1140	1148
				force/press	MKXIV	2.8	a3	TS1	0	60	1141, 1142, 1143	1149, 1150, 1151
				Roll sweep	MKXIV	2.8	a5	TS1	0-45	60	1144, 1145, 1146, 1147	1152, 1153, 1154, 1155
AS1 Config #1a		AS1	31	Reference	MKXIV	2.8	r1	TS1	0	90		
				Zsweep	MKXIV	2.8	a6	TS1	0	54-66	1179, 1180, 1181	1182, 1183, 1184

Series 31 cont'd

Mach			
1.50	1.70	1.90	2.00
1162	1166	1170	1174, 1175
1163, 1164, 1165	1167, 1168, 1169	1171, 1172, 1173	1176, 1177, 1178

Table 7.4-1. As-Run Summary (Continued)

CFD Code	WT Code	Model Config	Series	Data	Bal	Re	Alpha	Trip	Roll Angle	Height	Mach No	
											1.60	1.80
AS1 Config #1a		AS1	32	Reference	MKXIV	2.8	r1	TS1	0	90	1189	1193
				Zsweep	MKXIV	2.8	0	TS1	0	54-66	1190, 1191, 1192	1194,1195,1196
				Reference	MKXIV	2.8	0	TS1	0	86	1202	1198*
				time dep	MKXIV	2.8	0	TS1	0	54	1203	1199*
				time dep	MKXIV	2.8	0	TS1	0	60	1204	1200*
				time dep	MKXIV	2.8	0	TS1	0	66	1205	1201*
				Reference	MKXIV	2.8	0	TS1	0	86	1202	
				Reference	MKXIV	2.8	0	TS1	0	54	1203	
				Reference	MKXIV	2.8	0	TS1	0	60	1204	
8 deg Cone Fairing		CF	33	Reference	MKXIV	2.8	r1	TS1	0	86	1215	1226
				time dep	MKXIV	2.8	0	TS1	0	54	1216	1227
		PT2106		time dep	MKXIV	2.8	0	TS1	0	56	1217	1228
				time dep	MKXIV	2.8	0	TS1	0	58	1218	1229
				time dep	MKXIV	2.8	0	TS1	0	60	1219	1230
				time dep	MKXIV	2.8	0	TS1	0	62	1220	1231
				time dep	MKXIV	2.8	0	TS1	0	64	1221	1232
				time dep	MKXIV	2.8	0	TS1	0	66	1222	1233
				time dep	MKXIV	2.8	0	TS1	0	72	1223	1234
				time dep	MKXIV	2.8	0	TS1	0	75	1224	1235
				time dep	MKXIV	2.8	r1	TS1	0	86.8	1225	1236
				reference	MKXIV	2.8	r1	TS1	0	86.8	1236	1237
				time dep	MKXIV	2.8	0	TS1	0	60	1240	1238
				time dep	MKXIV	2.8	r1	TS1	0	86.8	1225	1236

*2 second data points x 30

7.5 Data Quality and Test Results

Pressure Data Signatures and Repeatability

Short-term repeatability of the pressure signatures was assessed during the test. A “snapshot” of the repeatability is presented herein for a representative configuration of each type of model tested. For each configuration, data comparisons are provided for the two nominal model heights above the rail (30 and 60 in, when available) and for the two Mach conditions tested (1.60 and 1.80). In general, dP/P overpressure repeatability for the BOR and boom models is within ± 0.002 for the 30-in rail heights and within ± 0.001 for the 60-in heights. The performance model repeatability data, only available at the $H = 60$ -in nominal position, is within ± 0.002 for both Mach conditions tested. Refer to Reference 28 for the complete repeatability assessments performed for all test configurations.

Figures 7.5-1 and 7.5-2 show the typical “ dP/P ” pressure repeatability for the BOR configurations (AS1 shown) for $M = 1.60$ and 1.80 , respectively. These results are similar for the other two BOR models.

Figures 7.5-3 and 7.5-4 show the typical pressure repeatability for the boom model configurations (Boom Model 1 [BM1], Configuration 4 shown) for $M = 1.60$ and 1.80 , respectively.

Figures 7.5-5 and 7.5-6 show the typical pressure repeatability for the performance model (Performance Model 1 [PM1], Configuration 4 shown) for $M = 1.60$ and 1.80 , respectively.

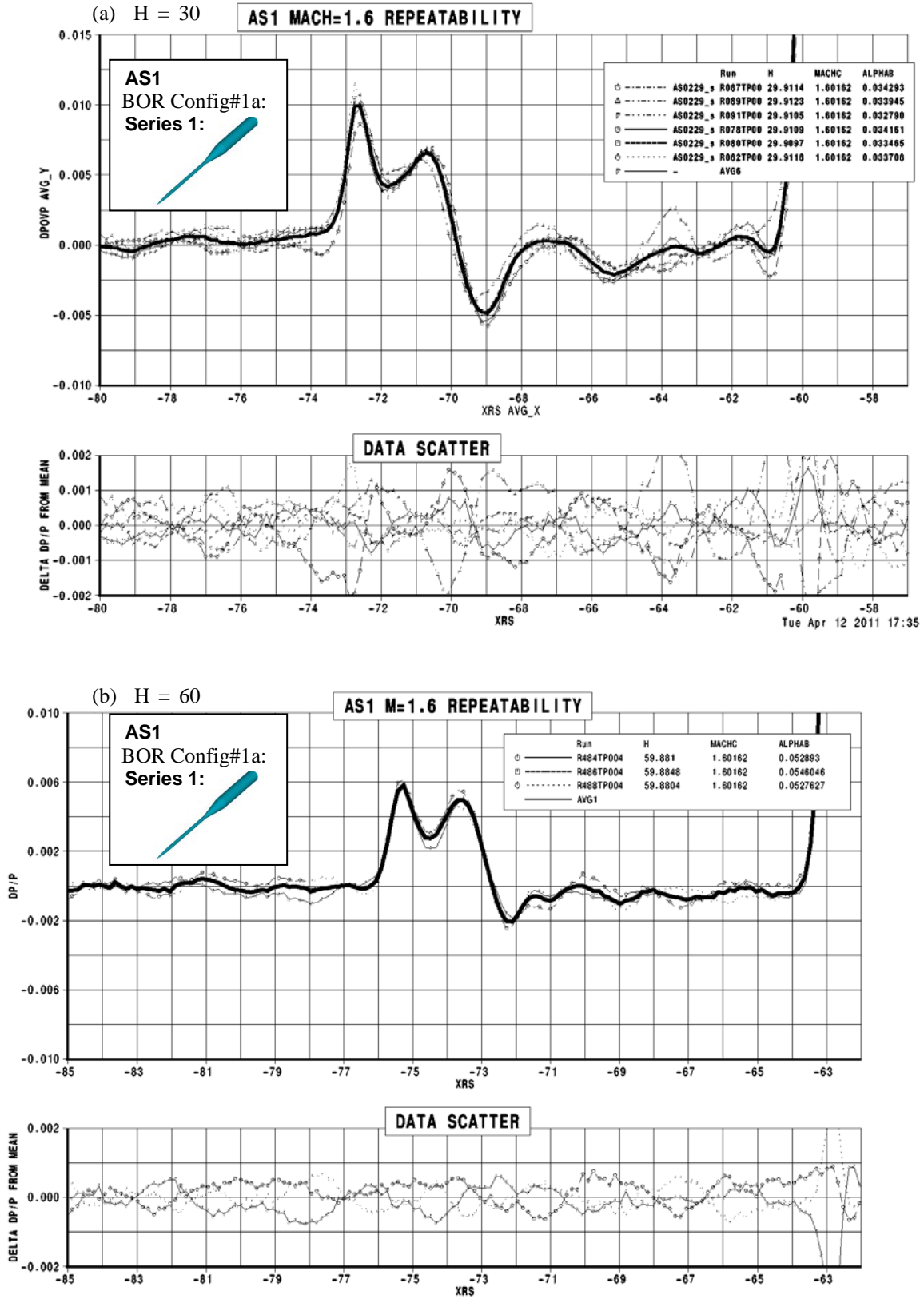


Figure 7.5-1. Typical BOR Pressure Data Repeatability, M = 1.60

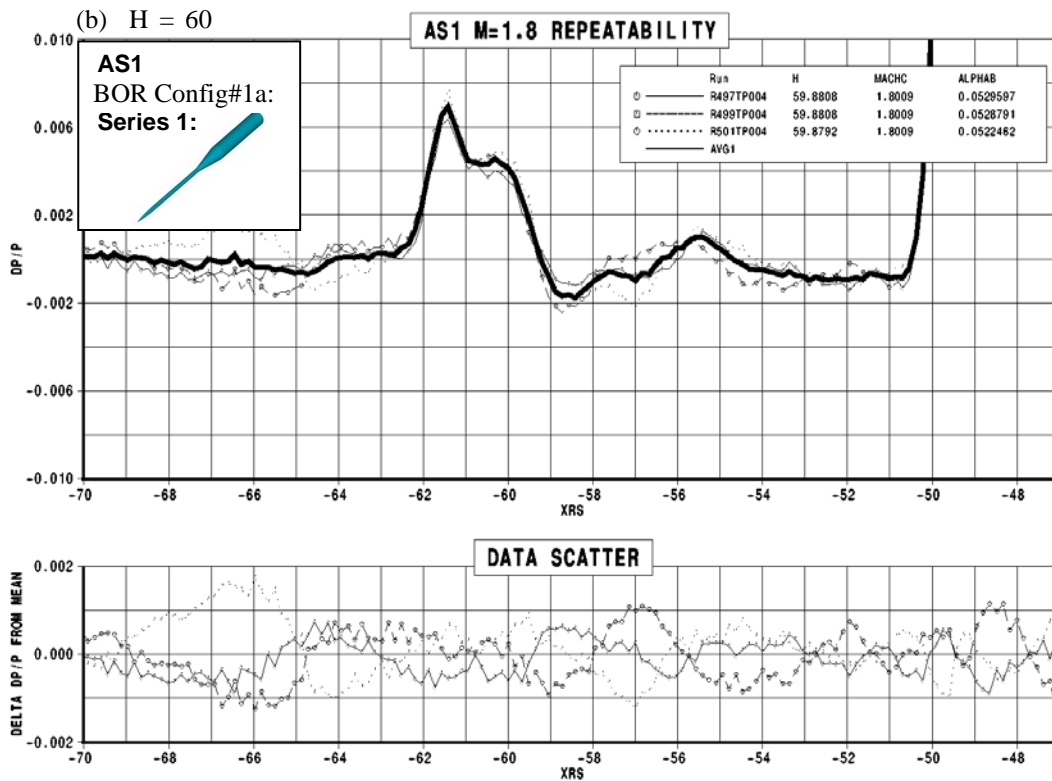
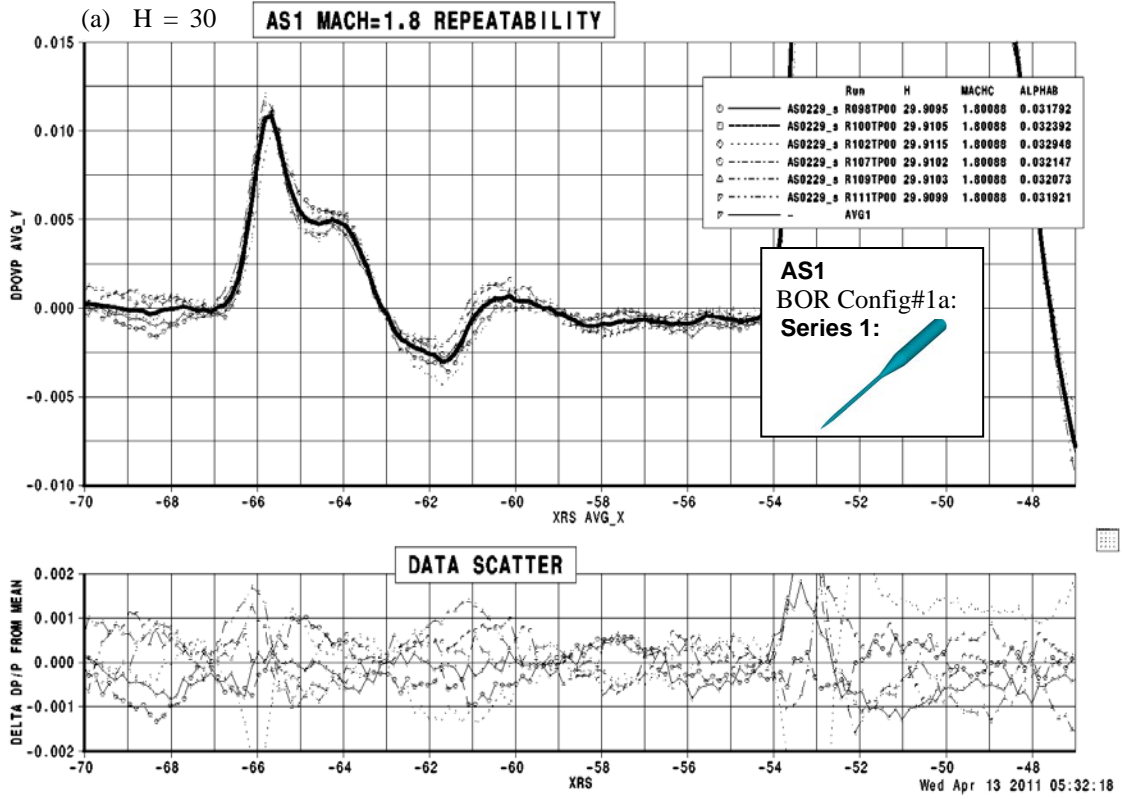
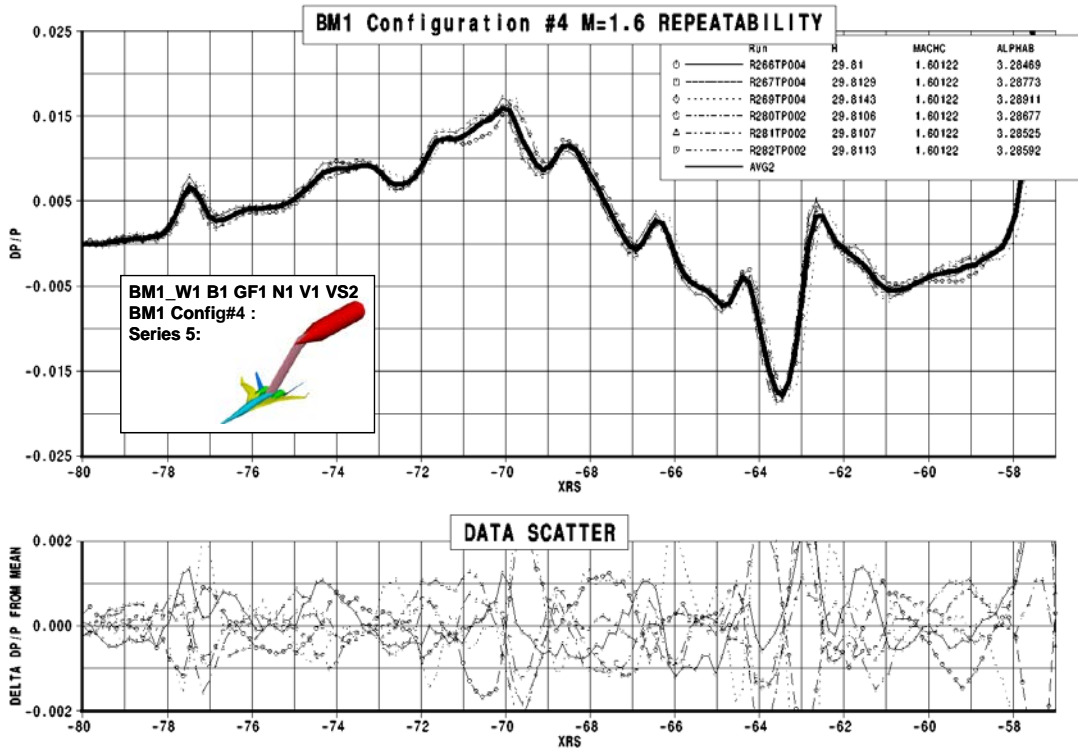


Figure 7.5-2. Typical BOR Pressure Data Repeatability, M = 1.80

(a) $H = 30$



(b) $H = 60$

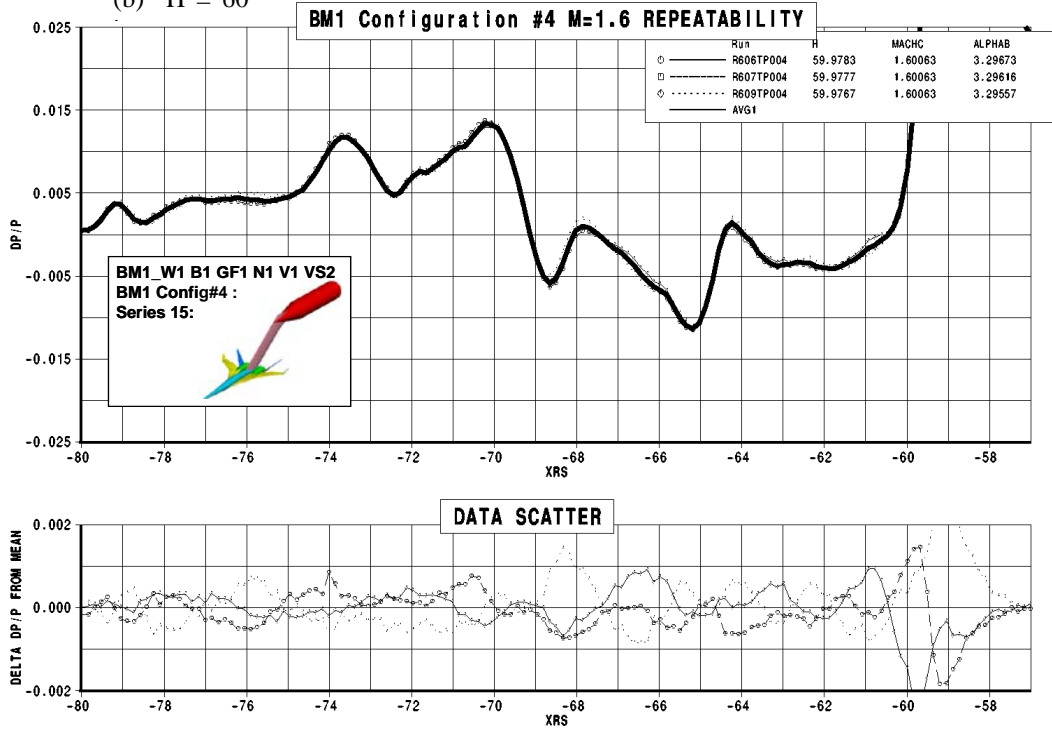
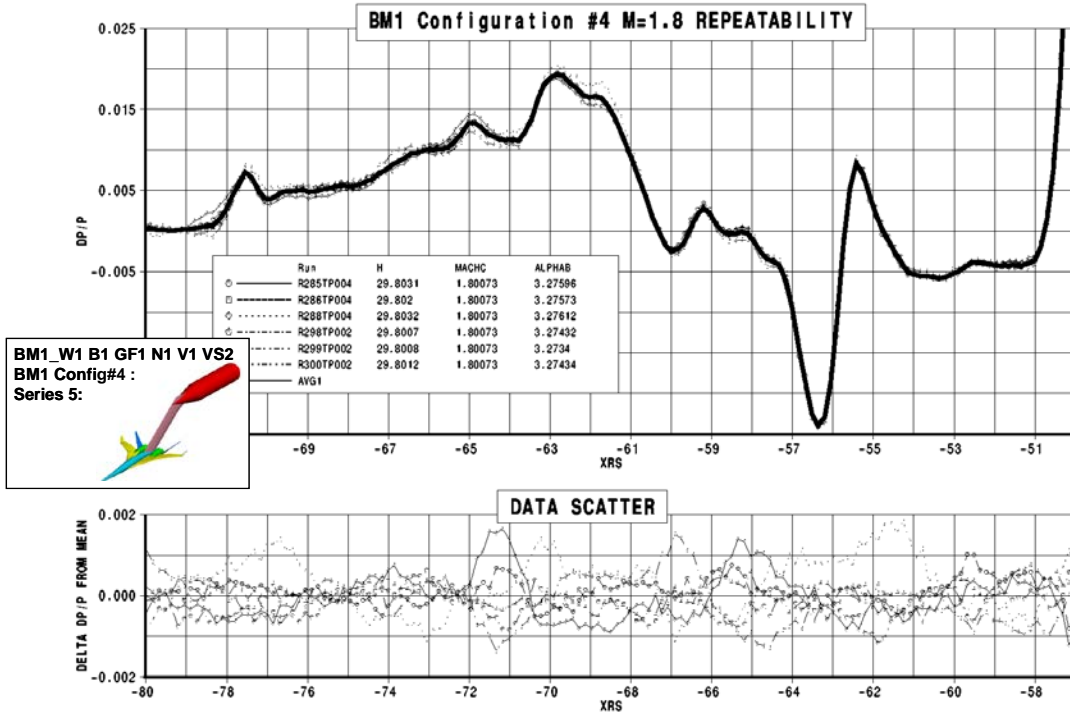


Figure 7.5-3. Typical Boom Model Pressure Data Repeatability, $M = 1.60$

(a) $H = 30$



(b) $H = 60$

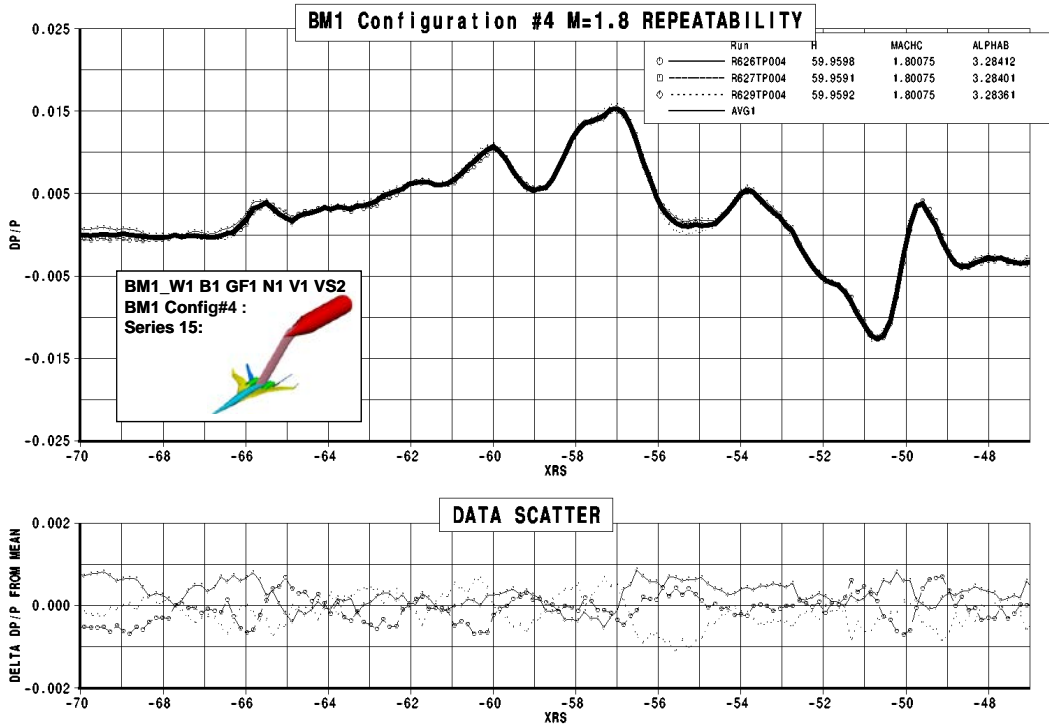
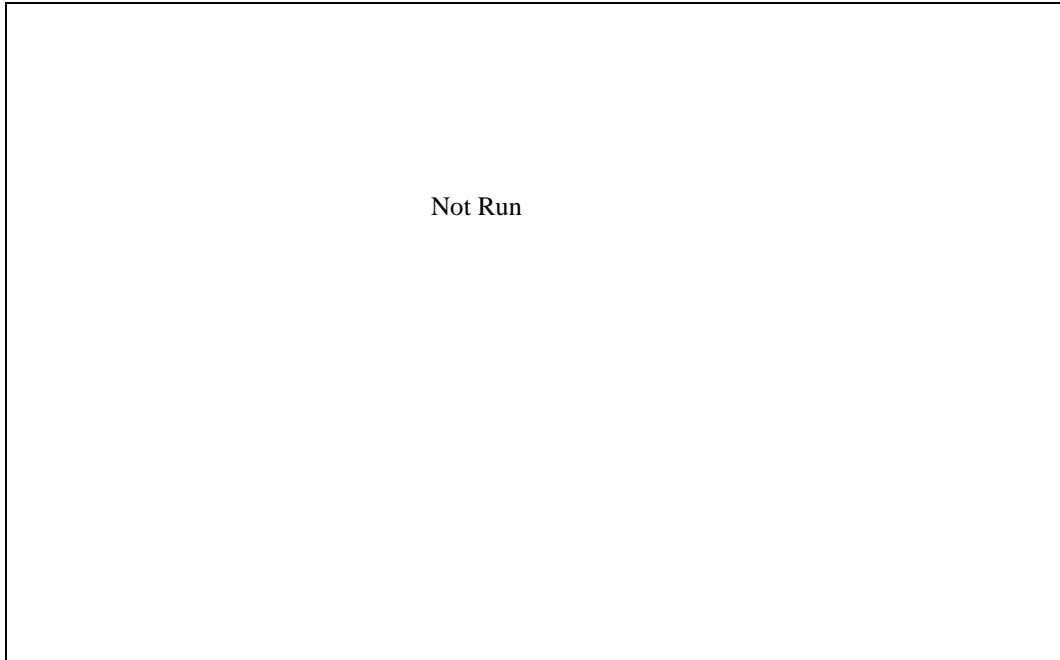


Figure 7.5-4. Typical Boom Model Pressure Data Repeatability, $M = 1.80$

(a) H = 30



(b) H = 60

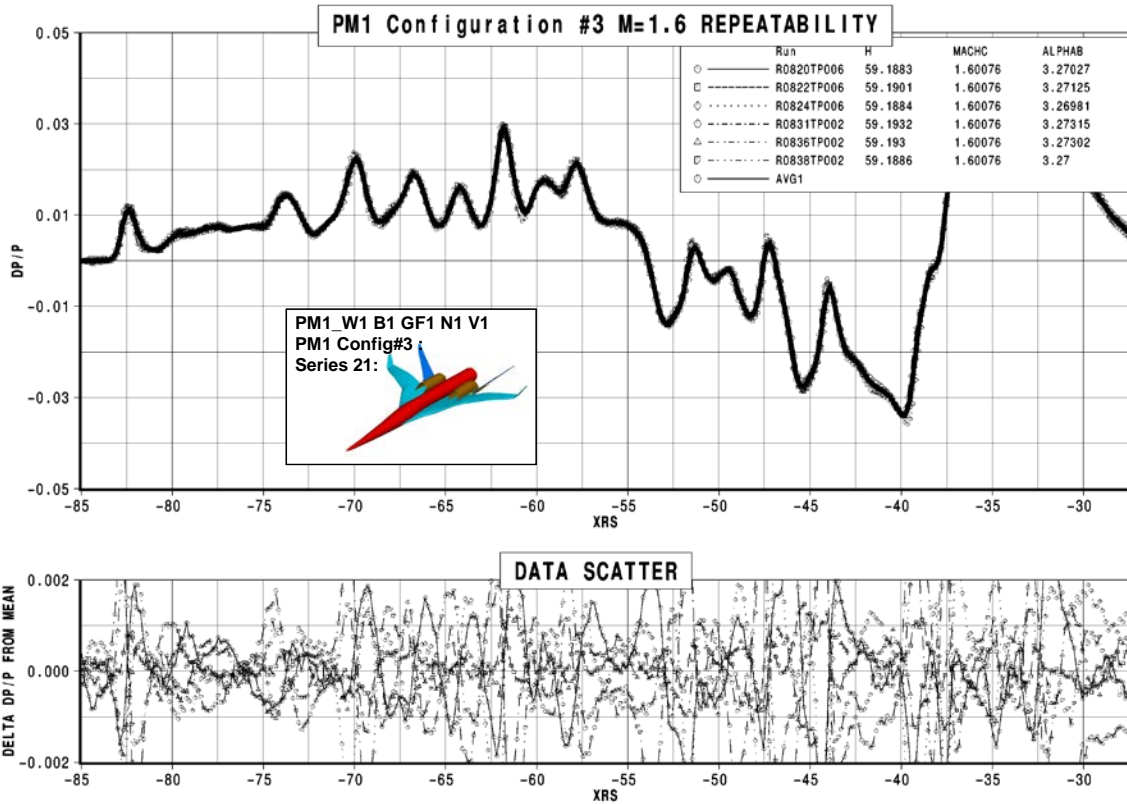
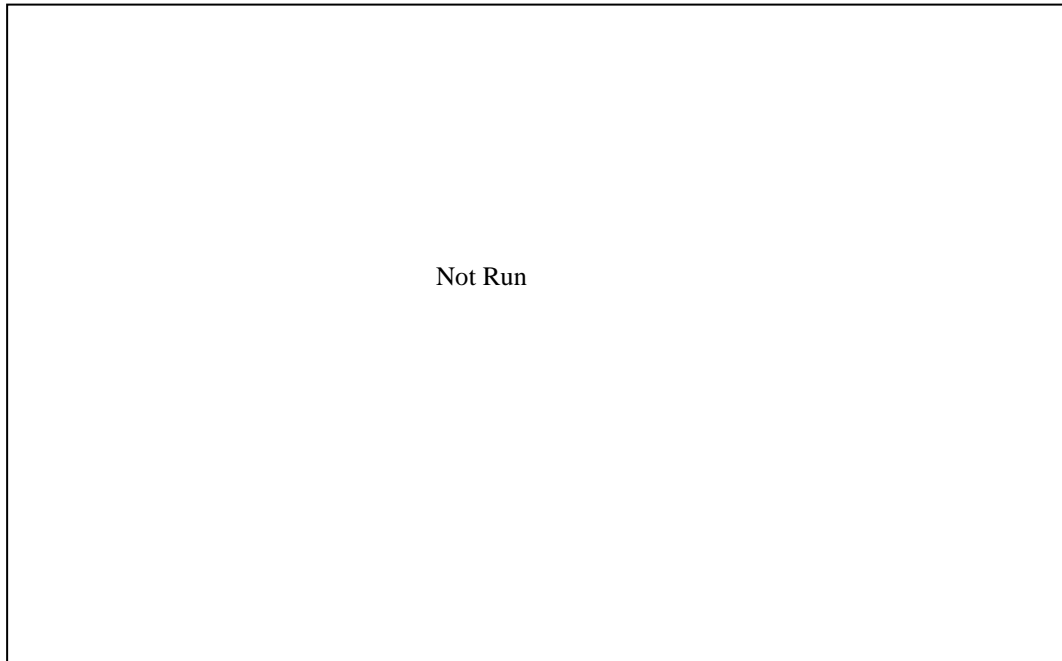


Figure 7.5-5. Typical Performance Model Pressure Data Repeatability, M = 1.60

(a) H = 30



(b) H = 60

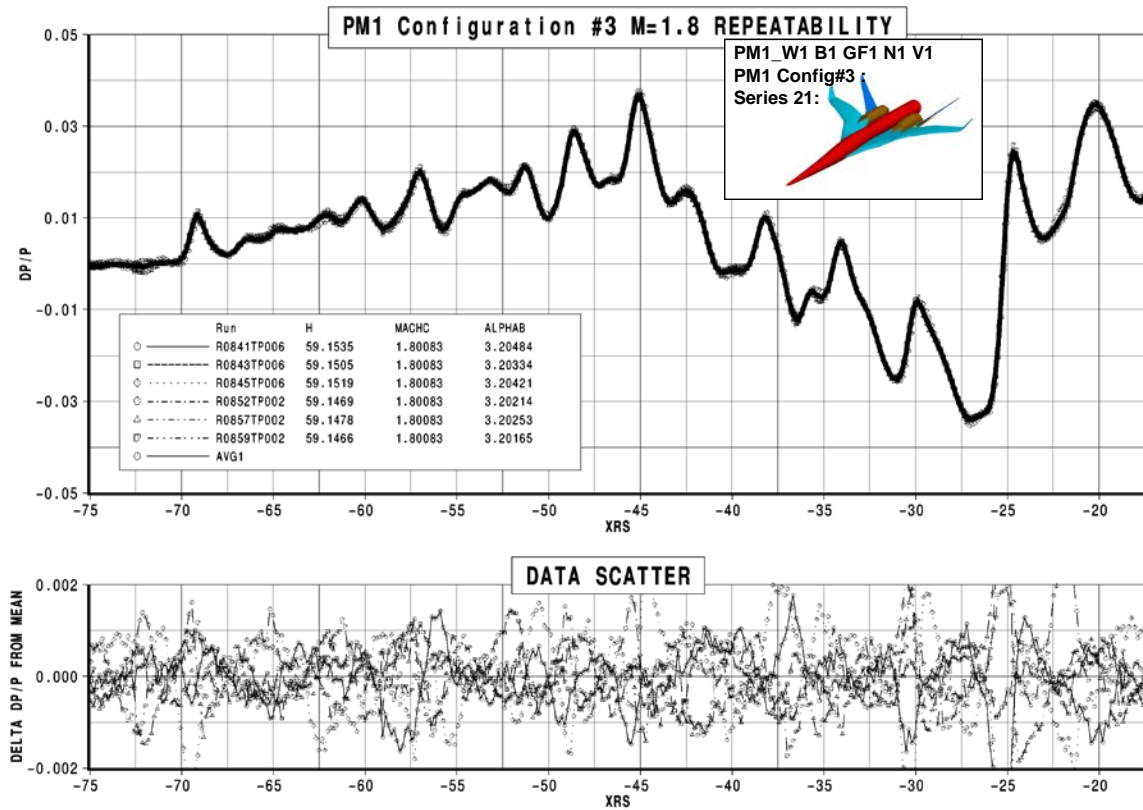


Figure 7.5-6. Typical Performance Model Pressure Data Repeatability, M = 1.80

Reference Run (“Up and Away”) Pressure Data Repeatability

A “snapshot” of the consistency of the reference run data used to “tare” the dP/P sonic boom signatures is provided herein for the same BOR and BM configurations discussed above. These reference runs were acquired frequently during a constant Mach run series by moving the model far away from the pressure rail to provide a rail signature void of any model influence. The acquired reference runs were averaged to create the tare correction for the run series. For each configuration, data comparisons are provided for the two nominal model heights above the rail (30 and 60 in, when available) and for the two Mach conditions tested (1.60 and 1.80). In general, the dP/P overpressure scatter for the reference runs is between ± 0.001 and ± 0.002 for both the 30-in and 60-in rail height run series, consistent with the rail pressure signature data repeatability.

Figures 7.5-7 and 7.5-8 show the typical “dP/P” reference run repeatability for the BOR configurations (AS1 shown) for $M = 1.60$ and 1.80 , respectively. These results are similar for the other two BOR models.

Figures 7.5-9 and 7.5-10 show the typical “dP/P” reference run repeatability for the Boom model configurations (BM1, Configuration 4 shown) for $M = 1.60$ and 1.80 , respectively.

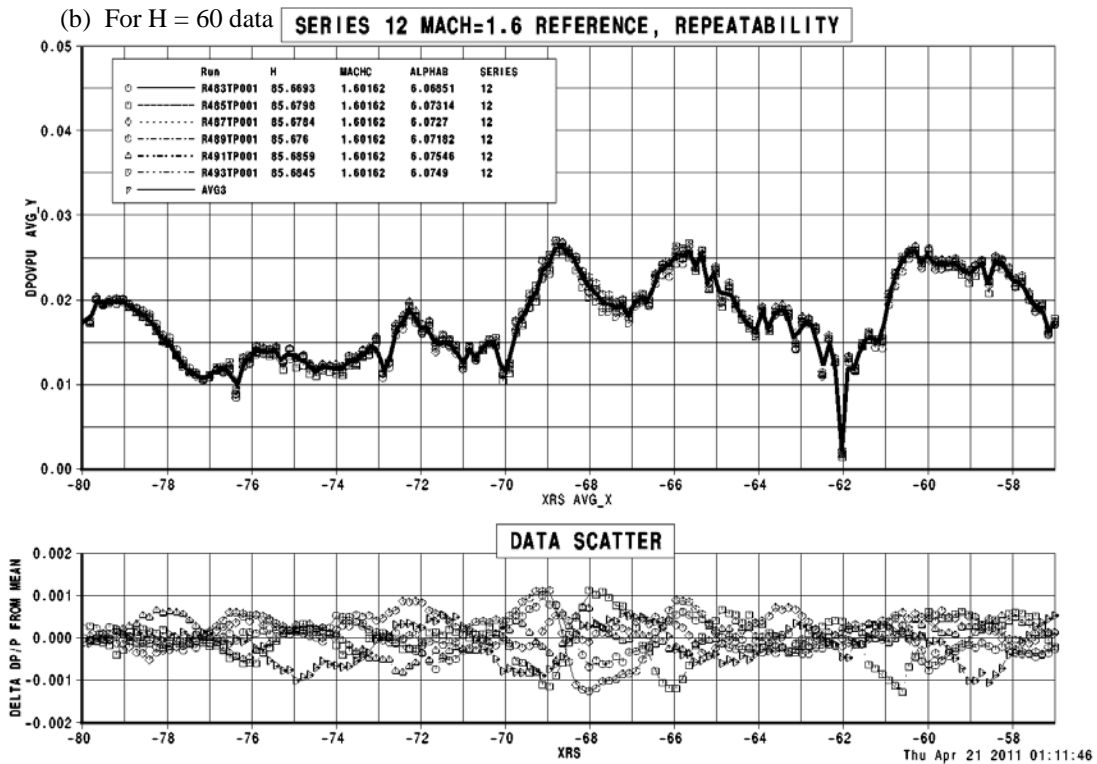
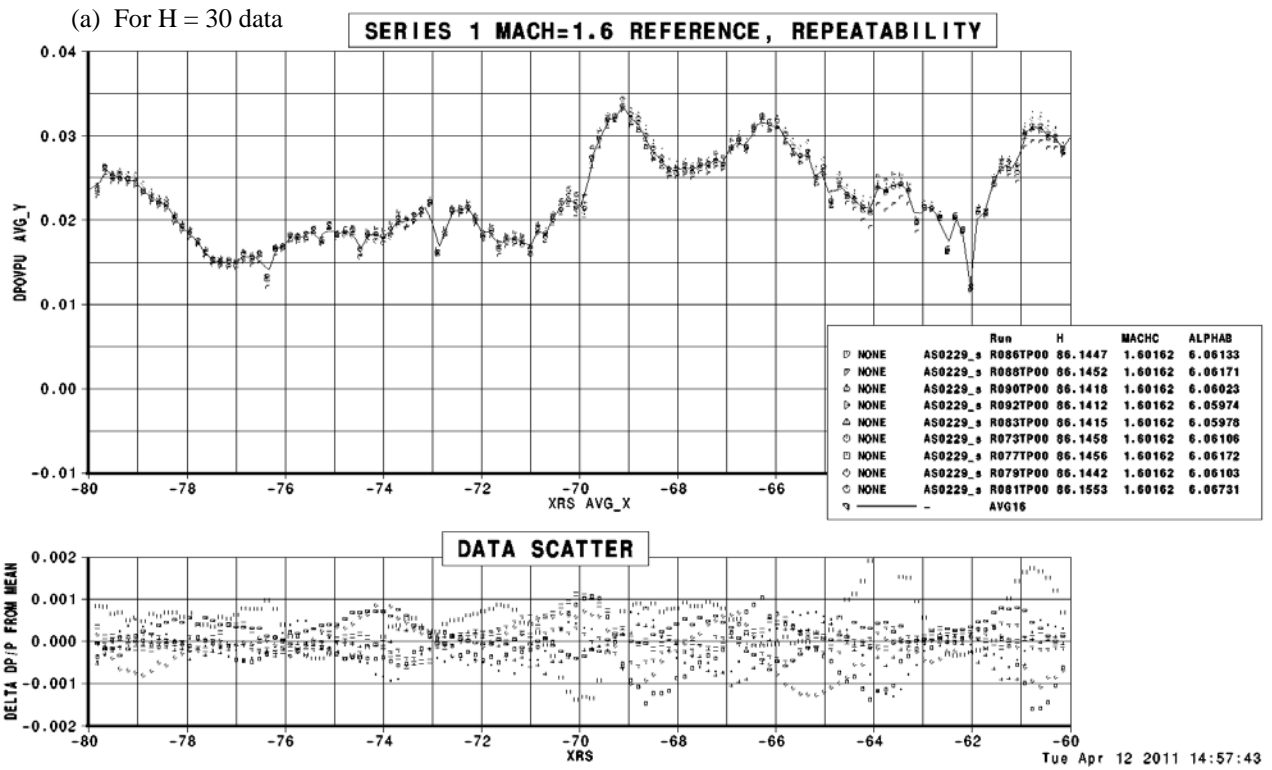
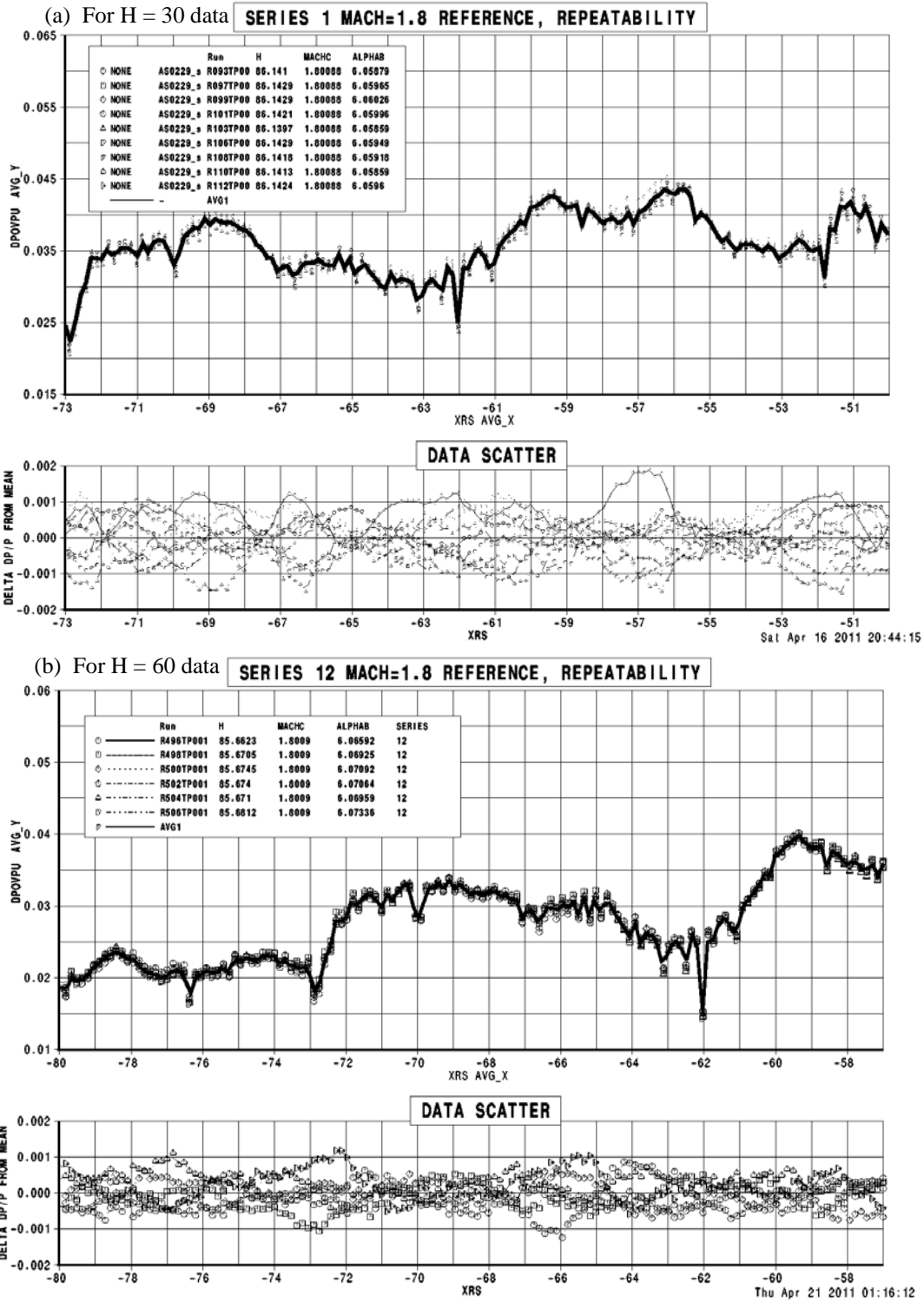
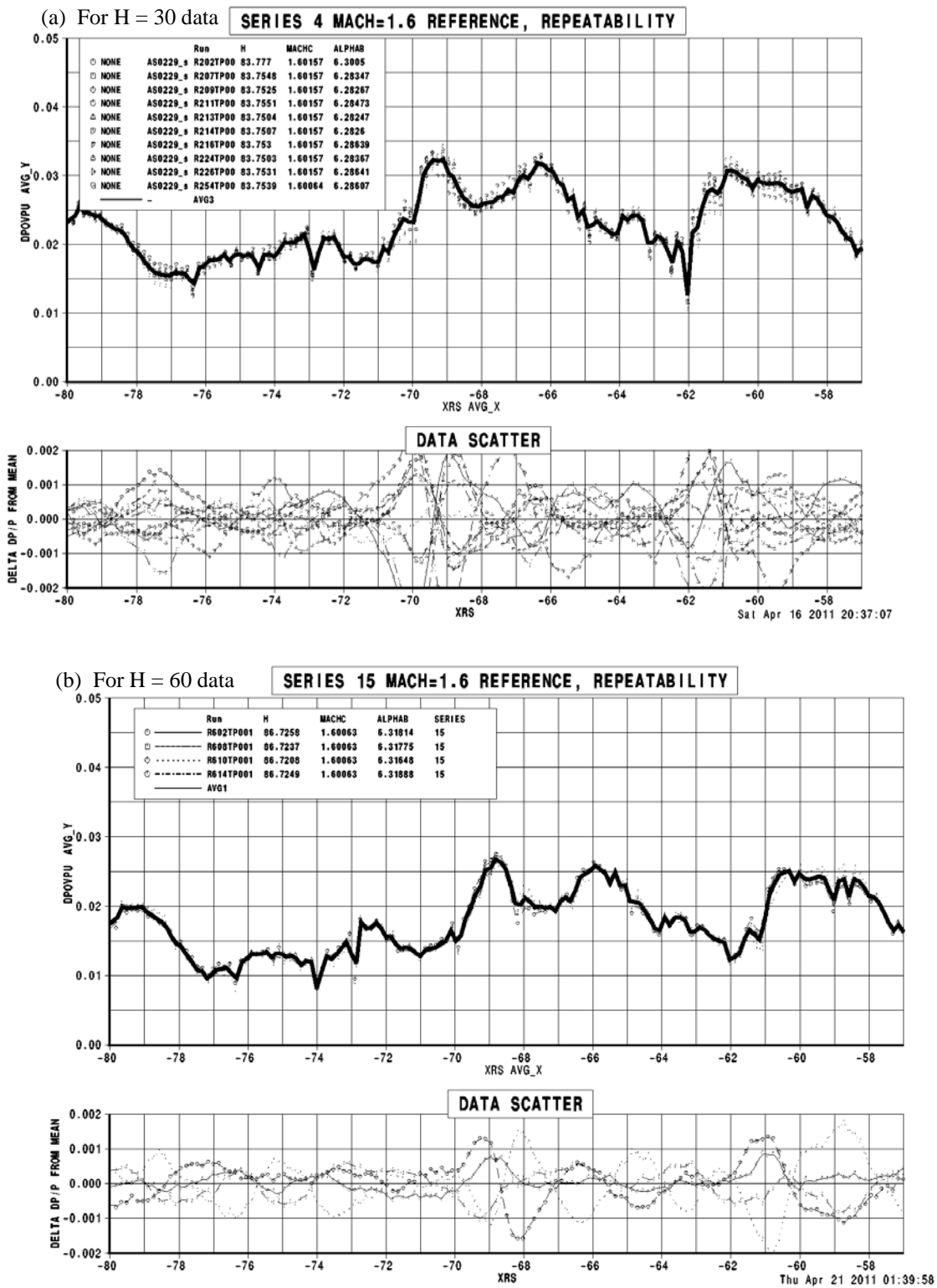


Figure 7.5-7. Typical BOR Reference Run Pressure Data Repeatability, M = 1.60, H = ~86”





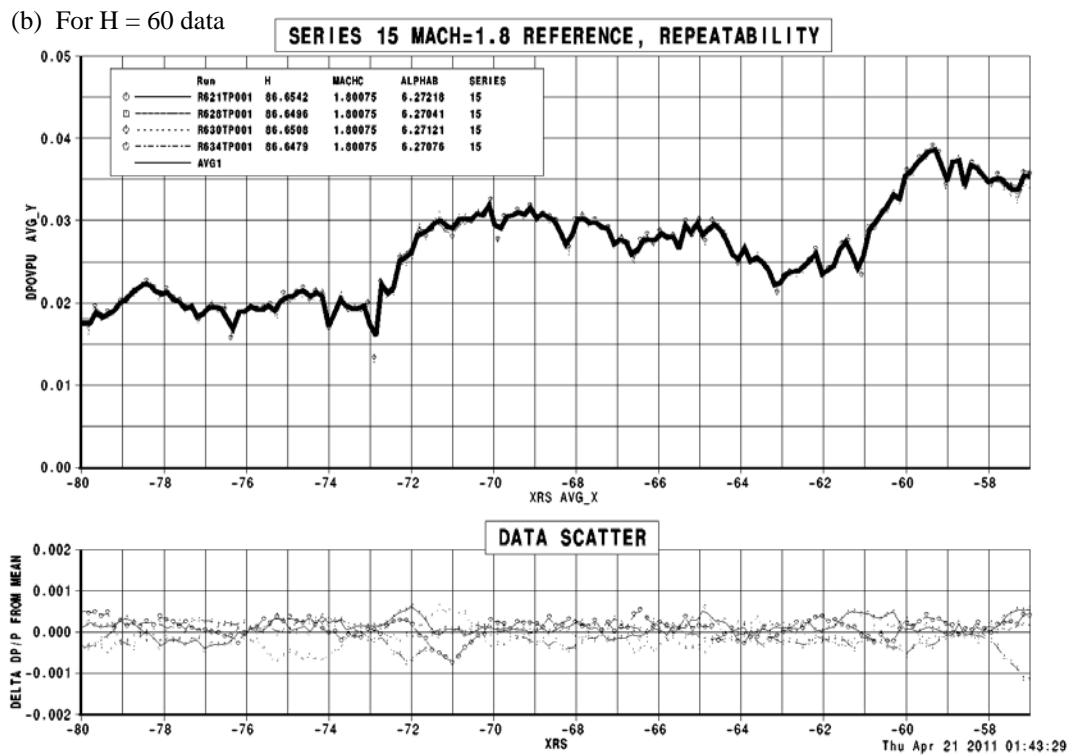
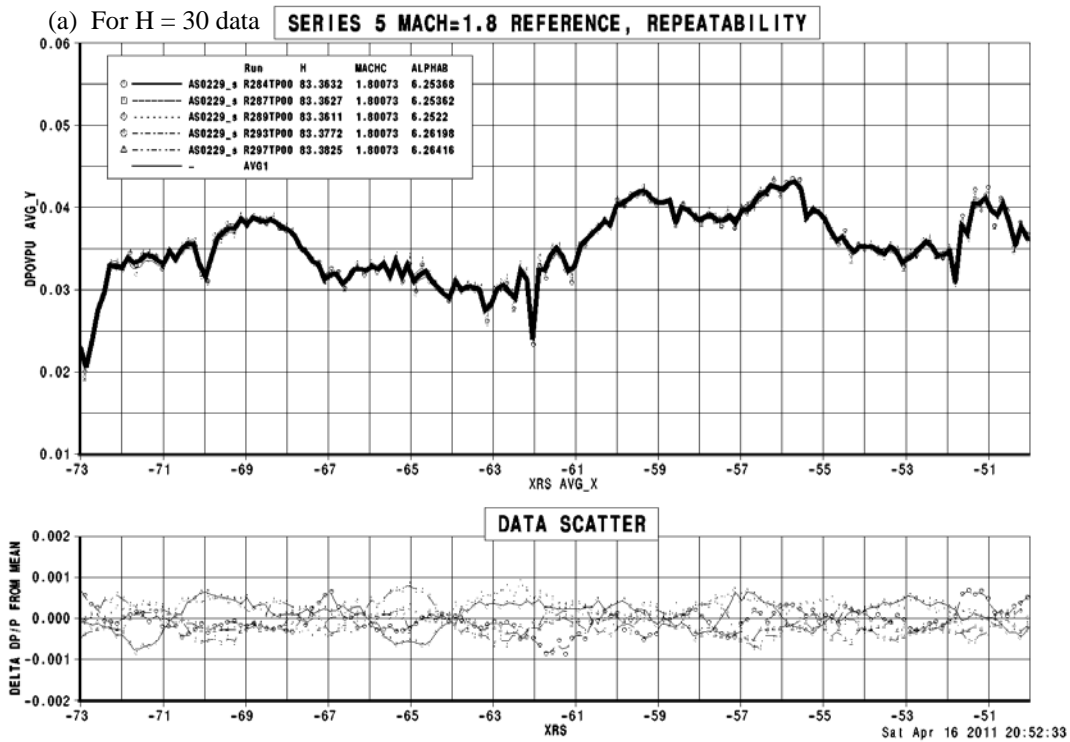


Figure 7.5-10. Typical Boom Model Reference Run Pressure Data Repeatability, $M = 1.80$, $H = \sim 86^\circ$

Pressure Data Alpha Variation

The effect of alpha (angle-of-attack) variation was assessed during the test. A “snapshot” of these comparisons is presented herein for the same configurations as those addressed above for the overpressure evaluations for consistency. For each configuration, data comparisons are provided for the two nominal model heights above the rail (30 and 60 in, when available) and for the two Mach conditions tested (1.60 and 1.80). Refer to Reference 28 for the complete repeatability assessments performed for all test configurations.

Figures 7.5-11 and 7.5-12 show the typical “dP/P” pressure variation with alpha for the BOR configurations (AS1 shown) for M = 1.60 and 1.80, respectively.

Figures 7.5-13 and 7.5-14 show the typical pressure variation with alpha for the boom model configurations (BM1, Configuration 4 shown) for M = 1.60 and 1.80, respectively.

Figures 7.5-15 and 7.5-16 show the typical pressure variation with alpha for the performance model (PM1, Configuration 4 shown) for M = 1.60 and 1.80, respectively.

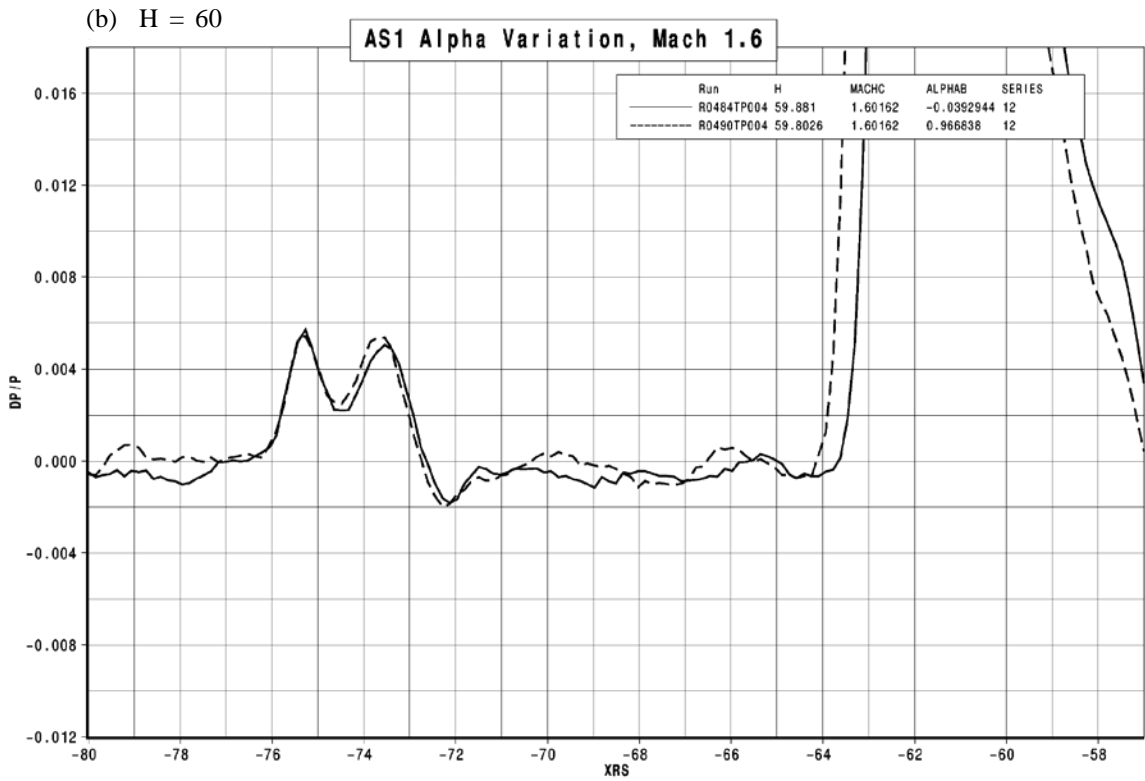
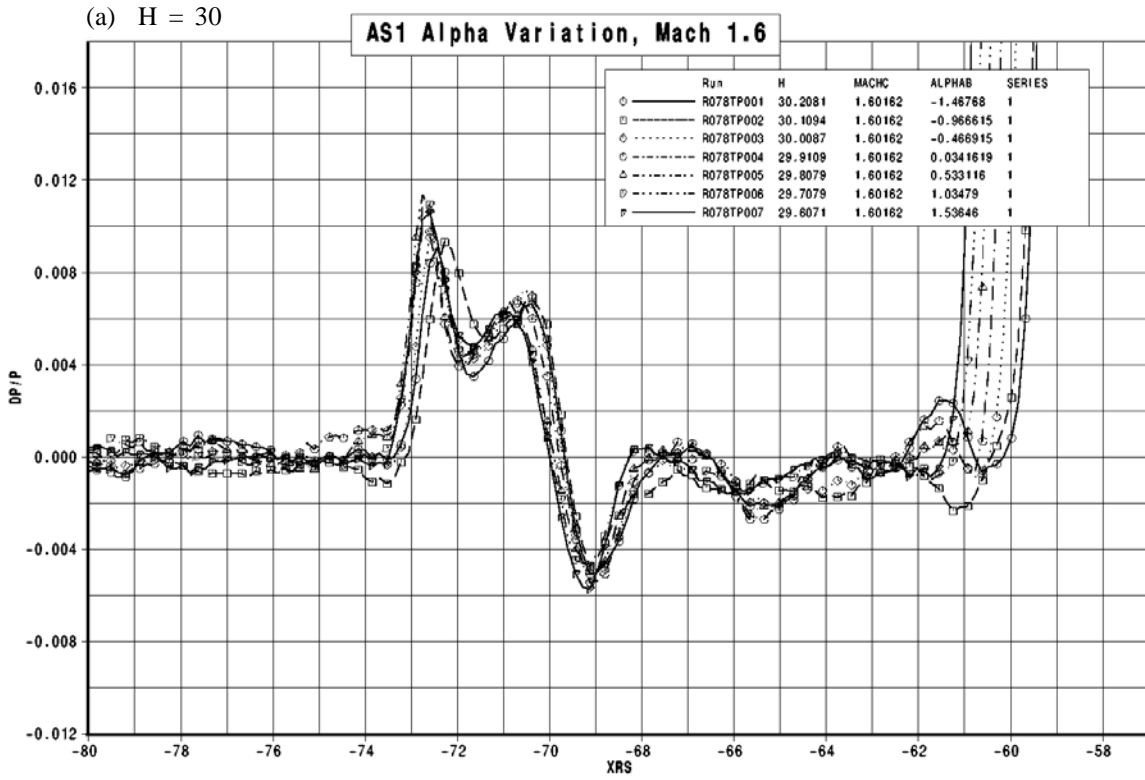
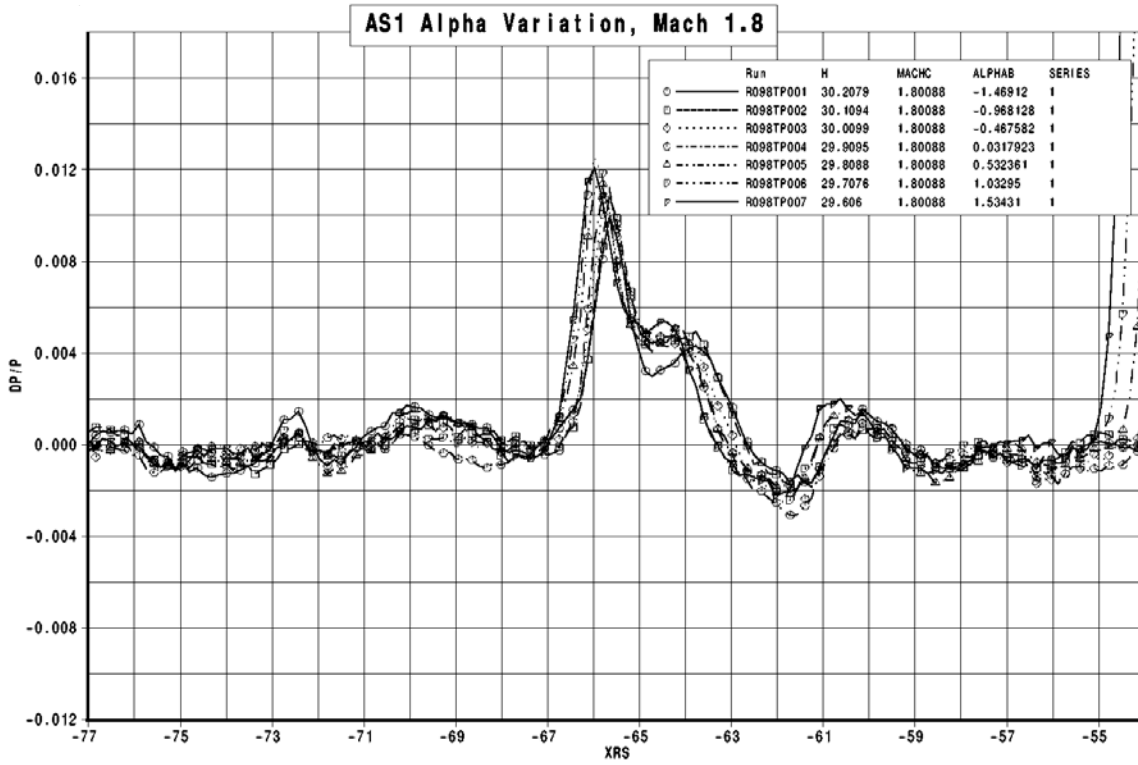


Figure 7.5-11. Typical BOR Pressure Data Variation with Angle of Attack, $M = 1.60$

(a) $H = 30$



(b) $H = 60$

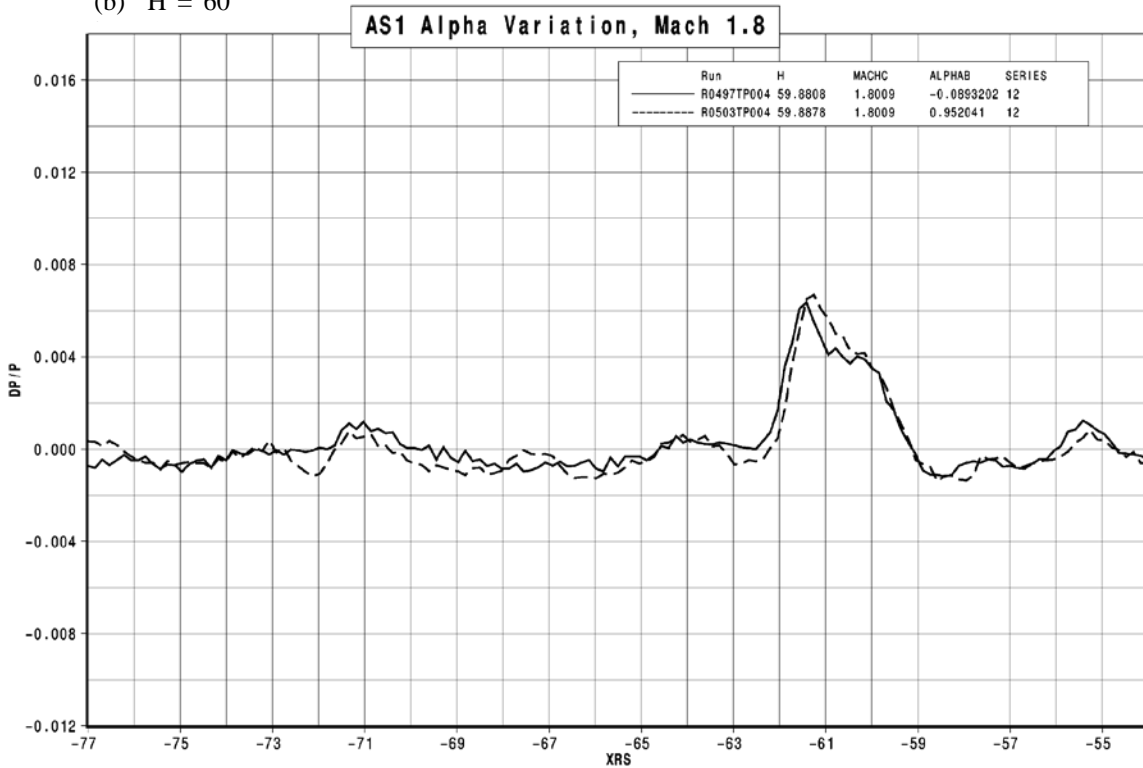
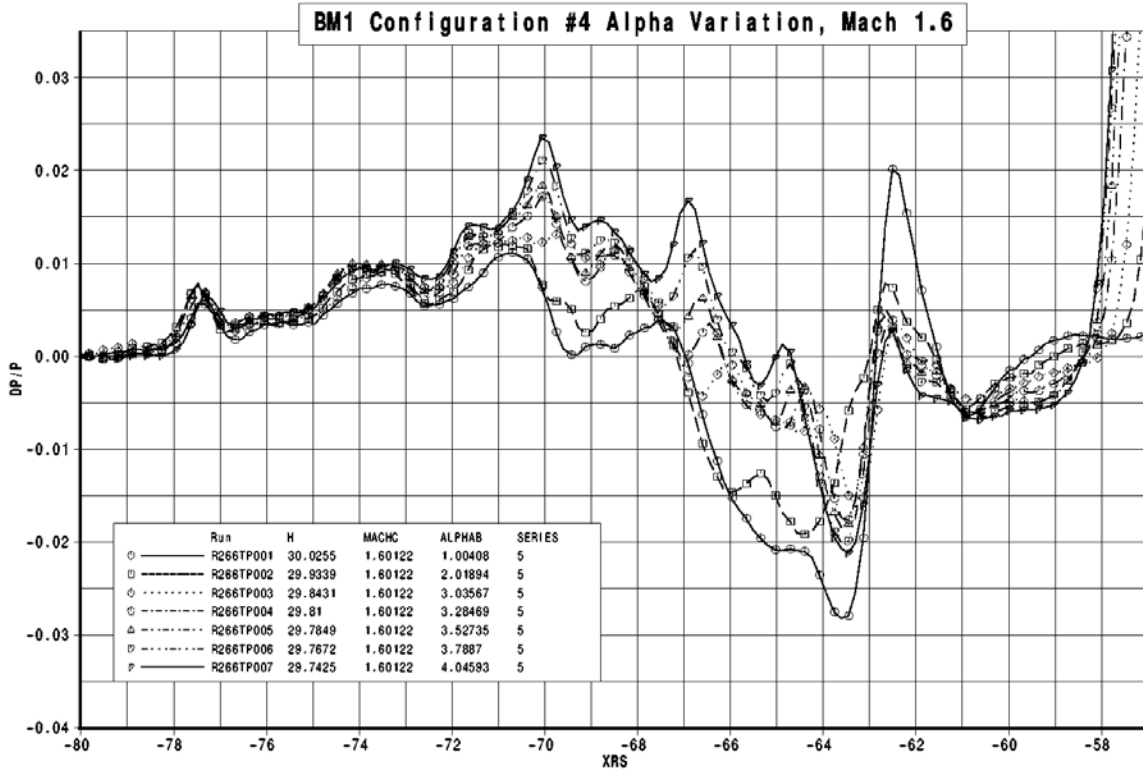


Figure 7.5-12. Typical BOR Pressure Data Variation with Angle of Attack, $M = 1.80$

(a) H = 30



(b) H = 60

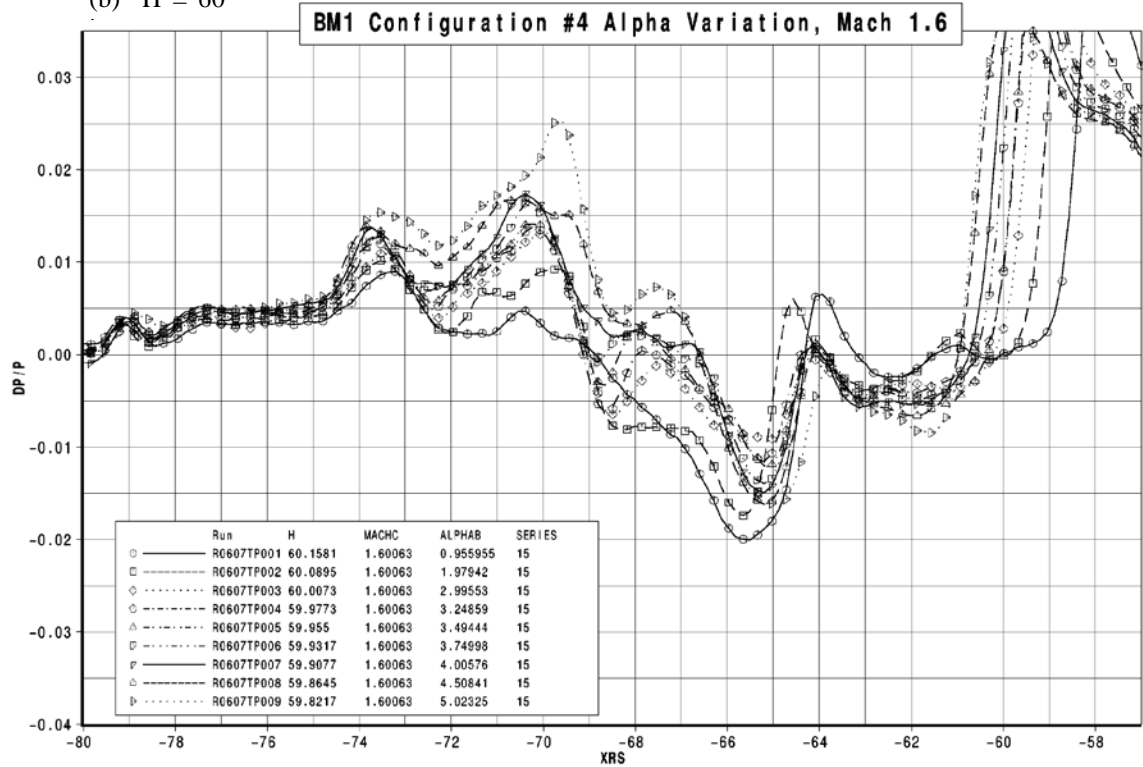


Figure 7.5-13. Typical Boom Model Pressure Data Variation with Angle of Attack, M = 1.60

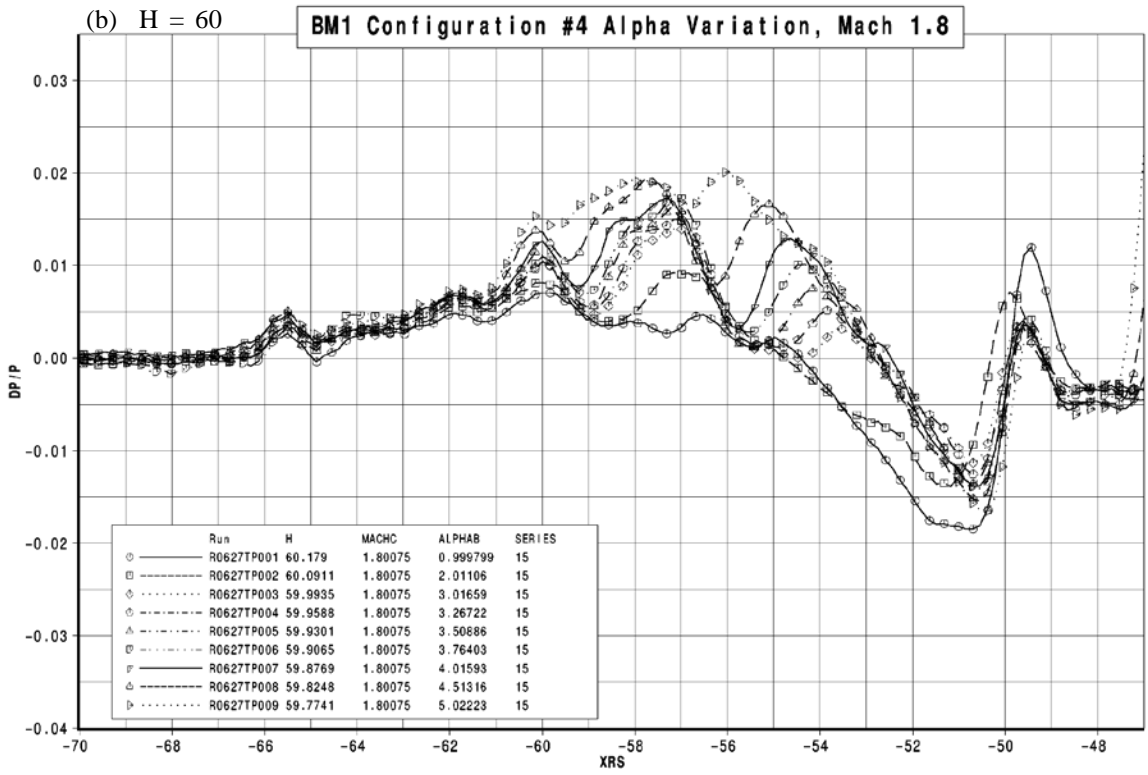
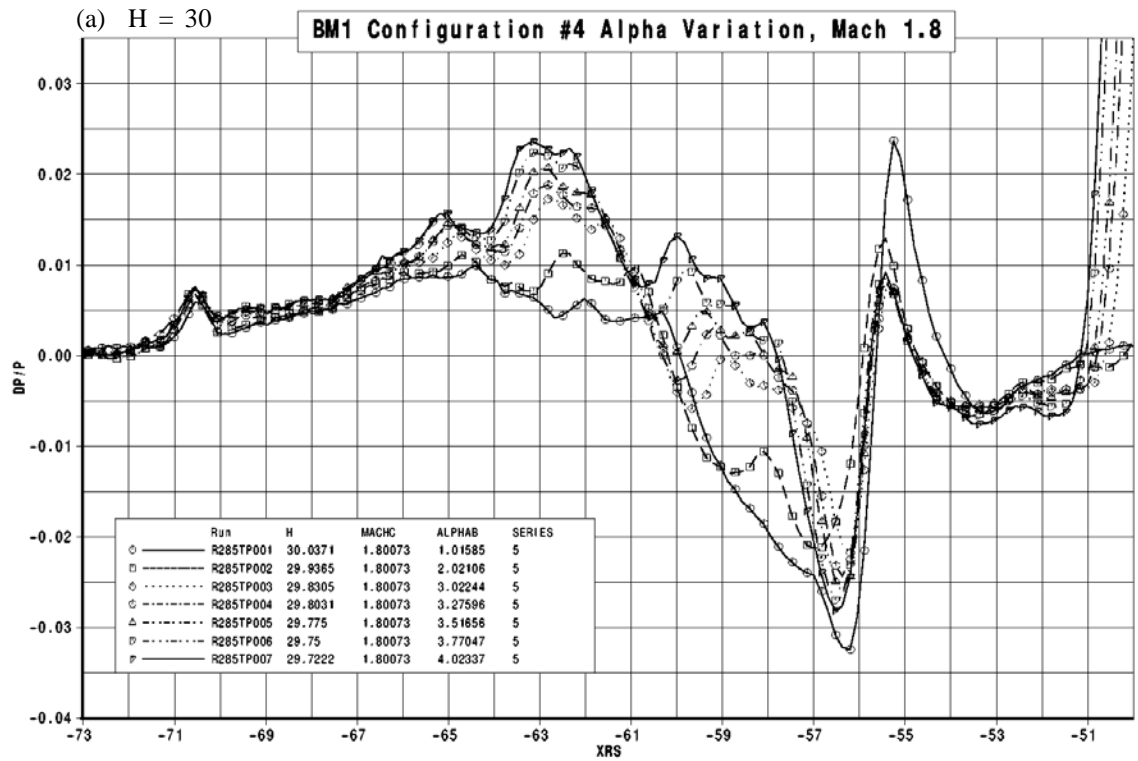


Figure 7.5-14. Typical BM Pressure Data Variation with Angle of Attack, M = 1.80

(a) $H = 30$

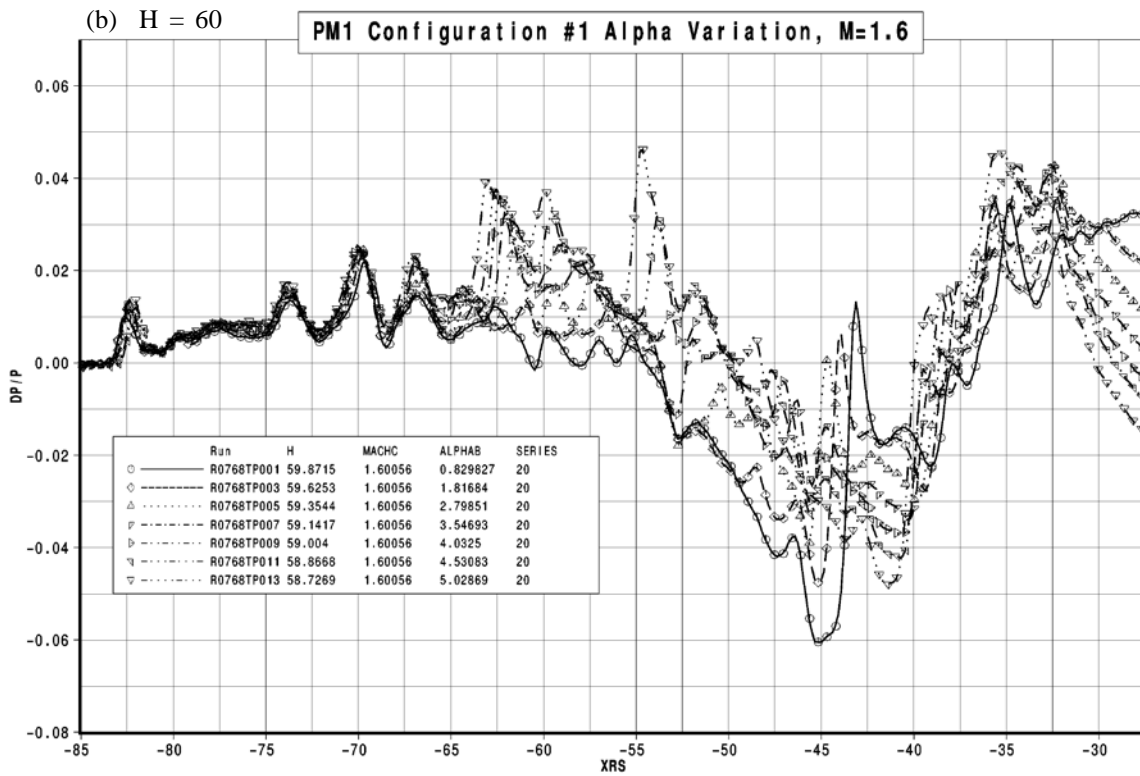
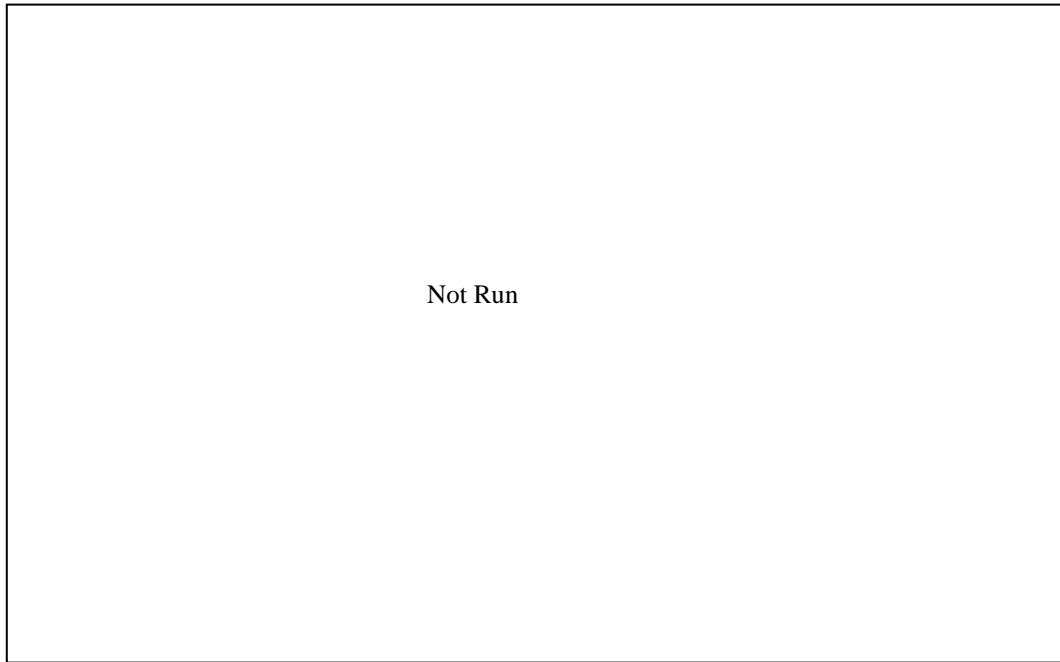
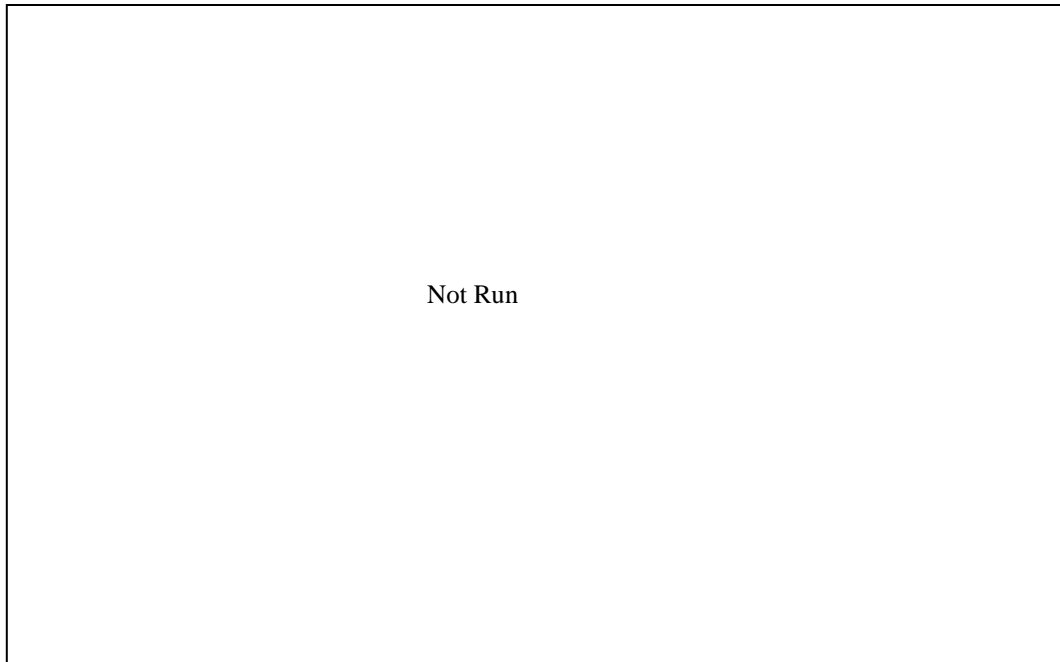


Figure 7.5-15. Typical Performance Model Pressure Data Variation with Angle of Attack, $M = 1.60$

(a) H = 30



(b) H = 60

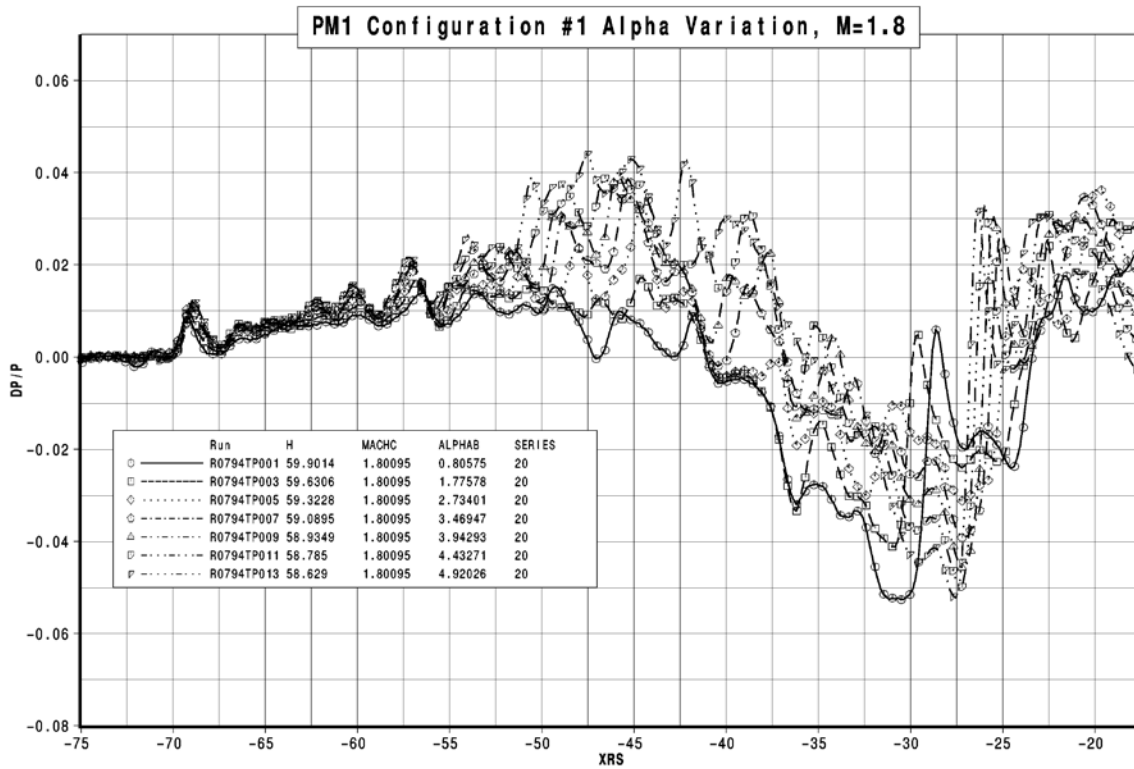


Figure 7.5-16. Typical Performance Model Pressure Data Variation with Angle of Attack, M = 1.80

Force and Moment (F&M) Data and Repeatability

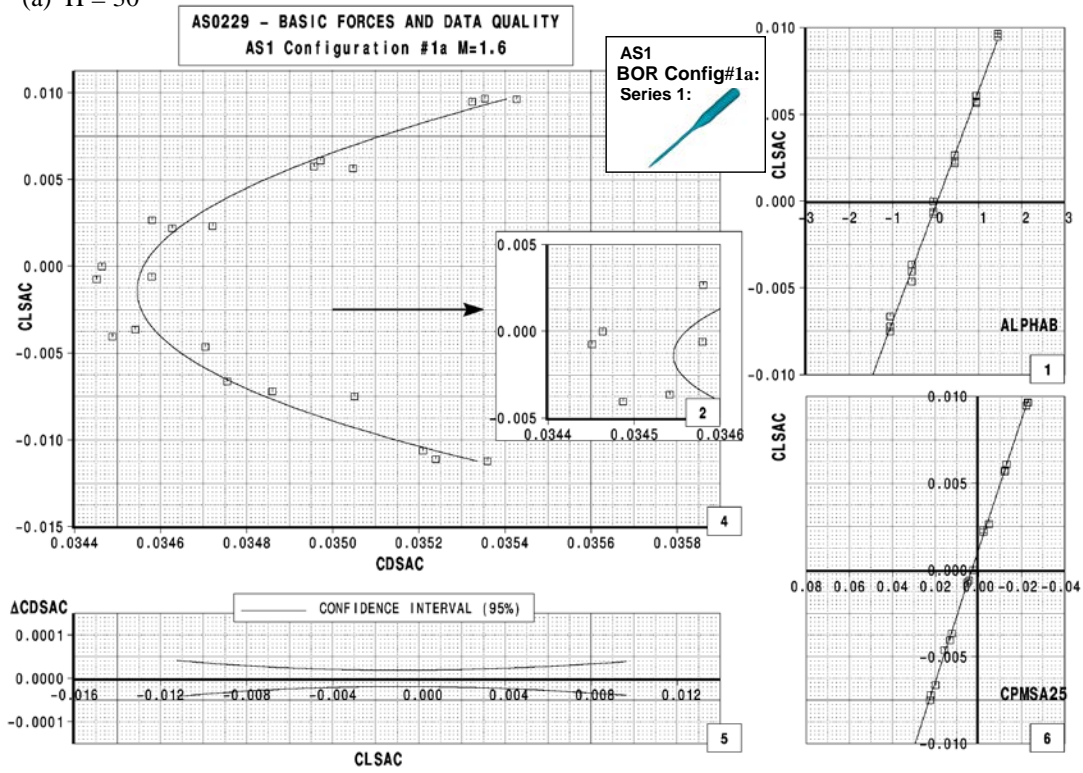
Force and moment data quality and repeatability was assessed for all model configurations. A “snapshot” of these repeatability comparisons is presented herein for the same configurations as those addressed above for the overpressure evaluations for consistency. The entire set of repeatability assessments are provided in Reference 28. The provided figures show the drag polar, lift, and moment curves for the nominal model heights of 30 and 60 inches above the rail and for the two Mach conditions tested (1.60 and 1.80) for each model type. The lower plot in each figure shows the 95% confidence interval based on all available data points and curve fit.

Figures 7.5-17 and 7.5-18 show the F&M data repeatability for the BOR configurations (AS1 shown) for $M = 1.60$ and 1.80 , respectively. These results are consistent with the other two BOR models. The data scatter is quite good considering the lower loads measured by the balance for these configurations.

Figures 7.5-19 and 7.5-20 show the F&M data repeatability for the boom model configurations (BM1, Configuration 4 shown) for $M = 1.60$ and 1.80 , respectively. Drag repeatability is shown to be within ± 2 drag counts for both within-series and over the test. The lower loads measured by the balance for the boom model configuration should be considered in these assessments.

Figures 7.5-21 and 7.5-22 show the F&M data repeatability for the performance model (PM1, Configuration 4 shown) for $M = 1.60$ and 1.80 , respectively. Drag repeatability is shown to be within ± 0.25 drag counts for the within-series comparisons and ± 1 count over the test (i.e., series-to-series).

(a) H = 30



(b) H = 60

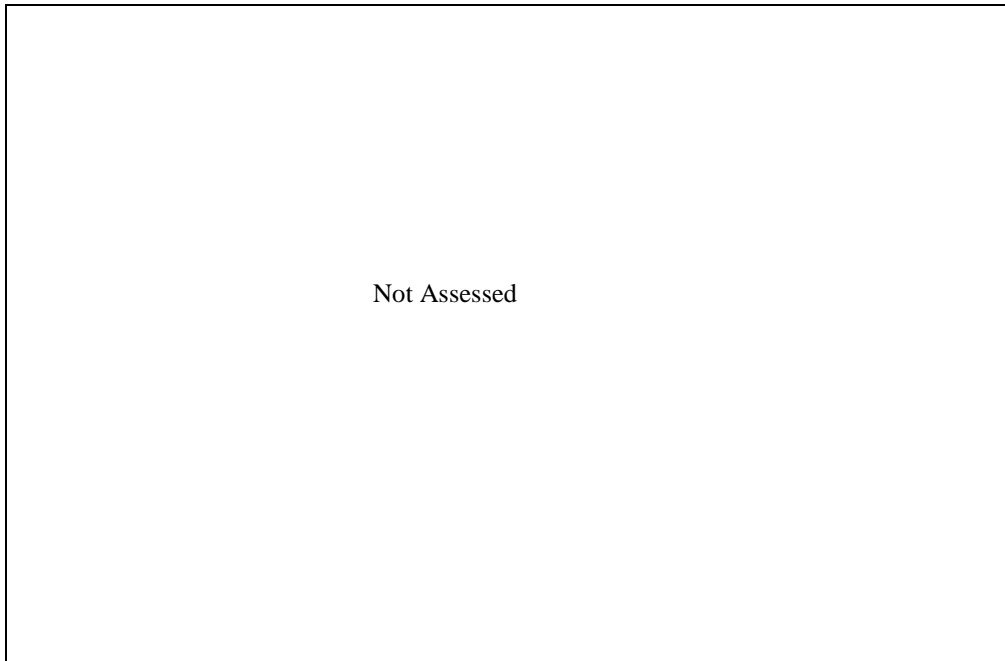
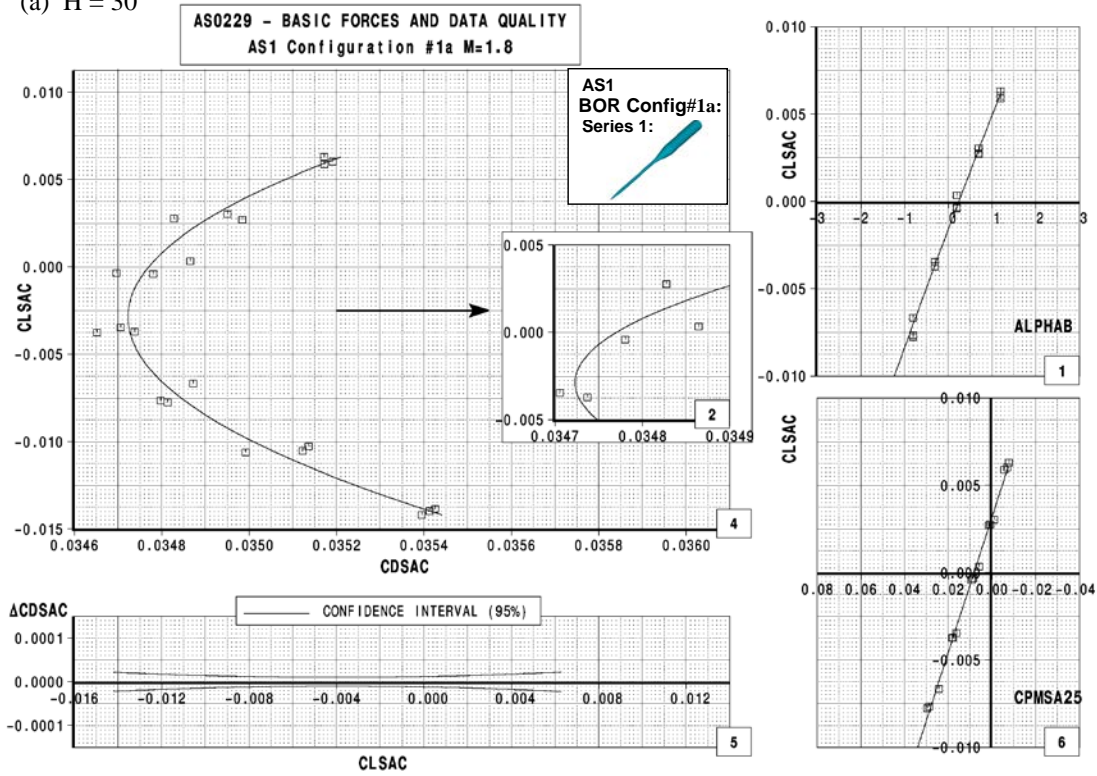


Figure 7.5-17. Typical BOR F&M Data Quality, M = 1.60

(a) H = 30



(b) H = 60

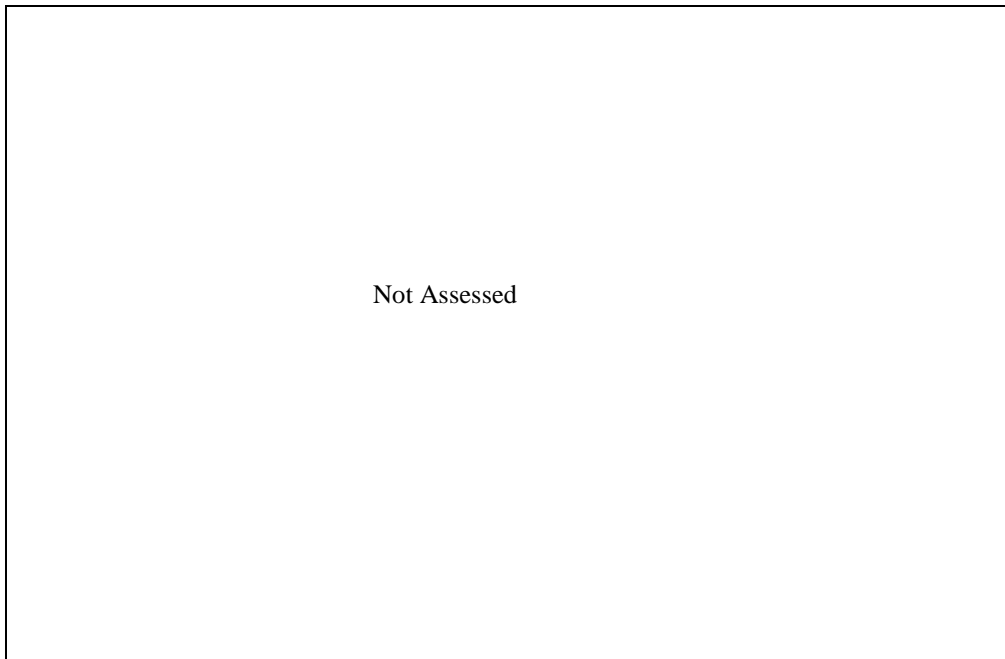
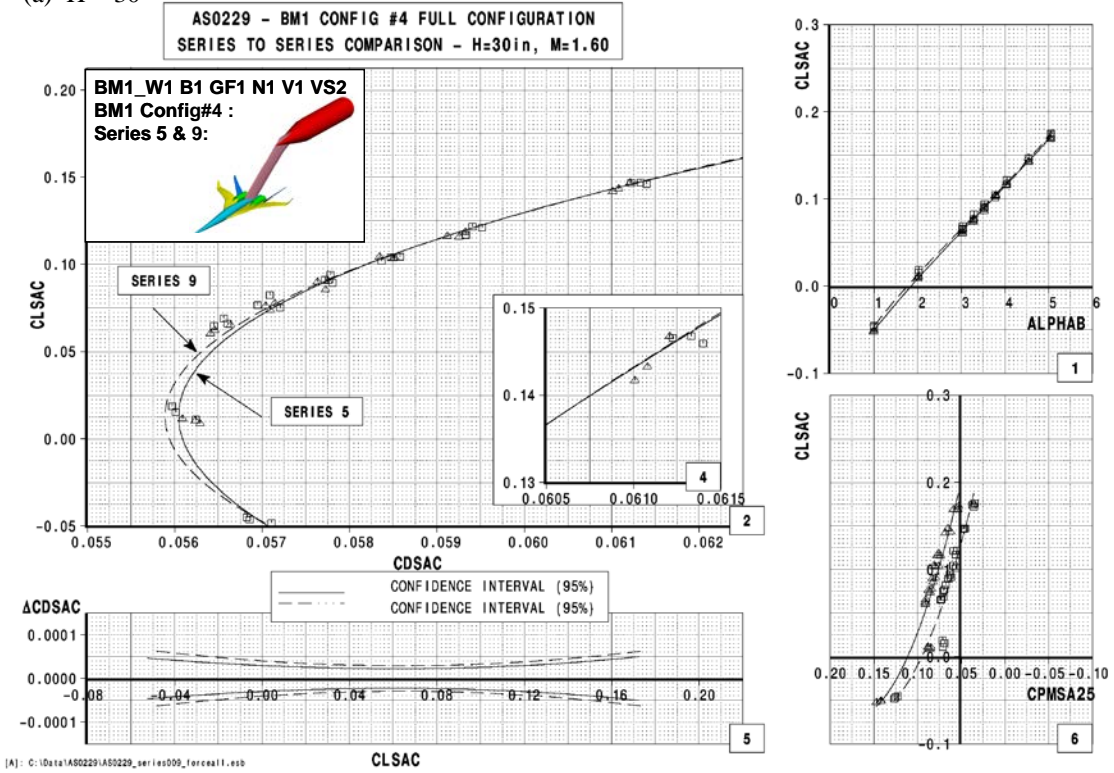


Figure 7.5-18. Typical BOR F&M Data Quality, M = 1.80

(a) H = 30



(b) H = 60

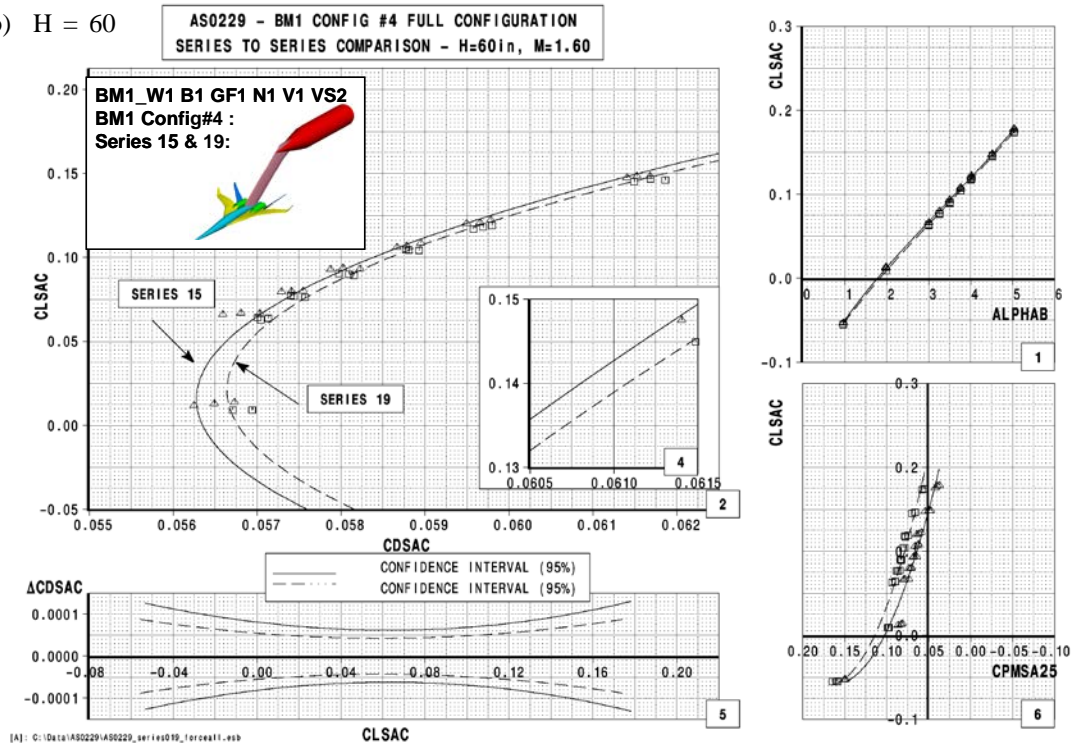
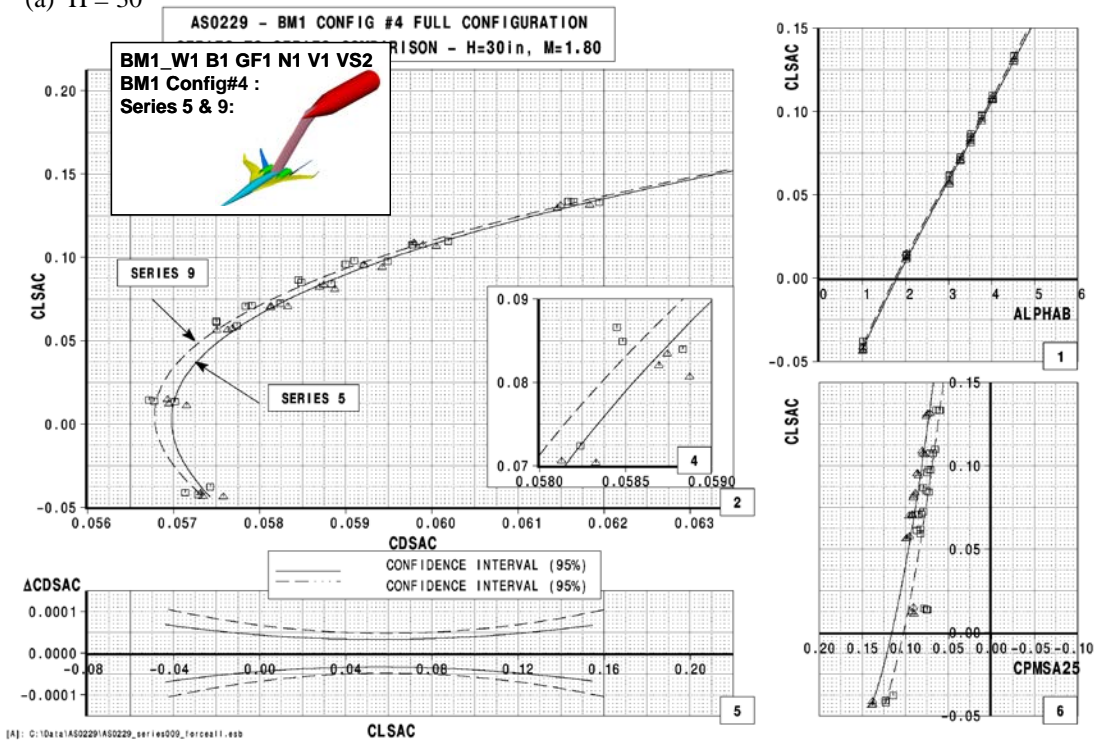


Figure 7.5-19. Typical BM F&M Data Repeatability, M = 1.60

(a) H = 30



(b) H = 60

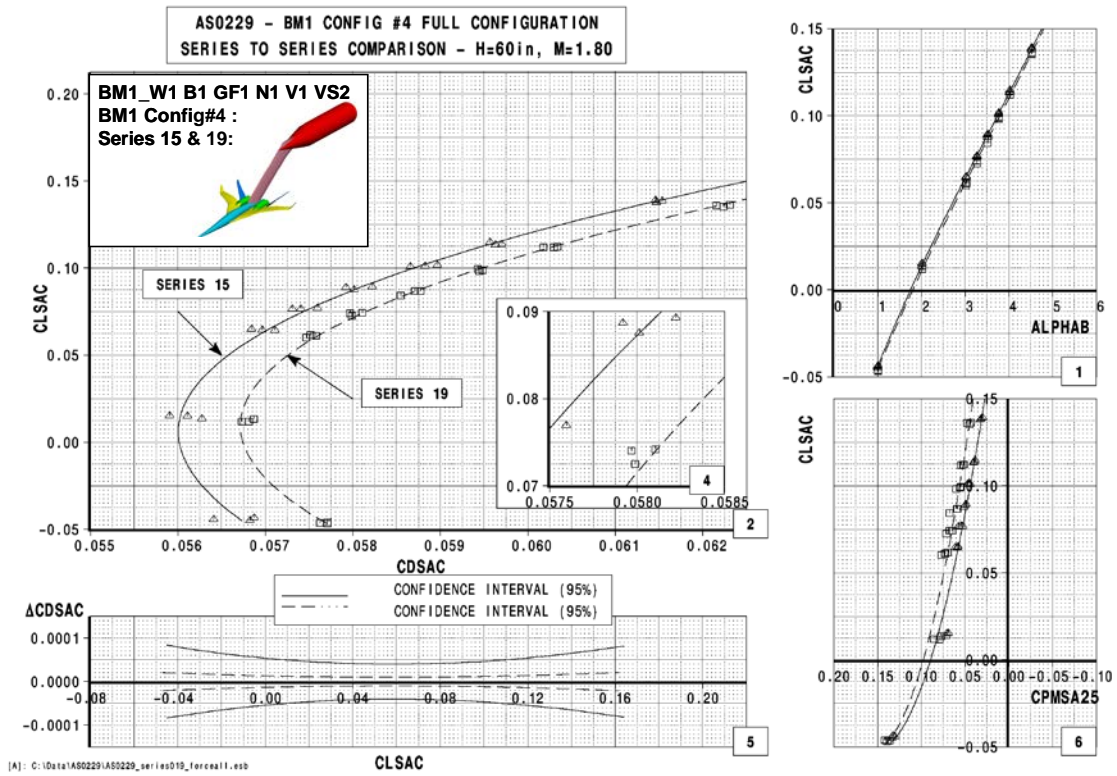
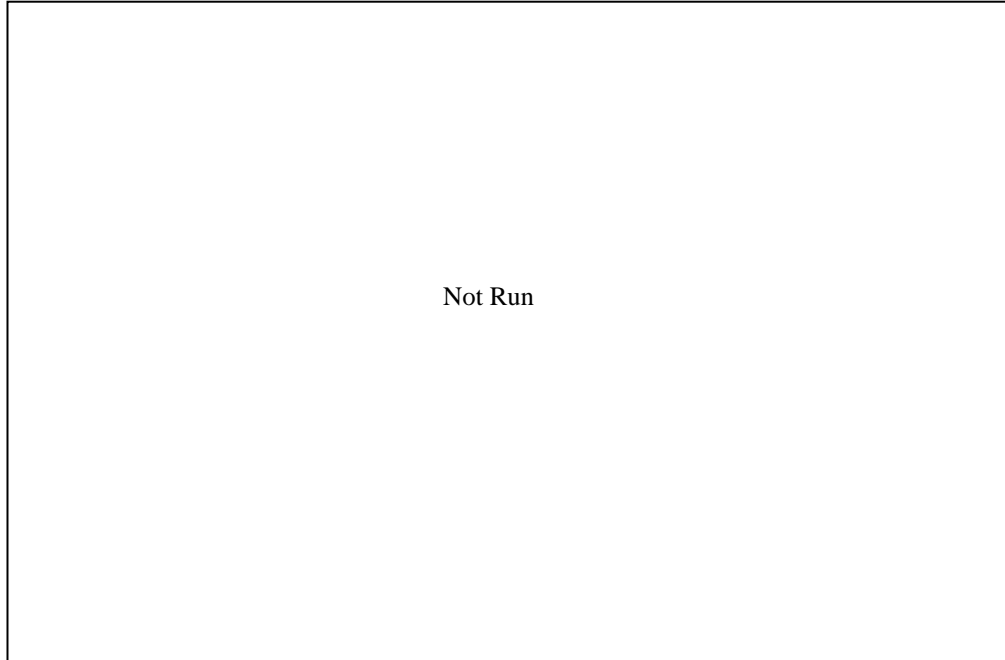


Figure 7.5-20. Typical BM F&M Data Repeatability, M = 1.80

(a) $H = 30$



(b) $H = 60$

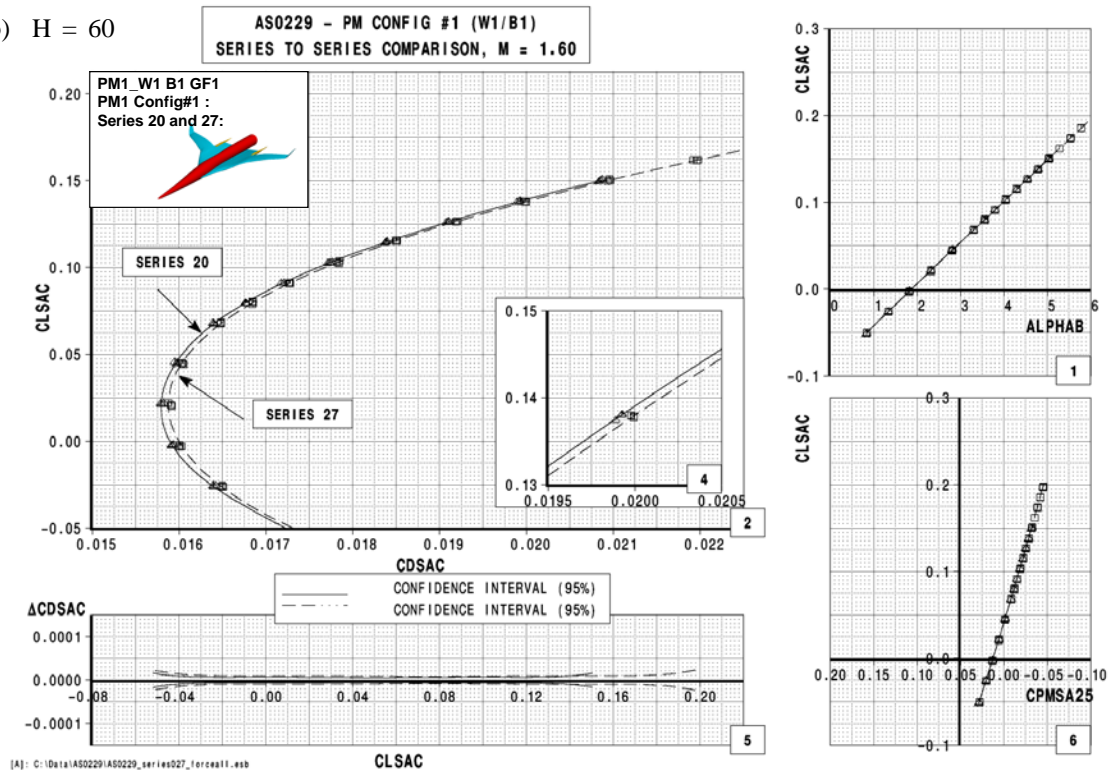
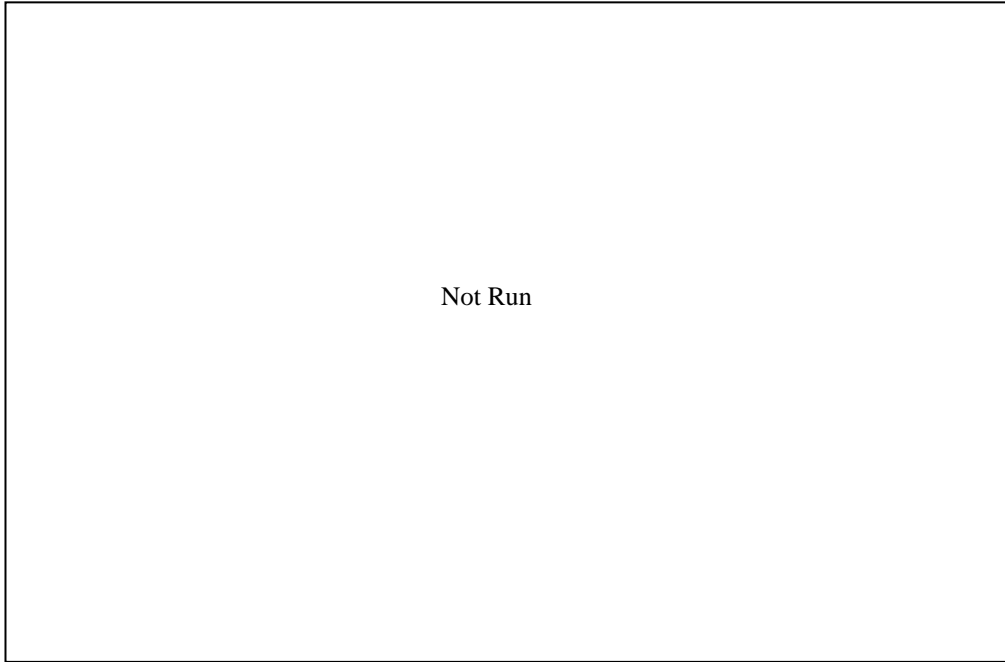


Figure 7.5-21. Typical PM F&M Data Repeatability, $M = 1.60$

(a) H = 30



(b) H = 60

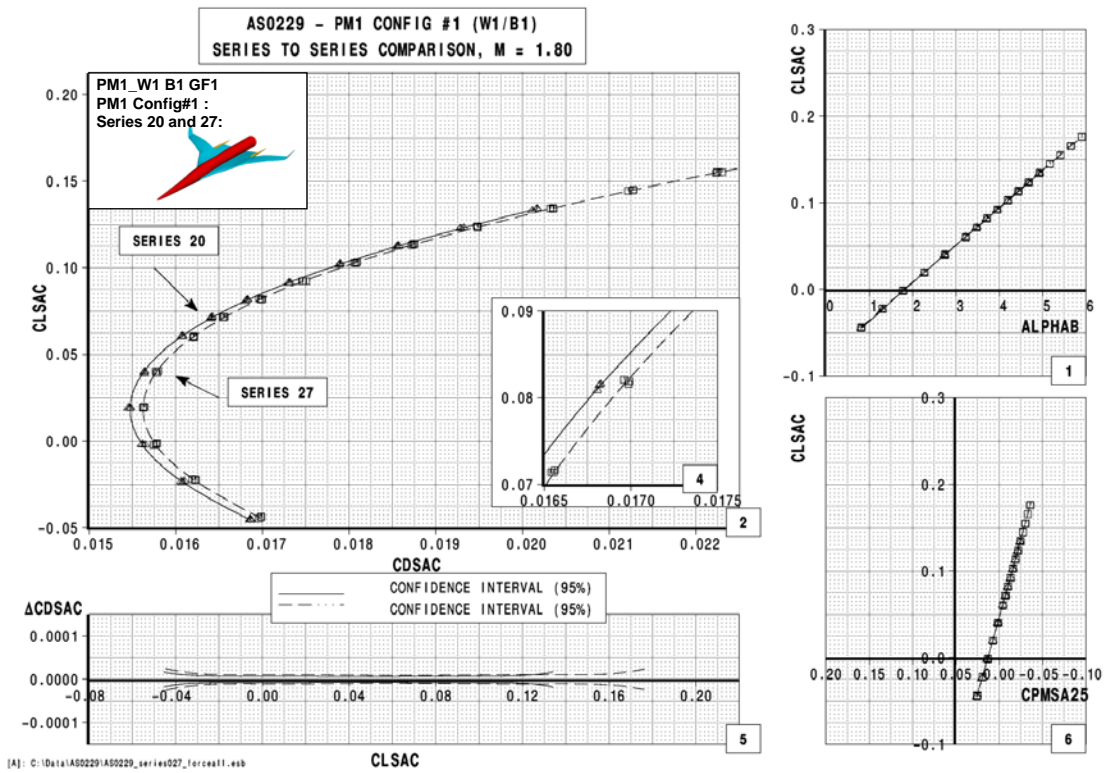


Figure 7.5-22. Typical PM F&M Data Repeatability, M = 1.80

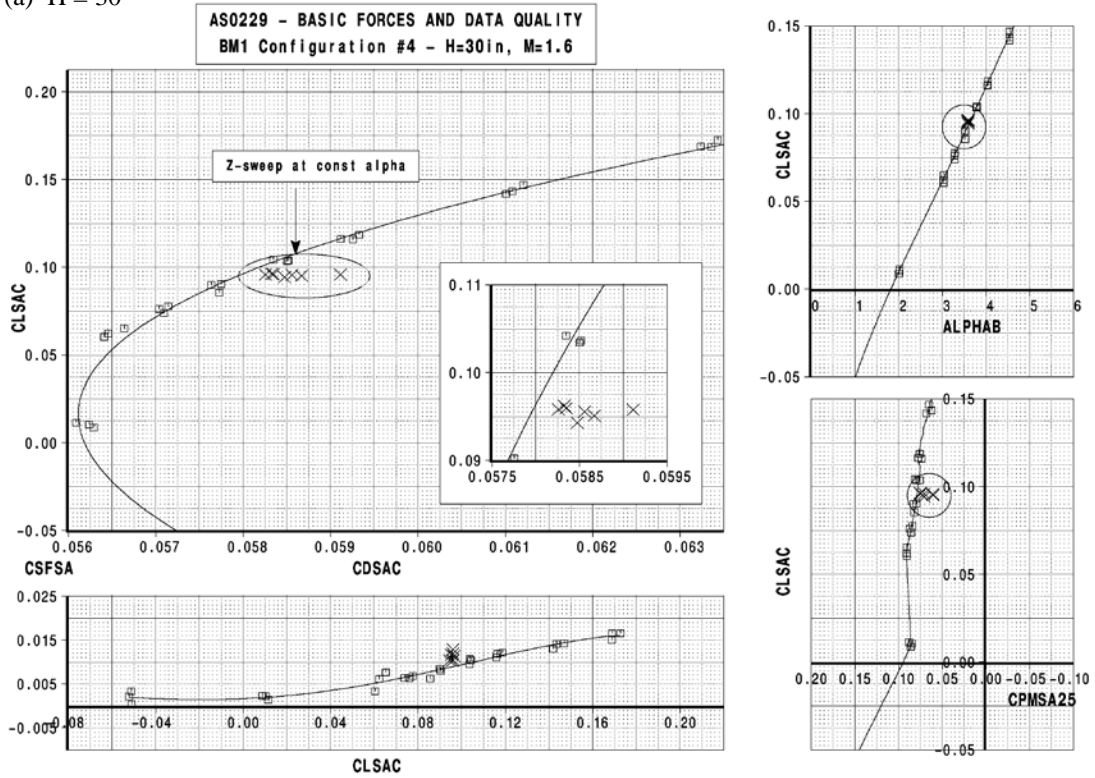
Force Data Variation With Height

The effect of model height above the rail on the force and moment data was assessed. For these runs, the model was moved in the \pm “z-direction” from the noted nominal model position while it remained at a constant angle of attack. A “snapshot” of height variation is presented herein for the same boom and performance model configurations as discussed in the previous sections. As can be seen in the figures, there is a notable effect of model position on the F&M data.

Figures 7.5-23 and 7.5-24 show the effect of the model height on the F&M data for the boom model configuration (BM1, Configuration 4 shown) for $M = 1.60$ and 1.80 , respectively. There is a noticeable (~ 11 counts) positive drag shift with model height at the nominal 30-inch position for both Mach numbers. This positive drag shift trend is also observed in the 60-inch Mach 1.80 data but the trend reverses at Mach 1.80 at the 30-in model position. There is also a positive trend in side force (~ 0.005) consistent with both Mach numbers. The pitching moment trend reverses from positive at $M = 1.60$ to negative at $M = 1.80$. It is perceived that these effects are attributable to an absence of flow uniformity in the test section.

Figures 7.5-25 and 7.5-26 show the effect of the model height on the F&M data for the performance model configurations (PM1, Configuration 1 shown) for $M = 1.60$ and 1.80 , respectively. There is little effect of model height on the lift, drag, or pitching moment at either Mach numbers. However, there still remains the positive trend in side force, ~ 0.005 at $M = 1.60$, that doubles in magnitude at $M = 1.80$.

(a) $H = 30$



(b) $H = 60$

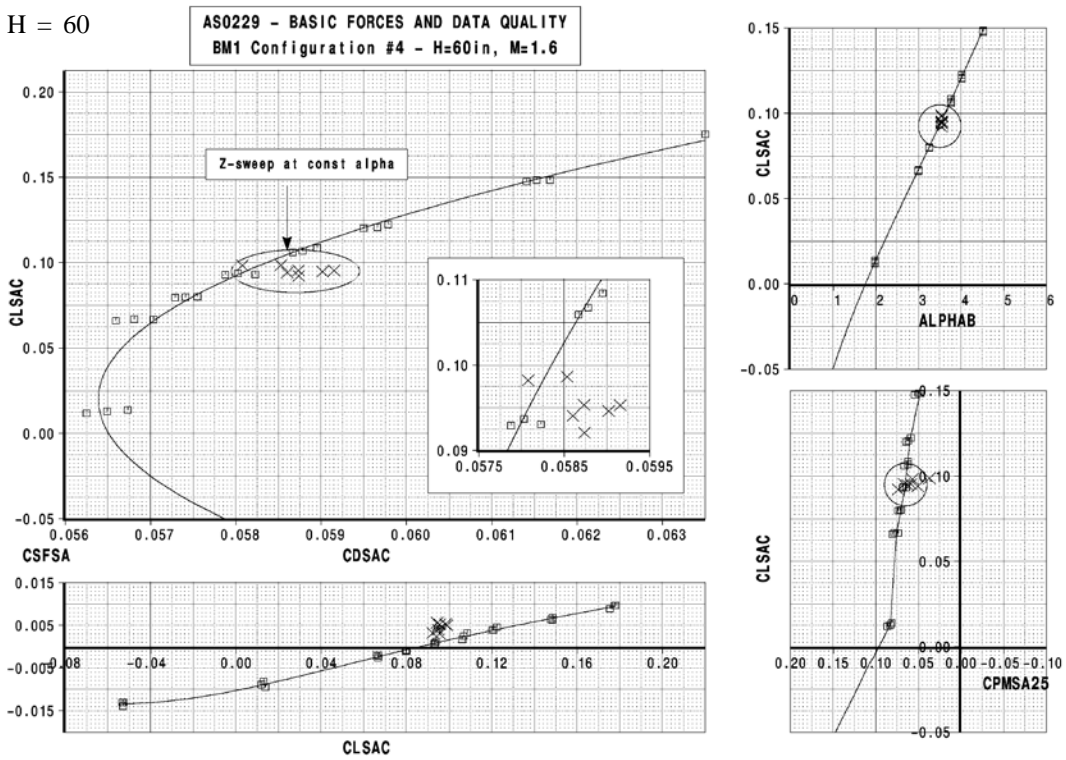
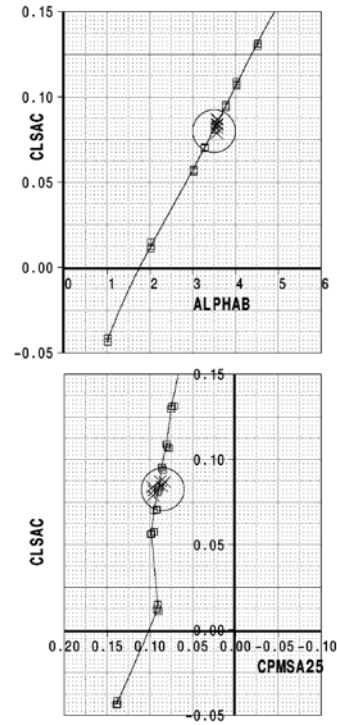
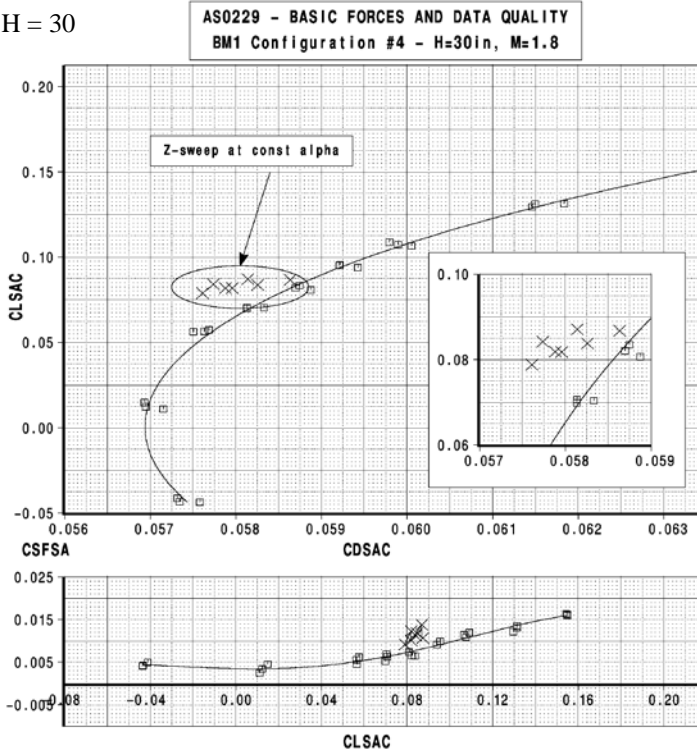


Figure 7.5-23. Typical Boom Model F&M Height Variation, $M = 1.60$

(a) $H = 30$



(b) $H = 60$

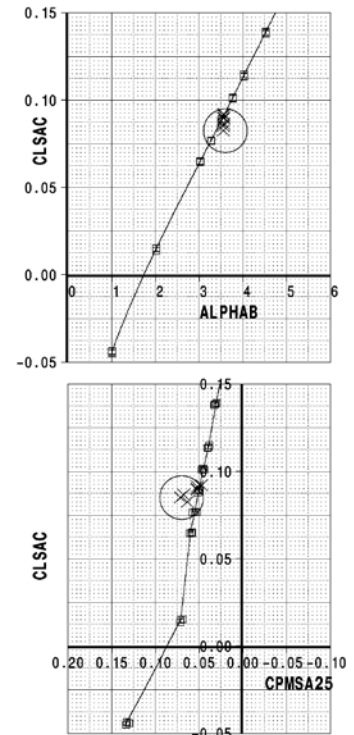
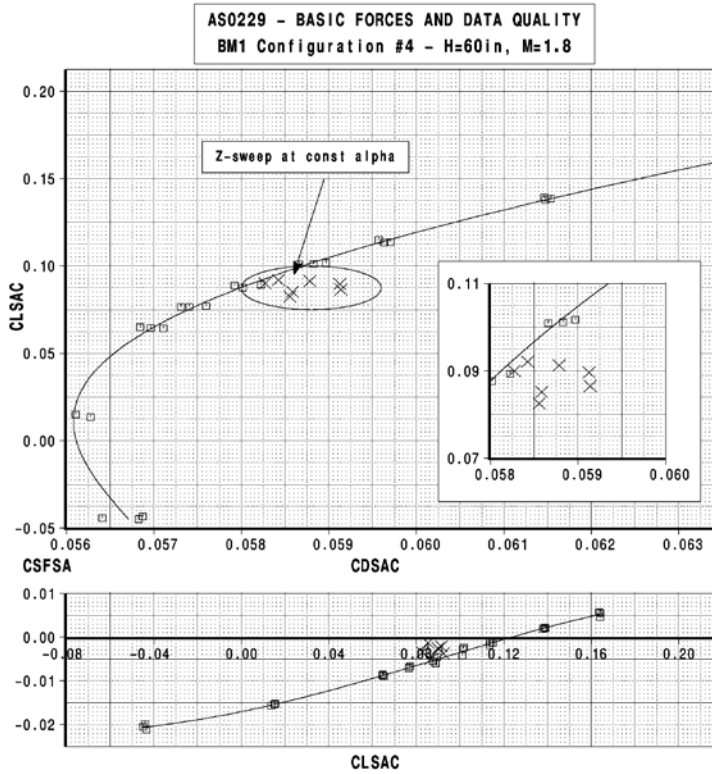
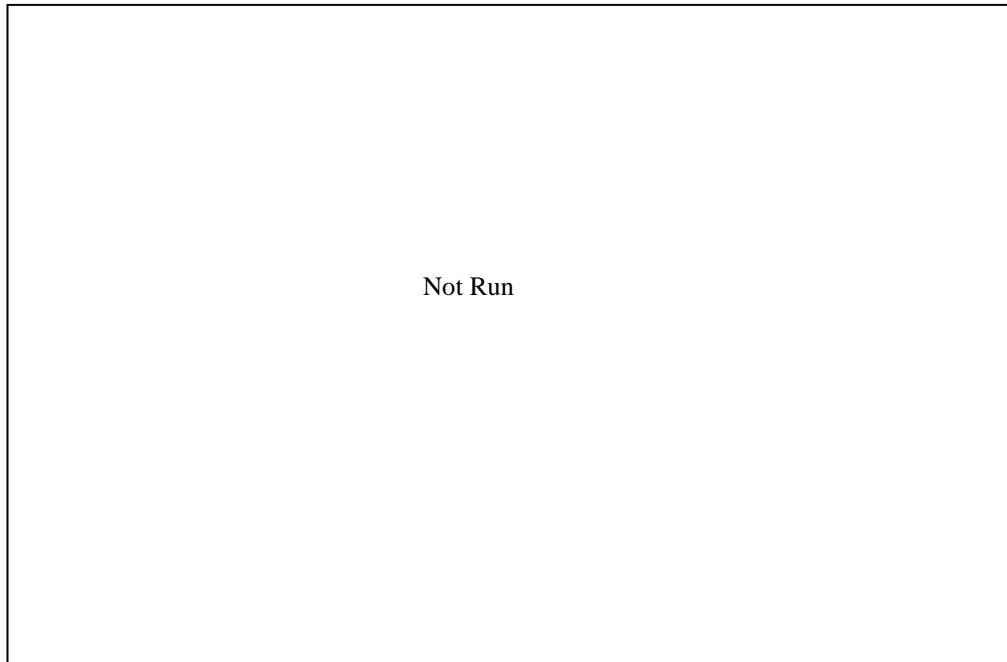


Figure 7.5-24. Typical Boom Model F&M Height Variation, $M = 1.80$

(a) $H = 30$



(b) $H = 60$

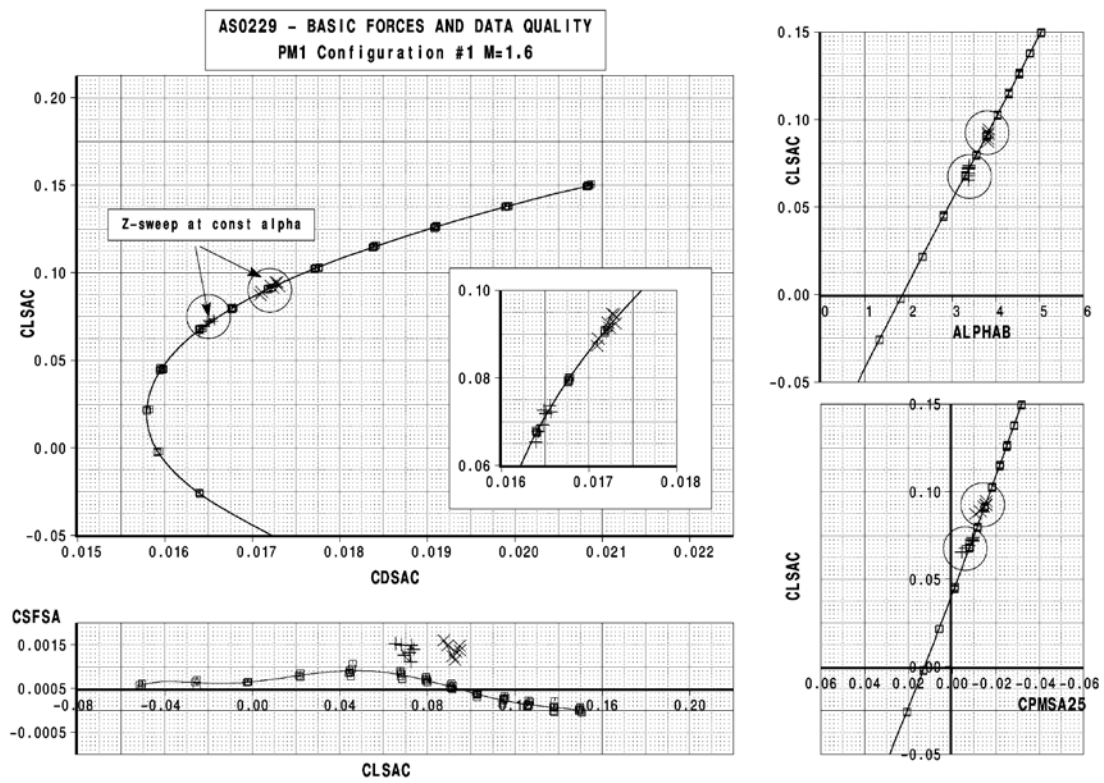
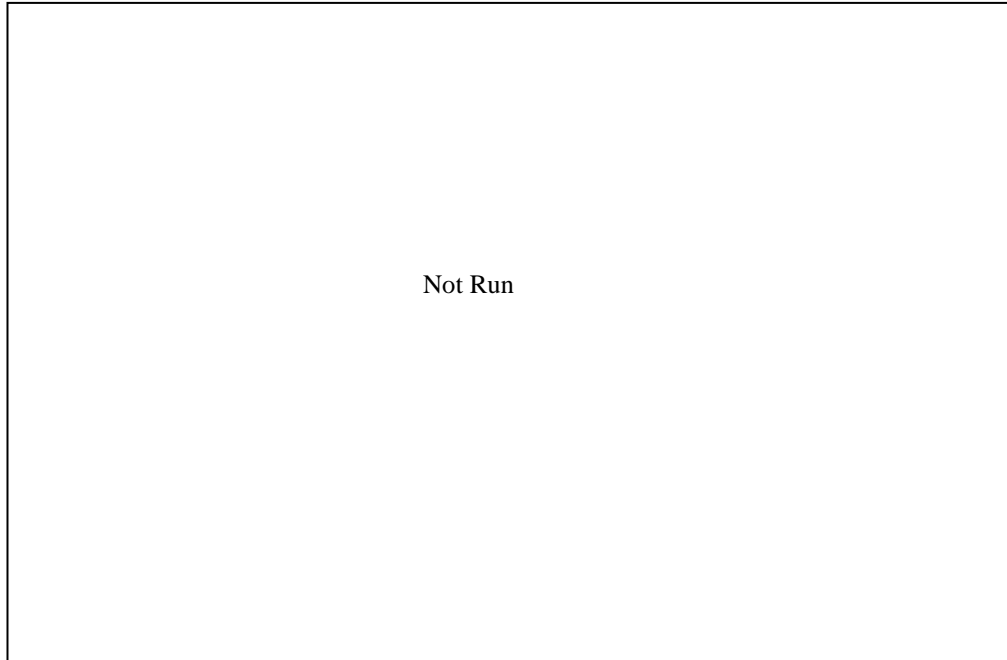


Figure 7.5-25. Typical Performance Model F&M Height Variation, $M = 1.60$

(a) H = 30



(b) H = 60

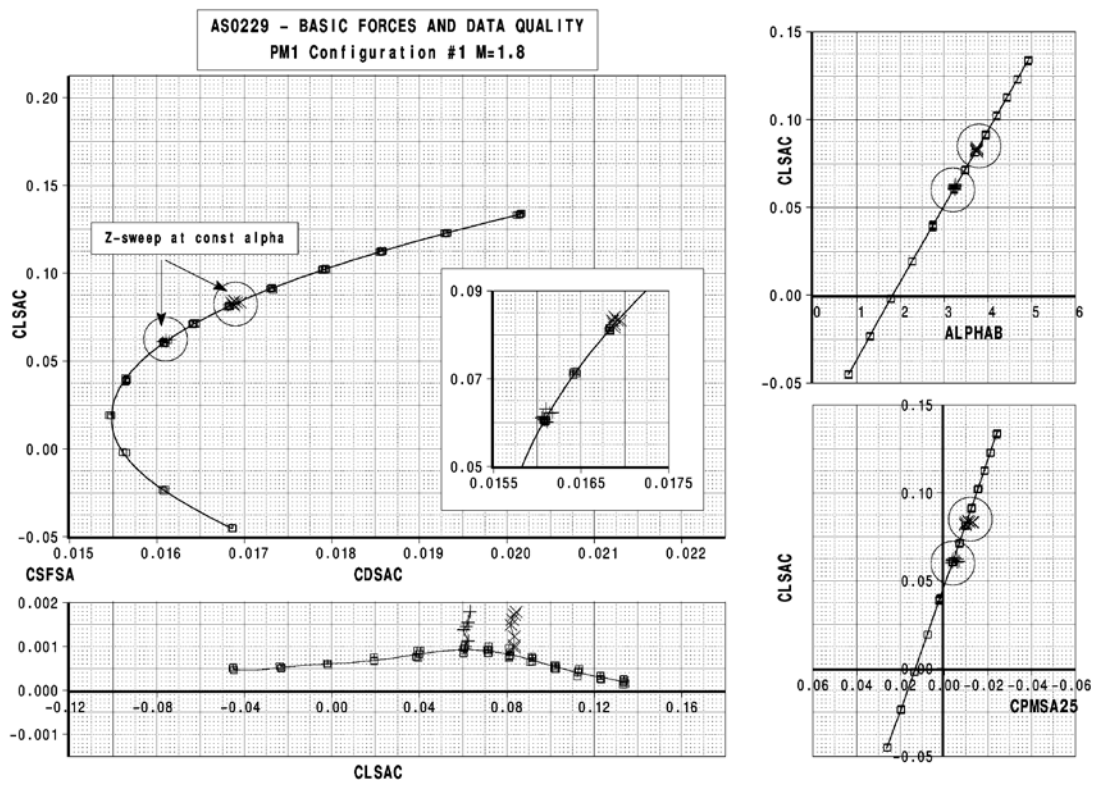


Figure 7.5-26. Typical Performance Model F&M Height Variation, M = 1.80

7.6 Wind Tunnel Test Summary and Conclusions

Through excellent teamwork and extensive pretest planning and preparation, the AS0229 N+2 Experimental Validation test was deemed very successful. The NASA Ames 9' x 7' supersonic wind tunnel test facility offered “world-class” productivity, with more than 1230 force and pressure runs acquired throughout a 20-shift entry. A total of 19 configurations were evaluated at various locations in the tunnel with more than 33 wind-on series.

Following a thorough, systematic calibration of the new 2” alternate pressure rail fabricated for the test using three calibration bodies (bodies of revolution), it was concluded that the rail met all desired Boeing criteria and provided commercial-level productivity for sonic boom testing. The rail was readily installed and its 458 pressures all remained healthy throughout the test. Although flow quality issues had been discovered in the NASA Ames 9' x 7' supersonic wind tunnel facility (e.g., sinusoidal pressure variation with strut location) that may have influenced the pressure rail evaluations, with proper corrections the rail should allow experimental validation of N+2 concepts.* Clean-tunnel variations and repeatability with body of revolution data are within ± 0.001 to ± 0.002 . Furthermore, there does not seem to be any interference issues with the alternate pressure rail.

Data quality was very good and within the accuracy/uncertainty of the instrumentation. Model dynamics were not a problem for any of the models tested, although precautions had been taken (e.g., additional boom model sting parts) before the test to potentially mitigate any effects had they arisen. There was no evidence of strong signal-to-rail/tunnel wall interferences, nor was there any evidence of strong shock/shock interference. Short- and long-term force and pressure repeatability were good. In addition, no strong time-dependency effects were observed.

It was observed that strut position can affect the reference run pressures. Model overall size and angle of attack also affect the pressures above and beyond the boom signal. Because similar effects have been seen previously on the 2-, 5.25-, 14- and 18-inch rails, it is reasonable to expect that these features span the test section and are not strictly wall-to-wall/boundary layer-dependent. For the test methods used in this test, the individual signatures at a specified axial and lateral (from wall) position in the tunnel must be viewed as having a signal with a bias and precision error built-in. That error was often on the same order as the signal. A “standard” correction (using a single reference run obtained in a specific manner) was not a sufficient tare for the pressure rail, given the facility capabilities and characteristics. Future tests should consider randomizing the bias, using spatial averaging to improve the data (i.e., use model movement), creating correlations (more instrumentation upstream in vanes), providing flow conditioning in front of the rail or aft of the model/strut, and, perhaps, changing how the model is positioned.* Additional test-methods development work is required to more fully capitalize on the total capability of the 9' x 7' facility with regard to sonic boom testing, and additional work is needed to reduce the overall uncertainty of the experimental datasets used for validation.

* Note: After the validation test, additional wind tunnel investigation of the 2” alternate and 14” blade rail were conducted. It was found that spatial averaging in the axial direction significantly improves the data quality. It was also determined that the rails had up to ~6 seconds of pressure lag due to the long line lengths in the rail instrumentation. The 14” blade rail provided for a consistent reflection factor of 1 and no tunnel wall reflections for model lengths less than ~35 inches at a Mach number of 1.6. The 2” alternate rail, due to its shorter height, does have a tunnel wall reflection for model lengths greater than ~5 inches at a Mach number of 1.6. Based on Boeing experience, testing in tunnels with porous walls may remove this issue. However, with proper corrections these reflections can be removed from the data in any tunnel. The preferred rail for future testing depends upon the size of the model. For small sonic boom models the 14 inch blade rail appears to be the best choice, especially for minimal corrections to the data. For models larger than 35 inches at Mach 1.6, the preferred choice may be the 2” alternate rail, especially if the interest is in the aft signature on a model with propulsion affects. In this situation both rails require corrections, but the H/L can be maximized with the 2” alternate rail.

8.0 CFD AND VALIDATION ANALYSIS

8.1 Overview

The AS-0229 NASA Ames 9' x 7' supersonic wind tunnel sonic boom and performance test performed in April 2011 provided a substantial database for CFD calibration. Data were acquired at $M = 1.6$ and $M = 1.8$ at heights of 24 to 36 inches and 54 to 66 inches from a wall-mounted pressure rail. Forces and moments of the model configurations were acquired by a full six-component force balance. Test models included three bodies of revolution, 5 configurations of a 15-inch-long boom model and 10 configurations of a 44-inch-long performance model. Figure 8.1-1 provides illustrations of the models and the corresponding test parameters.

Note: Configurations highlighted in **blue** are those used for validation of the Boeing Sonic Boom Tool Suite.

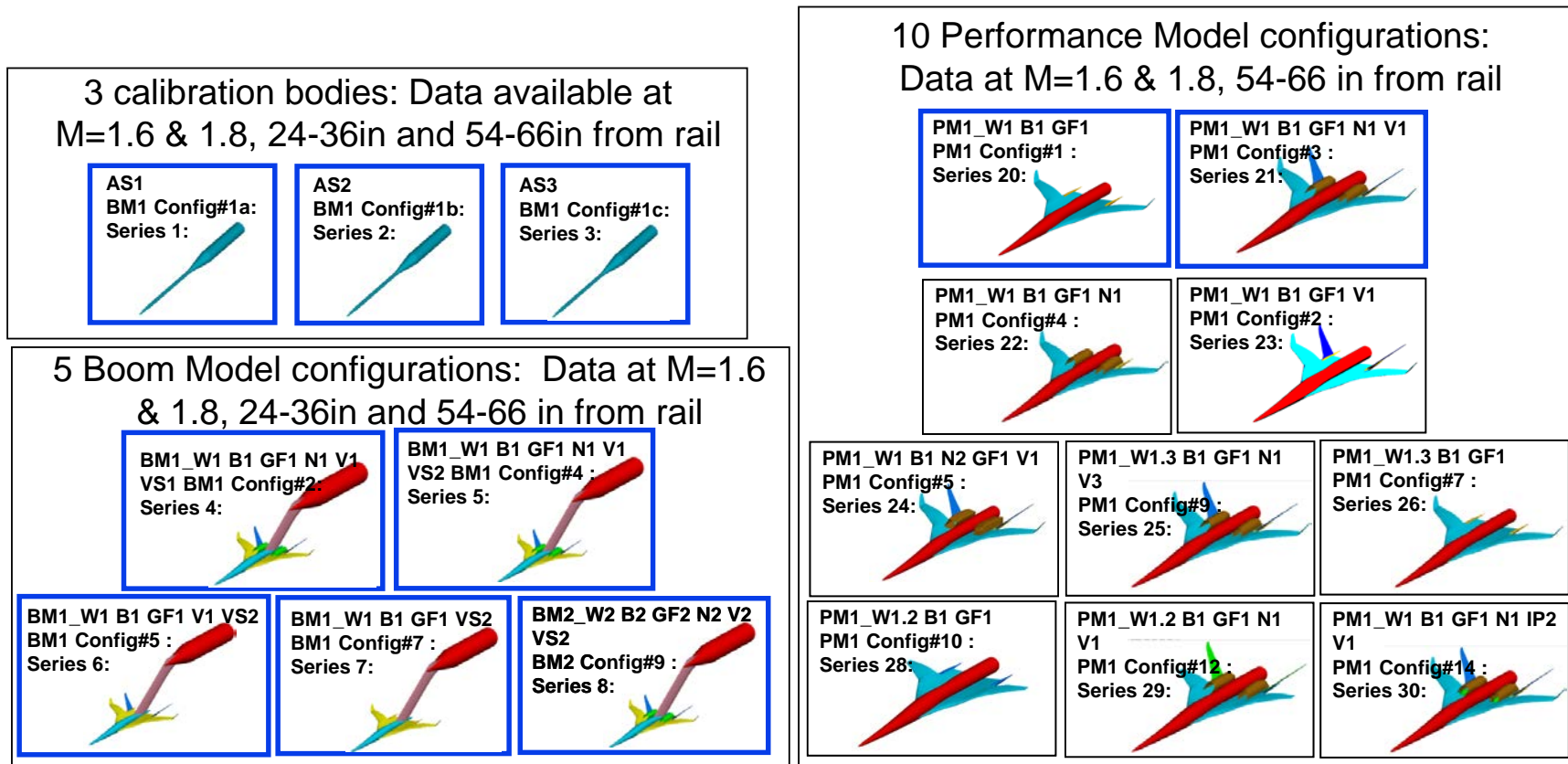



Figure 8.1-1. Available NASA Ames 9' x 7' Supersonic Wind Tunnel AS-0229 Test Configurations

8.2 Summary of CFD Cases


Pre-test and post-test OVERFLOW Euler and Navier Stokes analyses were run on 10 of the tested configurations (see the highlighted configurations in Figure 8.1-1), predominantly at the wind tunnel Reynolds number. Cases for all boom model configurations were run with and without the upper swept strut. Tables 8.2-1 through 8.2-3 define attributes of each of the CFD cases run for the body of revolution, boom and performance models, respectively. Each checked box in the tables indicates an available solution. The solutions for the performance model configurations were obtained with both a cylindrical wake and a sharp step sting. Additional analyses were undertaken to quantify the effects of model support hardware, aeroelastics and wind tunnel Reynolds numbers (WT Re) on the data. As expected, the wind tunnel test environment (modification for model support, WT Re) significantly alters the signatures. Overall, the correlation with test data was good and well within the accuracy/uncertainty of the experimental data.

Table 8.2-1. CFD Cases for BOR Models

AS1, Configuration 1a, CFD Analysis

BOR MODEL CASES	Mach	Alpha	CL	Euler F&M	NS F&M	H=30 in EU DP/P	H=60 in EUDP/P	H=90 in EU DP/P	H=30 in NS DP/P	H=60 in NS DP/P	H=90 in NS DP/P
Configuration # 1a AS1 	1.60	0.00		X	X	X	X	X	X	X	X
	1.60	1.00		X	X	X	X	X	X	X	X
	1.60	2.00		X	X	X	X	X	X	X	X
	1.60	3.00		X	X	X	X	X	X	X	X
	1.60	4.00		X	X	X	X	X	X	X	X
	1.60	5.00		X	X	X	X	X	X	X	X
	1.60		0.120								
	1.60		0.140								
	1.60		0.160								
	1.80	0.00		X	X	X	X	X	X	X	X
	1.80	1.00		X	X	X	X	X	X	X	X
	1.80	2.00		X	X	X	X	X	X	X	X
	1.80	3.00		X	X	X	X	X	X	X	X
	1.80	4.00		X	X	X	X	X	X	X	X
	1.80	5.00		X	X	X	X	X	X	X	X
	1.80		0.080								
	1.80		0.100								
	1.80		0.120								

AS2, Configuration 1b, CFD Analysis

BOR MODEL CASES	Mach	Alpha	CL	Euler F&M	NS F&M	H=30 in EU DP/P	H=60 in EUDP/P	H=90 in EU DP/P	H=30 in NS DP/P	H=60 in NS DP/P	H=90 in NS DP/P
Configuration # 1b AS2 	1.60	0.00		X	X	X	X	X	X	X	X
	1.60	1.00		X		X	X	X			
	1.60	2.00		X		X	X	X			
	1.60	3.00		X		X	X	X			
	1.60	4.00		X		X	X	X			
	1.60	5.00		X		X	X	X			
	1.60		0.120								
	1.60		0.140								
	1.60		0.160								
	1.80	0.00		X	X	X	X	X	X	X	X
	1.80	1.00		X		X	X	X			
	1.80	2.00		X		X	X	X			
	1.80	3.00		X		X	X	X			
	1.80	4.00		X		X	X	X			
	1.80	5.00		X		X	X	X			
	1.80		0.080								
	1.80		0.100								
	1.80		0.120								

AS3, Configuration 1c, CFD Analysis


BOR MODEL CASES	Mach	Alpha	CL	Euler F&M	NS F&M	H=30 in EU DP/P	H=60 in EUDP/P	H=90 in EU DP/P	H=30 in NS DP/P	H=60 in NS DP/P	H=90 in NS DP/P
Configuration # 1c AS3 	1.60	0.00		X	X	X	X	X	X	X	X
	1.60	1.00		X	X	X	X	X			
	1.60	2.00		X	X	X	X	X			
	1.60	3.00		X	X	X	X	X			
	1.60	4.00		X	X	X	X	X			
	1.60	5.00		X	X	X	X	X			
	1.60		0.120								
	1.60		0.140								
	1.60		0.160								
	1.80	0.00		X	X	X	X	X	X	X	X
	1.80	1.00		X	X	X	X	X			
	1.80	2.00		X	X	X	X	X			
	1.80	3.00		X	X	X	X	X			
	1.80	4.00		X	X	X	X	X			
	1.80	5.00		X	X	X	X	X			
	1.80		0.080								
	1.80		0.100								
	1.80		0.120								

Table 8.2-2. CFD Cases for BM Models

BM1, Configuration 2, CFD Analysis

BM MODEL CASE	Mach	Alpha	CL	F&M and Pressures with upper swept strut and balance shield									F&M and Pressures mounting hardware removed								
				Euler F&M	NS F&M	H=30 in EU DP/P	H=60 in EU DP/P	H=90 in EU DP/P	H=30 in NS DP/P	H=60 in NS DP/P	H=90 in NS DP/P	Euler F&M	NS F&M	H=30 in EU DP/P	H=60 in EU DP/P	H=90 in EU DP/P	H=30 in NS DP/P	H=60 in NS DP/P	H=90 in NS DP/P		
Configuration # 2 BM1 W1B1GF1N1V1 VS1 Full Configuration Short USS strut No stabs	1.60	0.00		X		X	X	X													
	1.60	1.00		X		X	X	X													
	1.60	2.00		X		X	X	X													
	1.60	3.00		X		X	X	X													
	1.60	4.00		X		X	X	X													
	1.60	5.00		X		X	X	X													
	1.60	3.39	0.120	X		X	X	X													
	1.60	3.74	0.140	X		X	X	X													
	1.60	4.10	0.160	X		X	X	X													
	1.80	0.00		X		X	X	X													
	1.80	1.00		X		X	X	X													
	1.80	2.00		X		X	X	X													
	1.80	3.00		X		X	X	X													
	1.80	4.00		X		X	X	X													
	1.80	5.00		X		X	X	X													
	1.80	2.85	0.080	X		X	X	X													
	1.80	3.24	0.100	X		X	X	X													
	1.80	3.63	0.120	X		X	X	X													

BM1, Configuration 4, CFD Analysis

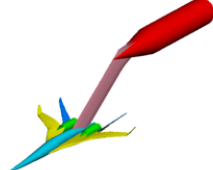
BM MODEL CASE	Mach	Alpha	CL	F&M and Pressures with upper swept strut and balance shield									F&M and Pressures mounting hardware removed								
				Euler F&M	NS F&M	H=30 in EU DP/P	H=60 in EU DP/P	H=90 in EU DP/P	H=30 in NS DP/P	H=60 in NS DP/P	H=90 in NS DP/P	Euler F&M	NS F&M	H=30 in EU DP/P	H=60 in EU DP/P	H=90 in EU DP/P	H=30 in NS DP/P	H=60 in NS DP/P	H=90 in NS DP/P		
Configuration # 4* BM1 W1B1GF1N1V1VS2 Full Configuration Long strut/No stabs	1.60	0.00		X	X	X	X	X	X	X											
	1.60	1.00		X	X	X	X	X	X	X											
	1.60	2.00		X	X	X	X	X	X	X											
	1.60	3.00		X	X	X	X	X	X	X											
	1.60	4.00		X	X	X	X	X	X	X											
	1.60	5.00		X	X	X	X	X	X	X											
	1.60	3.39	0.120	X	X	X	X	X	X	X	X	X	X	X	X	X	X	X	X		
	1.60	3.74	0.140	X	X	X	X	X	X	X	X	X	X	X	X	X	X	X	X		
	1.60	4.10	0.160	X	X	X	X	X	X	X	X	X	X	X	X	X	X	X	X		
	1.80	0.00		X	X	X	X	X	X	X	X										
	1.80	1.00		X	X	X	X	X	X	X	X										
	1.80	2.00		X	X	X	X	X	X	X	X										
	1.80	3.00		X	X	X	X	X	X	X	X										
	1.80	4.00		X	X	X	X	X	X	X	X										
	1.80	5.00		X	X	X	X	X	X	X	X										
	1.80	2.85	0.080	X	X	X	X	X	X	X	X	X	X	X	X	X	X	X	X		
	1.80	3.24	0.100	X	X	X	X	X	X	X	X	X	X	X	X	X	X	X	X		
	1.80	3.63	0.120	X	X	X	X	X	X	X	X	X	X	X	X	X	X	X	X		

BM1, Configuration 4, AE = -2 CFD Analysis

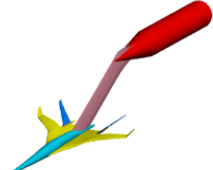
BM MODEL CASE	Mach	Alpha	CL	F&M and Pressures with upper swept strut and balance shield									F&M and Pressures mounting hardware removed								
				Euler F&M	NS F&M	H=30 in EU DP/P	H=60 in EU DP/P	H=90 in EU DP/P	H=30 in NS DP/P	H=60 in NS DP/P	H=90 in NS DP/P	Euler F&M	NS F&M	H=30 in EU DP/P	H=60 in EU DP/P	H=90 in EU DP/P	H=30 in NS DP/P	H=60 in NS DP/P	H=90 in NS DP/P		
Configuration # 4* BM1 W1B1GF1N1V1VS2 Full Configuration Long strut/No stabs Series #4 -2DEG aeroelastics	1.60	0.00																			
	1.60	1.00																			
	1.60	2.00																			
	1.60	3.00																			
	1.60	4.00																			
	1.60	5.00																			
	1.60	3.39	0.120		X				X	X	X	X	X	X	X	X	X	X	X		
	1.60	3.74	0.140		X				X	X	X	X	X	X	X	X	X	X	X		
	1.60	4.10	0.160		X				X	X	X	X	X	X	X	X	X	X	X		
	1.80	0.00																			
	1.80	1.00																			
	1.80	2.00																			
	1.80	3.00																			
	1.80	4.00																			
	1.80	5.00																			
	1.80	2.85	0.080		X				X	X	X	X	X	X	X	X	X	X	X		
	1.80	3.24	0.100		X				X	X	X	X	X	X	X	X	X	X	X		
1.80	3.63	0.120		X				X	X	X	X	X	X	X	X	X	X	X			

Table 8.2-2. CFD Cases for BM Models (Continued)

BM1, Configuration 4, AE = -4 CFD Analysis

BM MODEL CASE	Mach	Alpha	CL	F&M and Pressures with upper swept strut and balance shield									F&M and Pressures mounting hardware removed								
				Euler F&M	NS F&M	H=30 in EU DP/P	H=60 in EU DP/P	H=90 in EU DP/P	H=30 in NS DP/P	H=60 in NS DP/P	H=90 in NS DP/P	Euler F&M	NS F&M	H=30 in EU DP/P	H=60 in EU DP/P	H=90 in EU DP/P	H=30 in NS DP/P	H=60 in NS DP/P	H=90 in NS DP/P		
Configuration # 4* BM1 W1B1GF1N1V1VS2 Full Configuration Long strut/No stabs Series #4 4DEG aeroelastics 	1.60	0.00																			
	1.60	1.00																			
	1.60	2.00																			
	1.60	3.00																			
	1.60	4.00																			
	1.60	5.00																			
	1.60	3.39	0.120		X					X	X	X	X		X	X	X				
	1.60	3.74	0.140		X					X	X	X	X		X	X	X				
	1.60	4.10	0.160		X					X	X	X	X		X	X	X				
	1.80	0.00																			
	1.80	1.00																			
	1.80	2.00																			
	1.80	3.00																			
	1.80	4.00																			
	1.80	5.00																			
	1.80	2.85	0.080		X					X	X	X	X		X	X	X				
	1.80	3.24	0.100		X					X	X	X	X		X	X	X				
	1.80	3.63	0.120		X					X	X	X	X		X	X	X				

BM1, Configuration 5, CFD Analysis

BM MODEL CASE	Mach	Alpha	CL	F&M and Pressures with upper swept strut and balance shield									F&M and Pressures mounting hardware removed								
				Euler F&M	NS F&M	H=30 in EU DP/P	H=60 in EU DP/P	H=90 in EU DP/P	H=30 in NS DP/P	H=60 in NS DP/P	H=90 in NS DP/P	Euler F&M	NS F&M	H=30 in EU DP/P	H=60 in EU DP/P	H=90 in EU DP/P	H=30 in NS DP/P	H=60 in NS DP/P	H=90 in NS DP/P		
Configuration #5* BM1 W1B1GF1V1VS2 Nacelle off Long strut/No stabs 	1.60	0.00		X		X	X	X													
	1.60	1.00		X		X	X	X													
	1.60	2.00		X		X	X	X													
	1.60	3.00		X		X	X	X													
	1.60	4.00		X		X	X	X													
	1.60	5.00		X		X	X	X													
	1.60	3.35	0.120	X		X	X	X				X		X	X	X					
	1.60	3.70	0.140	X		X	X	X				X		X	X	X					
	1.60	4.06	0.160	X		X	X	X				X		X	X	X					
	1.80	0.00			X		X	X													
	1.80	1.00			X		X	X													
	1.80	2.00			X		X	X													
	1.80	3.00			X		X	X													
	1.80	4.00			X		X	X													
	1.80	5.00			X		X	X													
	1.80	2.79	0.080		X		X	X				X		X	X	X					
	1.80	3.18	0.100		X		X	X				X		X	X	X					
	1.80	3.57	0.120		X		X	X				X		X	X	X					

BM1, Configuration 6, CFD Analysis

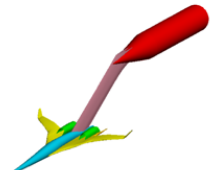
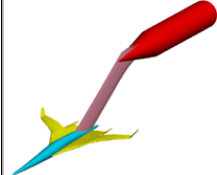
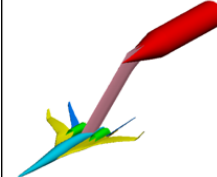
BM MODEL CASE	Mach	Alpha	CL	F&M and Pressures with upper swept strut and balance shield									F&M and Pressures mounting hardware removed								
				Euler F&M	NS F&M	H=30 in EU DP/P	H=60 in EU DP/P	H=90 in EU DP/P	H=30 in NS DP/P	H=60 in NS DP/P	H=90 in NS DP/P	Euler F&M	NS F&M	H=30 in EU DP/P	H=60 in EU DP/P	H=90 in EU DP/P	H=30 in NS DP/P	H=60 in NS DP/P	H=90 in NS DP/P		
Configuration # 6 BM1 W1B1GF1N1VS2 Tail off Long strut/No stabs 	1.60	0.00		X		X	X	X													
	1.60	1.00		X		X	X	X													
	1.60	2.00		X		X	X	X													
	1.60	3.00		X		X	X	X													
	1.60	4.00		X		X	X	X													
	1.60	5.00		X		X	X	X													
	1.60	3.73	0.120	X		X	X	X				X		X	X	X					
	1.60	4.12	0.140	X		X	X	X				X		X	X	X					
	1.60	4.51	0.160	X		X	X	X				X		X	X	X					
	1.80	0.00			X		X	X													
	1.80	1.00			X		X	X													
	1.80	2.00			X		X	X													
	1.80	3.00			X		X	X													
	1.80	4.00			X		X	X													
	1.80	5.00			X		X	X													
	1.80	3.08	0.080		X		X	X				X		X	X	X					
	1.80	3.51	0.100		X		X	X				X		X	X	X					
	1.80	3.94	0.120		X		X	X				X		X	X	X					

Table 8.2-2. CFD Cases for BM Models (Continued)

BM1, Configuration 7, CFD Analysis

BM MODEL CASE	Mach	Alpha	CL	F&M and Pressures with upper swept strut and balance shield									F&M and Pressures mounting hardware removed								
				Euler F&M	NS F&M	H=30 in EU DP/P	H=60 in EU DP/P	H=90 in EU DP/P	H=30 in NS DP/P	H=60 in NS DP/P	H=90 in NS DP/P	Euler F&M	NS F&M	H=30 in EU DP/P	H=60 in EU DP/P	H=90 in EU DP/P	H=30 in NS DP/P	H=60 in NS DP/P	H=90 in NS DP/P		
Configuration # 7 BM1 W1B1GF1N1VS2 Nacelle & Tail off Long strut/No stabs 	1.60	0.00																			
	1.60	1.00		X		X	X	X													
	1.60	2.00		X		X	X	X													
	1.60	3.00		X		X	X	X													
	1.60	4.00		X		X	X	X													
	1.60	5.00		X		X	X	X													
	1.60	3.71	0.120	X		X	X	X					X		X	X	X				
	1.60	4.10	0.140	X		X	X	X					X		X	X	X				
	1.60	4.49	0.160	X		X	X	X					X		X	X	X				
	1.80	0.00																			
	1.80	1.00			X		X	X	X												
	1.80	2.00			X		X	X	X												
	1.80	3.00			X		X	X	X												
	1.80	4.00			X		X	X	X												
	1.80	5.00			X		X	X	X												
	1.80	3.06	0.080		X		X	X	X					X		X	X	X			
	1.80	3.48	0.100		X		X	X	X					X		X	X	X			
	1.80	3.91	0.120		X		X	X	X					X		X	X	X			

BM2, Configuration 9, CFD Analysis

BM MODEL CASE	Mach	Alpha	CL	F&M and Pressures with upper swept strut and balance shield									F&M and Pressures mounting hardware removed								
				Euler F&M	NS F&M	H=30 in EU DP/P	H=60 in EU DP/P	H=90 in EU DP/P	H=30 in NS DP/P	H=60 in NS DP/P	H=90 in NS DP/P	Euler F&M	NS F&M	H=30 in EU DP/P	H=60 in EU DP/P	H=90 in EU DP/P	H=30 in NS DP/P	H=60 in NS DP/P	H=90 in NS DP/P		
Configuration # 9* BM2 W2B2GF2N2V2VS2 Full Configuration Long strut/No stabs 	1.60	0.00		X	X	X	X	X	X	X											
	1.60	1.00		X	X	X	X	X	X	X	X										
	1.60	2.00		X	X	X	X	X	X	X	X										
	1.60	3.00		X	X	X	X	X	X	X	X										
	1.60	4.00		X	X	X	X	X	X	X	X										
	1.60	5.00		X	X	X	X	X	X	X	X										
	1.60	4.98	0.120	X	X	X	X	X	X	X	X	X	X	X	X	X	X	X	X	X	
	1.60	5.32	0.140	X	X	X	X	X	X	X	X	X	X	X	X	X	X	X	X	X	
	1.60	5.66	0.160	X	X	X	X	X	X	X	X	X	X	X	X	X	X	X	X	X	
	1.80	0.00			X	X	X	X	X	X	X										
	1.80	1.00			X	X	X	X	X	X	X										
	1.80	2.00			X	X	X	X	X	X	X										
	1.80	3.00			X	X	X	X	X	X	X										
	1.80	4.00			X	X	X	X	X	X	X										
	1.80	5.00			X	X	X	X	X	X	X										
	1.80	4.36	0.080		X	X	X	X	X	X	X	X	X	X	X	X	X	X	X	X	
	1.80	4.74	0.100		X	X	X	X	X	X	X	X	X	X	X	X	X	X	X	X	
	1.80	5.13	0.120		X	X	X	X	X	X	X	X	X	X	X	X	X	X	X	X	

BM2, Configuration 10, CFD Analysis

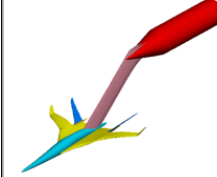
BM MODEL CASE	Mach	Alpha	CL	F&M and Pressures with upper swept strut and balance shield									F&M and Pressures mounting hardware removed								
				Euler F&M	NS F&M	H=30 in EU DP/P	H=60 in EU DP/P	H=90 in EU DP/P	H=30 in NS DP/P	H=60 in NS DP/P	H=90 in NS DP/P	Euler F&M	NS F&M	H=30 in EU DP/P	H=60 in EU DP/P	H=90 in EU DP/P	H=30 in NS DP/P	H=60 in NS DP/P	H=90 in NS DP/P		
Configuration # 10* BM2 W2B2GF2V2VS2 Nacelle off Long strut/No stabs 	1.60	0.00		X		X	X	X													
	1.60	1.00		X		X	X	X													
	1.60	2.00		X		X	X	X													
	1.60	3.00		X		X	X	X													
	1.60	4.00		X		X	X	X													
	1.60	5.00		X		X	X	X													
	1.60	4.95	0.120	X		X	X	X					X		X	X	X				
	1.60	5.28	0.140	X		X	X	X					X		X	X	X				
	1.60	5.62	0.160	X		X	X	X					X		X	X	X				
	1.80	0.00			X		X	X	X												
	1.80	1.00			X		X	X	X												
	1.80	2.00			X		X	X	X												
	1.80	3.00			X		X	X	X												
	1.80	4.00			X		X	X	X												
	1.80	5.00			X		X	X	X												
	1.80	4.31	0.080		X		X	X	X					X		X	X	X			
	1.80	4.69	0.100		X		X	X	X					X		X	X	X			
	1.80	5.07	0.120		X		X	X	X					X		X	X	X			

Table 8.2-2. CFD Cases for BM Models (Continued)

BM2, Configuration 12, CFD Analysis

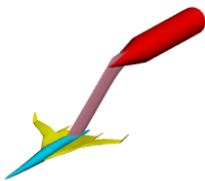

BM MODEL CASE	F&M and Pressures with upper swept strut and balance shield										F&M and Pressures mounting hardware removed								
	Mach	Alpha	CL	Euler F&M	NS F&M	H=30 in EU DP/P	H=60 in EU DP/P	H=90 in EU DP/P	H=30 in NS DP/P	H=60 in NS DP/P	H=90 in NS DP/P	Euler F&M	NS F&M	H=30 in EU DP/P	H=60 in EU DP/P	H=90 in EU DP/P	H=30 in NS DP/P	H=60 in NS DP/P	H=90 in NS DP/P
Configuration # 12 BM2 W2B2GF2VS2 Nacelle & Tail off Long strut/No stabs 	1.60	0.00		X		X	X	X											
	1.60	1.00		X		X	X	X											
	1.60	2.00		X		X	X	X											
	1.60	3.00		X		X	X	X											
	1.60	4.00		X		X	X	X											
	1.60	5.00		X		X	X	X											
	1.60	5.19	0.120	X		X	X	X				X		X	X	X			
	1.60	5.56	0.140	X		X	X	X				X		X	X	X			
	1.60	5.93	0.160	X		X	X	X				X		X	X	X			
	1.80	0.00		X		X	X	X											
	1.80	1.00		X		X	X	X											
	1.80	2.00		X		X	X	X											
	1.80	3.00		X		X	X	X											
	1.80	4.00		X		X	X	X											
	1.80	5.00		X		X	X	X											
	1.80	4.50	0.080	X		X	X	X				X		X	X	X			
	1.80	4.92	0.100	X		X	X	X				X		X	X	X			
	1.80	5.34	0.120	X		X	X	X				X		X	X	X			

Table 8.2-3. CFD Cases for PM Models

PM1, Configuration 1, CFD Analysis

PM MODEL CASE	F&M and Pressures with Flared aftbody and cylindrical wake										
	Mach	Alpha	CL	Euler F&M	NS F&M	H=30 in EU DP/P	H=60 in EU DP/P	H=90 in EU DP/P	H=30 in NS DP/P	H=60 in NS DP/P	H=90 in NS DP/P
Configuration # 1 PM1 W1B1.1GF1 Winq/body 	1.60	0.00		X	X	X	X	X	X	X	X
	1.60	1.00		X	X	X	X	X	X	X	X
	1.60	2.00		X	X	X	X	X	X	X	X
	1.60	3.00		X	X	X	X	X	X	X	X
	1.60	4.00		X	X	X	X	X	X	X	X
	1.60	5.00		X	X	X	X	X	X	X	X
	1.60	4.14	0.120	X	X	X	X	X	X	X	X
	1.60	4.52	0.140	X	X	X	X	X	X	X	X
	1.60	4.91	0.160	X	X	X	X	X	X	X	X
	1.80	0.00		X	X	X	X	X	X	X	X
	1.80	1.00		X	X	X	X	X	X	X	X
	1.80	2.00		X	X	X	X	X	X	X	X
	1.80	3.00		X	X	X	X	X	X	X	X
	1.80	4.00		X	X	X	X	X	X	X	X
	1.80	5.00		X	X	X	X	X	X	X	X
	1.80	3.46	0.080	X	X	X	X	X	X	X	X
	1.80	3.88	0.100	X	X	X	X	X	X	X	X
	1.80	4.30	0.120	X	X	X	X	X	X	X	X

PM1, Configuration 3, CFD Analysis

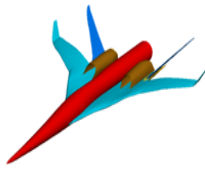
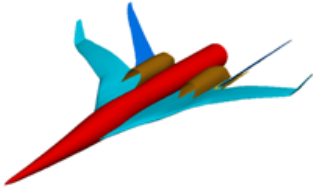
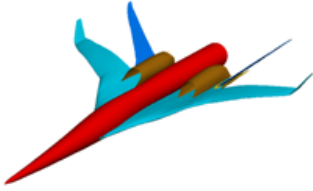
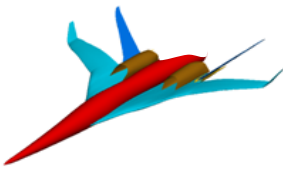
PM MODEL CASE	F&M and Pressures with Flared aftbody and cylindrical wake										F&M and Pressures with Flared aftbody and step to sting modeled								
	Mach	Alpha	CL	Euler F&M	NS F&M	H=30 in EU DP/P	H=60 in EU DP/P	H=90 in EU DP/P	H=30 in NS DP/P	H=60 in NS DP/P	H=90 in NS DP/P	Euler F&M	NS F&M	H=30 in EU DP/P	H=60 in EU DP/P	H=90 in EU DP/P	H=30 in NS DP/P	H=60 in NS DP/P	H=90 in NS DP/P
Configuration # 3 PM1 W1B1.1GF1N1V1 Full Configuration 	1.60	0.00		X	X	X	X	X	X	X									
	1.60	1.00		X	X	X	X	X	X	X									
	1.60	2.00		X	X	X	X	X	X	X									
	1.60	3.00		X	X	X	X	X	X	X									
	1.60	4.00		X	X	X	X	X	X	X									
	1.60	5.00		X	X	X	X	X	X	X									
	1.60	3.39	0.120	X	X	X	X	X	X	X		X					X	X	X
	1.60	3.74	0.140	X	X	X	X	X	X	X		X					X	X	X
	1.60	4.10	0.160	X	X	X	X	X	X	X		X					X	X	X
	1.80	0.00		X	X	X	X	X	X	X									
	1.80	1.00		X	X	X	X	X	X	X									
	1.80	2.00		X	X	X	X	X	X	X									
	1.80	3.00		X	X	X	X	X	X	X									
	1.80	4.00		X	X	X	X	X	X	X									
	1.80	5.00		X	X	X	X	X	X	X									
	1.80	2.85	0.080	X	X	X	X	X	X	X		X					X	X	X
	1.80	3.24	0.100	X	X	X	X	X	X	X		X					X	X	X
	1.80	3.63	0.120	X	X	X	X	X	X	X		X					X	X	X

Table 8.2-3. CFD Cases for PM Models (Continued)

PM1, Configuration 3, with Aeroelastics CFD Analysis

F&M and Pressures with Flared aftbody and cylindrical wake											
PM MODEL CASE	Mach	Alpha	CL	Euler F&M	NS F&M	H=30 in EU DP/P	H=60 in EU DP/P	H=90 in EU DP/P	H=30 in NS DP/P	H=60 in NS DP/P	H=90 in NS DP/P
Configuration # 3 PM1 W1B1.1GF1N1V1 Full Configuration -2DEG aeroelastics 	1.60	0.00									
	1.60	1.00									
	1.60	2.00									
	1.60	3.00									
	1.60	4.00									
	1.60	5.00									
	1.60	3.39	0.120		X				X	X	X
	1.60	3.74	0.140		X				X	X	X
	1.60	4.10	0.160		X				X	X	X
	1.80	0.00									
	1.80	1.00									
	1.80	2.00									
	1.80	3.00									
	1.80	4.00									
	1.80	5.00									
	1.80	2.85	0.080		X				X	X	X
	1.80	3.24	0.100		X				X	X	X
	1.80	3.63	0.120		X				X	X	X
F&M and Pressures with Flared aftbody and cylindrical wake											
PM MODEL CASE	Mach	Alpha	CL	Euler F&M	NS F&M	H=30 in EU DP/P	H=60 in EU DP/P	H=90 in EU DP/P	H=30 in NS DP/P	H=60 in NS DP/P	H=90 in NS DP/P
Configuration # 3 PM1 W1B1.1GF1N1V1 Full Configuration -4DEG aeroelastics 	1.60	0.00									
	1.60	1.00									
	1.60	2.00									
	1.60	3.00									
	1.60	4.00									
	1.60	5.00									
	1.60	3.39	0.120		X				X	X	X
	1.60	3.74	0.140		X				X	X	X
	1.60	4.10	0.160		X				X	X	X
	1.80	0.00									
	1.80	1.00									
	1.80	2.00									
	1.80	3.00									
	1.80	4.00									
	1.80	5.00									
	1.80	2.85	0.080		X				X	X	X
	1.80	3.24	0.100		X				X	X	X
	1.80	3.63	0.120		X				X	X	X

PM1, Configuration 3, with Closed Aft-Body CFD Analysis

F&M and Pressures with closed aftbody											
PM MODEL CASE	Mach	Alpha	CL	Euler F&M	NS F&M	H=30 in EU DP/P	H=60 in EU DP/P	H=90 in EU DP/P	H=30 in NS DP/P	H=60 in NS DP/P	H=90 in NS DP/P
Configuration # 3 PM1 W1B1.1GF1N1V1 Full Configuration 	1.60	0.00									
	1.60	1.00									
	1.60	2.00									
	1.60	3.00									
	1.60	4.00									
	1.60	5.00									
	1.60	3.39	0.120		X				X	X	X
	1.60	3.74	0.140		X				X	X	X
	1.60	4.10	0.160		X				X	X	X
	1.80	0.00									
	1.80	1.00									
	1.80	2.00									
	1.80	3.00									
	1.80	4.00									
	1.80	5.00									
	1.80	2.85	0.080		X				X	X	X
	1.80	3.24	0.100		X				X	X	X
	1.80	3.63	0.120		X				X	X	X

8.3 Body of Revolution CFD vs. Test Pressure Signature Comparisons

Pressure Signatures

Comparisons of the CFD results with the Ames 9' x 7' supersonic wind tunnel AS-0229 test data for each of the BOR model configurations at $\alpha = 0$ deg are provided in this section. The CFD results assume an isolated model corrected with a 30% amplification factor to account for the effect of the flat-top reflective nature of the rail.

Figures 8.3-1 and 8.3-2 compare the “dP/P” pressure signatures from the CFD OVERFLOW solutions and the corresponding wind tunnel test data for the AS1 body of revolution configuration for $M = 1.60$ and 1.80 , respectively, and at heights (of nose) of 24 and 58 inches above the rail. In addition to the amplification factor, the CFD data were extracted at 30 and 60 inches off-body and corrected for amplitude by a factor of 30/24 and 60/58, respectively.

Figures 8.3-3 and 8.3-4 compare the “dP/P” pressure signatures from the CFD OVERFLOW solutions and the corresponding wind tunnel test data for the AS2 body of revolution configuration for $M = 1.60$ and 1.80 , respectively, and at heights (of nose) of 24 and 56 inches above the rail. In addition to the amplification factor, the CFD data were extracted at 30 and 60 inches off-body and corrected for amplitude by a factor of 30/24 and 60/56, respectively.

Figures 8.3-5 and 8.3-6 compare the “dP/P” pressure signatures from the CFD OVERFLOW solutions and the corresponding wind tunnel test data for the AS3 body of revolution configuration for $M = 1.60$ and 1.80 , respectively, and at heights (of nose) of 24 and 56 (for $M = 1.60$) or 58 (for $M = 1.80$) inches above the rail. In addition to the amplification factor, the CFD data were extracted at 30 and 60 inches off-body and corrected for amplitude by a factor of 30/24 and 60/56 (or 60/58), respectively.

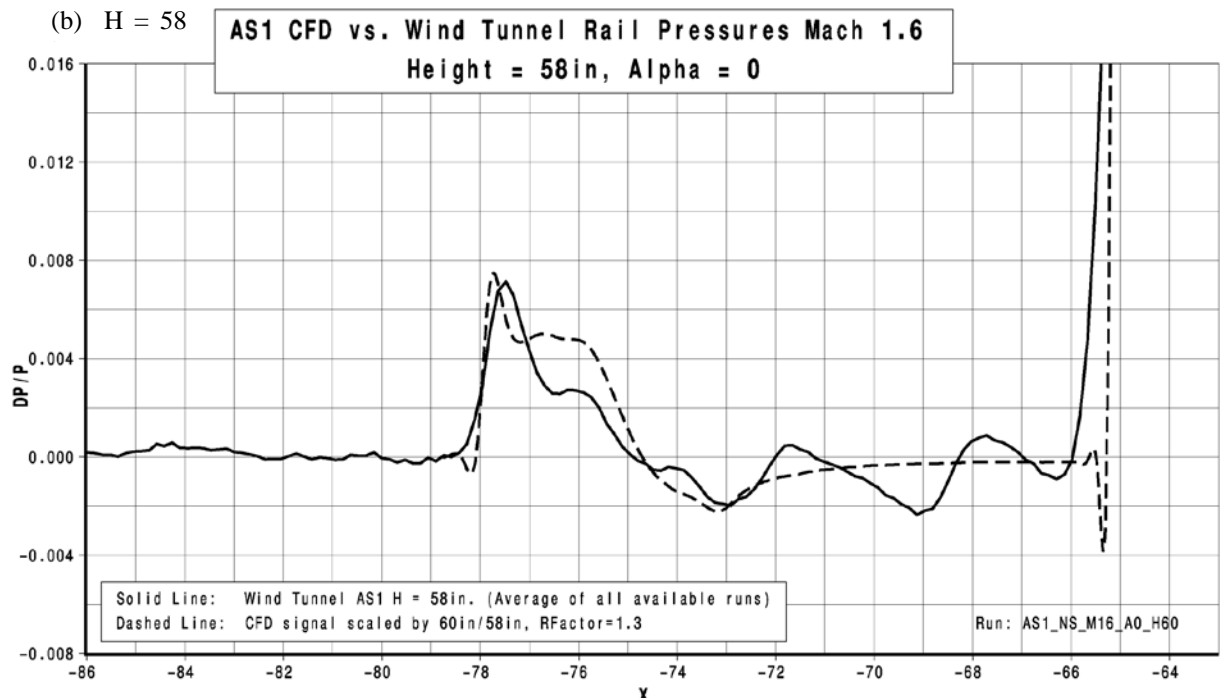
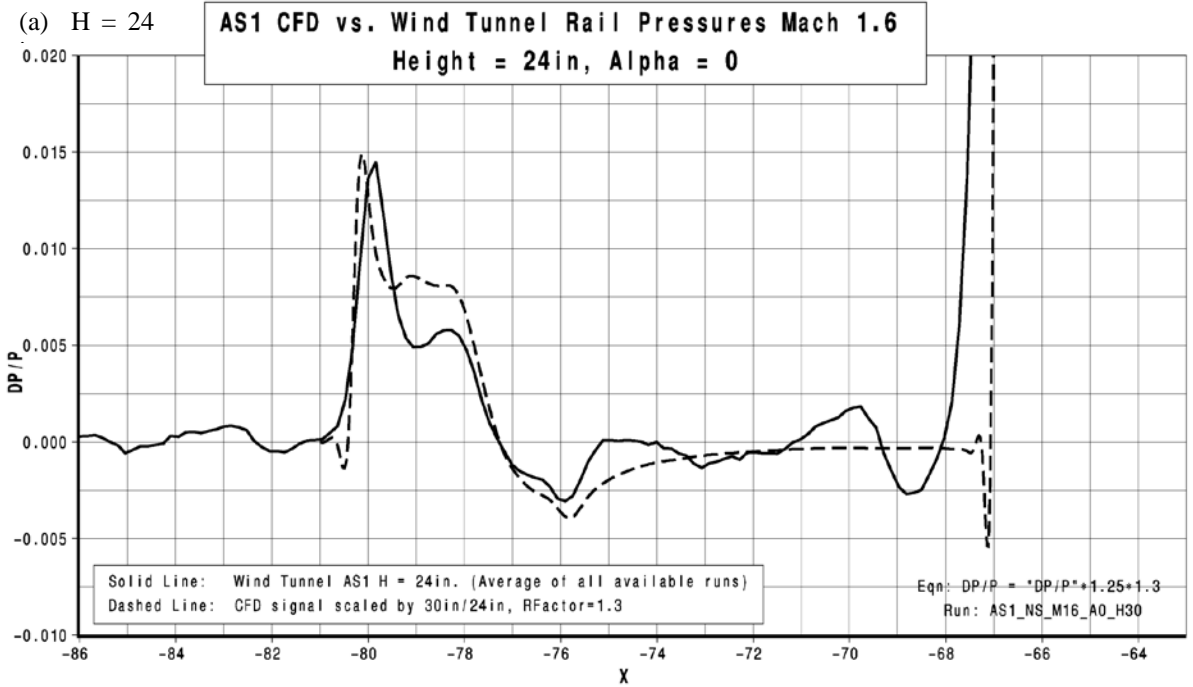
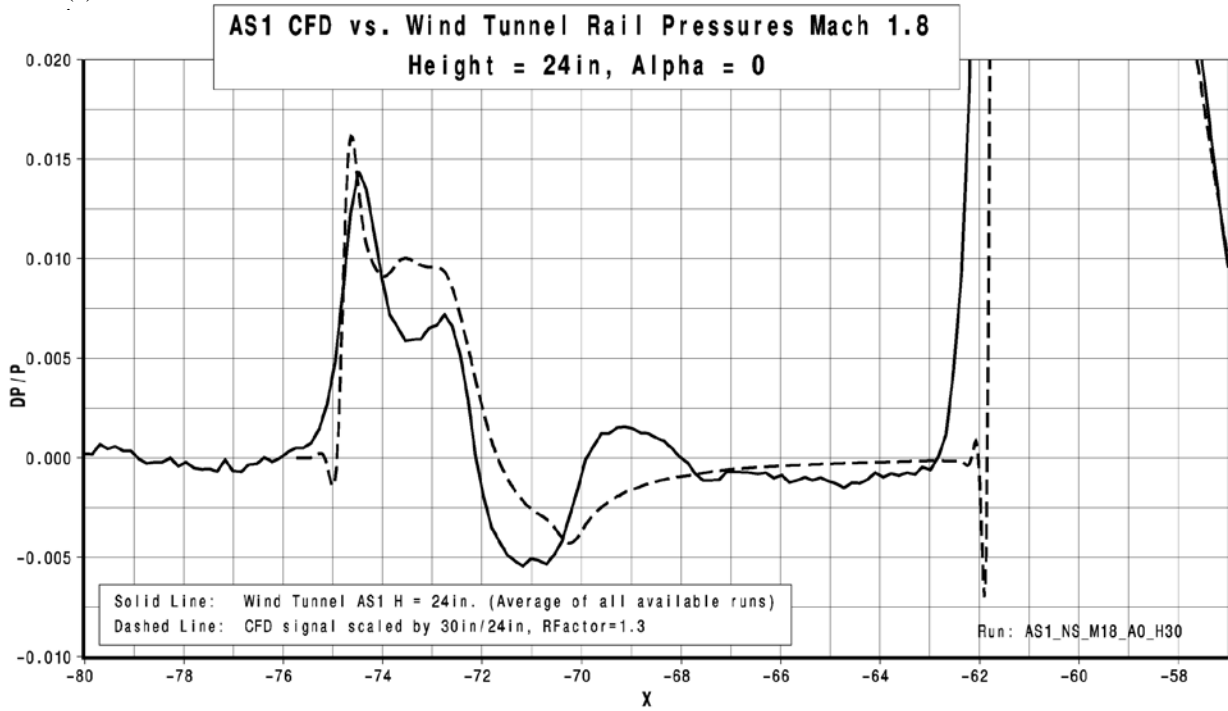


Figure 8.3-1. AS1 Pressure Signature Comparison of OVERFLOW vs. Test, M = 1.60

(a) H = 24



(b) H = 58

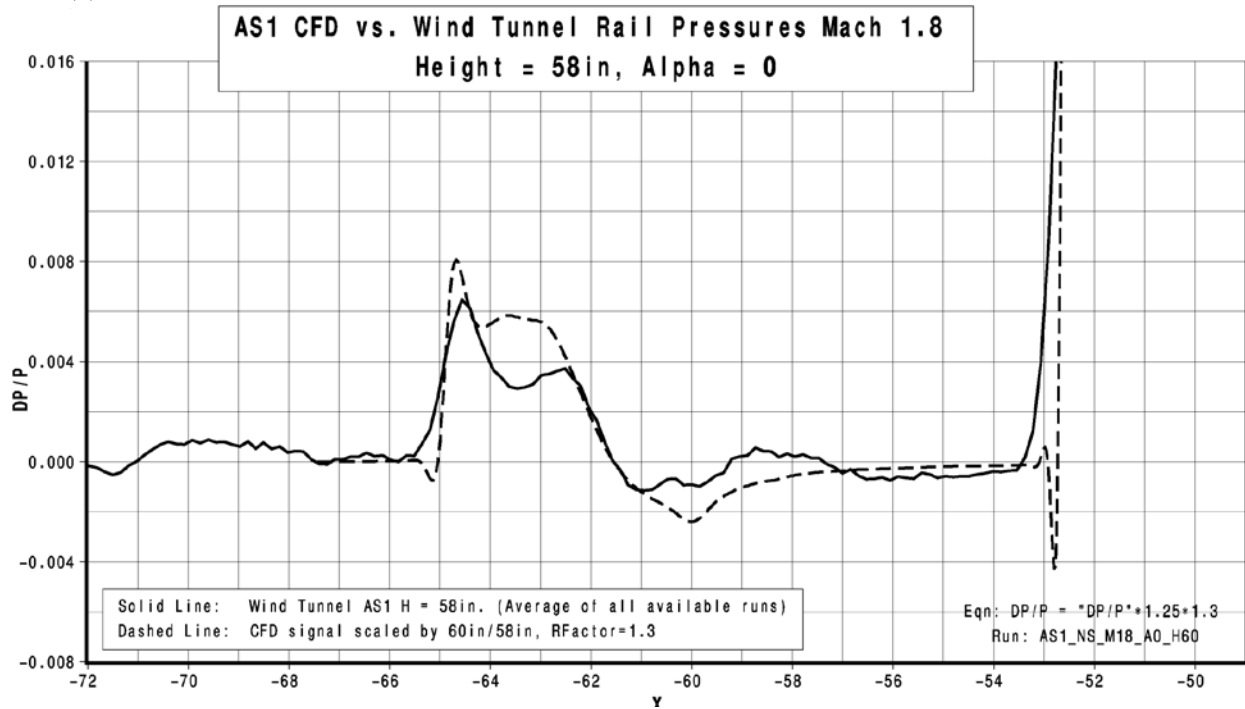
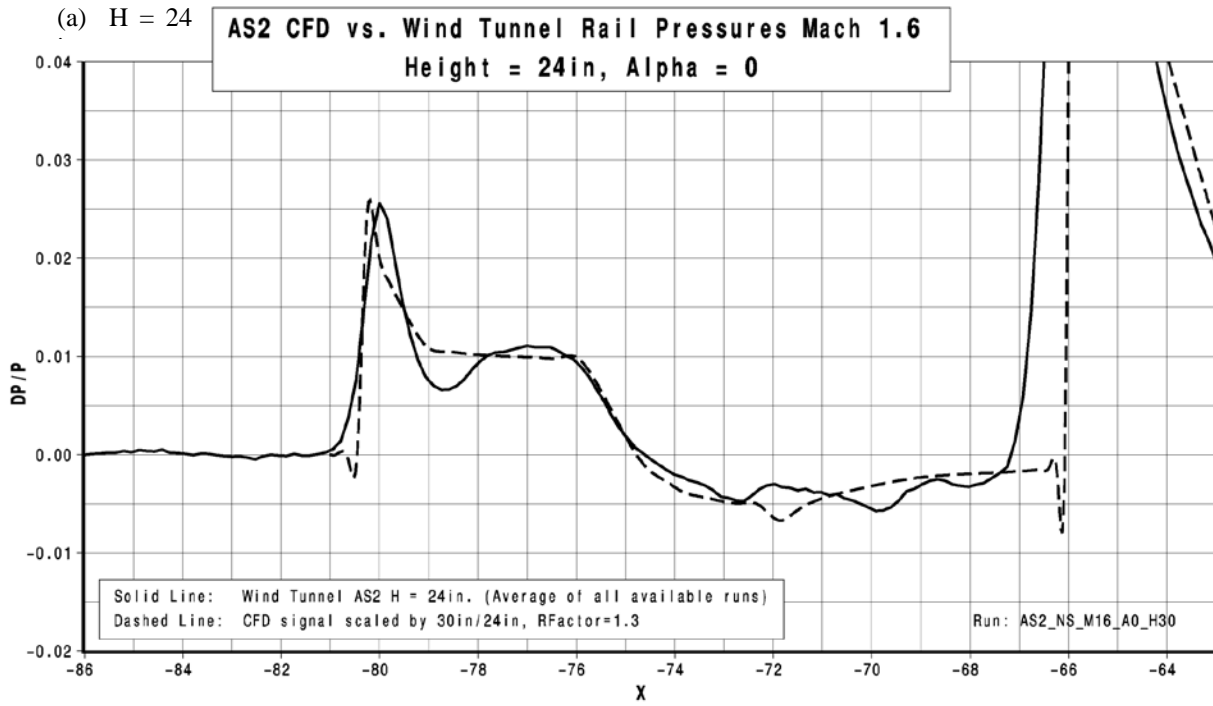


Figure 8.3-2. AS1 Pressure Signature Comparison of OVERFLOW vs. Test, M = 1.80



(b) $H = 56$

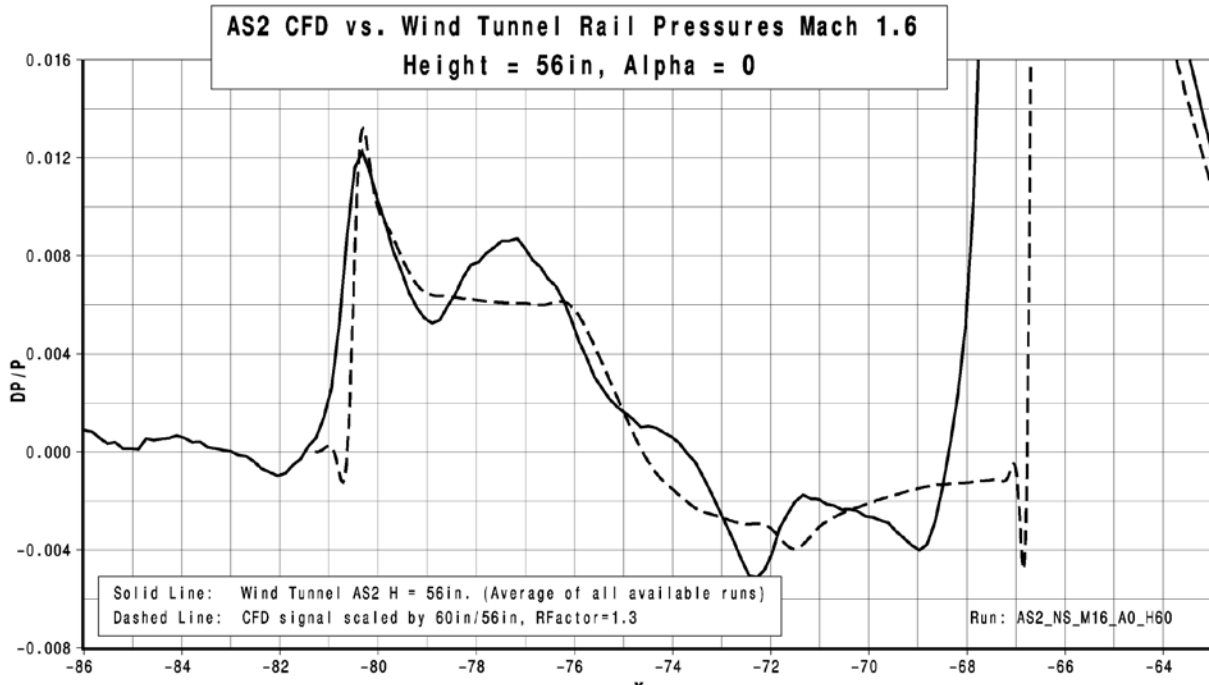
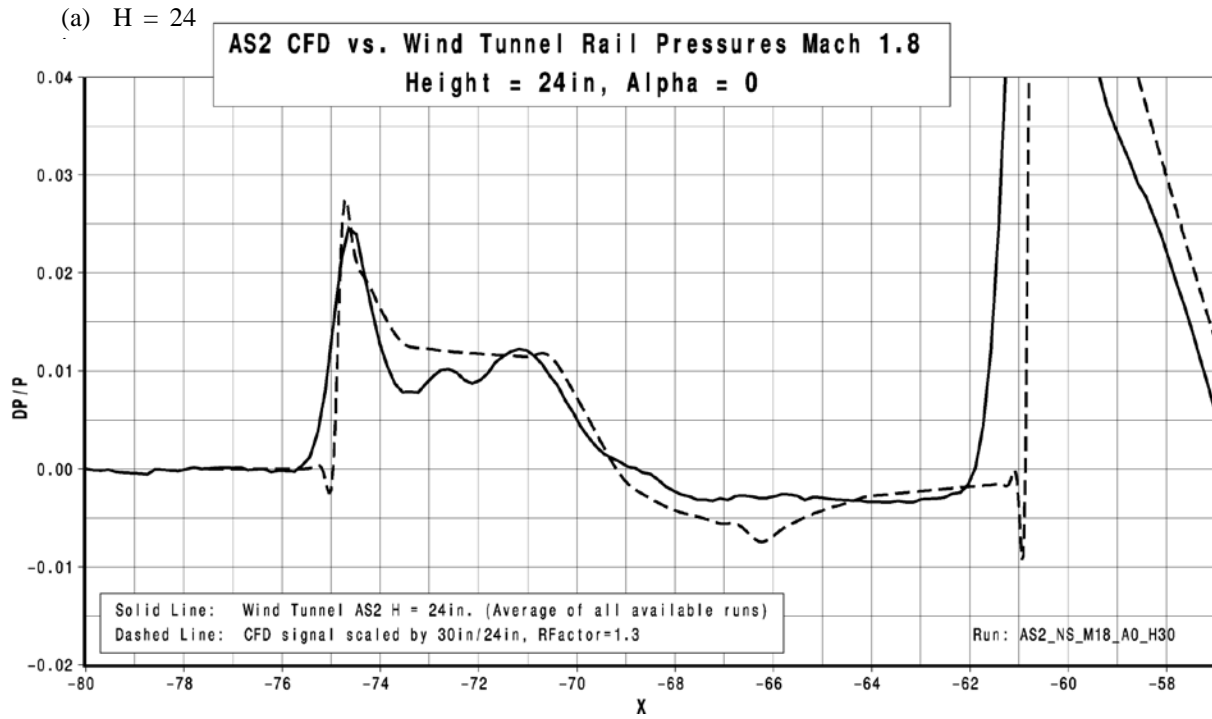


Figure 8.3-3. AS2 Pressure Signature Comparison of OVERFLOW vs. Test, $M = 1.60$



(b) $H = 56$

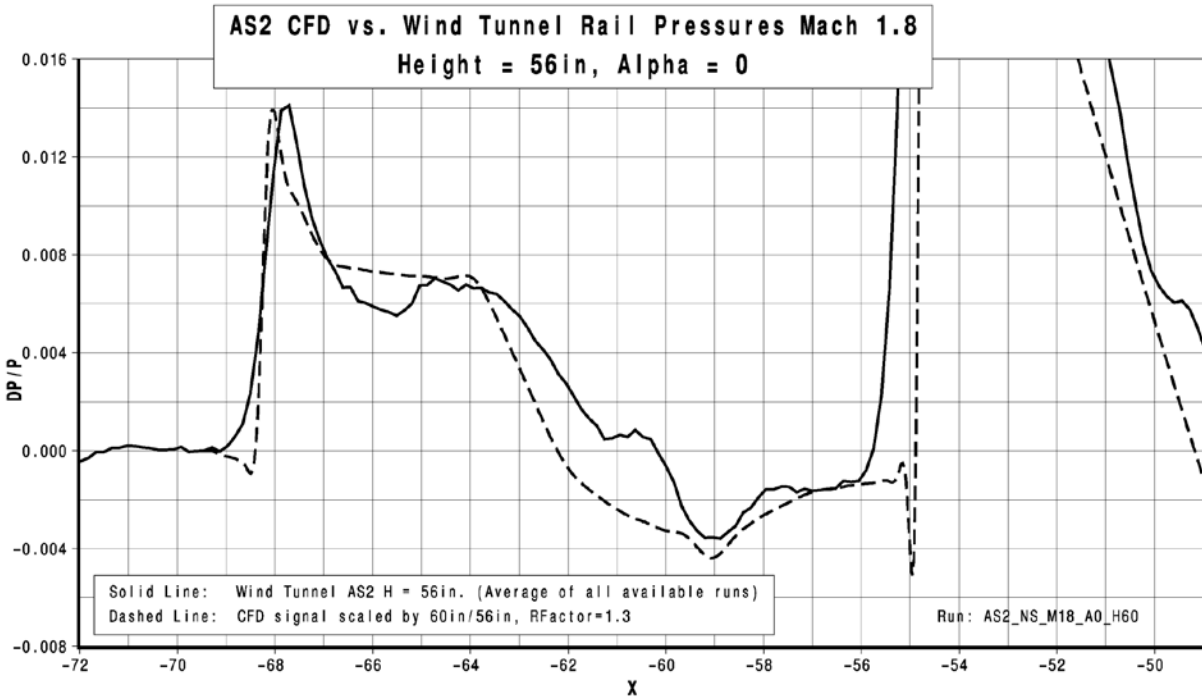


Figure 8.3-4. AS2 Pressure Signature Comparison of OVERFLOW vs. Test, $M = 1.80$

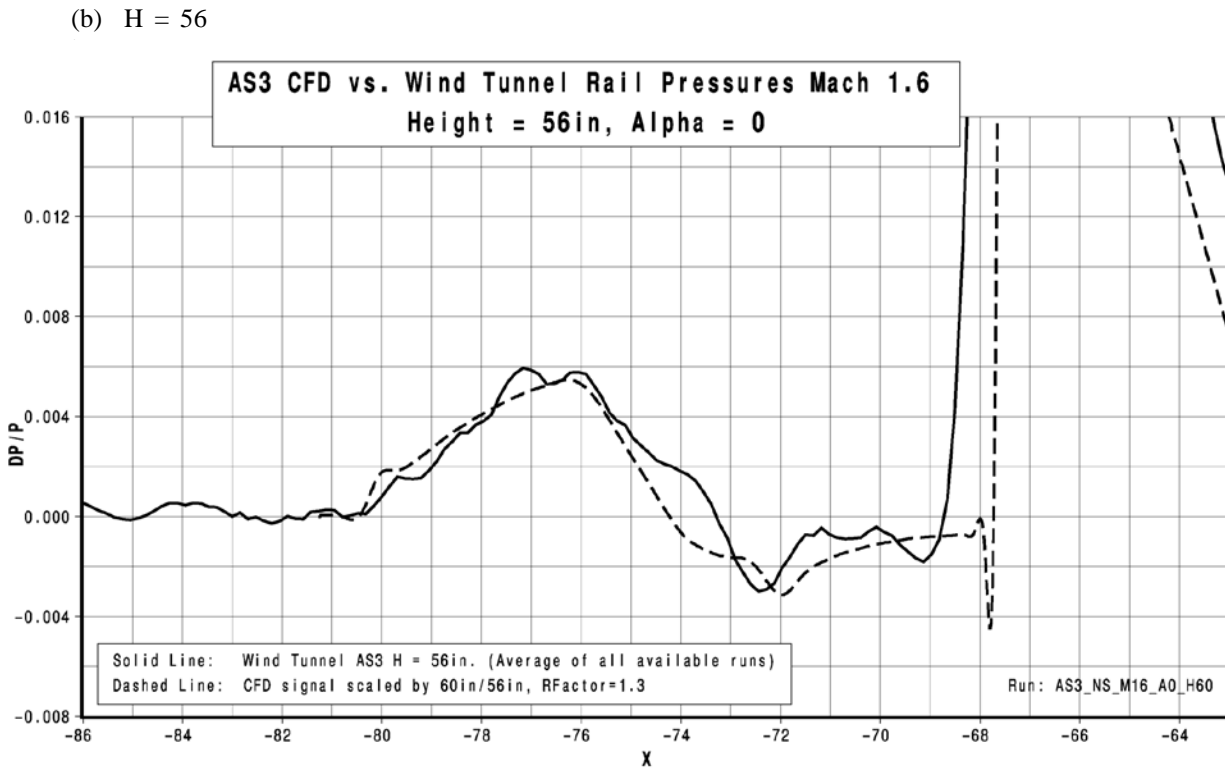
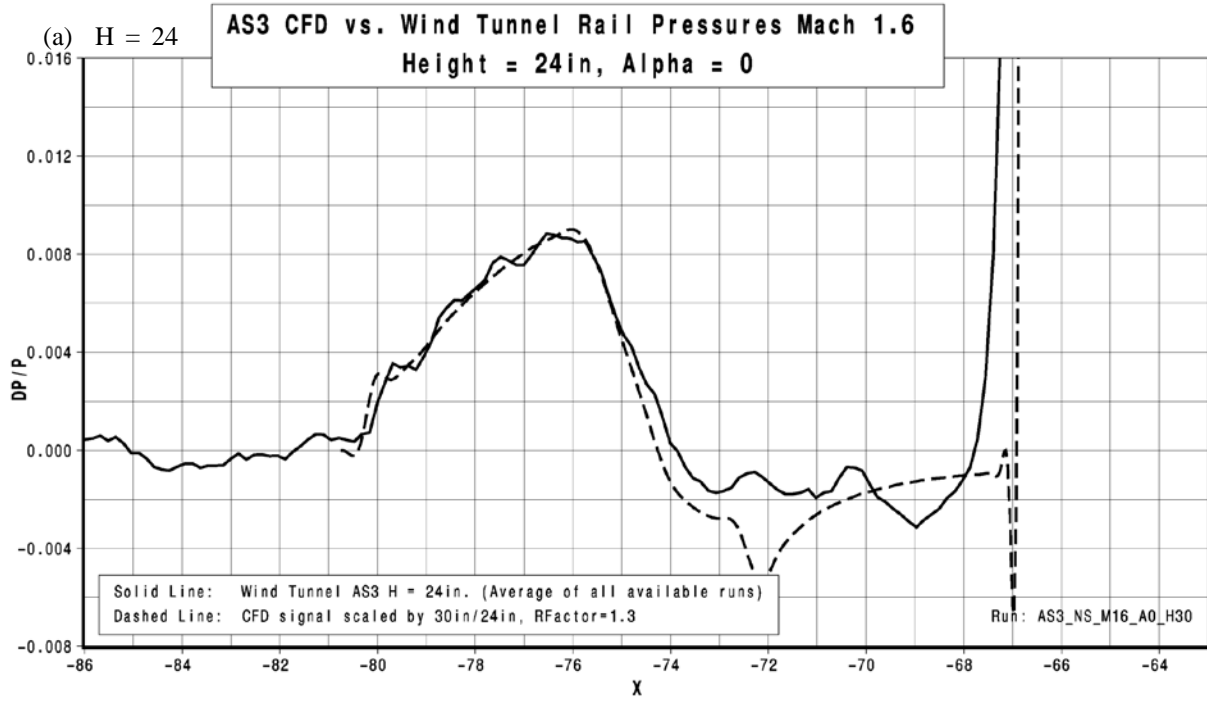
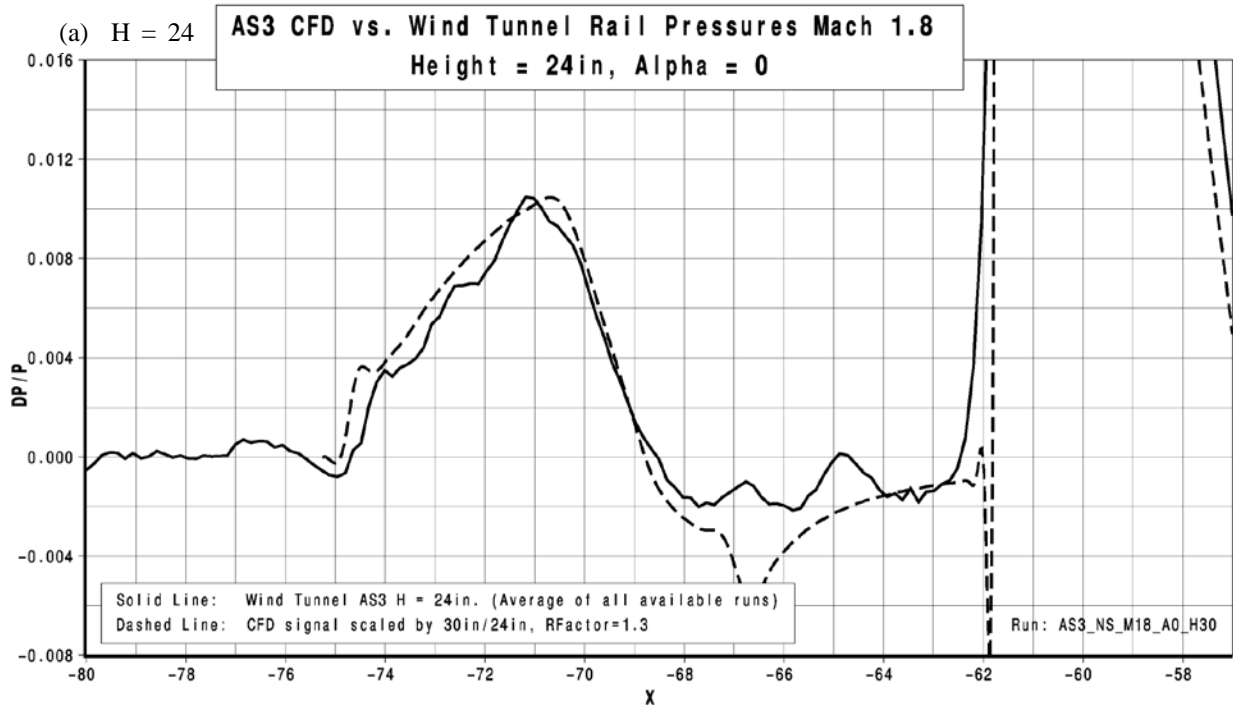


Figure 8.3-5. AS3 Pressure Signature Comparison of OVERFLOW vs. Test, M = 1.60



(b) H = 58

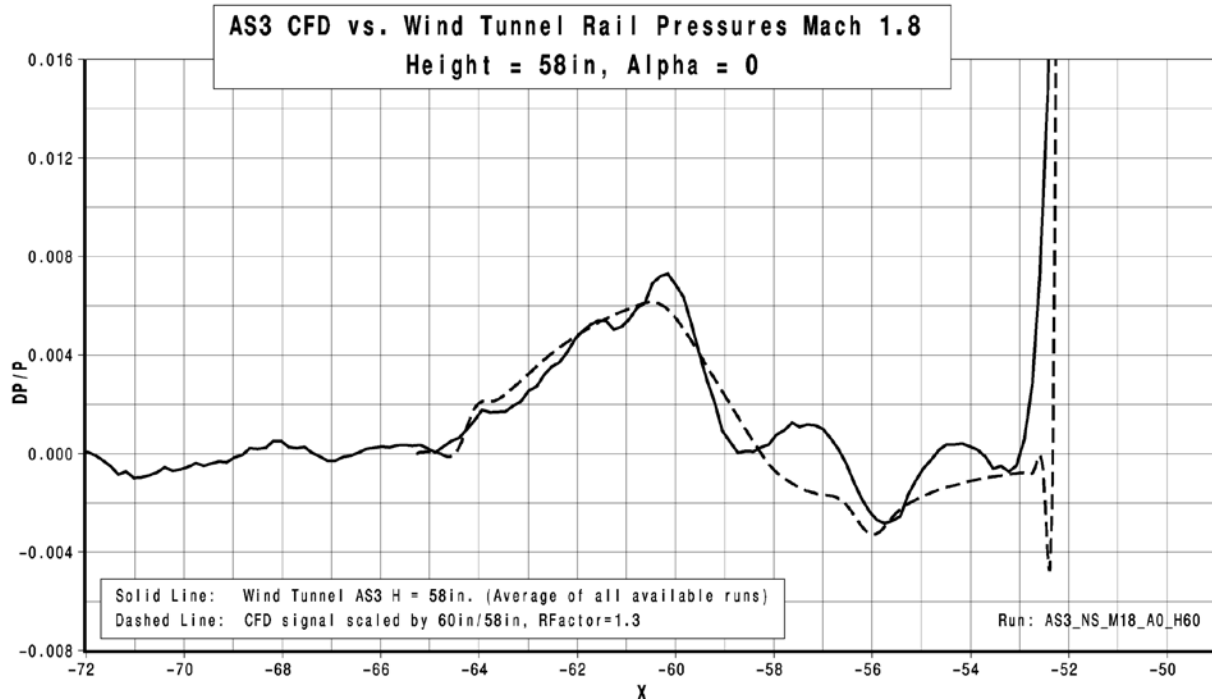


Figure 8.3-6. AS3 Pressure Signature Comparison of OVERFLOW vs. Test, M = 1.80

8.4 Boom Model CFD vs. Test Pressure Signature and F&M Comparisons

Pressure Signatures

Comparisons of the CFD results with the NASA Ames 9' x 7' supersonic wind tunnel AS-0229 pressure signature test data for boom models BM1, Configuration 4 and BM2, Configuration 9 at $\alpha = 3.6$ deg are provided in this section. The CFD results assume an isolated model corrected with a 30% amplification factor to account for the effect of the flat-top reflective nature of the rail. In addition to the amplification factor, CFD data were extracted at 30 and 60 inches off-body and corrected for amplitude by a factor of 30/24 and 60/56, respectively. See Reference 30 for the complete validation results.

Figures 8.4-1 and 8.4-2 compare the “dP/P” pressure signatures from the CFD OVERFLOW solutions and the corresponding wind tunnel test data for BM1, Configuration 4 for $M = 1.60$ and 1.80 , respectively, and at heights (of nose) of 24 and 56 inches above the rail.

Figures 8.4-3 and 8.4-4 compare the “dP/P” pressure signatures from the CFD OVERFLOW solutions and the corresponding wind tunnel test data for BM2, Configuration 9 for $M = 1.60$ and 1.80 , respectively, and at heights (of nose) of 24 and 56 inches above the rail.

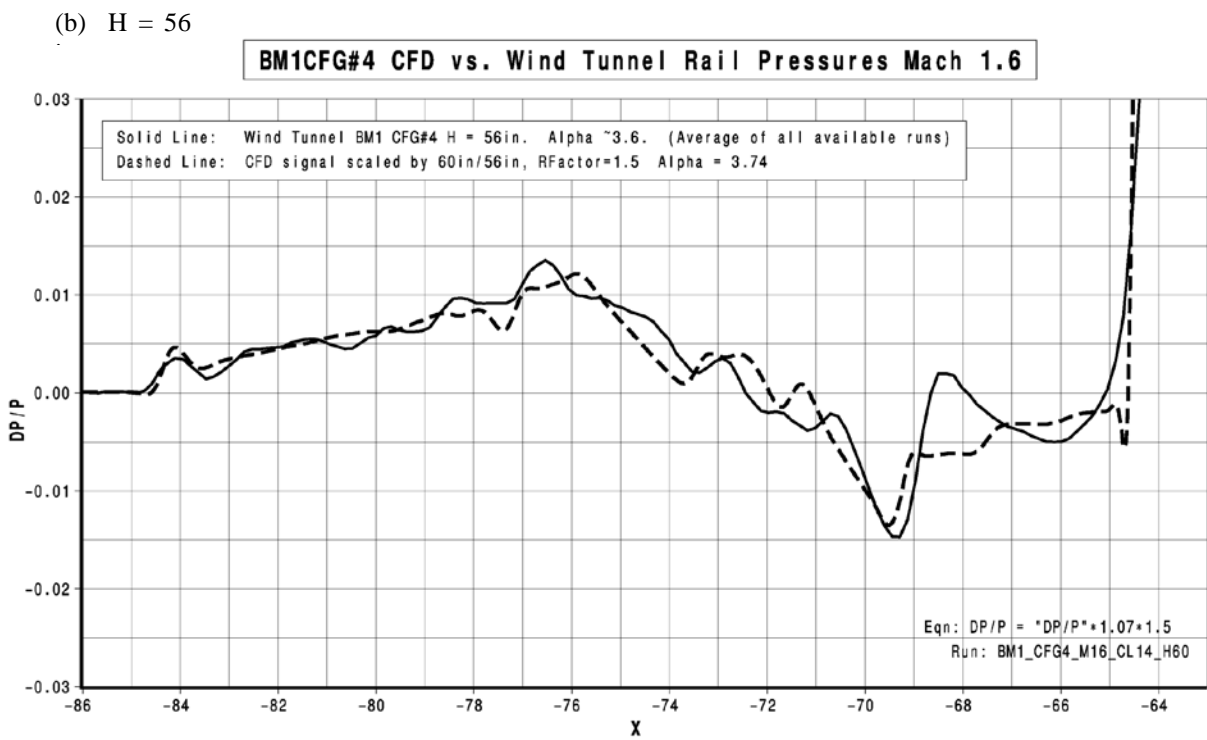
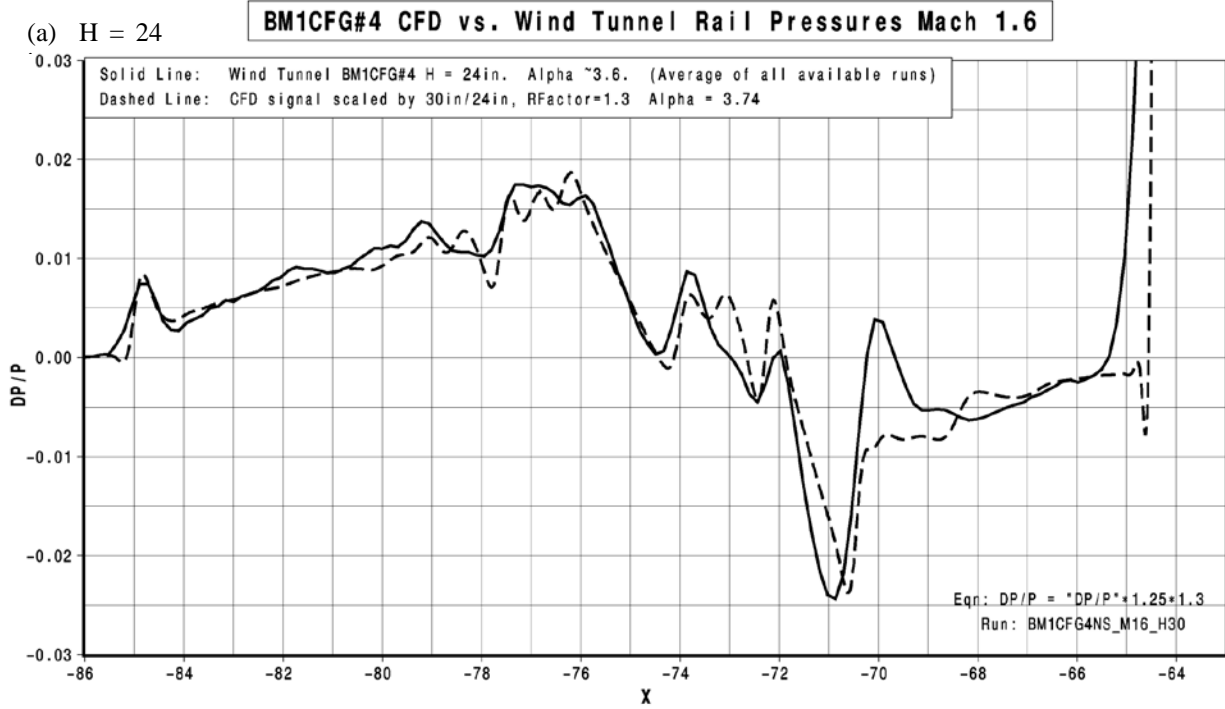
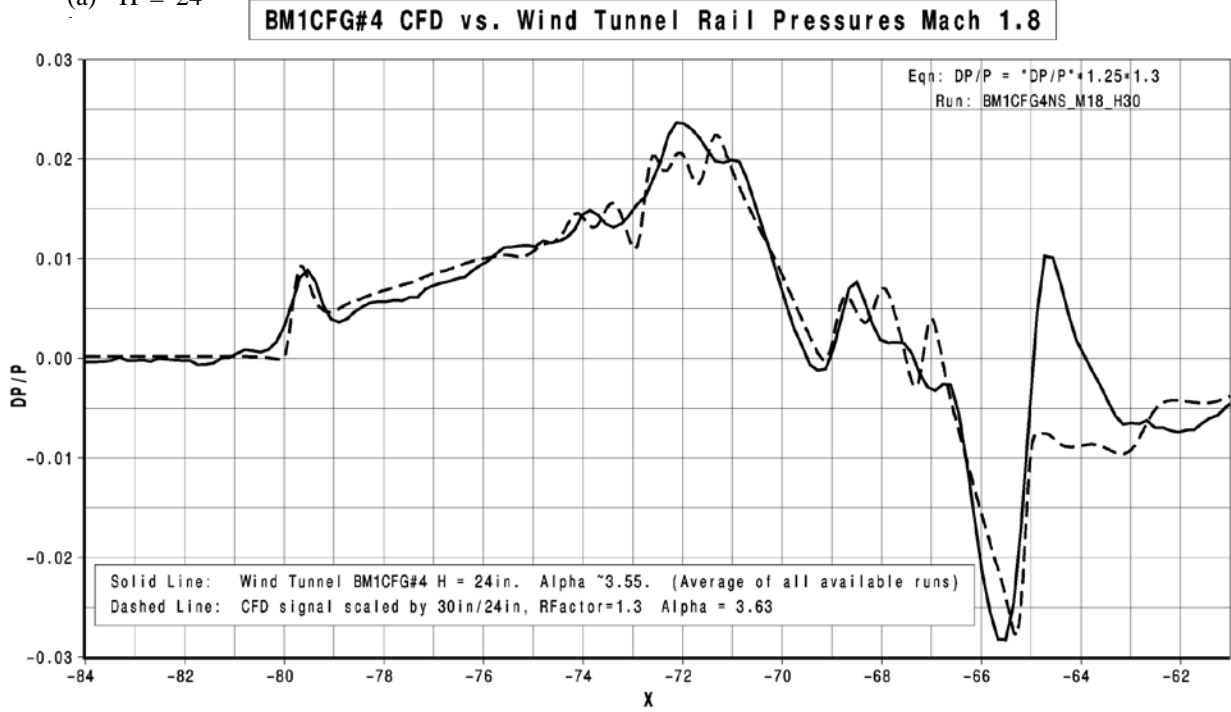


Figure 8.4-1. BM1, Configuration 4,
 Pressure Signature Comparison of OVERFLOW vs. Test, M = 1.60

(a) H = 24



(b) H = 56

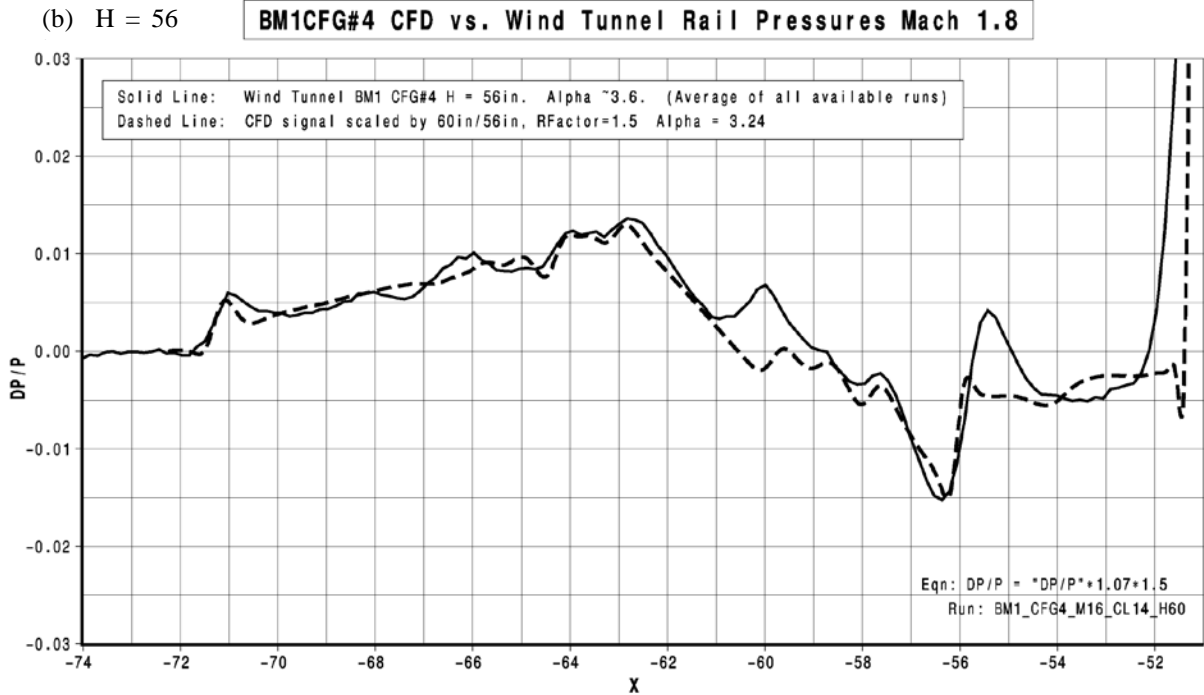


Figure 8.4-2. BM1, Configuration 4,
Pressure Signature Comparison of OVERFLOW vs. Test, M = 1.80

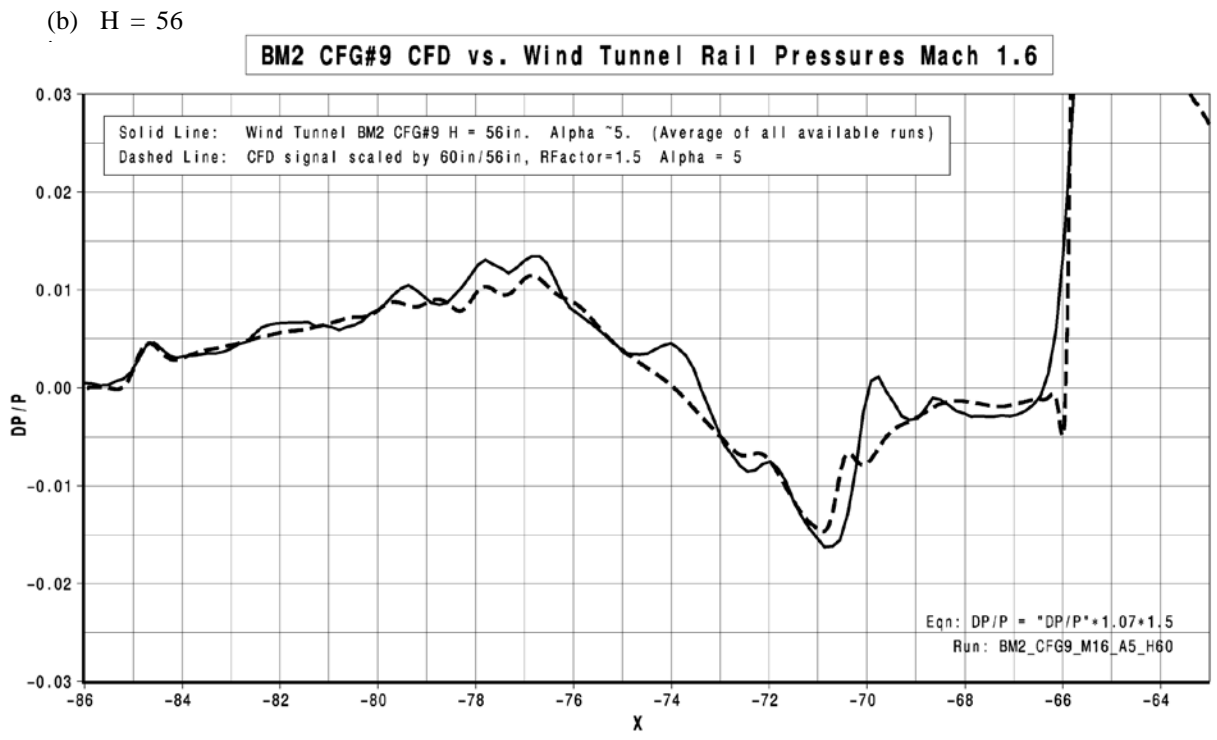
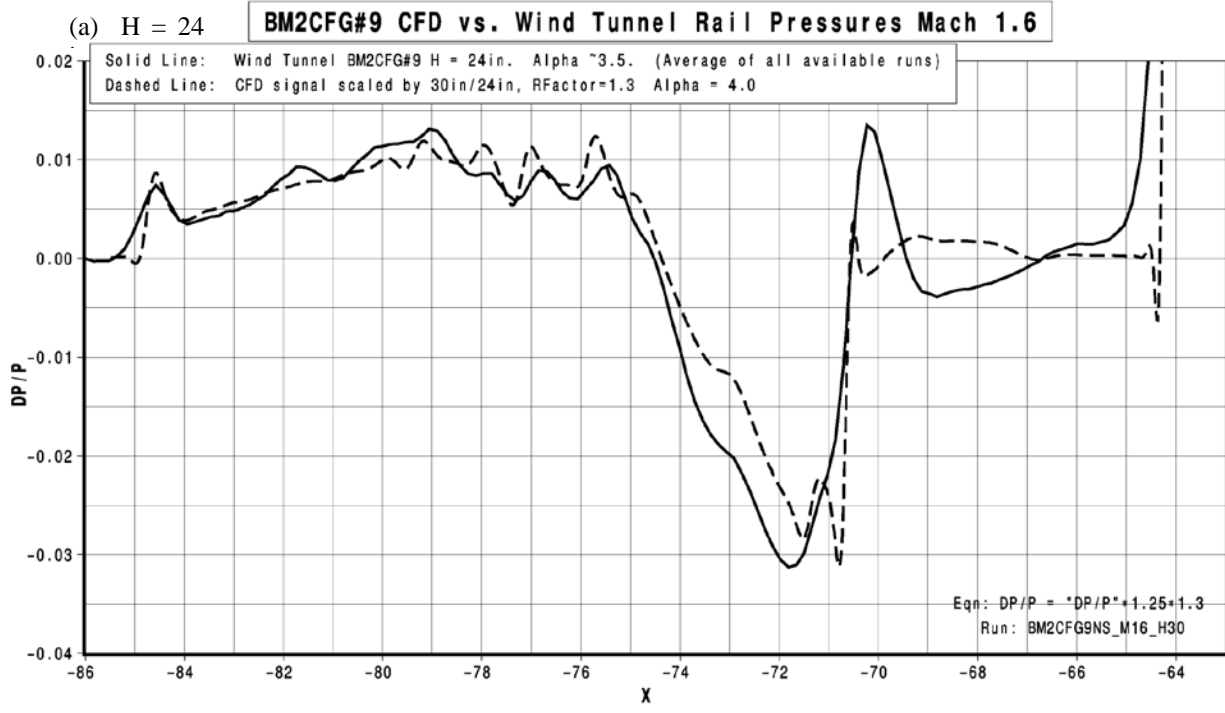


Figure 8.4-3. BM2, Configuration 9, Pressure Signature Comparison of OVERFLOW vs. Test, M = 1.60

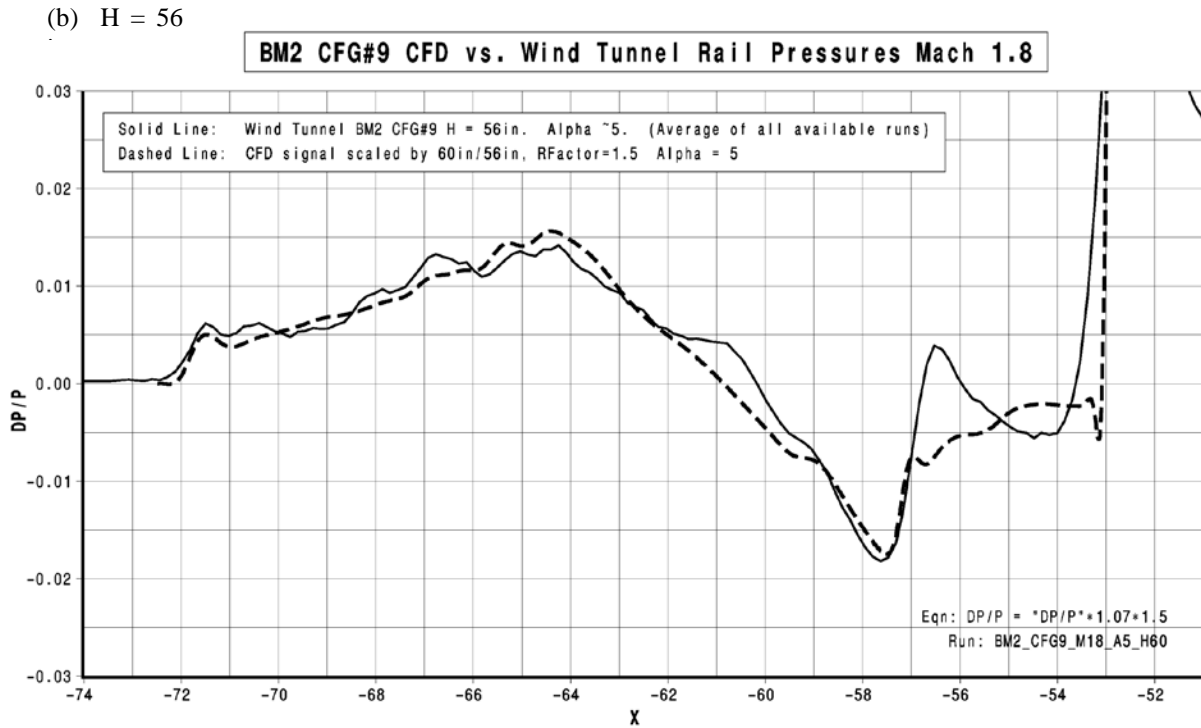
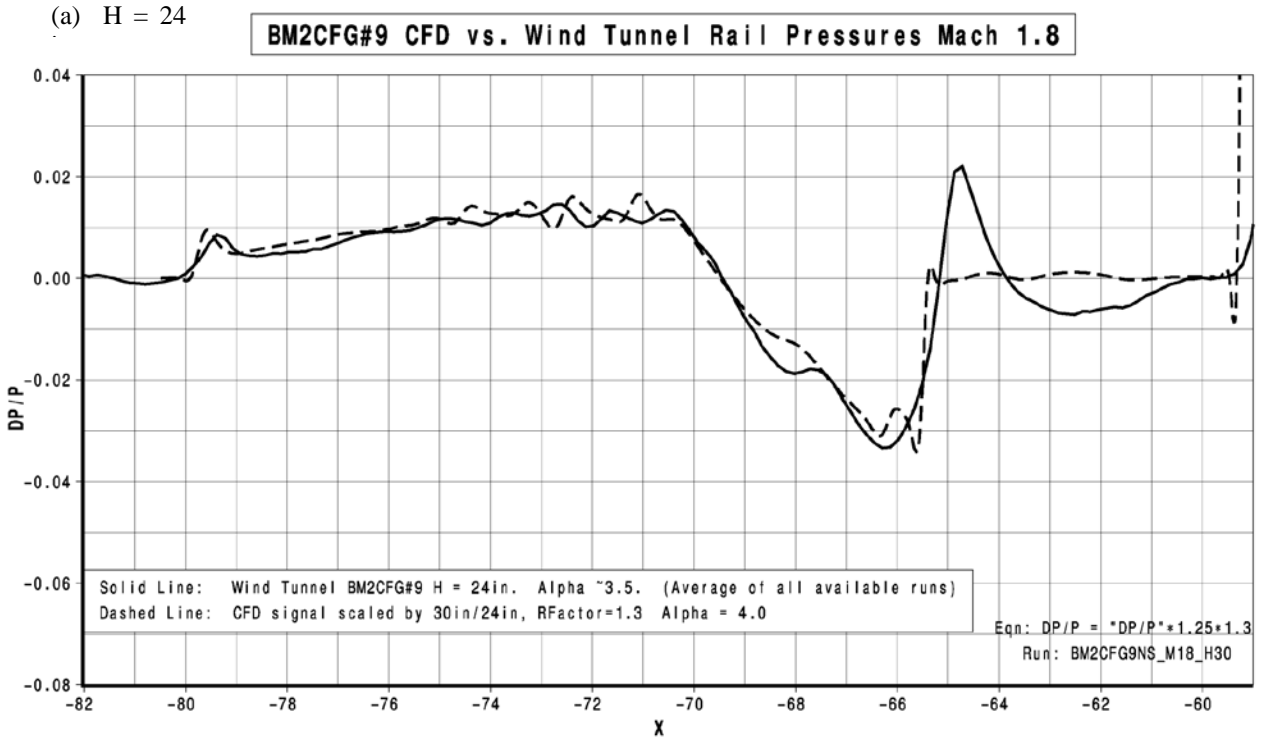


Figure 8.4-4. BM2, Configuration 9,
Pressure Signature Comparison of OVERFLOW vs. Test, M = 1.80

Forces and Moments

Comparisons of the CFD results with the NASA Ames 9' x 7' supersonic wind tunnel AS-0229 force and moment test data for boom models BM1, Configuration 4 and BM2, Configuration 9 are provided in this section. The provided figures show the drag polar, lift, and moment curves for the nominal model height of 30 inches above the rail and for the two Mach conditions tested (1.60 and 1.80) for each model type.

Figures 8.4-5 and 8.4-6 compare the force and moment characteristics from the CFD OVERFLOW solutions and the corresponding wind tunnel test data for BM1, Configuration 4 for M = 1.60 and 1.80, respectively, at H = 30 inches.

Figures 8.4-7 and 8.4-8 compare the force and moment characteristics from the CFD OVERFLOW solutions and the corresponding wind tunnel test data for BM2, Configuration 9 for M = 1.60 and 1.80, respectively, at H = 30 inches.

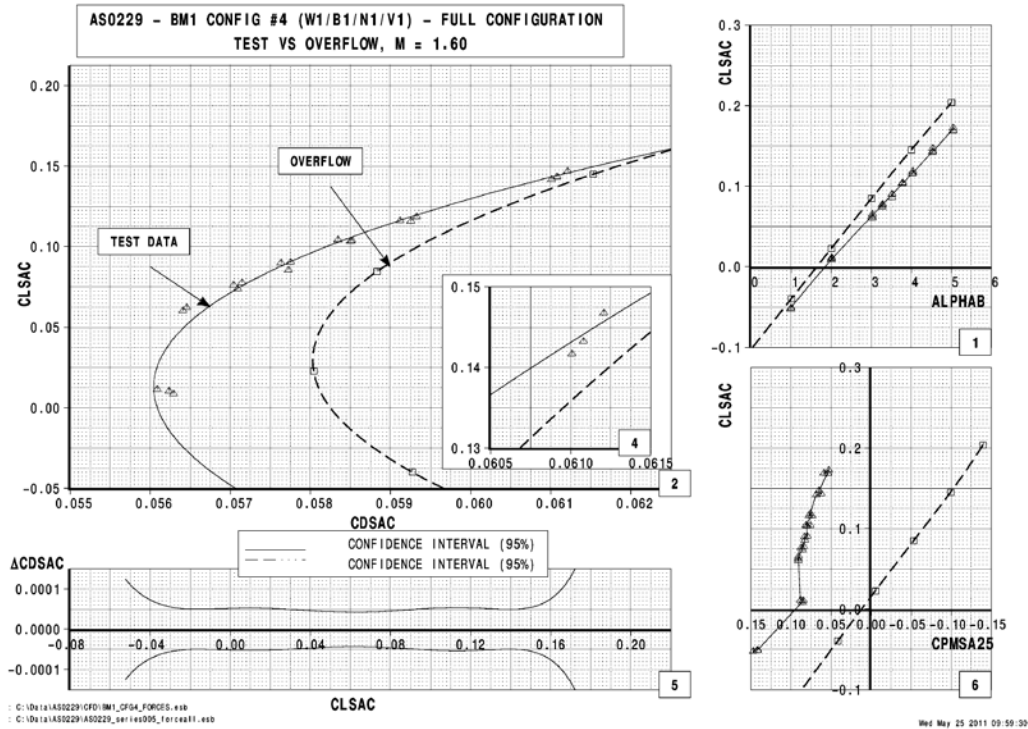


Figure 8.4-5. BM1, Configuration 4, F&M Comparison of OVERFLOW vs. Test, M = 1.60

Figure 8.4-6. BM1, Configuration 4, F&M Comparison of OVERFLOW vs. Test, M = 1.80

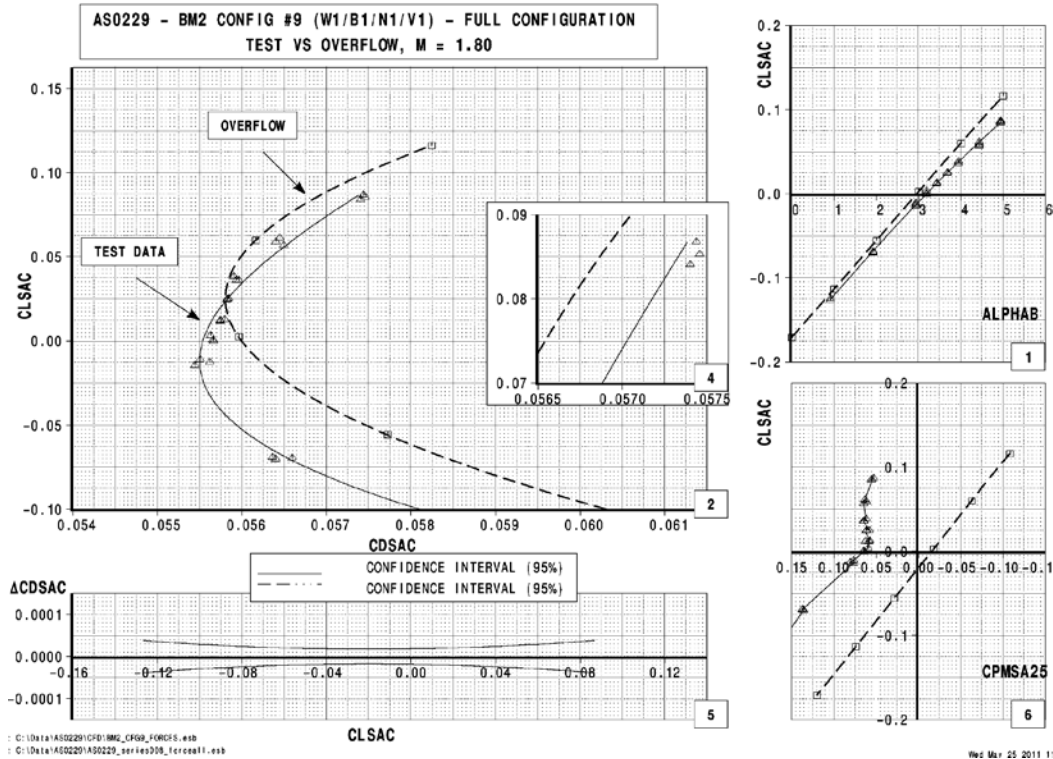


Figure 8.4-8. BM2, Configuration 9, F&M Comparison of OVERFLOW vs. Test, M = 1.80

Incremental Forces and Moments

Comparisons between OVERFLOW isolated model CFD and wind tunnel force and pressure increments at a height of 30 inches are provided in this section. The configuration increment is between BM1, Configuration 4 and BM2, Configuration 9 and is shown at both Mach 1.6 and Mach 1.8.

Figure 8.4-9 compares the pressure and F&M increments between the CFD OVERFLOW solutions and the corresponding wind tunnel test data. The CFD data have been corrected with a 60% amplification factor to account for the effect of the flat-top reflective nature of the rail. The top plots show the increment in the pressure signature between the two configurations, whereas the bottom plots show the force increments in lift, drag, and pitching moment between BM1 and BM2.

Figures 8.4-10 and 8.4-11 compare the pressure and F&M increments between the OVERFLOW isolated model CFD and wind tunnel force and pressure increments at Mach 1.6 and 1.8, respectively. The results shown are for a height of 30 in. The configuration increment is between BM1, Configuration 4 and BM2, Configuration 9. The CFD data have been corrected with a 60% amplification factor to account for the effect of the flat-top reflective nature of the rail. The top left plots in each figure show the CFD and wind tunnel pressure results for the two configurations, whereas the top right plots show the increment in the pressure signature. The bottom plots show the force increments in lift, drag, and pitching moment between BM1 and BM2.

Delta=BM1#4 – BM2#9 (Full config comparison)

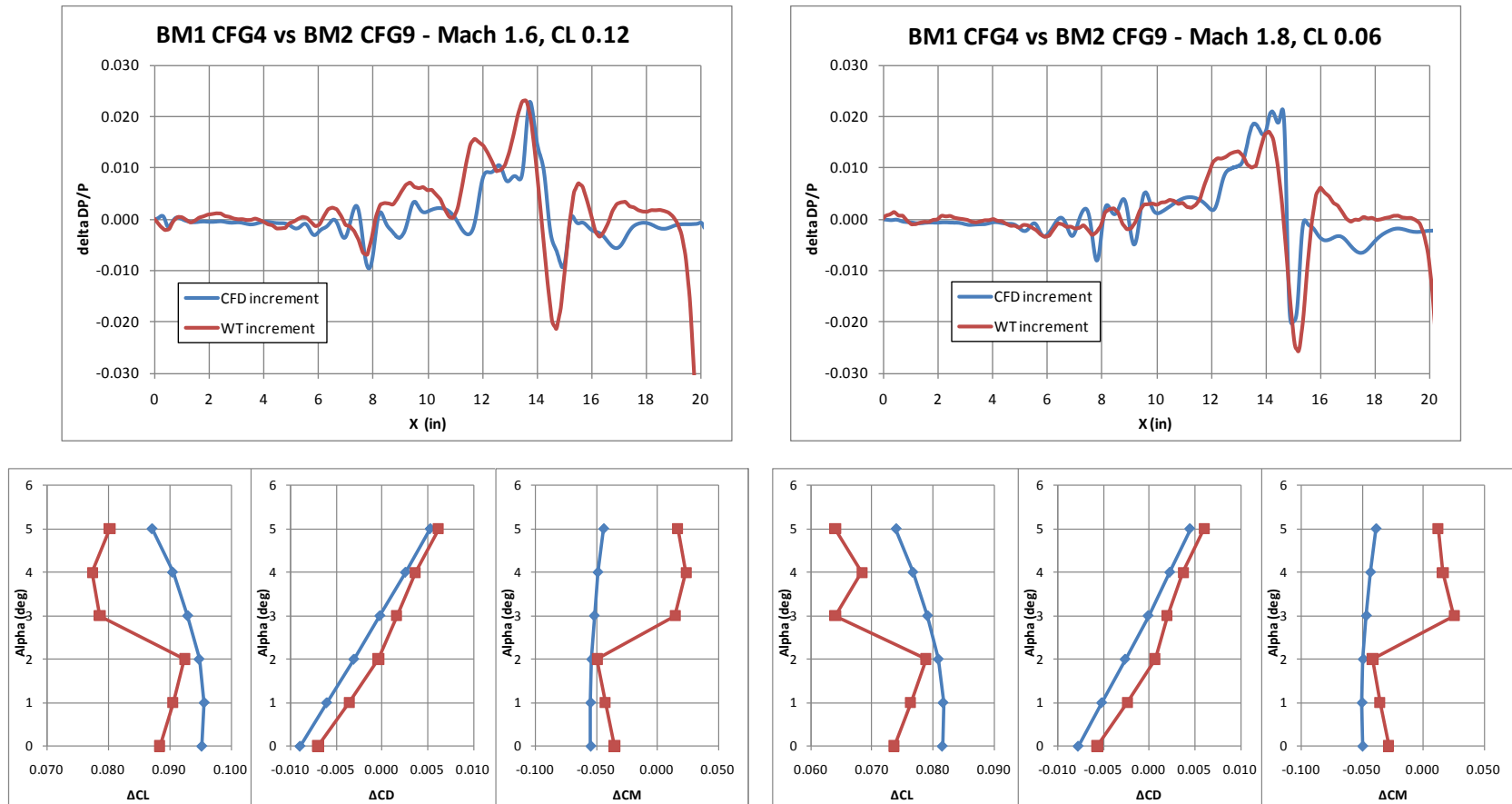


Figure 8.4-9. BM1, Configuration 4 to BM2, Configuration 9, Pressure and F&M Increments—Comparison of OVERFLOW vs. Test

Delta=BM1#4 – BM2#9 (Full config comparison)

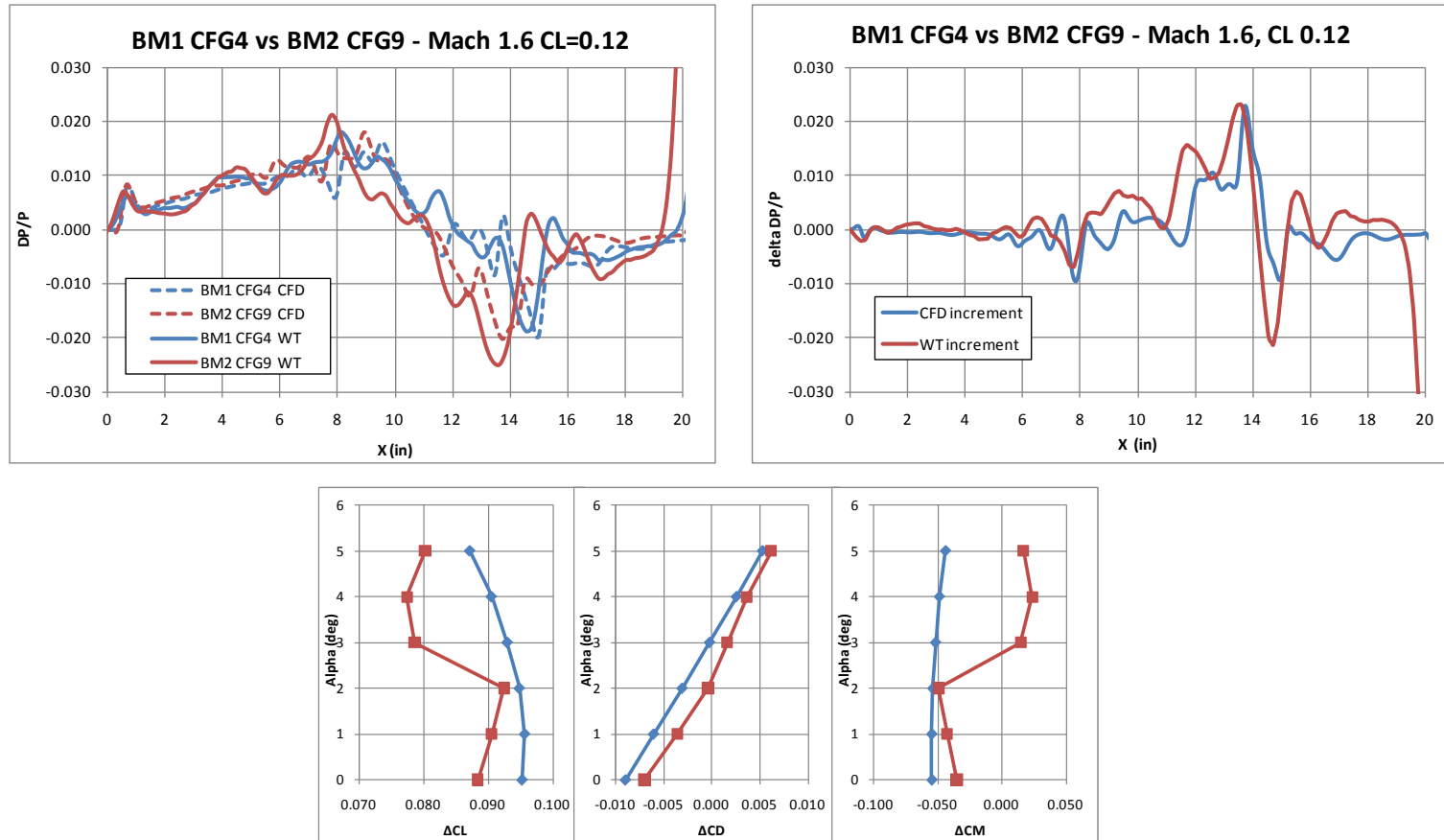


Figure 8.4-10. BM1, Configuration 4 to BM2, Configuration 9, Pressure and F&M Increments, M = 1.60, Comparison of OVERFLOW vs. Test

Delta=BM1#4 – BM2#9 (Full config comparison)

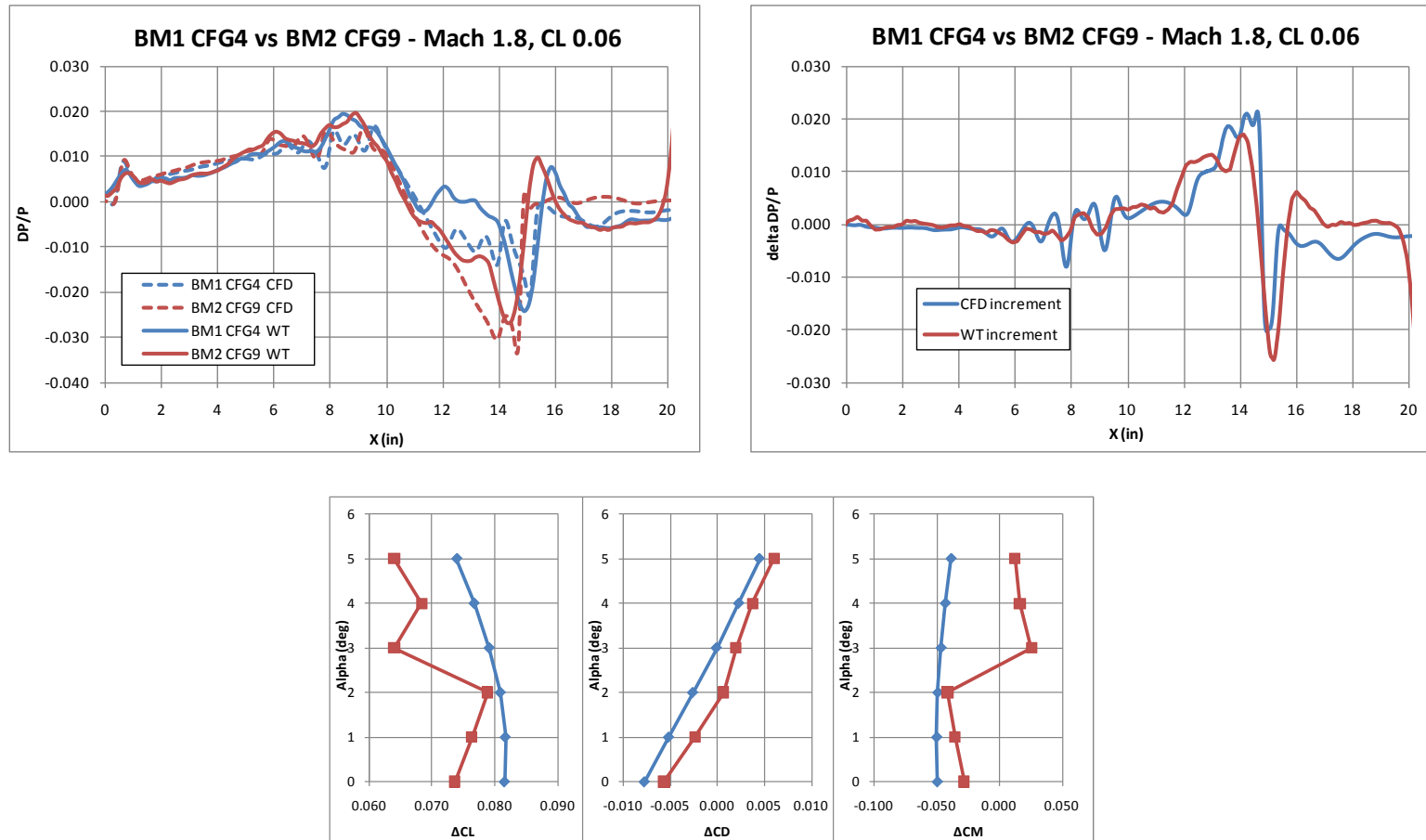
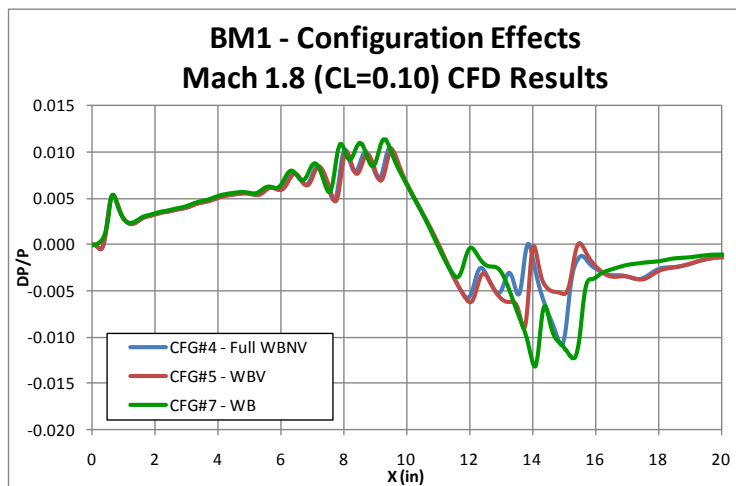
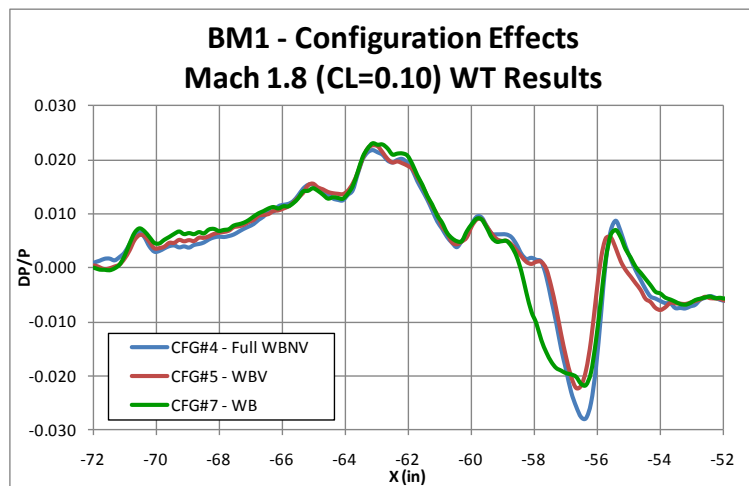
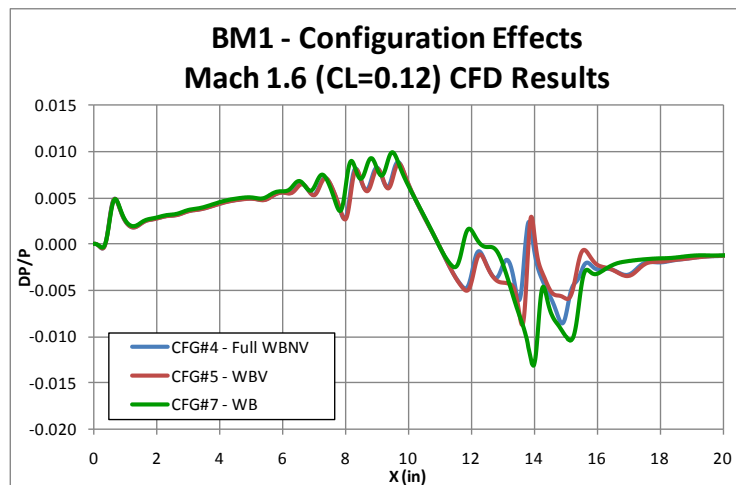
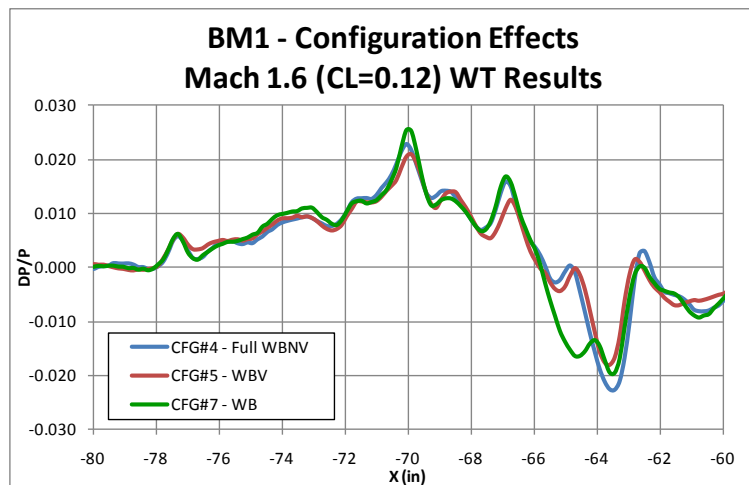


Figure 8.4-11. BM1, Configuration 4 to BM2, Configuration 9, Pressure and F&M Increments, M = 1.80, Comparison of OVERFLOW vs. Test

Configuration Effects

Comparisons between OVERFLOW isolated model CFD and wind tunnel pressures for three Boom Model 1 configurations at both Mach 1.6 and Mach 1.8 at a height of 30 inches are presented in Figure 8.4-12. The configurations shown are full configuration (Configuration 4), nacelle off (Configuration 5), and nacelle/tail off (Configuration 7). The plots on the left show wind tunnel results and the plots on the right show CFD results. The CFD was run using Euler and does not have an amplification factor applied.

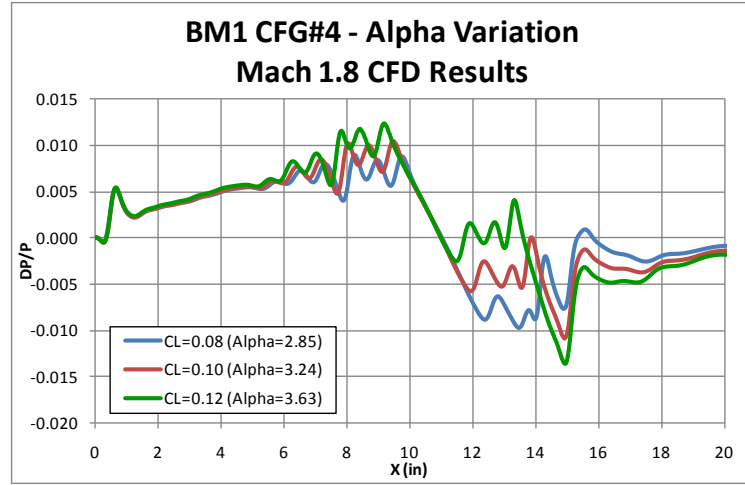
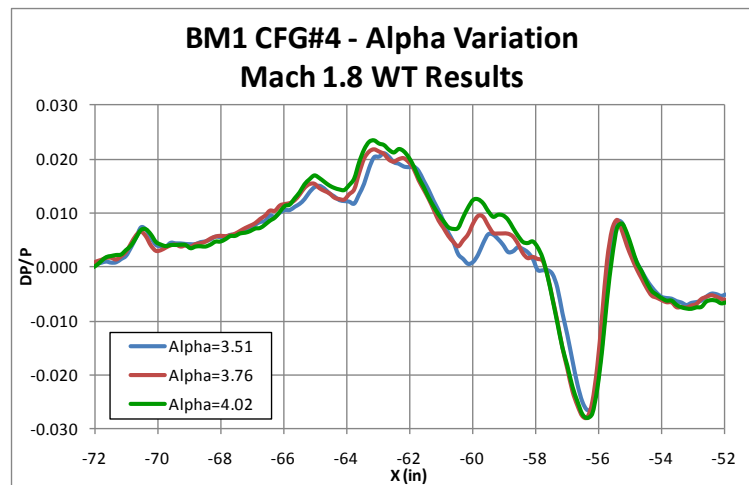
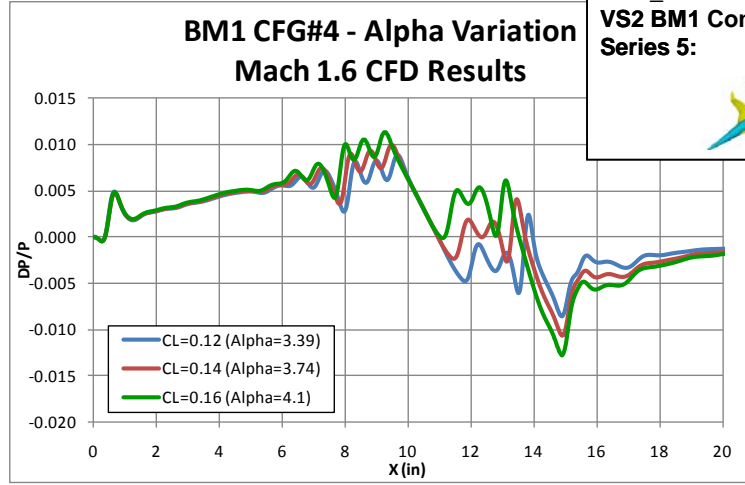
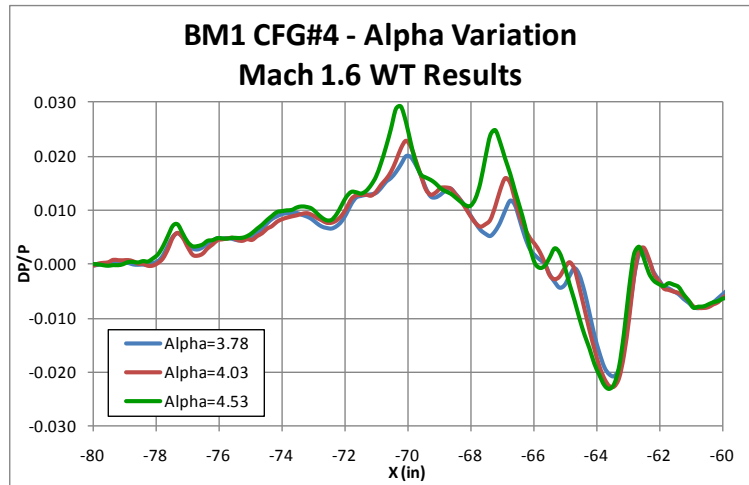


***CFD results are Euler and have NO reflection factor**

Figure 8.4-12. BM1 Configuration Effects—Comparison of OVERFLOW vs. Test

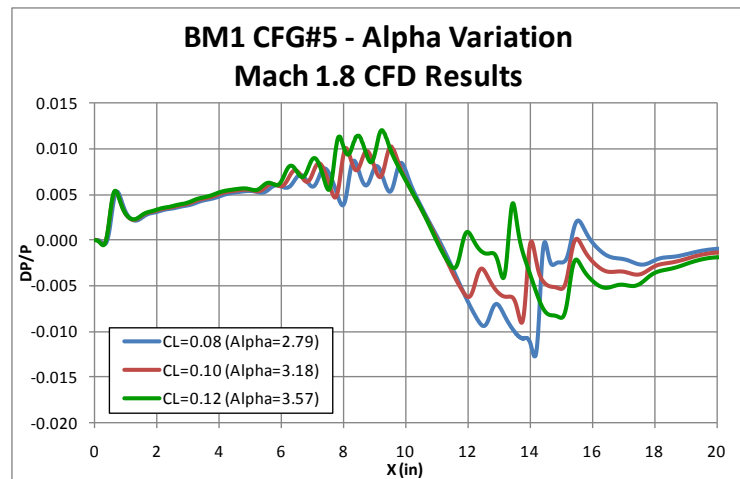
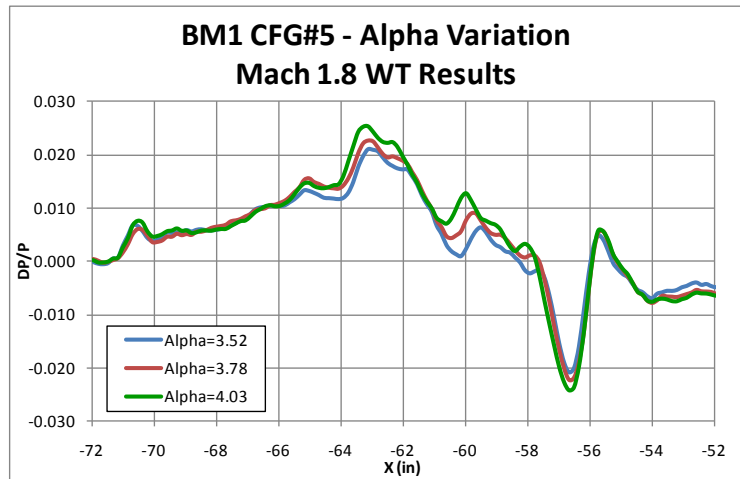
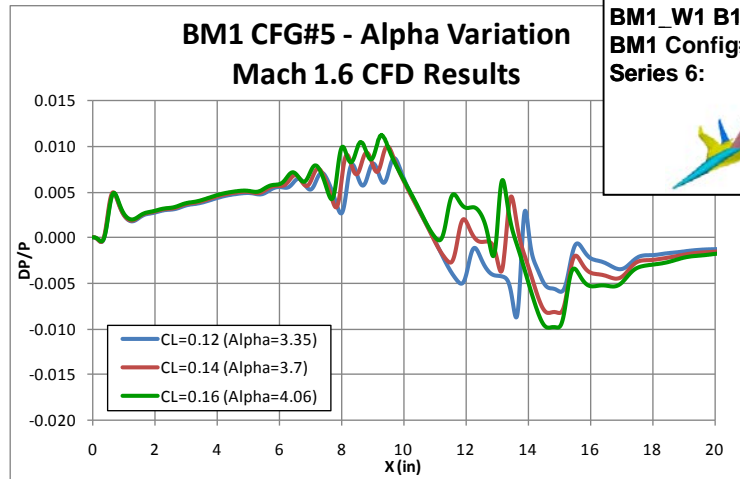
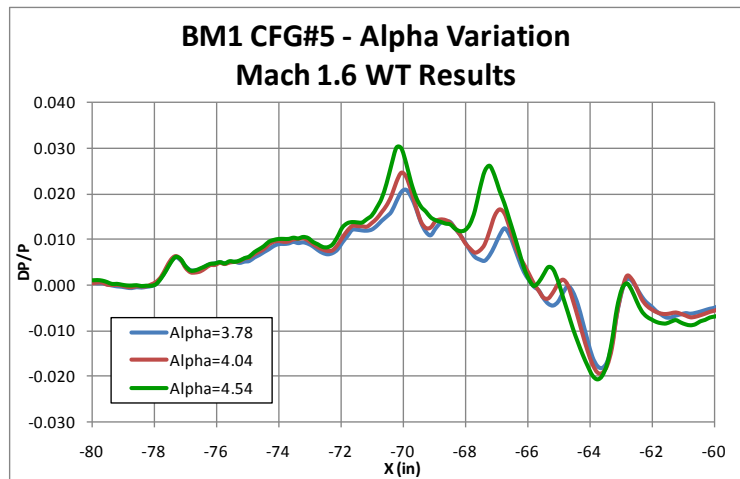
Variation with Alpha

Comparisons between OVERFLOW isolated model CFD and wind tunnel pressures at both Mach 1.6 and Mach 1.8 at various angles of attack are presented in Figures 8.4-13, 8.4-14, and 8.4-15 for boom models BM1, Configuration 4; BM1, Configuration 5; and BM1, Configuration 7, respectively. The results shown are for a height of 30 in. In each figure, the plots on the left show the wind tunnel results and the plots on the right show the CFD results. The CFD was run using Euler and does not have an amplification factor applied.



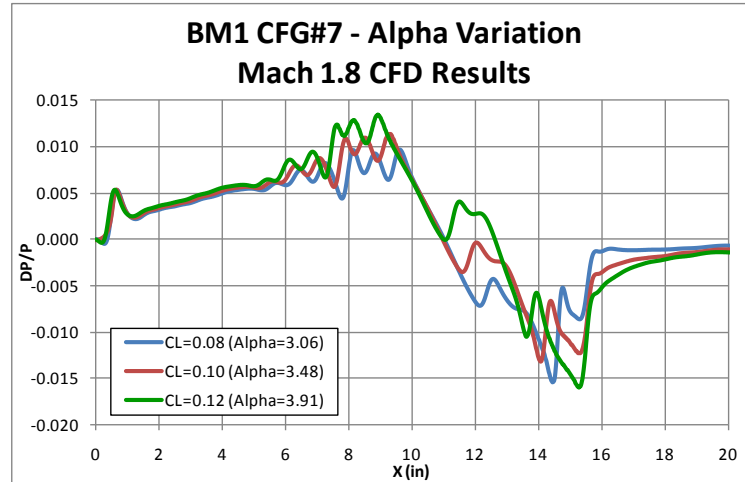
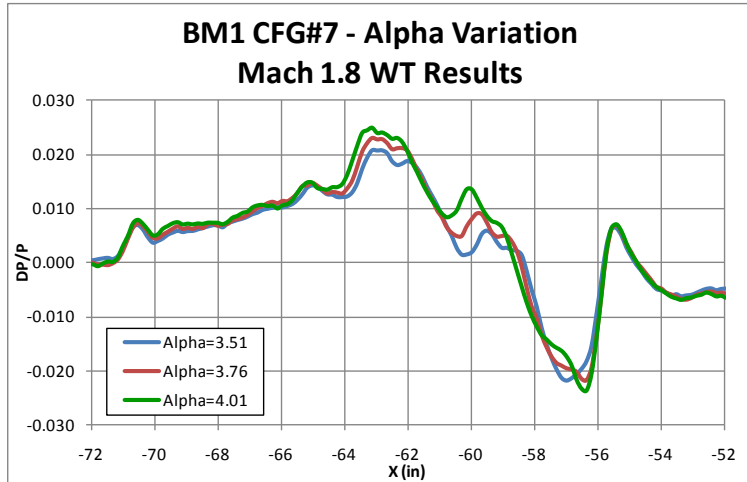
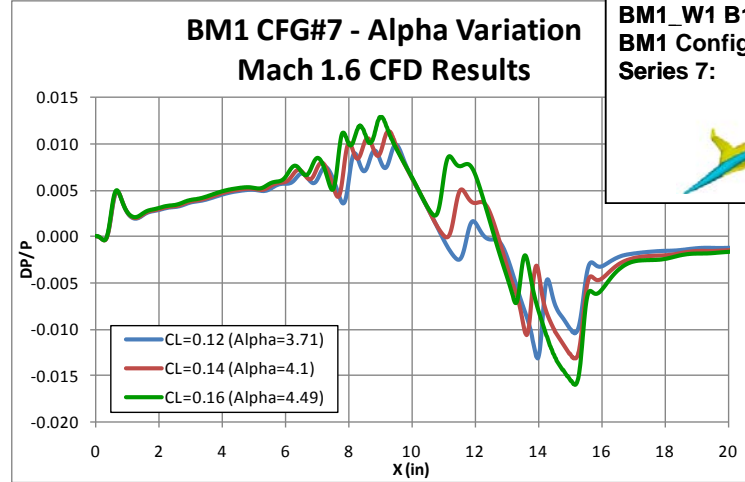
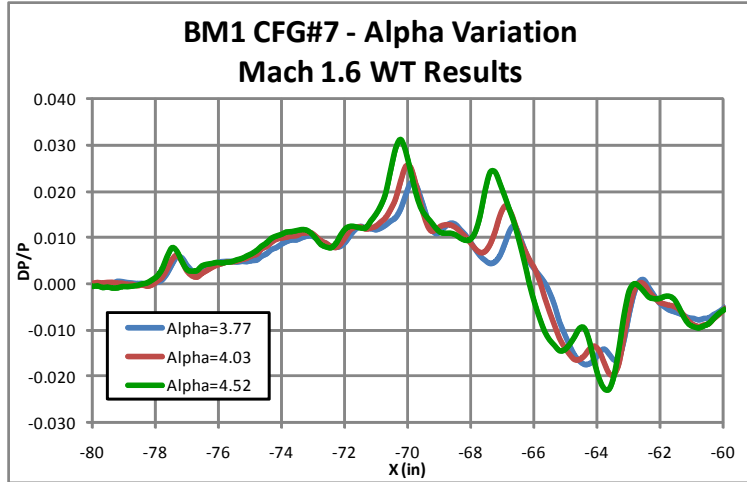
***CFD results are Euler and have NO reflection factor**

Figure 8.4-13. BM1, Configuration 4, Alpha Variation—Comparison of OVERFLOW vs. Test



***CFD results are Euler and have NO reflection factor**

Figure 8.4-14. BM1, Configuration 5, Alpha Variation—Comparison of OVERFLOW vs. Test



***CFD results are Euler and have NO reflection factor**

Figure 8.4-15. BM1, Configuration 7, Alpha Variation—Comparison of OVERFLOW vs. Test

8.5 Performance Model CFD vs. Test Pressure Signature and F&M Comparisons

Pressure Signatures

Comparisons of the CFD results with the NASA Ames 9' x 7' supersonic wind tunnel AS-0229 pressure signature test data are provided at $\alpha = 3.3$ deg and for both Mach 1.60 and 1.80 in Figures 8.5-1 and 8.5-2 for the performance models PM1, Configuration 1 and PM1, Configuration 3, respectively. The CFD results assume an isolated model corrected with an 80% amplification factor to account for the effect of the flat-top reflective nature of the rail. The CFD cases are run with the aft-body extended aft but with no attempt to model the step down to the sting or the tape for the base pressures. dP/P values are calculated using the nearest reference run.

Pressure Signatures—Aft-Body Effects

Comparisons of the CFD results with the NASA Ames 9' x 7' supersonic wind tunnel AS-0229 pressure signature test data are provided in Figure 8.5-3 for PM1, Configuration 3 at Mach 1.6 and 1.8 with a nose height of 60 inches and an α of approximately 3.3 deg. The OVERFLOW isolated model data are corrected with an 80% amplification factor to account for the effect of the flat-top reflective nature of the rail. Shown in the figure are CFD solutions with the aft-body run two ways: (1) the aft-body extended aft with no attempt to model the step down to the sting or the tape for the base pressures and (2) an attempt to model what was tested (step from body to sting and tape). dP/P values are calculated using the nearest reference run.

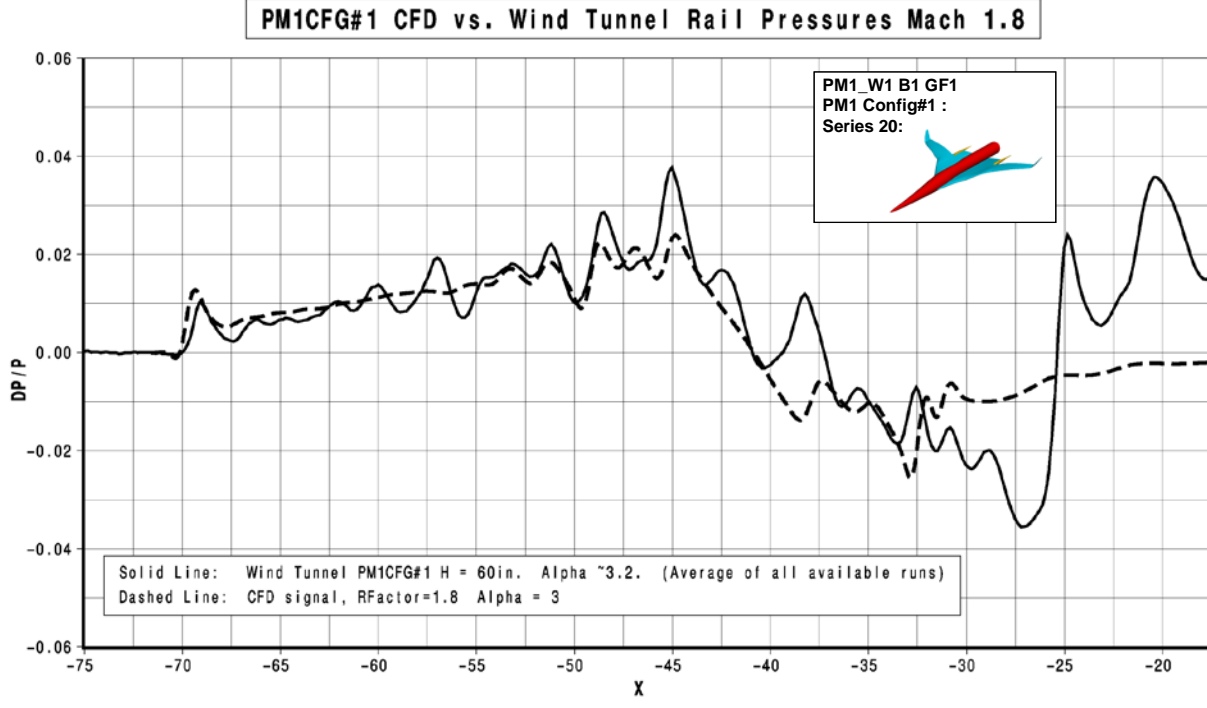
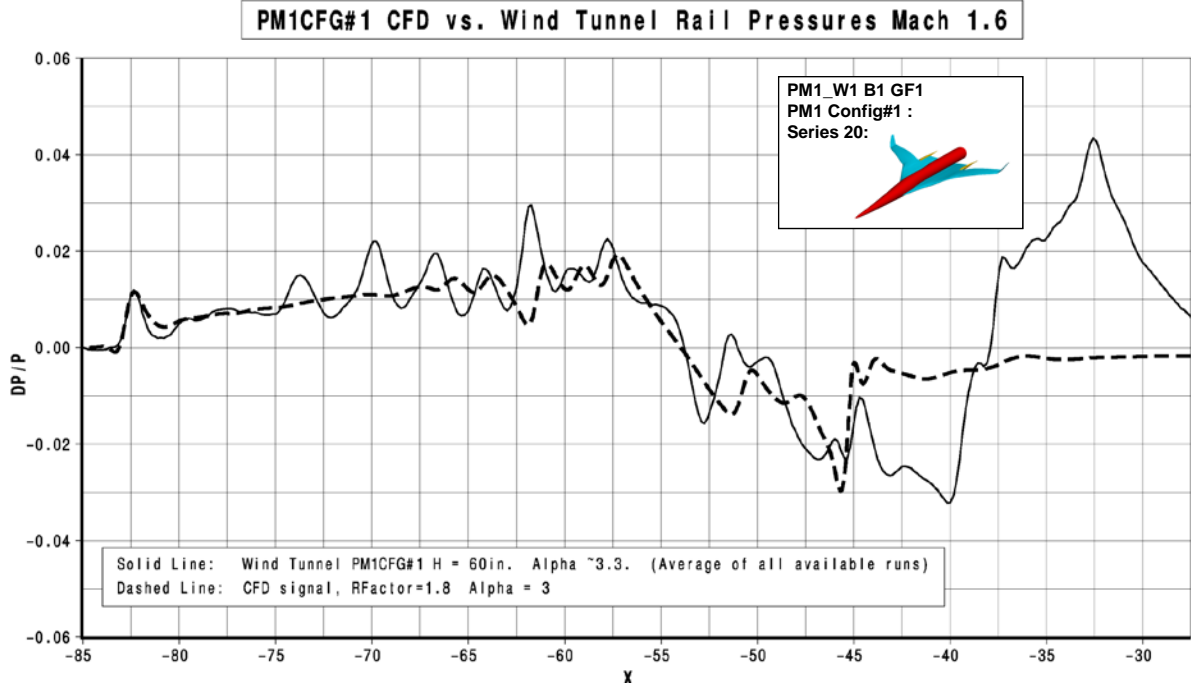


Figure 8.5-1. PM1, Configuration 1, Pressure Signature Comparison of OVERFLOW vs. Test, H = 60

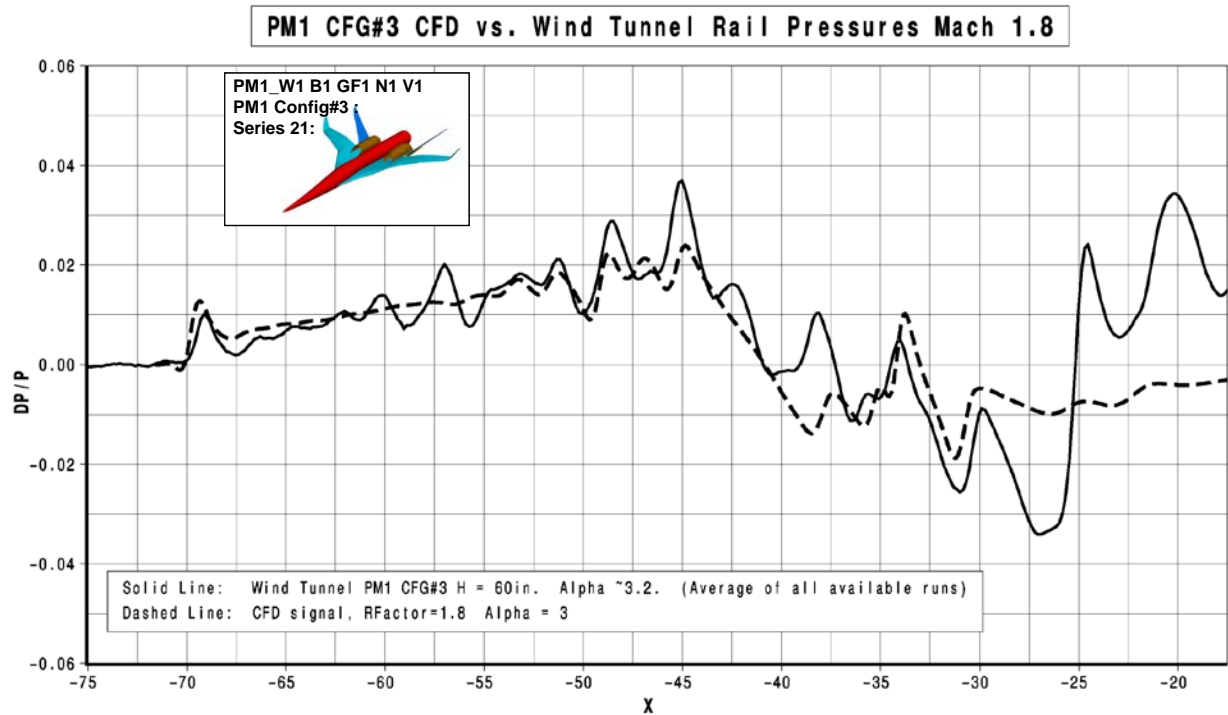
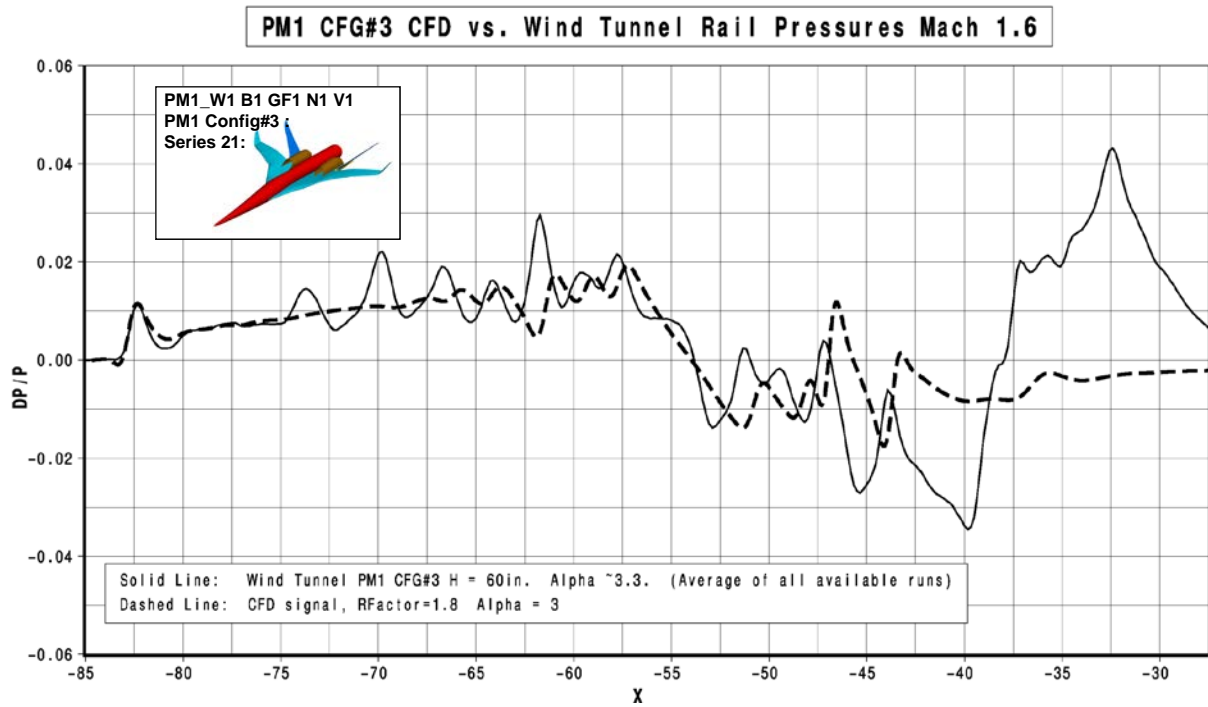


Figure 8.5-2. PM1, Configuration 3, Pressure Signature Comparison of OVERFLOW vs. Test, H = 60

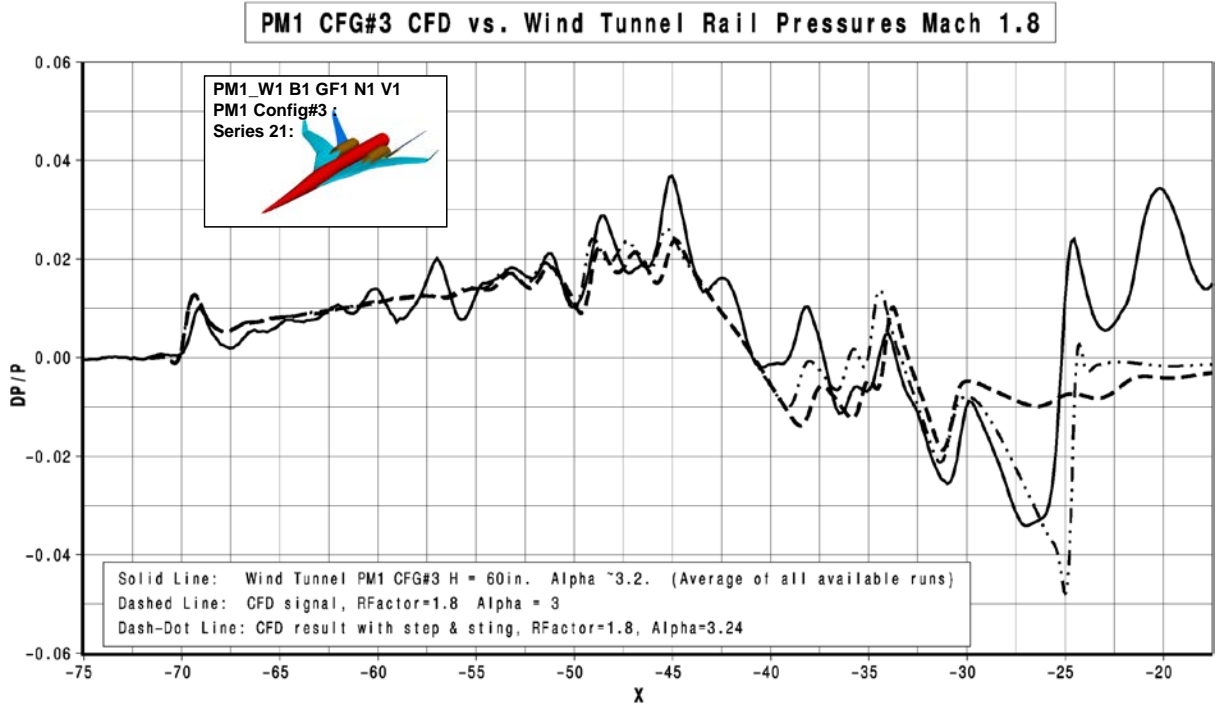
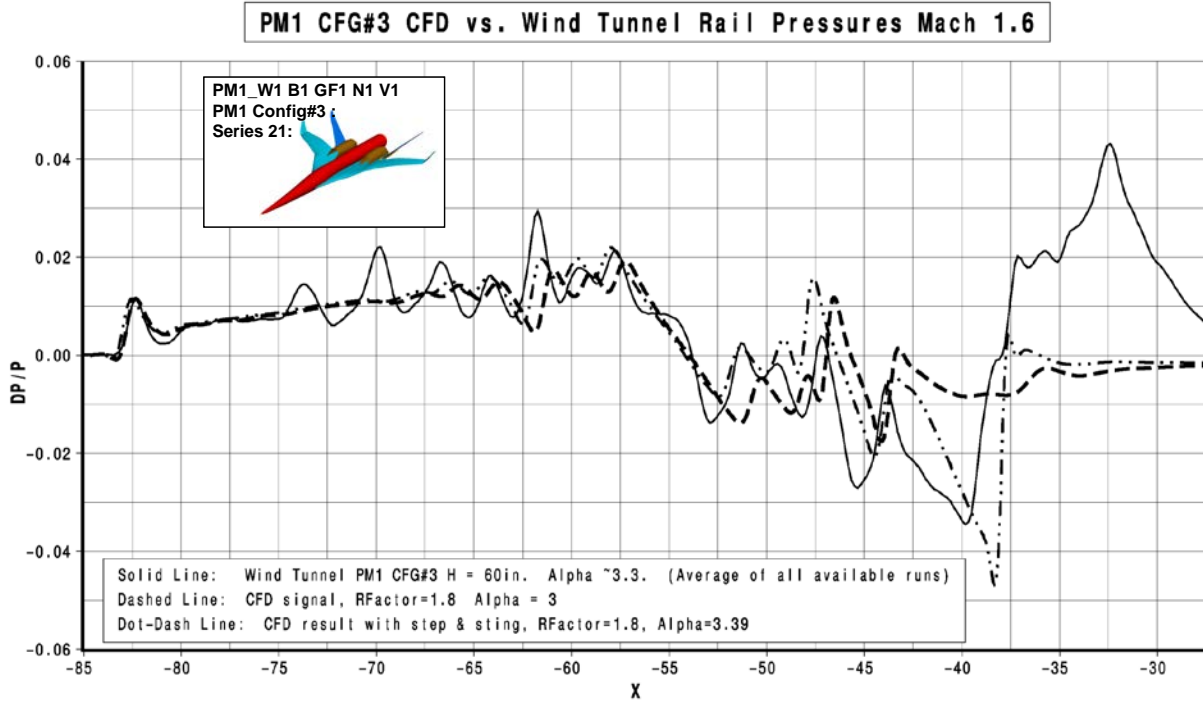


Figure 8.5-3. PM1, Configuration 3, Pressure Signature Comparison of OVERFLOW vs. Test, H = 60

Forces and Moments

Comparisons of the CFD results with the NASA Ames 9' x 7' supersonic wind tunnel AS-0229 force and moment test data for performance models PM1, Configuration 1 and PM1, Configuration 3 are provided in this section. The provided figures show the drag polar, lift, and moment curves for the nominal model height of 60 inches above the rail and for the two Mach conditions tested (1.60 and 1.80) for each model type. A correction for trip and transition has been applied to the CFD data.

Figures 8.5-4 and 8.5-5 compare the force and moment characteristics from the CFD OVERFLOW solutions and the corresponding wind tunnel test data for the PM1, Configuration 1 performance model for M = 1.60 and 1.80, respectively, at H = 60 in.

Figures 8.5-6 and 8.5-7 compare the force and moment characteristics from the CFD OVERFLOW solutions and the corresponding wind tunnel test data for the PM1, Configuration 3 performance model for M = 1.60 and 1.80, respectively, at H = 60 in.

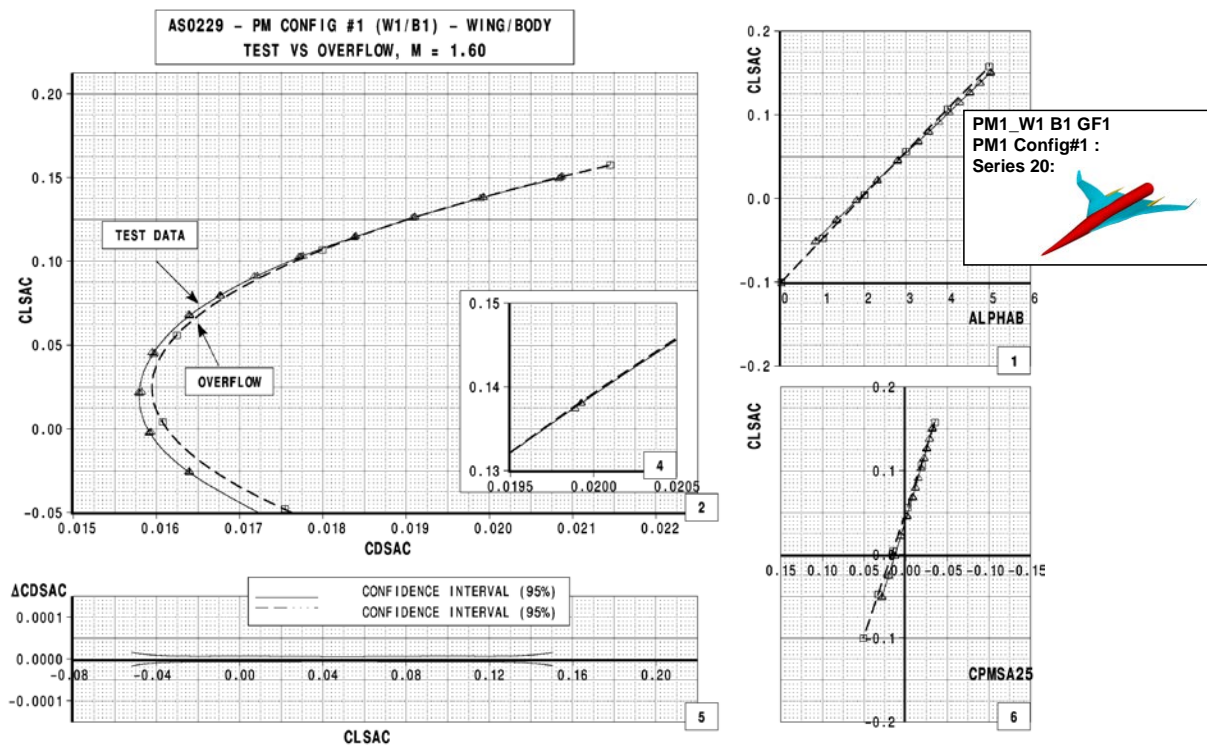


Figure 8.5-4. PM1, Configuration 1, F&M Comparison of OVERFLOW vs. Test, M = 1.60

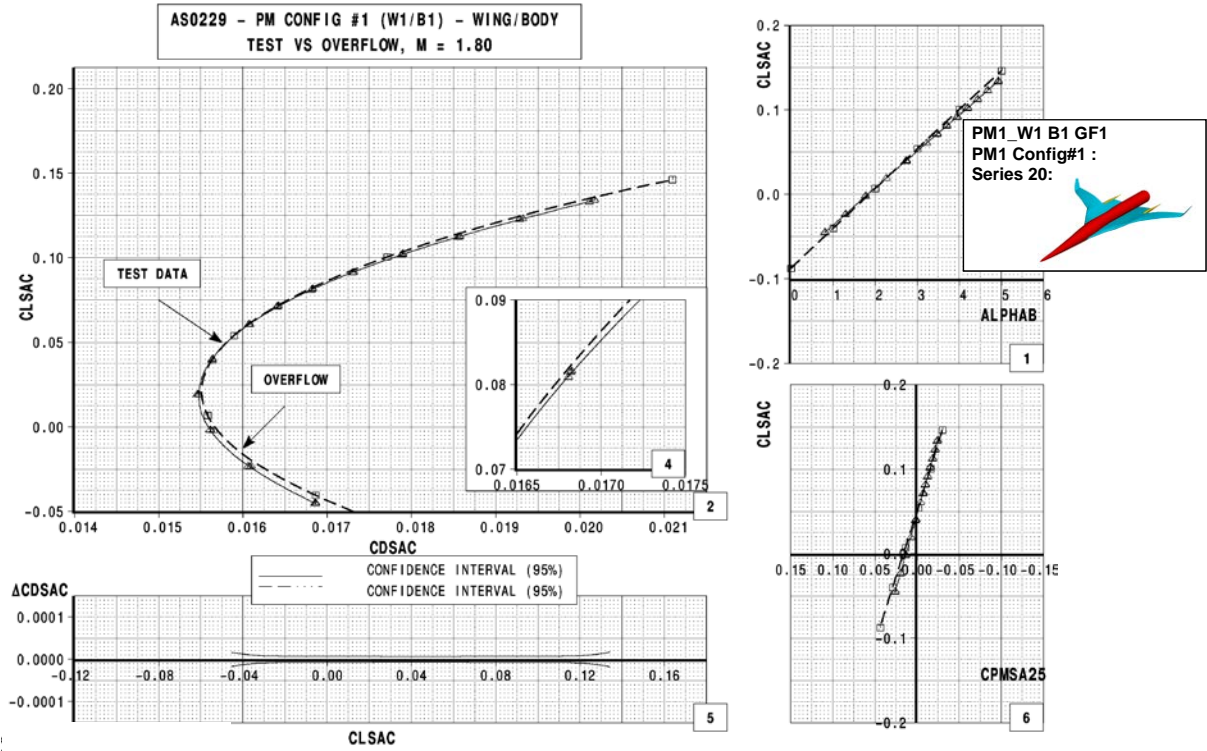


Figure 8.5-5. PM1, Configuration 1, F&M Comparison of OVERFLOW vs. Test, M = 1.80

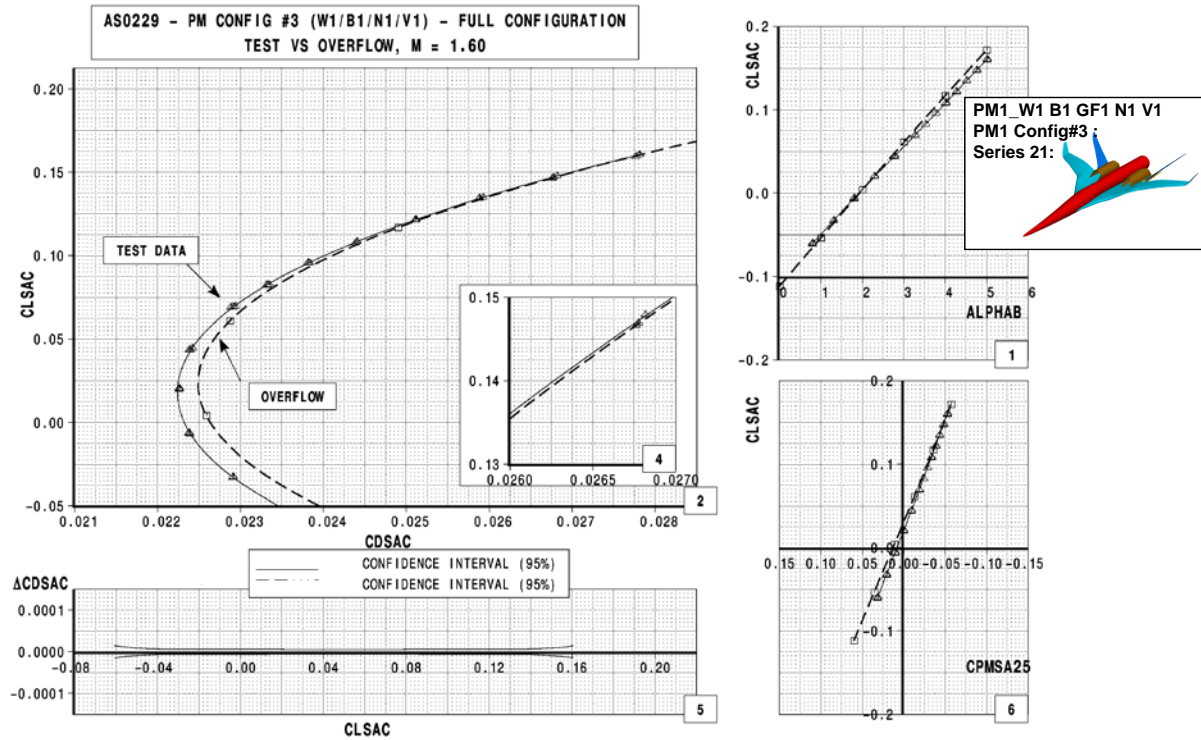


Figure 8.5-6. PM1, Configuration 3, F&M Comparison of OVERFLOW vs. Test, M = 1.60

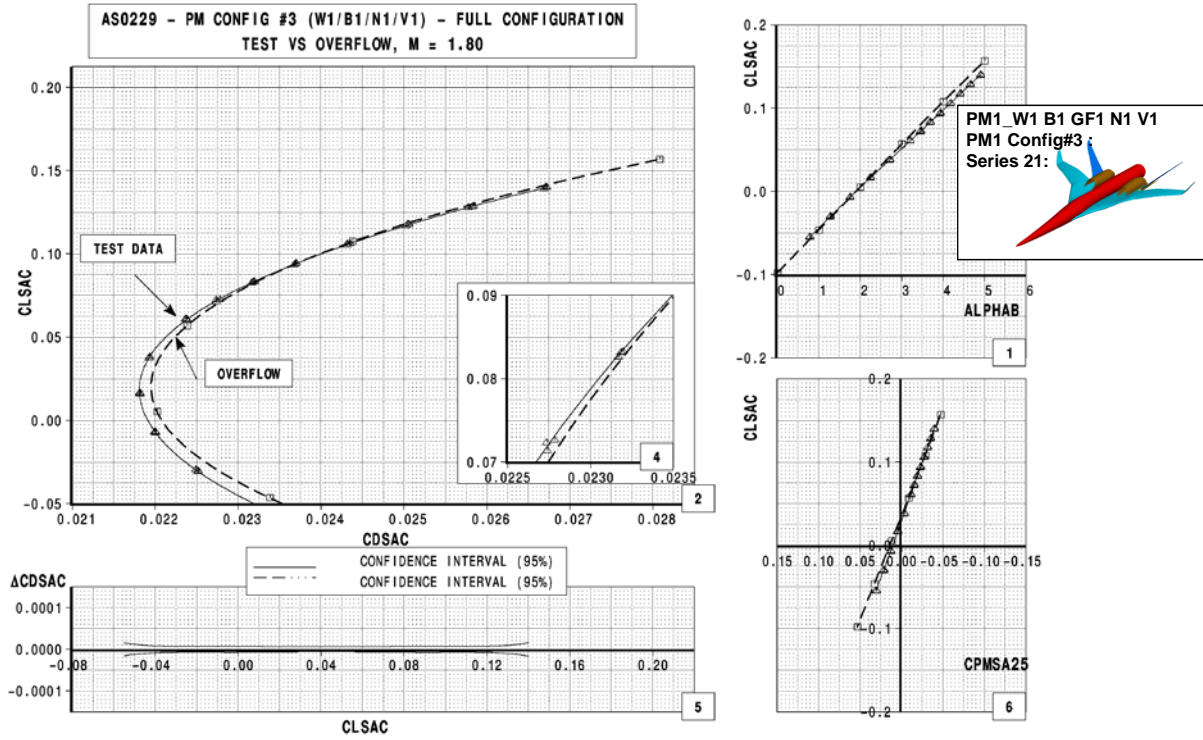


Figure 8.5-7. PM1, Configuration 3, F&M Comparison of OVERFLOW vs. Test, M = 1.80

Incremental Forces and Moments

Comparisons between OVERFLOW isolated model CFD and wind tunnel force and pressure increments at a height of 60 inches are provided in this section. The configuration increment is between PM1, Configuration 1 (wing/body) and PM1, Configuration 3 (full configuration) and is shown at both Mach 1.6 and Mach 1.8.

Figure 8.5-8 compares the pressure and F&M increments between the CFD OVERFLOW solutions and the corresponding wind tunnel test data. The CFD data have been corrected with an 80% amplification factor to account for the effect of the flat-top reflective nature of the rail. The top plots show the increment in the pressure signature between the two configurations. The bottom plots show the force increments in lift, drag, and pitching moment between Configuration 1 and Configuration 3. The CFD was run with the aft-body extended aft with no attempt to model the step down to the sting or the tape for the base pressures.

Figures 8.5-9 and 8.5-10 compare the pressure and F&M increments between the OVERFLOW isolated model CFD and wind tunnel force and pressure increments at Mach 1.6 and 1.8, respectively. The results are shown for a height of 60 inches. The configuration increment is between PM1, Configuration 3 (full configuration) and PM1, Configuration 1 (wing/body). The CFD data have been corrected with a 60% amplification factor to account for the effect of the flat-top reflective nature of the rail. The top left plot shows the CFD and wind tunnel pressure results for the two configurations, whereas the top right plot shows the increment in the pressure signature. The bottom plots show the force increments in lift, drag, and pitching moment between Configuration 3 and Configuration 1. The CFD was run with the aft-body extended aft but with no attempt to model the step down to the sting or the tape for the base pressures.

Delta=PM1 cfg #3 – PM1 cfg #1 (Full Config – Wing/body)

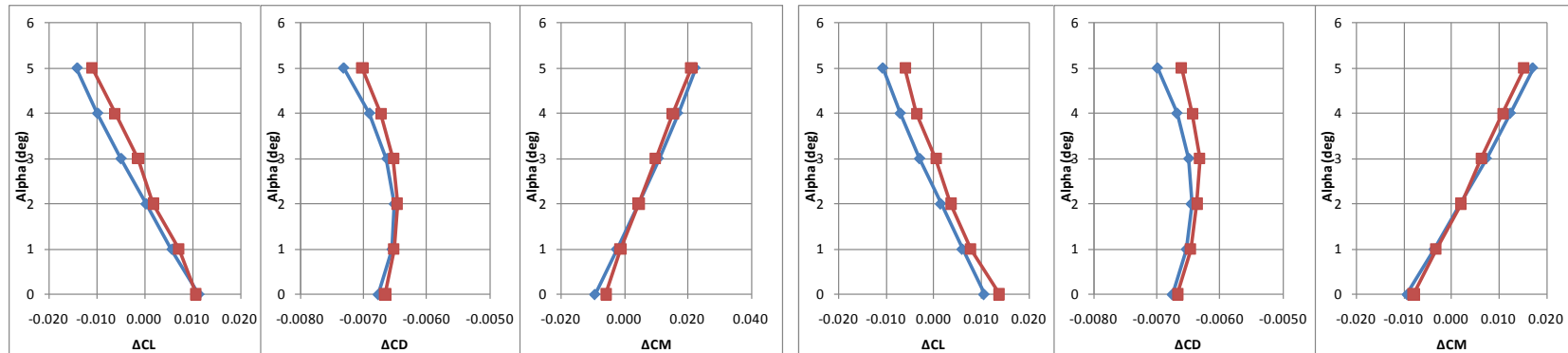
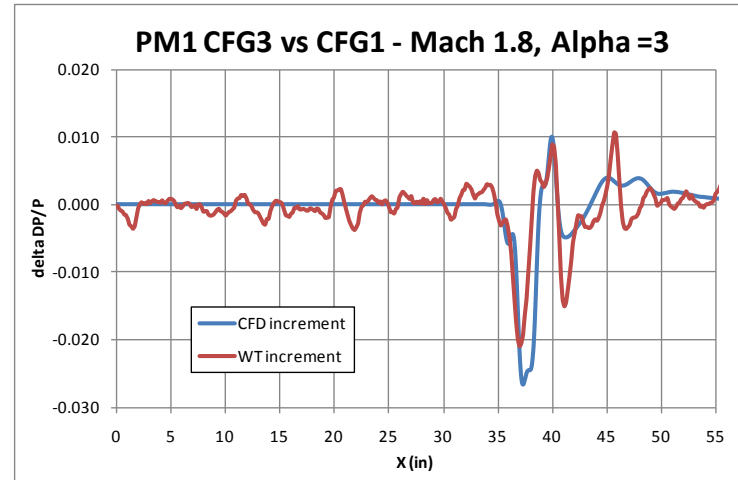
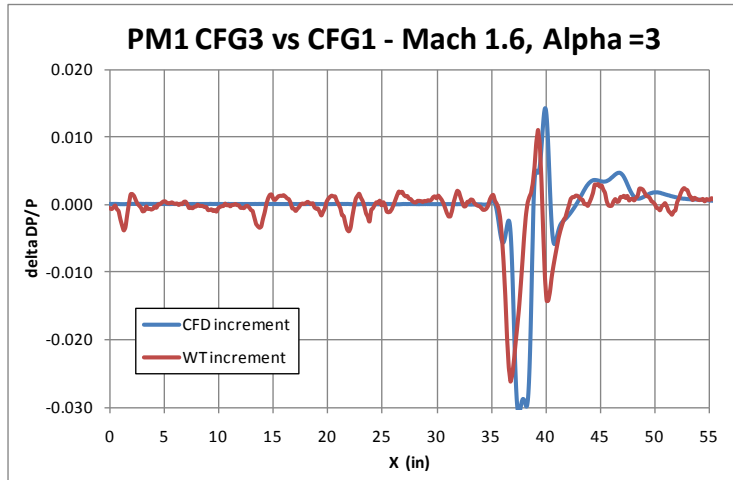


Figure 8.5-8. PM1, Configuration 1 to PM1, Configuration 3, Pressure and F&M Increments—Comparison of OVERFLOW vs. Test

Delta=PM1 cfg #3 – PM1 cfg #1 (Full Config – Wing/body)

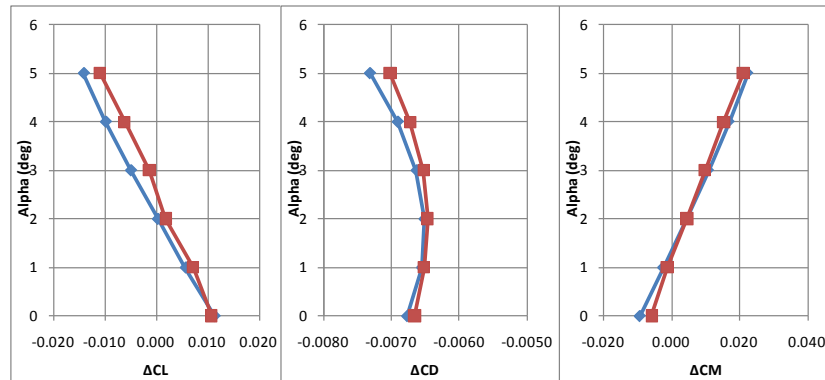
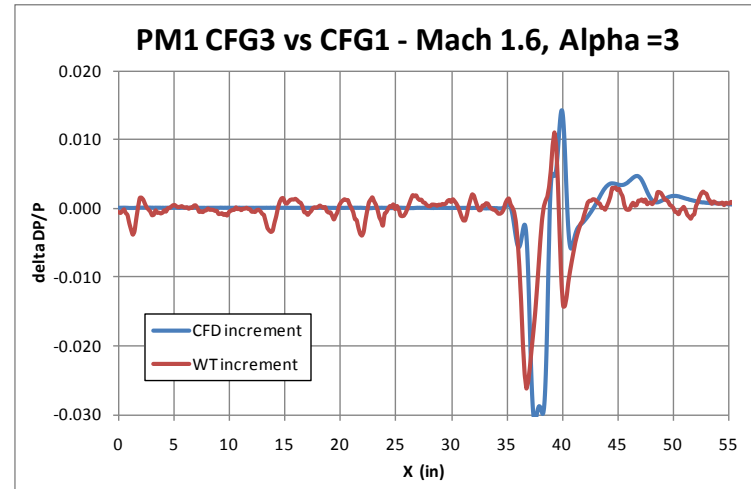
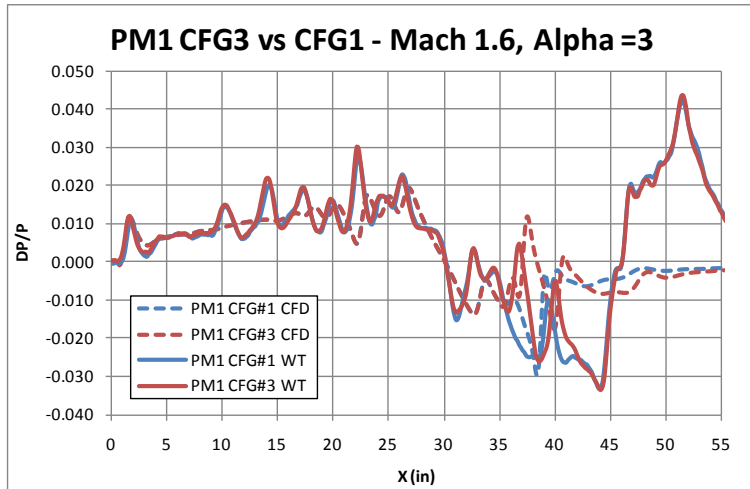


Figure 8.5-9. PM1, Configuration 1 to PM1, Configuration 3, Pressure and F&M Increments, M = 1.60
Comparison of OVERFLOW vs. Test

Delta=PM1 cfg #3 – PM1 cfg #1 (Full Config – Wing/body)

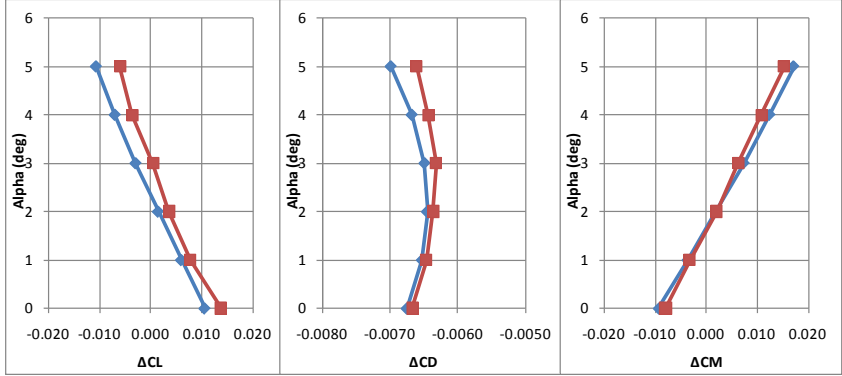
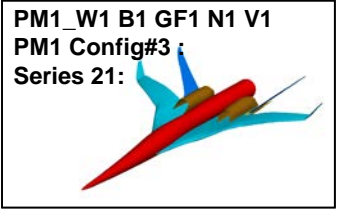
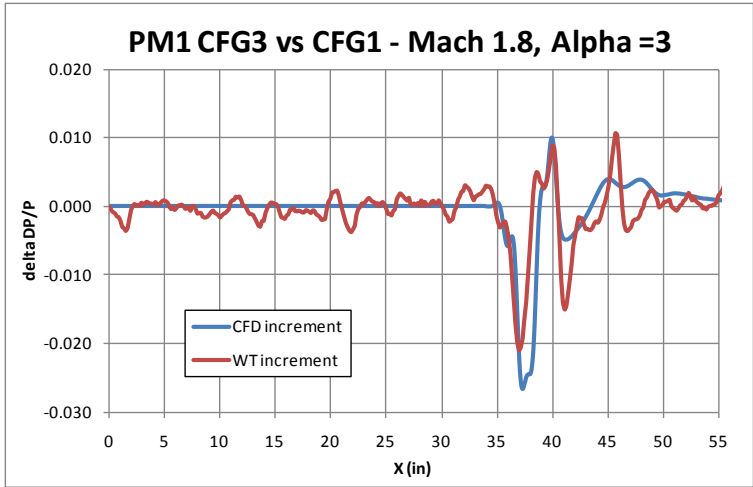
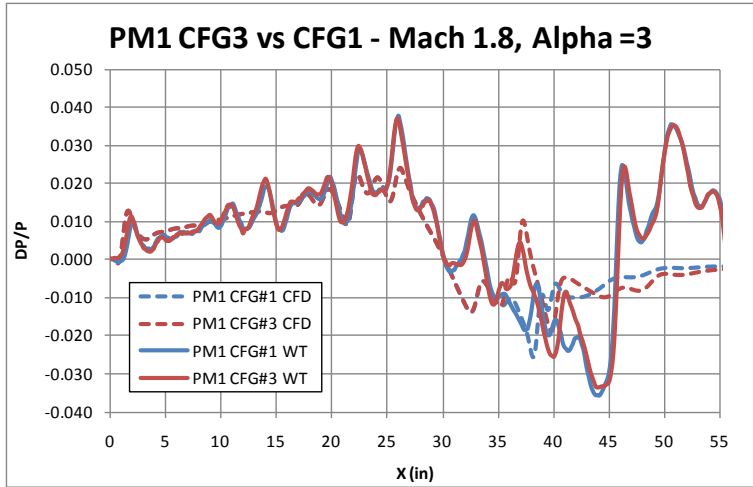


Figure 8.5-10. PM1, Configuration 1 to PM1, Configuration 3, Pressure and F&M Increments, M = 1.80
Comparison of OVERFLOW vs. Test

8.6 Additional Tare and Interference Assessments

CFD-Based Reynolds Number Corrections for Boom Model

Figures 8.6-1 and 8.6-2 show the CFD-predicted effect on pressures and forces for the BM1, Configuration 4 geometry at $M = 1.6$ and 1.8 , respectively, as a result of Reynolds number variations. The upper left plot shows the pressure variation of an Euler analysis (an approximation for flight Re) versus wind tunnel Reynolds number (~ 2.8 million/ft). The dP/P signals are 30 inches off-body at model scale and 4615 inches full scale. The upper right-hand plot shows the delta between the two (Euler/Flt-WtRe). The lower plot shows the delta in forces.

Figure 8.6-3 combines the CFD predicted pressure and forces deltas for BM1, Configuration 4 geometry at $M = 1.6$ and $M = 1.8$ into a single illustration for comparison.

CFD-Based Reynolds Number Corrections for Performance Model

Figures 8.6-4 and 8.6-5 show the CFD-predicted effect on pressures and forces for the PM1 Configuration 3 geometry at $M = 1.6$ and 1.8 , respectively, as a result of Reynolds number variations. The upper left plot shows the pressure variation of an Euler analysis (an approximation for flight Re) versus wind tunnel Reynolds number (~ 2.8 million/ft). The dP/P signals are 60 inches off-body at model scale and 3357 inches full scale. The upper right-hand plot shows the delta between the two (Euler/Flt-WtRe). The lower plot shows the delta in forces.

Figure 8.6-6 combines the CFD predicted pressure and forces deltas for BM1, Configuration 4 geometry at $M = 1.6$ and $M = 1.8$ onto a single illustration for comparison.

CFD-Based Upper Swept Strut Corrections for Boom Model

The upper plots in Figure 8.6-7 show a CFD-based pressure comparison at $M = 1.6$ and 1.8 between the BM1, Configuration 4 geometry modeled with the upper swept strut (wind tunnel hardware) and with the full-scale concept aircraft with a closed aft-body. The lower plots in the figure show the increment between the closed aft-body and the wind tunnel upper swept strut configurations. The dP/P signals are 60 inches off-body at model scale and 4615 inches full scale.

CFD-Based Flared Aft-Body Correction for Performance Model

The upper plots in Figure 8.6-8 show a CFD-based pressure comparison at $M = 1.6$ and 1.8 between the PM1, Configuration 3 geometry (flared aft-body) with the step sting modeled and the full-scale concept aircraft with a closed aft-body. The lower plots show the increment between the closed aft-body and the wind tunnel flared aft-body with the step sting modeled. The dP/P signals are 60 inches off-body at model scale and 3357 inches full scale.

All CFD-Based Corrections for Boom Model

Figure 8.6-9 shows a comparison at $M = 1.6$ and 1.8 at an alpha of approximately 3.5 deg between the BM1, Configuration 4 geometry (flared aft-body) test data, CFD, and test data with corrections for Reynolds number and the upper swept strut tare and interference.

Delta-Re=Configuration_{Fit} - Configuration_{Wt-re}

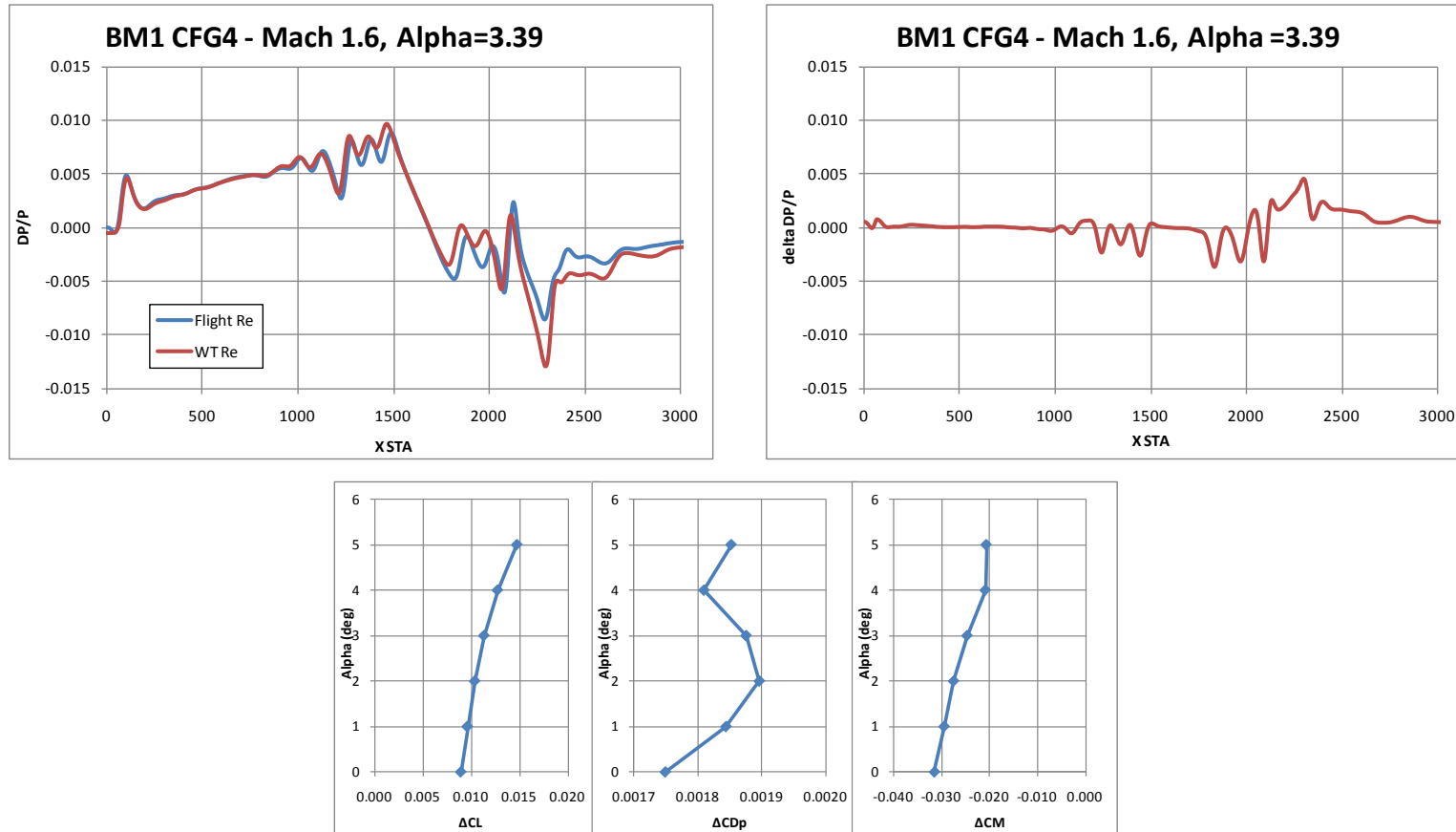


Figure 8.6-1. CFD-Based Reynolds Number Correction for BM1, Configuration 4, M = 1.60

Delta-Re=Configuration_{Flt} - Configuration_{Wt-re}

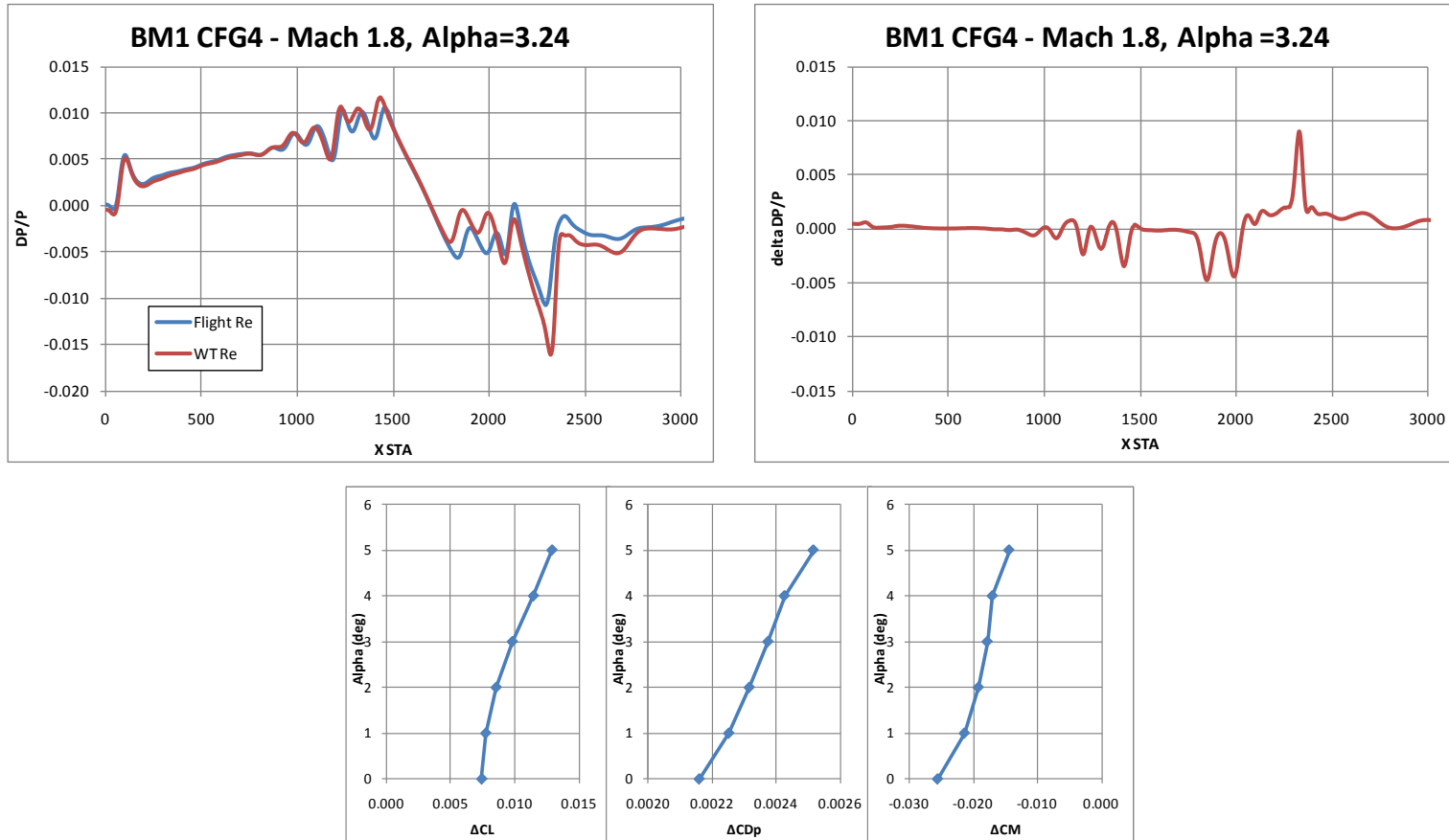


Figure 8.6-2. CFD-Based Reynolds Number Correction for BM1, Configuration 4, M = 1.80

Delta-Re=Configuration_{Fit} - Configuration_{Wt-re}

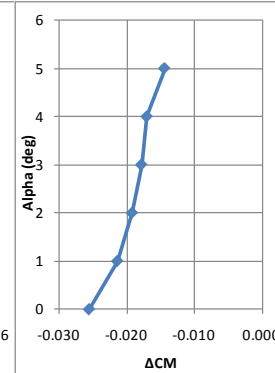
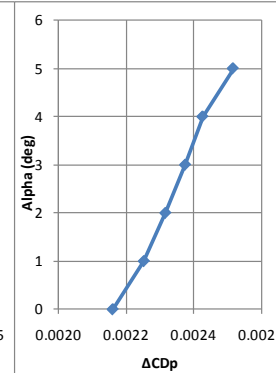
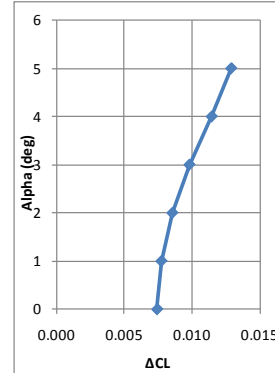
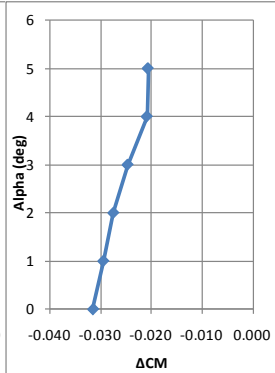
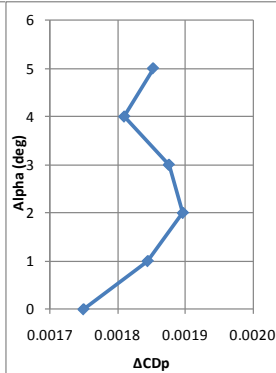
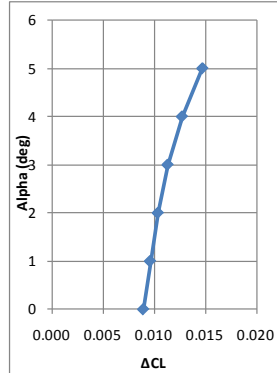
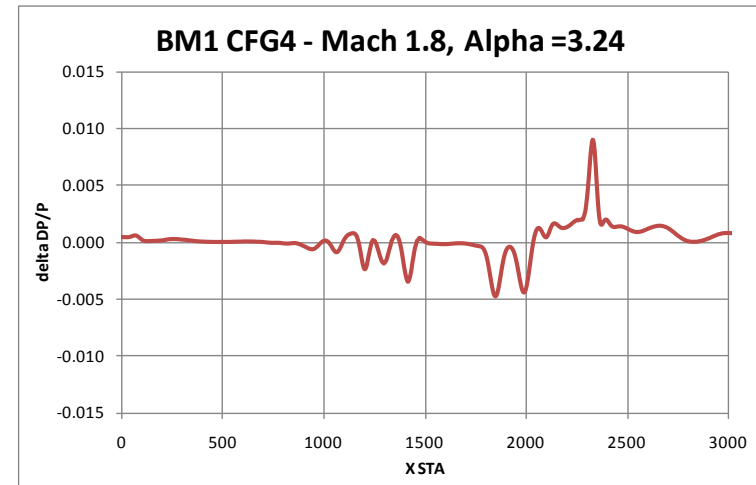
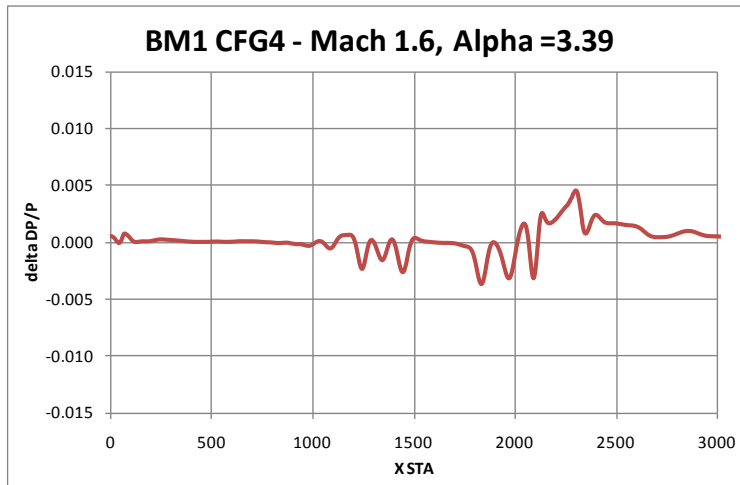


Figure 8.6-3. CFD-Based Reynolds Number Correction for BM1, Configuration 4, M = 1.60 and 1.80

Delta-Re=Configuration_{Flt} - Configuration_{Wt-re}

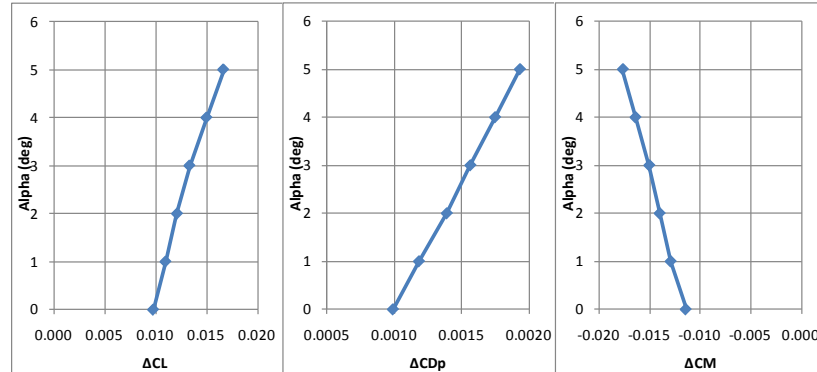
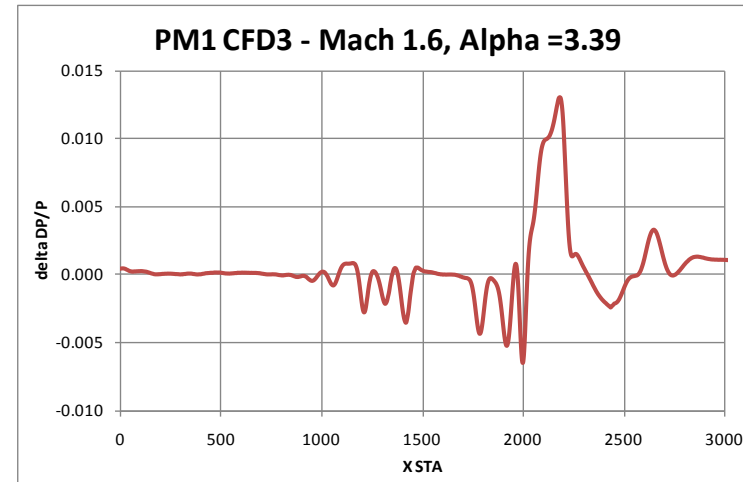
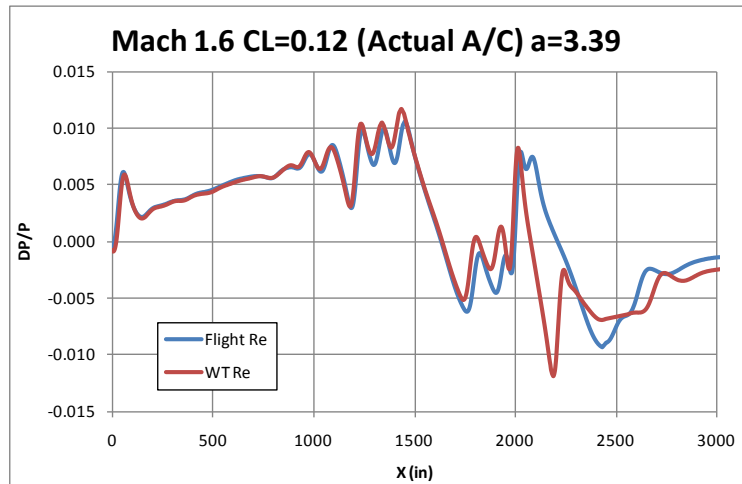
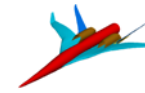


Figure 8.6-4. CFD-Based Reynolds Number Correction for PM1, Configuration 3, M = 1.60

Delta-Re=Configuration_{Flt} - Configuration_{Wt-re}

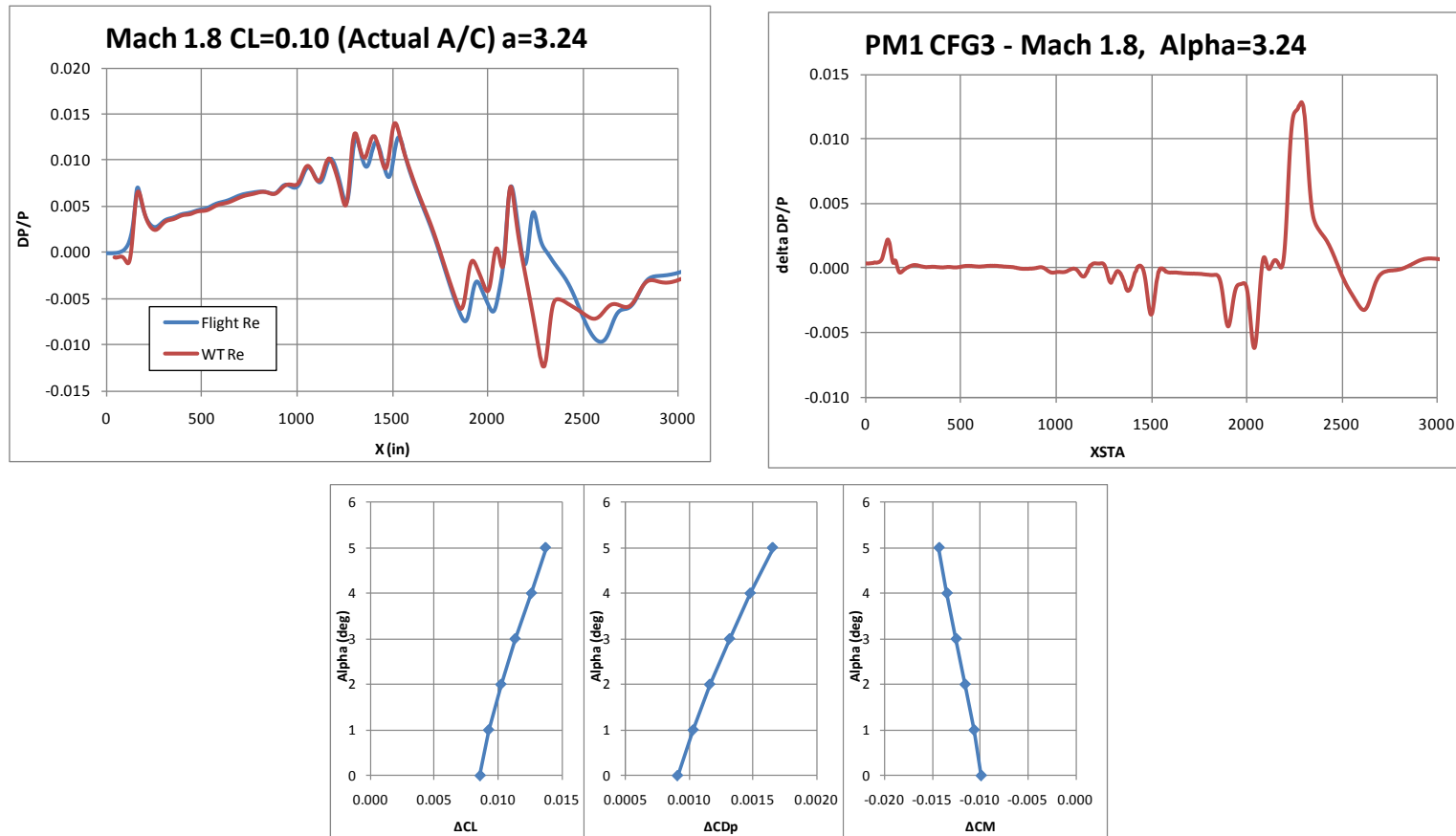


Figure 8.6-5. CFD-Based Reynolds Number Correction for PM1, Configuration 3, M = 1.80

Delta-Re=Configuration_{Flt} - Configuration_{Wt-re}

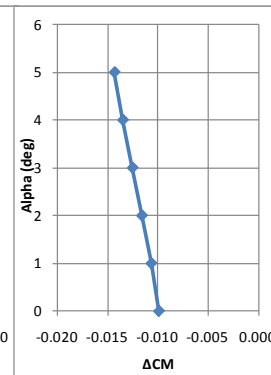
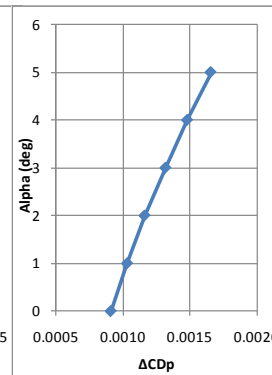
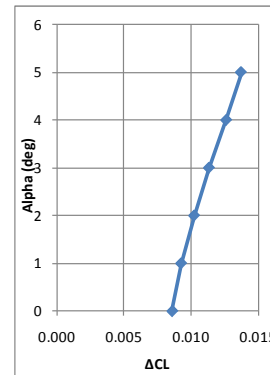
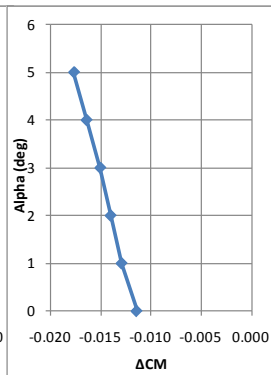
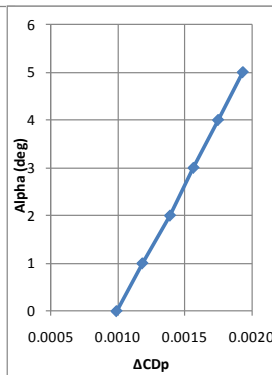
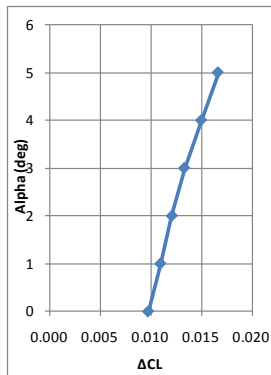
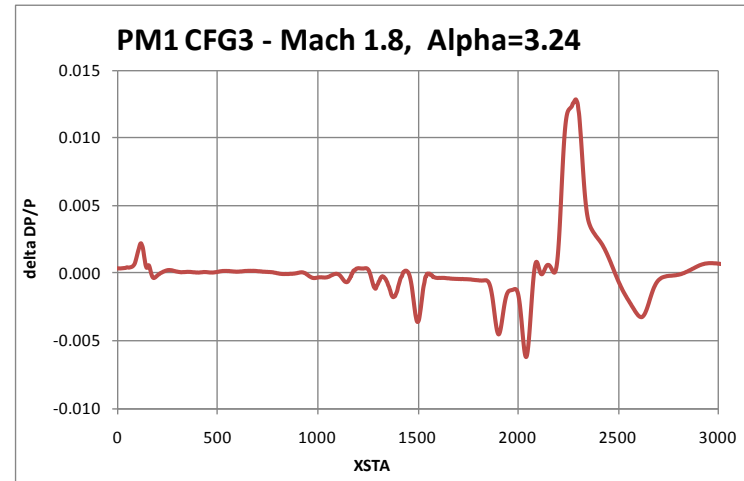
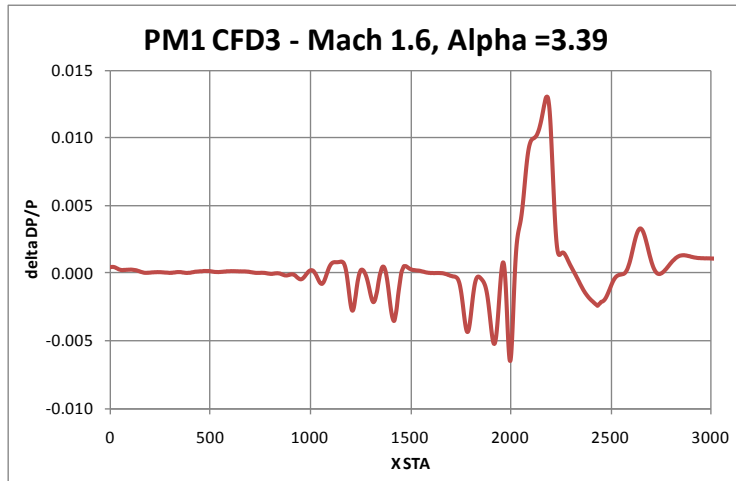


Figure 8.6-6. CFD-Based Reynolds Number Correction for PM1, Configuration 3, M = 1.60 and 1.80

Delta-USS T&I=Configuration_{no-strut} - Configuration_{With-Upper-swept Strut}

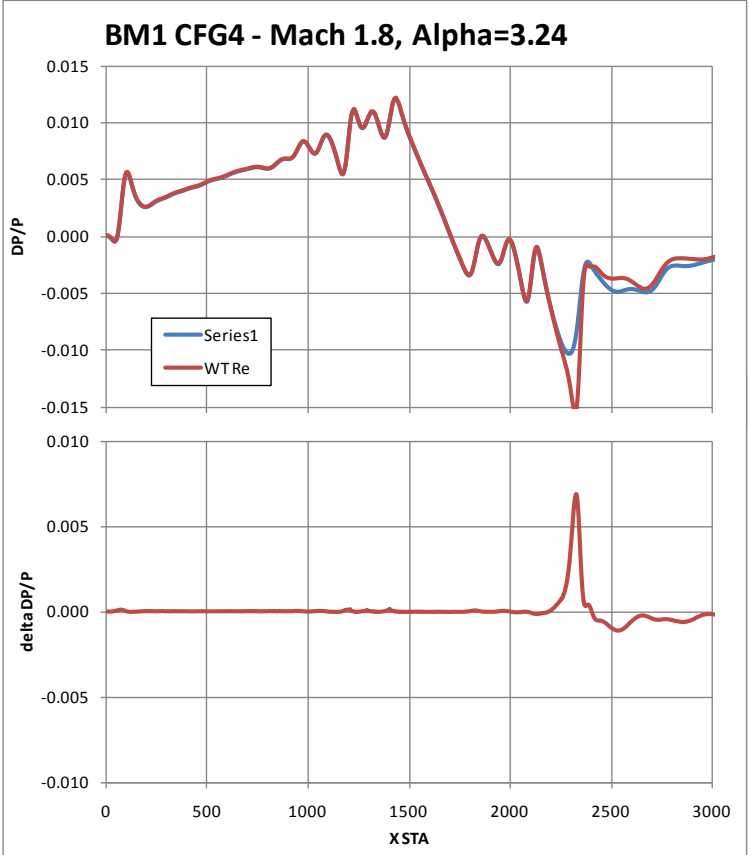
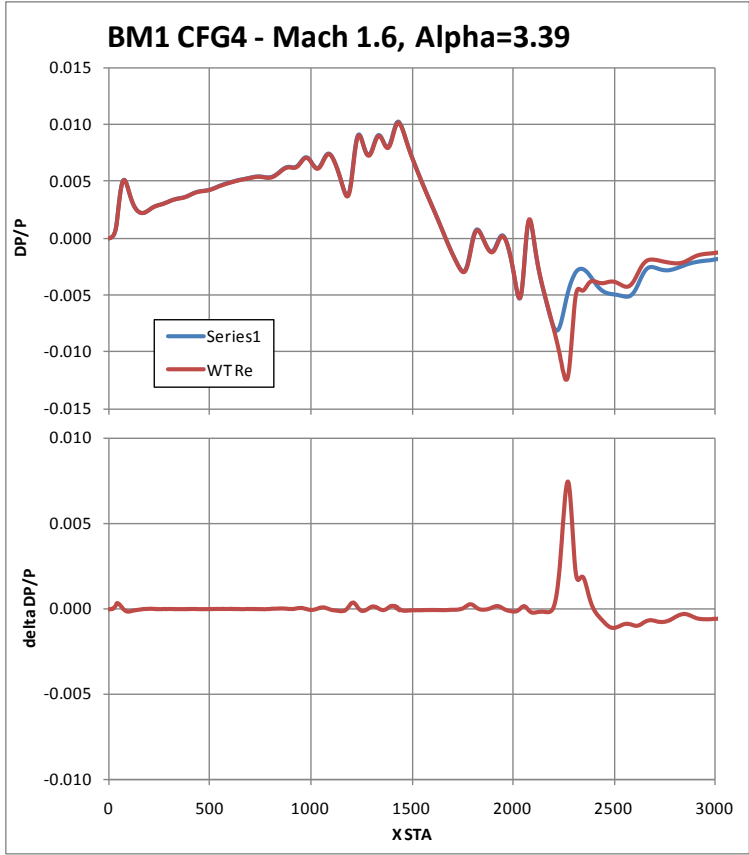


Figure 8.6-7. CFD-Based Upper Swept Strut Correction for BM1, Configuration 4, M = 1.60 and 1.80

Delta-Body Flare T&I=Configuration_{no-Flare} - Configuration_{With-Flare}

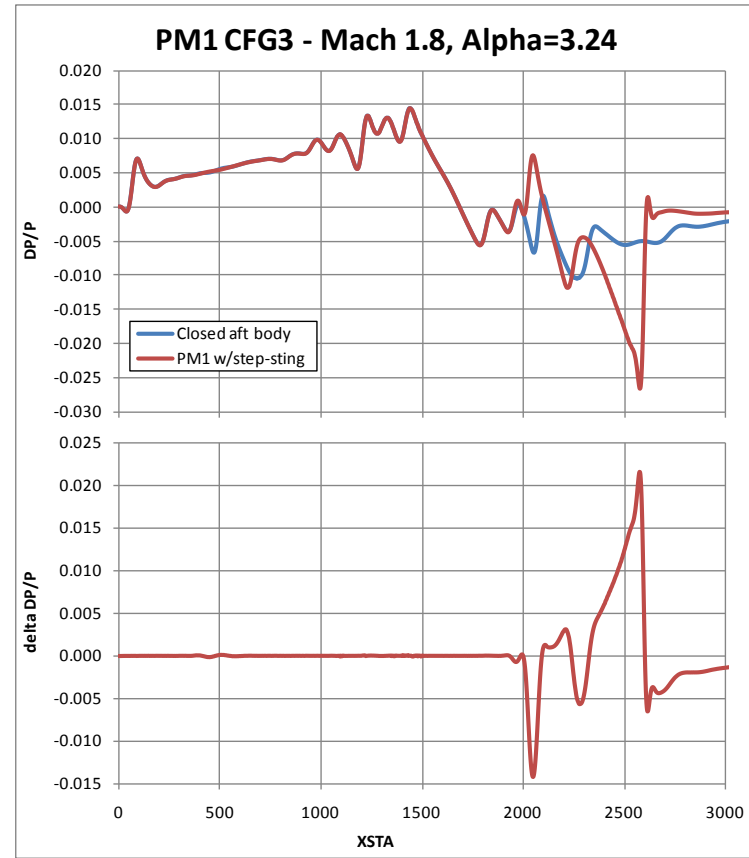
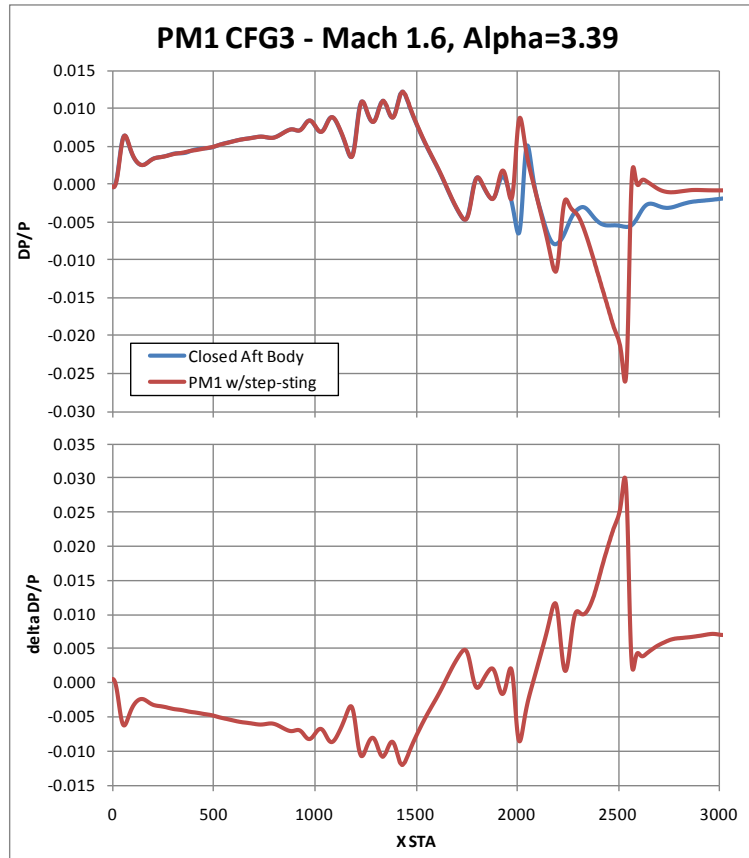
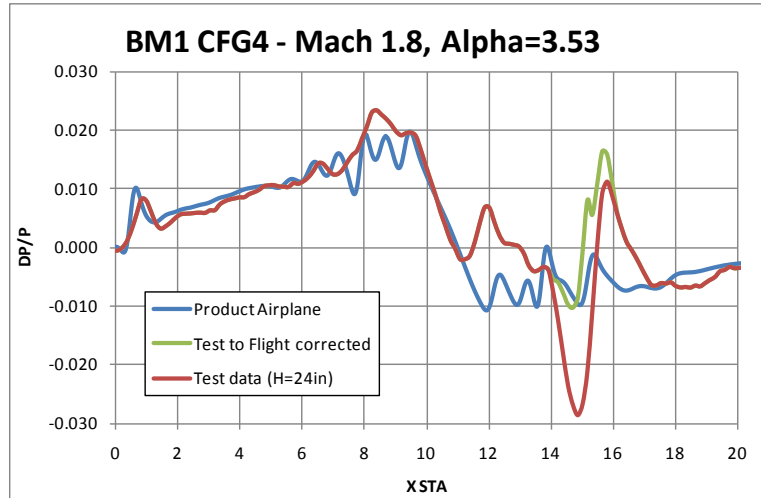
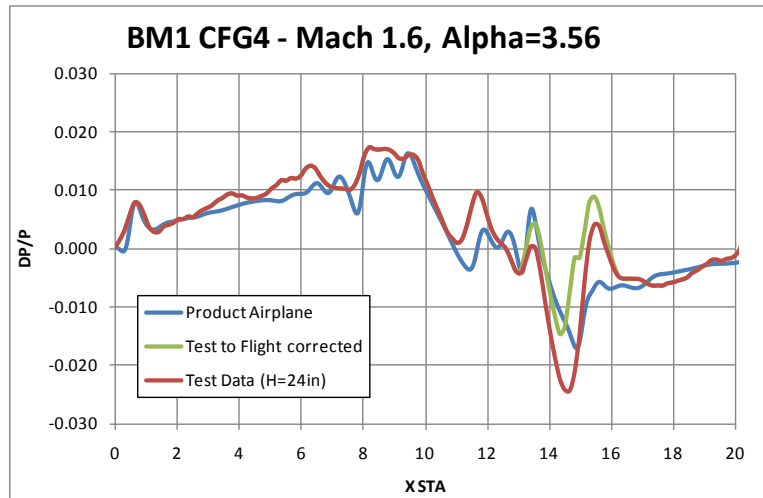


Figure 8.6-8. CFD-Based Upper Swept Strut Correction for BM1, Configuration 4, M = 1.60 and 1.80



Notes:

“Product Airplane” is signature of isolated model with no mounting hardware, scaled by x1.5.

“Test to Flight corrected” has RE and strut increments applied.

Figure 8.6-9. Experimental Results with CFD-Based Corrections Applied for BM1, Configuration 4, M = 1.60 and 1.80

8.7 CFD Validation Summary and Conclusions

The CFD to AS0229 test results validate the predictive capability to assess signatures and performance of an N+2 generation transport aircraft. This validation demonstrates the capability of the low-boom-design to achieve an overland sonic boom of <85 PLdB, with progress toward the longer term goal of 65 to 70 PLdB. The support system tare and interference and wind tunnel Reynolds number effects of the ground-based testing were significant and thus complicate the interpretation of results. It is recommended that additional work in this area be considered.

OVERFLOW analyses were run on 10 of the configurations tested (as well as two that were not tested due to time constraints). In most cases, both Euler and Navier-Stokes solutions at the wind tunnel test Reynolds number were obtained. For all boom models, the configurations were run with and without the upper swept strut. For the performance model configurations, solutions were obtained with both a cylindrical wake and a sharp step sting. As expected, the wind tunnel test environment (modification for model support, WT Re) significantly alters the signatures. Overall, the correlation with test data was good and within the accuracy/uncertainty of the experimental data.

In-depth off-body pressure comparisons were made between CFD and test data for the 10 configurations. When the rail pressure data is filtered to consider only data with minimal perceived tunnel flow non-uniformity, pressure comparisons with CFD are reasonable. There was no evidence of strong shock/shock interference or unexpected rail interference effects seen in the CFD-to-test comparisons. However, there was some evidence of wind tunnel wall shock reflections in the 2" alternate rail measurements. Corrections must be applied to the test results to remove these tunnel wall shock reflections.

The force and moment CFD-to-experiment correlation for the performance model is good and within acceptable uncertainty. As-predicted sonic boom levels were achieved (boom model results), as were predicted levels of L/D (performance model results).

All of the CFD correlation work utilized the as-designed lofts for each of the wind tunnel models. Although the CFD-to-experiment correlations were good, improved correlations might be possible using as-built and as-tested (as-built with deflections). However, this type of analysis was beyond the scope and funding of the phase I contract.

9.0 RECOMMENDATIONS AND FUTURE WORK

Recommendations

The following recommendations are made.

- Further testing at the NASA Ames 9' x 7' supersonic wind tunnel facility requires additional diagnostic testing to better characterize the wind tunnel and develop test methods to avoid issues (tunnel flow non-uniformity) seen during the AS0229 test.** This may help further identify the source of the sinusoidal flow variation observed during the AS0229 test.
- Additional testing at alternate facilities, such as the NASA Ames 11-ft, NASA Glenn 8- by 6-ft, and NASA Glenn 10-ft, should be investigated to see if the results obtained at the NASA Ames 9' x 7' supersonic wind tunnel are related to the experimental set-up or the facility.
- CFD-to-test correlation would benefit from more scrutiny in the area of the terminal recompression.
 - Test data show recompression past freestream whereas CFD does not.
 - Model fidelity tolerance effect should be checked (i.e. as-built and as-tested).
- When appropriate test data are available for comparison, CFD validations should include off-track signatures. The AS0229 test gathered off-track near-field signature data, but because of the way in which the data was gathered it was un-usable in any of the CFD-to-test correlation work. Further work is needed in off-track test techniques to fix this problem.
- For minimum post-test corrections, it is recommended that the 14" blade rail be utilized for small models (model lengths < 35 inches for Mach 1.6 testing) in future testing. For larger models (model lengths greater > 35 inches for Mach 1.6 testing) the 2" alternate rail may be the preferred choice because it maximizes the H/L. However, data corrections will be required to remove the tunnel wall reflected shock from the data. In fact, all of the rails require some level of data corrections depending upon the size of the model and the test objectives.

** Note: After the validation test, additional wind tunnel investigation in the NASA Ames 9' x 7' supersonic wind tunnel of the 2" alternate and 14" blade rail were conducted (Tests 97-231 and 97-250). It was found that spatial averaging in the axial direction significantly improves the data quality and essentially removes much of the tunnel non-uniformities. It was also determined that the rails had up to ~6 seconds of pressure lag due to the long line lengths in the rail instrumentation.

10.0 SUMMARY AND CONCLUSION

During Phase I, all objectives established at the beginning of the project were met. A low-boom concept that meets the main goals of the project was developed. The characteristics (i.e., sonic boom, aerodynamics, performance, trim, and CG) of this concept were evaluated and presented at Gate Review 1. The low-boom concept successfully passed the review, and performance (i.e., large force and moment) and sonic boom wind tunnel models were designed and fabricated for testing in the NASA Ames 9' x 7' supersonic wind tunnel.

The models were tested in the NASA Ames 9' x 7' supersonic wind tunnel during the AS-0229 test in April 2011. The results from that test validated the low-boom design and correlated well with pretest CFD data. However, the test did uncover flow quality issues in the wind tunnel that merit further investigation.

Existing NASA sonic boom pressure measurement rails were evaluated, and recommendations were made to build two new rails. The first, the NASA 14" Blade Rail design, was tested in November 2010 and the second, the Boeing 2" Alternate Rail design, was tested during the April 2011 low-boom validation test. Both new rails showed improved performance compared with the previous NASA rails. The best rail for future testing depends upon the test objectives and the size of the model. For small sonic-boom models the 14" blade rail requires the least amount of post test corrections. However, the 2" Alternate Rail may be the best choice for larger model testing, because it maximizes the achievable H/L. Both rails for the larger model will require more corrections to remove unwanted tunnel wall reflections.

The low-boom concept achieved and, in some cases, exceeded all sonic boom goals for the project. The low-boom concept was designed at Mach = 1.8 and achieved a shaped front and aft sonic boom signature. The front portion of the under-track signature is sinusoidal in shape, and the aft portion of the signature has a flat-top shape. The under-track signature has a ground-perceived loudness of 81 PLdB, which exceeds the goal of 85 PLdB. The low-boom concept also retains its low-boom characteristics at off-design conditions of Mach and CL and at some off-track locations.

The second-priority goal for the project was to meet or exceed the same level of aerodynamic performance as the 765-076E configuration developed under the N+2 Supersonic Systems Study. Although this goal was not achieved, it was noted that with a notional 3% technology projection by the year 2025, this configuration would indeed meet the performance goals of the project.

Several areas in addition to the sonic boom and performance were also assessed. These included fuel loading, stability, trim, and center-of-gravity. It was determined that sufficient space could be found in the configuration to load enough fuel to meet the mission. The low-boom concept is statically stable at cruise. However, the concept cruise CG was not within current fuel tank loadability limits and, therefore, the trim for the low-boom concept design did not close.

With these issues in mind, a second sonic boom concept was developed with the objective of improved L/D and off-track performance. This second sonic boom concept focused on a Mach = 1.6 cruise condition, and the pitching moment was constrained to improve the trim. The resulting concept had improved performance with essentially the same sonic boom and was able to achieve the lower pitching moment for improved trim. This second configuration had significantly different shaping and, with its different implementation of design objectives, resulted in a concept worthy of validation. Thus a second sonic boom model was designed and fabricated for testing in the NASA Ames 9' x 7' supersonic wind tunnel.

The ultimate purpose of this project was to validate in a wind tunnel environment the tools and processes required to achieve low-boom aerodynamically-efficient concepts. This goal was successfully achieved. The main design objective was to develop a low-boom configuration optimized for minimum sonic boom levels and maximum performance efficiency. The resulting low-boom concepts were never meant to be closed aircraft designs. The project assessed several design disciplines and noted some shortcomings in the concepts. Additionally, there were many areas not addressed, including structures and aeroelastics. These future challenges will have to be overcome once low-boom design methods are fully validated and matured.

In conclusion, the wind tunnel test results show that the designed low-boom configuration is indeed low-boom with both front and aft near-field shaping that matches pretest predictions. However, not all test data were consistent and some measured signatures did not match as well as desired. It is conjectured that these anomalous results stem from the NASA Ames 9' x 7' facility flow quality issues. These anomalous results were sinusoidal and seem to be tied to the movement of the wind tunnel strut. Further study is required to determine the source of these flow issues, and testing at alternate wind tunnel facilities may help determine a solution to these problems.

Phase II of the project will focus on the effect of propulsion on the low-boom design.

11.0 NOMENCLATURE

Term	Description
2D	Two-Dimensional
3D	Three-Dimensional
765-076E	Boeing N+ 2 System Study baseline concepts
AOA	Angle-of-Attack
ARC	Ames Research Center
ARRA	American Recovery and Reinvestment Act
BCA	Boeing Commercial Airplanes
BOR	Body of Revolution
BR&T	Boeing Research and Technology
CA	Axial Force Coefficient
Cart3d	A high-fidelity inviscid analysis package for conceptual and preliminary aerodynamic design
CD	Drag Coefficient
CFD	Computational Fluid Dynamics
CG	Center of Gravity
CL	Lift Coefficient
CM	Pitching Moment Coefficient
CN	Normal Force Coefficient
COTR	Contracting Officer's Technical Representative
Count	1 count of drag is $CD = 0.0001$
CR	Contractor Report
DFRC	Dryden Flight Research Center
dP/P	$(P-P_{inf})/P_{inf}$
DPOVP AVG_Y	Averaged $(P-P_{inf})/P_{inf}$ with the reference pressure run removed
DPOVPU AVG_Y	Averaged $(P-P_{inf})/P_{inf}$ with the reference pressure run not removed
F&M	Force and Moment
FAA	Federal Aviation Administration
FAP	Fundamental Aeronautics Program
FAR	Federal Aviation Regulation
FS	Full Scale
GFI	Government-Furnished Information
GRC	Glenn Research Center

H	Height
H/L	Height/Length
HB	Huntington Beach, California
L/D	Lift-to-Drag ratio
LH/RH	Left Hand/Right Hand
LaRC	Langley Research Center
MDA	Multidisciplinary Analysis
MDBOOM	A Boeing linear wave propagation code
MDO	Multidisciplinary Optimization
MDOPT	A Multidisciplinary Design OPTimization system
MDPLOT	A Boeing noise metrics calculation tool used with MDBOOM
MPR	Model Preparation Room
NASA	National Aeronautics and Space Administration
nmi	Nautical Mile
NPSS	Numerical Propulsion System Simulation
NRA	NASA Research Announcement
OML	Outer Mold-Line
OVERFLOW	The OVERset grid FLOW solver. This code solves the Reynolds-Averaged Navier-Stokes equations
PDR	Preliminary Design Review
Placeholder Nacelle	Representative nacelle used on validation concept. A refined nacelle (inlet and nozzle) will be designed in phase II of the project.
PLdB	Perceived Loudness in decibels
QEVC	Quiet Experimental Validation Concept
S&C	Stability and Control
SEEB	Seebass and George minimum sonic boom theory (equivalent area body of revolution)
SFC	Specific Fuel Consumption
SSBD	Shaped Sonic Boom Demonstrator
t/c	Thickness to Chord ratio
TIM	Technical Interchange Meeting
TRANAIR	Nonlinear, full-potential equation code developed to analyze compressible flow over arbitrary complex configurations at subsonic, transonic, or supersonic freestream Mach numbers
UPWT	Unitary Plan Wind Tunnel
V-tail	Vertical Tail

W/B/N/V	Wing/Body/Nacelle/Vertical
WBS	Work Breakdown Structure
WT Re	Wind Tunnel Reynolds Number
x/L	Axial location/Length
Zephyrus	Boeing sonic boom propagation computer code that predicts the expected sonic boom waveform at ground level and incorporates as many physical effects as possible

12.0 REFERENCES

Report References

1. Pawlowski, J. W., D. H. Graham, C. H. Boccadoro, P. G. Coen, and D. J. Maglieri, "Origins and Overview of the Shaped Sonic Boom Demonstration Program," AIAA 2005-5-703, 43rd AIAA Aerospace Sciences Meeting and Exhibit, 10–13 January 2005, Reno, Nevada.
2. Welge, H. R., J. Bonet, T. Magee, D. Chen, S. Hollowell, A. Kutzmann, A. Mortlock, J. Stengle, C. Nelson, A. Adamson, S. Baughcum, R. T. Britt, G. Miller, and J. Tai, "N+2 Supersonic Concept Development and Systems Integration," NASA /CR-2010-216842, August 2010.
3. Welge, H. R., C. Nelson, and J. Bonet, "Supersonic Vehicle Systems for the 2020 to 2035 Timeframe," AIAA 2010-4930, 28th AIAA Applied Aerodynamics Conference, 28 June–1 July 2010, Chicago, Illinois.
4. Wintzer, M., M. Nemeć, and M. J. Aftosmis, "Adjoint-Based Adaptive Mesh Refinement for Sonic Boom Prediction," AIAA 2008-6593, 26th AIAA Applied Aerodynamics Conference, 18–21 August 2008, Honolulu, Hawaii.
5. Nichols, R. H., R.W. Tramel, and P. G. Buning, "Solver and Turbulence Model Upgrades to OVERFLOW 2 for Unsteady and High-Speed Applications," AIAA 2006-2824-824, 24th Applied Aerodynamics Conference, 5–8 June 2006, San Francisco, California.
6. Plotkin, K. J., and J. A. Page, "MDBOOM and MDPLOT Computer Programs for Sonic Boom Analysis and Design," Wyle Report WR 02-03, February 2002.
7. Robinson, L., "Sonic Boom Propagation through an Inhomogeneous, Windy Atmosphere," PhD dissertation, 1991.
8. Robinson, L., "Modifications to the Zephyrus Sonic Boom Propagation Model," final report to The Boeing Company, 11 September 1996.
9. Furukawa, T., Y. Makino, N. Masayoshi, and T. Ito, "Supporting System Study of Wind-Tunnel Models for Validation of Aft-Sonic-Boom Shaping Design," AIAA 2008-6596-787, 26th AIAA Applied Aerodynamics Conference, 18–21 August 2008, Honolulu, Hawaii.

Additional Sonic Boom References

10. Yoshida, K., Y. Makino, and Y. Shimbo, "An Experimental Study on Unmanned Scaled Supersonic Experimental Airplane," AIAA-2002-2842, 2002.
11. Haglund, G. T., "HSCT Designs for Reduced Sonic Boom," AIAA-91-3103, 1991.
12. Mack, R.J., and G. T. Haglund, "A Practical Low-Boom Overpressure Signature Based on Minimum Sonic Boom Theory," NASA CP-3173, vol. II, 1992.
13. Hayes, W. D., R. C. Haefeli, and H. E. Kulsrud, "Sonic Boom Propagation in a Stratified Atmosphere, with Computer Program," NASA CR 1299, 1969.
14. Darden, C. M., "Sonic-Boom Minimization with Nose-Bluntness Relaxation," NASA TP 1348, 1979.
15. Shepherd, K. P., and B. M. Sullivan, "A Loudness Calculation Procedure Applied to Shaped Sonic Booms," NASA Technical Paper 3134, November 1991.
16. Brown, J. G., and G. T. Haglund, "Sonic Boom Loudness Study and Airplane Configuration Development," AIAA-88-4467, 1988.
17. Seebass, R., and A. R. George, "Sonic-Boom Minimization," *Journal of the Acoustical Society of America*, vol. 51, no. 2, pt. 3, February 1972, pp. 686–694.
18. Seebass, R., and B. Argrow, "Sonic Boom Minimization Revisited," AIAA Paper 98-2956, AIAA 2nd Theoretical Fluid Mechanics Meeting, Albuquerque, New Mexico, 1998.
19. Victor, L., and J. M. Morgenstern, "Calculated and Measured Pressure Fields for an Aircraft Designed for Sonic-boom Alleviation," AIAA 2004-4846, 2004.
20. Morgenstern, J. M., "Wind Tunnel Testing of a Sonic Boom Minimized Tail-Braced Wing Transport Configuration," AIAA 2004-4536, 2004.
21. Graham, D., J. Dahlin, J. A. Page, K. J. Plotkin, and P. G. Coen, "Wind Tunnel Validation of Shaped Sonic Boom Demonstration Aircraft Design", AIAA 2005-7, 2005
22. Mack, R. J., and N. Kuhn, "Determination of Extrapolation Distance With Measured Pressure Signatures From Two Low-Boom Models," NASA/TM-2004-213264, 2004.

23. Mack, R. J., "An Integrated Fuselage-Sting Balance for a Sonic-Boom Wind-Tunnel Model," NASA/TM-2004-213265, 2004.
24. Carlson, H. W., F. E. Mc Lean, and B. L. Shrout, "A wind tunnel study of sonic boom characteristics for basic and modified models of a supersonic transport configuration," NASA-TM-X-1236, 1966.
25. MS Excel file, "Occ Log_QEVC Test_97-0229.xls," 2 May 2011.
26. MS Excel file, "Run Log_All Runs_QEVC Test_97-0229.xls," 28 April 2011.
27. MS Word document, "Test Notes_QEVC Test_97-0229.doc," 2 May 2011.
28. MS PowerPoint file, "N+2 Supersonic System Level Experimental Validation-April 2011 Ames 9x7 Test Summary Report," E. Adamson, A. Bidwell, K. Mejia, and S. Shaw, 27 May 2011.
29. NASA Ames Wind Tunnel Customer Agreement, "TBC1: QEVC Boom and Performance Test, Test No. 97-0229," 25 March 2011.
30. MS PowerPoint file, "N+2 Supersonic System Level Experimental Validation-Phase 1 Validation Report," E. Adamson, A. Bidwell, S. Fugal, K. Mejia, S. Shaw, D. Trieber, and E. Unger, 10 June 2011.

REPORT DOCUMENTATION PAGE

*Form Approved
OMB No. 0704-0188*

The public reporting burden for this collection of information is estimated to average 1 hour per response, including the time for reviewing instructions, searching existing data sources, gathering and maintaining the data needed, and completing and reviewing the collection of information. Send comments regarding this burden estimate or any other aspect of this collection of information, including suggestions for reducing this burden, to Department of Defense, Washington Headquarters Services, Directorate for Information Operations and Reports (0704-0188), 1215 Jefferson Davis Highway, Suite 1204, Arlington, VA 22202-4302. Respondents should be aware that notwithstanding any other provision of law, no person shall be subject to any penalty for failing to comply with a collection of information if it does not display a currently valid OMB control number.
PLEASE DO NOT RETURN YOUR FORM TO THE ABOVE ADDRESS.

1. REPORT DATE (DD-MM-YYYY) 01-02-2013		2. REPORT TYPE Contractor Report		3. DATES COVERED (From - To)	
4. TITLE AND SUBTITLE System-Level Experimental Validations for Supersonic Commercial Transport Aircraft Entering Service in the 2018–2020 Time Period - Phase I Final Report				5a. CONTRACT NUMBER NNL08AA16B	
				5b. GRANT NUMBER	
				5c. PROGRAM ELEMENT NUMBER	
6. AUTHOR(S) Magee, Todd E.; Wilcox, Peter A.; Fuqal, Spencer R.; Acheson, Kurt E.; Adamson, Eric; Bidwell, Alicia L.; Shaw, Stephen G.				5d. PROJECT NUMBER	
				5e. TASK NUMBER NNL10AA00T	
				5f. WORK UNIT NUMBER 475122.02.07.03.03	
7. PERFORMING ORGANIZATION NAME(S) AND ADDRESS(ES) NASA Langley Research Center Hampton, Virginia 23681-2199				8. PERFORMING ORGANIZATION REPORT NUMBER	
9. SPONSORING/MONITORING AGENCY NAME(S) AND ADDRESS(ES) National Aeronautics and Space Administration Washington, DC 20546-0001				10. SPONSOR/MONITOR'S ACRONYM(S) NASA	
				11. SPONSOR/MONITOR'S REPORT NUMBER(S) NASA/CR-2013-217797	
12. DISTRIBUTION/AVAILABILITY STATEMENT Unclassified - Unlimited Subject Category 01 Availability: NASA CASI (443) 757-5802					
13. SUPPLEMENTARY NOTES Langley Technical Monitor: Linda S. Bangert					
14. ABSTRACT This report describes the work conducted by The Boeing Company under American Recovery and Reinvestment Act (ARRA) and NASA funding to experimentally validate the conceptual design of a supersonic airliner feasible for entry into service in the 2018 to 2020 timeframe (NASA N+2 generation). The report discusses the design, analysis and development of a low-boom concept that meets aggressive sonic boom and performance goals for a cruise Mach number of 1.8. The design is achieved through integrated multidisciplinary optimization tools. The report also describes the detailed design and fabrication of both sonic boom and performance wind tunnel models of the low-boom concept. Additionally, a description of the detailed validation wind tunnel testing that was performed with the wind tunnel models is provided along with validation comparisons with pretest Computational Fluid Dynamics (CFD). Finally, the report describes the evaluation of existing NASA sonic boom pressure rail measurement instrumentation and a detailed description of new sonic boom measurement instrumentation that was constructed for the validation wind tunnel testing.					
15. SUBJECT TERMS Aerodynamics; Sonic boom; Supersonic; System study					
16. SECURITY CLASSIFICATION OF:			17. LIMITATION OF ABSTRACT	18. NUMBER OF PAGES	19a. NAME OF RESPONSIBLE PERSON
a. REPORT	b. ABSTRACT	c. THIS PAGE			STI Help Desk (email: help@sti.nasa.gov)
U	U	U	UU	192	19b. TELEPHONE NUMBER (Include area code) (443) 757-5802